AN INVESTIGATION OF HIGH-G MANEUVERS OF THE AH-1G HELICOPTER

James R. Van Gaasbeek

Bell Helicopter Company

Prepared for:

Army Air Mobility Research and Development Laboratory

April 1975

USAAMRDL-TR-75-18

204034

AN INVESTIGATION OF HIGH-G MANEUVERS OF THE AH-1G HELICOPTER

Bell Helicopter Company
P. O. Box 482
Fort Worth, Tex. 76101

April 1975

Approved for public release; distribution unlimited.

Prepared for

EUSTIS DIRECTORATE
U. S. ARMY AIR MOBILITY RESEARCH AND DEVELOPMENT LABORATORY
Fort Eustis, Va. 23604

UNCLASSIFIED

SECURITY CLASSIFICATION OF THIS PAGE (When Data Entered)

REPORT DOCUMENTATION PAGE		READ INSTRUCTIONS BEFORE COMPLETING FORM
1. REPORT NUMBER USAAMRDL-TR-75-18	2. GOVT ACCESSION NO.	3. RECIPIENT'S CATALOG NUMBER
4. TITLE (and Subtitle) AN INVESTIGATION OF HIGH-G MANEUVERS OF THE AH-1G HELICOPTER		5. TYPE OF REPORT & PERIOD COVERED 6. PERFORMING ORG. REPORT NUMBER
7. AUTHOR(s) James R. Van Gaasbeek		8. CONTRACT OR GRANT NUMBER(s) DAAJ02-73-C-0092
9. PERFORMING ORGANIZATION NAME AND ADDRESS Bell Helicopter Company P. O. Box 482 Ft. Worth, Tex. 76101		10. PROGRAM ELEMENT, PROJECT, TASK AREA & WORK UNIT NUMBERS 62208A 1F162208AA43 04 008 EK
11. CONTROLLING OFFICE NAME AND ADDRESS Eustis Directorate U.S. Army Air Mobility R&D Laboratory Fort Eustis, Va. 23604		12. REPORT DATE April 1975 13. NUMBER OF PAGES 120
14. MONITORING AGENCY NAME & ADDRESS(if different from Controlling Office)		15. SECURITY CLASS. (of this report) Unclassified 15a. DECLASSIFICATION/DOWNGRADING SCHEDULE

16. DISTRIBUTION STATEMENT (of this Report)

Approved for public release; distribution unlimited.

17. DISTRIBUTION STATEMENT (of the abstract entered in Block 20, if different from Report)

18. SUPPLEMENTARY NOTES

PRICES SUBJECT TO CHANGE

19. KEY WORDS (Continue on reverse side if necessary and identify by block number)

High-g Maneuvers
Statistical Analysis of Flight Test Data
Rotorcraft Flight Simulation
Rotor Contour Plots
Absolute Aerodynamic Limit

20. ABSTRACT (Continue on reverse side if necessary and identify by block number)

The high-g maneuver capabilities of the AH-1G have been investigated in this effort. Flight test data for 132 high-g maneuvers have been studied and statistically analyzed to determine the relationships among the variables. A series of fixed-collective symmetric pullups was simulated, using the Rotorcraft Flight Simulation Program C81, to determine the mechanisms limiting high-g maneuvers of the AH-1G. Statistical analysis

DD FORM 1 JAN 73 1473 EDITION OF 1 NOV 65 IS OBSOLETE

UNCLASSIFIED

SECURITY CLASSIFICATION OF THIS PAGE (When Data Entered)

Block 20. Continued.

of the C81 data was used to supplement the analysis of the test data. Three additional maneuvers, similar to the most severe test maneuvers, were simulated. Blade element lift coefficient and contour plots for ten of the simulated maneuvers have been used as an aid in determining the mechanisms involved in the absolute aerodynamic limit.

PREFACE

This report covers research conducted under Contract DAAJ02-73-C-0092 awarded in June, 1973 by the Eustis Directorate of the U. S. Army Air Mobility Research and Development Laboratory (USAAMRDL). Technical program direction was provided by Mr. D. J. Merkley of USAAMRDL.

The author wishes to acknowledge Mr. B. L. Blankenship for his assistance with the statistical analysis and Mr. C. L. Livingston for his helpful insights into high-g maneuvering flight.

TABLE OF CONTENTS

LIST OF ILLUSTRATIONS

LIST OF ILLUSTRATIONS - Continued

LIST OF ILLUSTRATIONS - Continued

LIST OF ILLUSTRATIONS - Concluded

LIST OF TABLES

LIST OF TABLES - Concluded

INTRODUCTION

Helicopter maneuverability at moderate and high forward speeds has become important to the aircraft operator in recent years. In civilian applications, maneuverability in this speed range is necessary for pipeline/powerline patrol, course change, and terrain avoidance purposes, while military operations require vehicle agility for evasive reaction to hostile fire and for close air support missions. High-speed, high-g maneuverability requirements are more stringent for the military user; Southeast Asia operational flight data (References 1 and 2) have established that gunship missions require significantly more maneuver capability than any other, as shown in Figure 1. The AH-1G (Huey Cobra) was entering service at the time these data were collected, and gunship maneuverability requirements were not well established. The Cobra was well suited to its mission requirements, but some adverse flight characteristics were encountered in certain high normal-load-factor maneuvers, such as transient engine torque pressure changes during high roll rate maneuvers. Cyclic control force feedback at high load factors was encountered, but this phenomenon was intentionally designed into the helicopter to warn the pilot that the maneuver should be limited in severity.

A series of flight tests was conducted at Edwards Air Force Base (Reference 3) in the spring of 1970 "to study in detail the characteristics of maneuvering flight and to identify any limitations required to improve flight safety." A heavily instrumented AH-1G was used to gather additional data to quantify the descriptions of phenomena encountered in Southeast Asia. These data, and the data of the structural demonstration flight tests (Reference 4), identify the high-g boundaries of the flight envelope and describe the symptoms associated with these boundaries. The referenced studies do not address themselves to determining the causes of the maneuver limitations.

The objective of the present investigation was to study the maneuvering flight data of References 3 and 4 and, with the aid of computer simulated maneuvers, describe the mechanics involved in the phenomena which limit high-g maneuvers of the AH-1G. For the purposes of the investigation, all maneuver limitations were classified into four categories: avoidable, subjective, design, and absolute limits. The first two categories constitute the "soft" limits in the sense that revision of training or operating techniques will modify or eliminate them, while the latter two categories contain those limits which are intrinsically hardware oriented, and will require technological breakthroughs to modify. The scope of these four categories is best delineated by examples.

Avoidable maneuver limitations include such problems as "inadequate altitude margins to recover from high-g turns at low airspeeds." This difficulty can be avoided by initiating such maneuvers from higher altitudes. If the low entry altitude is required for some reason, such as accuracy of ordnance delivery, then this restriction is unavoidable and is actually a design limitation.

Subjective limits are related, in general, to human factors considerations and pilot judgment. These limits are partially avoidable, as one pilot might terminate a maneuver sooner than another because he felt that the pitch rate was too great. In this area, the limit might be modified by training pilots to accept larger angular rates (within the confines of safety-of-flight considerations). Another example of a subjective maneuver limit is the termination of a maneuver due to excessive vibration, as individual pilots have different tolerances. But this limitation is also a design limitation, as the solution requires better vibration isolation for the crew, necessitating design changes. Limits imposed due to structural considerations are also design limits and their elimination would require a stronger structure.

The boundaries of the flight envelope are normally not defined by structural limitations as other limits are encountered first. Among these are the absolute limits, one of which is physiological in nature, i.e., the structure is usually designed such that the crew would terminate the maneuver before the primary structure would fail. The other major absolute limit is the aerodynamic limit of the rotor. This is a design limit, in that the rotor size, airfoil, and rotational speed can be varied, but Duhon (Reference 5) has shown that the maximum lift capability of contemporary rotors is limited to a C_T/σ of about 0.17 to 0.19.

These different types of limitations have been studied in the current effort. Structural limitations were specifically excluded, as they were being investigated under a separate contract (Reference 6). The high-g maneuver data of References 3 and 4 were selected for analysis in this study, as they describe a wide range of AH-1G maneuvers. These data have been supplemented with data from a series of simulated fixed collective symmetric pullups and all the maneuver data have been statistically analyzed. In addition, three of the flight test maneuvers have been simulated and the aerodynamic conditions have been analyzed using contour plots. The results of this analysis have been used to determine the interrelationships among the variables and to determine the mechanisms which limit AH-1G high-g maneuvers.

FLIGHT TEST DATA

The test programs of References 3 and 4 provide a large, diverse body of AH-1G maneuvering flight data, as several types of maneuvers were flown with the aircraft in different configurations and under varying atmospheric conditions. The Bell Helicopter Company tests were conducted to demonstrate the structural integrity of the aircraft throughout the specified flight envelope while the Army tests were intended to determine if any maneuvering limitations should be imposed on the AH-1G. Although the tests were flown for different purposes, the aircraft were instrumented in a similar manner and the data generated by the two programs constitute a unified set of quantitative information that can be drawn upon to study the mechanisms limiting high-g maneuvers.

Maneuvers with mean normal load factors in excess of 1.3 g were selected for this study. (In some instances, the normal load factor reported on the pilot card was greater than that recorded by the instrumentation, so a few maneuvers with normal load factors less than 1.3 g are included in the data.) One hundred thirty-two such maneuvers of the types listed in Table I were selected from the data. The teardrop turns, level-return-to-target and combat maneuvers of the Army test program were excluded from the selection process because, unlike the 132 maneuvers chosen, these are very complex and cannot be described by a small set of parameters.

The records for a maximum of twenty-one variables were examined for each maneuver as listed in Table II. These variables were chosen to describe the aircraft trajectory as completely as possible and to indicate the loading, power, and vibration levels experienced during the maneuver. Several of the variables listed in Table II are of secondary value to the analysis; the primary variables, and the maximum values observed, are listed in Table III.

The data were reduced for that 2 to 2-1/2 second interval of the maneuver which contained the time of maximum mean normal load factor. The method of data reduction was to band the trace (see Figure 2) and to determine the value at the upper and lower edges of the envelope at each 1/10 second. The mean value of the trace was computed as the average of these two values and the oscillatory amplitude was taken to be one-half the difference of the values, i.e., the one-half peak-to-peak value.

Several instrumentation problems were encountered during the reduction of the data which caused either the loss of data for one or more variables for a particular maneuver or introduced uncertainty into the data set. As an example of data loss,

the oscillograph paper speed was reduced for Army Flight 22, so that many of the overlapping traces were indecipherable in the period of maximum mean normal load factor.

The problem of uncertainty was due to four different effects. For many of the maneuvers the rate and attitude information were contradictory, i.e., the pitch attitude trace showed a different pitch rate than that given by the pitch rate trace. A second effect was the shift in trace zeros between the beginning and end of a flight. This means that the absolute value of a variable could not be known. A third problem is the lack of a calibration constant for the copilot vertical acceleration trace in the Army data. It was assumed to be equal to the desired sensitivity given in Reference 4, 1.05 g/inch. The fourth cause of uncertainty was a possible reading error of ±0.01 inch, which is about the width of the oscillograph trace. No attempt was made to account for these different measures of uncertainty, as they either could not be quantified or, in the case of the reading error, were less than one percent of the full throw value of the trace.

Table IV identifies the 132 selected maneuvers by flight number and oscillograph counter numbers and the measured maximum mean normal load factor achieved. The table also lists the missing variables for a given counter and notes major discrepancies between the recorded value of the maximum mean normal load factor and the value reported on the pilot card.

The AH-1G high-g maneuver data have been statistically analyzed to render them into a more usable form. The discipline of descriptive statistics has been used to reduce the large body of data to a small set of numbers which define the parameters of the high-g maneuvers examined. As the maneuver data constitutes a sample of the population of all high-g maneuvers, statistical inference has been used to draw conclusions about the entire population. Since data were not available for each variable for each observation, special provisions were made for calculating the statistics of the set. In particular, the sample correlation coefficient between the i^{th} and j^{th} variable, r_{ij}, depends on the number of observations of each variable contained in the data set. Formulas for r_{ij} and other statistical quantities are given in Appendix I. The computer program used for the calculations, also described in the appendix, computes and lists the mean and standard deviation for each variable, the standard error of estimate, computed value of t, and probability of a deviation less than t.

The 35 variables chosen for the statistical analysis are listed in Table V with their mean value and standard deviation. Nine of these variables are designated as <u>base variables</u> because

excessive values or oscillation in these traces would indicate that a maneuver limit had been reached. The nine base variables and their variable numbers are:

Variable Number	Variable
2	Oscillatory Copilot Vertical Acceleration at the time of Maximum Mean Normal Load
4	Oscillatory Main Rotor Pitch Link Axial Force at the time of Maximum Mean Normal Load
7	Δ(Longitudinal Cyclic Stick Position)*
9	Δ(Lateral Cyclic Stick Position)
10	Engine Torque Pressure at the time of Maximum Mean Normal Load Factor
13	Oscillatory Main Rotor Chordwise Bending Moment, Station 135, at the time of Maximum Mean Normal Load
15	Oscillatory Longitudinal Cyclic Stick Force at the time of Maximum Mean Normal Load
17	Oscillatory Lateral Cyclic Stick Force at the time of Maximum Mean Normal Load
35	Maximum Mean Normal Load Factor

The matrix of correlation coefficients for the nine base variables is given in Table VI. The sign of the correlation coefficient indicates the slope of the regression line. For the cyclic stick positions and the fuselage angular rates, the sign of the correlation coefficient depends on the convention used for the positive sense of the measured variable.

The means and standard deviations for the 35 variables used in the study are listed in Table V. The full 35 x 35 matrix of correlation coefficients was computed but only specific values are included herein. Scatter diagrams were plotted for each variable pair and examples of these plots (Figures 3 through 8) are discussed in the next section.

---

*Δ() indicates the difference between the value of the variable at the time of maximum mean normal load and the value at the beginning of the maneuver record.

Simple and multiple linear regression analyses of the flight test data are described in the following sections.

SIMPLE LINEAR REGRESSION ANALYSIS

A simple linear regression analysis was done to provide a one-to-one comparison of each variable pair formed from the 35 variables listed in Table V. Although the results of this procedure were not entirely adequate to reveal the physical phenomena involved in limiting maneuvers at high-g levels for the AH-1G helicopter, several observations can be made on the basis of these results.

The mean and standard deviation are measures of the average value and dispersion of the variable about that average. Since the sample covers the spectrum of AH-1G high-g maneuvers, the mean gives the average value of the variable to be expected in such maneuvers. The standard deviation, s_j, of the j^{th} variable is a measure of the "bandwidth" of that variable about the mean value, $\bar{x}_j$. If the distribution is normal, or nearly normal, then 68 percent of the values of the variable lie within one standard deviation of the mean ($\bar{x}_j \pm s_j$) and 95 percent of the values lie within two standard deviations of the mean ($\bar{x}_j \pm 2s_j$). For all distributions, normal or otherwise, s_j is a measure of the dispersion of the variable about its mean. For example, the maximum mean normal load factor encountered in the test data has a mean value of 1.76g and a standard deviation of 0.39g (Table V). The sample data for maximum mean normal load factor varied from 1.19g to 2.61g.

Table V shows near zero mean values for roll and yaw rates (variables 27 through 30), indicating a near equal proportion of left and right turns together with symmetric maneuvers. The scatter diagram of maximum roll rate versus the maximum mean normal load shows roll rates clustered about zero with a few large magnitude values (Figure 3). These large values result in a maximum roll rate standard deviation of 15.6 degrees/second. The scatter diagram for maximum yaw rate versus maximum mean normal load does not show clustering about zero, but rather an almost equal density dispersion from -15 degrees/second to +15 degrees/second (Figure 4).

Variable 12, Δ(Engine Torque Pressure), gives a measure of the difference between power required at the time of maximum mean normal load factor and that required at the beginning of the maneuver record. The low mean value and significant standard deviation show that power required sometimes went up and sometimes went down for the maneuvers. The scatter diagram of this

variable versus the maximum mean normal load (Figure 5) shows a cluster of zero values and considerable dispersion. Attempts to relate these variations to other measured quantities are further discussed in the next section.

The square of the simple correlation coefficient, r_{kp}^2, gives the variation in the k^{th} variable associated with the variation in the p^{th} variable, with no consideration taken of any variation in the other variables. For example, if $r_{kp} = -0.21479$, then $r_{kp}^2 = 0.0461$, which means that 4.6 percent of the variation in variable k is explained by the variation of variable p. When several variables are interrelated, the simple correlation coefficients between the pairs may be misleading. A correlation coefficient r_{ij} such that r_{ij}^2 is near one may indicate that x_i and x_j are two similar quantities, or that there is a formal linear relationship between the two, or that some other functional relation exists.

Data are included for pairs of variables such that one represents the value of the quantity measured at the time of occurrence of maximum mean load factor and the other represents the maximum value of the quantity observed during the maneuver. A list of pairs of variables representing such similar quantities and the correlation coefficient for each pair follows:

Variable Numbers	Variable	Correlation Coefficient
2 and 3	Oscillatory Copilot Vertical Accelerations	0.90
4 and 5	Oscillatory Main Rotor Pitch Link Axial Forces	0.93
10 and 11	Engine Torque Pressures	0.95
13 and 14	Oscillatory Main Rotor Chordwise Bending Moments, Station 135	0.82
15 and 16	Oscillatory Longitudinal Cyclic Stick Forces	0.95
17 and 18	Oscillatory Lateral Cyclic Stick Forces	0.81
25 and 26	Pitch Rates	0.86
27 and 28	Roll Rates	0.85
29 and 30	Yaw Rates	0.96

The pairs were included in the data set because it was not known in advance whether a significant difference would be found. The results show that there are differences although the correlation coefficients are high. Generally,

$$r_{2,i} \neq r_{3,i}, \text{ etc.}$$

for the pairs. That is, the components of a pair are not statistically the same.

The formal linear relationship between the referred thrust (maximum mean normal load divided by the density ratio) and the disc loading (variables 32 and 33) leads to a correlation coefficient of one. Variables related in this manner are statistically identical and result in the equalities

$$r_{32,i} = r_{33,i}$$

Accurate evaluation of main rotor rpm at the time of maximum mean normal load factor from the flight test records was not possible and a nominal, constant value of 324 rpm was used. This caused the calibrated airspeed and advance ratio (variables 23 and 34) to be statistically identical. These duplicates were taken into account in the evaluation discussed under multiple regression analysis.

The maximum mean normal load factor (variable 35) is defined as maximum mean normal load (variable 1) divided by gross weight. The flight tests were flown at three different gross weights, resulting in a scatter diagram for this pair (variables 1 and 35) consisting of three straight-line groups of points (Figure 6) and in a correlation coefficient of 0.88. In the scatter diagram for referred thrust (variables 32) and maximum mean normal load factor (variable 35) the variations in density ratio as well as gross weight contribute to the scatter (Figure 7). For this pair of variables the correlation coefficient is 0.82.

As would be expected, the correlation coefficient for the referred thrust and collective pitch (variables 32 and 22) is significantly high at 0.64. The scatter diagram for these variables is given in Figure 8. However, neither the longitudinal cyclic stick position at maximum mean normal load (variable 6) nor the difference in longitudinal stick position at the beginning of the maneuver and at the time of maximum normal load (variable 7) show significant correlation with the referred thrust. The highest correlation coefficient for the longitudinal cyclic stick differential (variable 7) is observed when it is paired with pitch rate (0.30).

The specific cause-effect or input-output connections related to maneuver limits are principally the oscillatory loads as functions of thrust, power, forward speed, control positions, and fuselage angular rates.

The most complete set of variables available for this comparison are those measured at the time of maximum normal load factor. The maximum normal load factor and the referred thrust are included as separate variables in the group of "cause" or independent variables since their correlation coefficients are different. The independent variables considered are:

Variable Number	Variable
6	Longitudinal Cyclic Stick Position
8	Lateral Cyclic Stick Position
22	Collective Stick Position
10	Engine Torque Pressure
32	Referred Thrust
35	Mean Normal Load Factor
25	Pitch Rate
27	Roll Rate
29	Yaw Rate
34	Advance Ratio

The dependent variables considered are:

Variable Number	Variable
2	Oscillatory Copilot Vertical Acceleration at the time of Maximum Mean Normal Load
4	Oscillatory Main Rotor Pitch Link Axial Force at the time of Maximum Mean Normal Load
13	Oscillatory Main Rotor Chordwise Bending Moment, Station 135, at the time of Maximum Mean Normal Load Factor

15	Oscillatory Longitudinal Cyclic Stick Force at the time of Maximum Mean Normal Load Factor
17	Oscillatory Lateral Cyclic Stick Force at the time of Maximum Mean Normal Load Factor

The Student-t test is used to test the hypothesis that the correlation coefficient is significantly different from zero. For a given correlation coefficient, r_{ij}, and number of observations, M_j, the value of t is computed as

$$t_{comp} = \frac{|r_{ij}| \sqrt{M_j-2}}{\sqrt{1-r_{ij}^2}}$$

If the computed-t value is greater than the value of t in the Student-t distribution for a given probability, p, and (M_j-2) degrees of freedom, then the probability that r_{ij} is not significantly different from zero is less than or equal to p. There were a total of 121 observations of test data available for this analysis. For a probability of 5 percent that the true value of the correlation coefficient is not significantly different from zero and with $M_j = 121$, the tabulated value of t is 1.64 (Reference 7). Then if t_{comp} is greater than 1.64, there is at least a 95-percent probability that the correlation coefficient is significantly different from zero. The values of r_{ij} for which t_{comp} is greater than 1.64 are found by solving the inequality

$$\frac{|r_{ij}| \sqrt{119}}{\sqrt{1-r_{ij}^2}} \geq 1.64$$

Whence $$|r_{ij}| \geq 0.15$$

Table VII gives the correlation coefficients which are greater than 0.15 for the variable listed above.

The correlation coefficients in Table VII suggest that the cyclic stick position, engine torque pressure, and mean normal load are the most significant parameters in predicting fuselage

vibration. For the oscillatory main rotor pitch link axial force, the collective stick position, referred thrust and mean normal load predominate. Collective stick position and mean normal load also dominate in the case of the oscillatory main rotor chordwise bending moments. The results are inconclusive for the oscillatory cyclic stick forces. The significance of the relationships between the dependent and independent variables is considered further in the discussions of multivariable analysis.

MULTIPLE REGRESSION ANALYSIS

Since the set of data acquired for this study relates output variables to several input variables, multiple regression analysis is probably a better statistical approach than one-to-one considerations. The analysis consists of developing a linear function of the several independent variables to approximate the dependent variable.

The set of standard normal variables, X_i, obtained from the variables, x_i, given in Table V, by the relationship

$$X_i = \frac{x_i - \bar{x}_i}{s_i}$$

has the same correlation coefficient matrix as the original set. Furthermore, the X_i may be employed in an equation for the regression plane for the case of several variables as

$$X_1' = - \frac{R_{12}}{R_{11}} X_2 - \frac{R_{13}}{R_{11}} X_3 - \ldots - \frac{R_{1k}}{R_{11}} X_k$$

where X_1' indicates the approximation to X_1 from the regression plane and the R_{ij} are the cofactors of $\bar{R}$, the correlation coefficient matrix. The coefficients in the equation are called coefficients of partial regression and are interpreted as the average change in the dependent variable associated with a unit change in the particular independent variable. These coefficients are denoted thus:

$$m_{ij} = - \frac{R_{ij}}{R_{ii}}$$

Note that $m_{ij} \neq m_{ji}$.

Table VIII gives the coefficients of partial regression for the standard normal variables corresponding to the variables listed in Table VII. The coefficient m_{ij} may be compared directly since the X_i's have unit standard deviations.

Thus, the predominant elements in approximating the dependent variable from the regression plane are revealed. Generally, the tabulation shows that vibration levels increase with advance ratio and with lateral cyclic stick position to the left of neutral. In addition, oscillatory main rotor pitch link axial force is a strong function of referred thrust, and the oscillatory main rotor chordwise bending moments are highly sensitive to collective stick position. The oscillatory loads are only slightly dependent on roll and yaw rate while the fuselage vibrations, as measured by the oscillatory copilot vertical acceleration, appear to decrease with increasing pitch rate. Indications from Table VIII of the effects of longitudinal cyclic stick position, engine torque pressure and mean normal load factor on vibration are somewhat ambiguous.

A quantity which is closely allied to the coefficient of partial regression is the partial correlation coefficient,

$$r_{ij.kl...} = - \frac{R_{ij}}{\sqrt{R_{ii}\ R_{jj}}}$$

This is the correlation coefficient between X_i and X_j when the remaining variables X_k, X_l, ..., are held fixed.

The values of the partial regression coefficient range from -1.0 to 1.0. The significance of this parameter is determined by use of the z-test, in which the partial regression coefficient is transformed to a variable ranging from $-\infty$ to $+\infty$ with a zero mean. The transformation is

$$z = \frac{1}{2} \ln \frac{(1+r_{ij.kl...})}{(1-r_{ij.kl...})}$$

The standard deviation of the transformed variable is

$$\sigma_z = \frac{1}{\sqrt{n-3}}$$

To establish the confidence levels for the partial correlation coefficients, the standard deviation is revised to

$$\sigma_z = \frac{1}{\sqrt{n-3-k}}$$

where k is the number of independent variables (Reference 8).

For the variables in question,

$$\sigma_z = \frac{1}{\sqrt{65-3-10}} = 0.139$$

Further, the statistic

$$Z = \frac{z - \zeta_H}{\sigma_z}$$

has the standard normal distribution when ζ, the actual mean of the z-distribution, is equal to ζ_H, the hypothetical mean (Reference 8). To test the hypothesis that there is no correlation of x_i with x_j, take $\zeta_H = 0$.

Since Z is a standard normal variable (Reference 8), 95 percent of the distribution lies within 1.96 standard deviations of the mean. The critical value of $r_{ij.kl...}$ for the 5-percent confidence level is found from

$$\frac{1}{2} \ln \frac{1+r_{ij.kl...}}{1-r_{ij.kl...}} = z_{crit} = 1.96\ \sigma_z = 0.272$$

Whence $r_{ij.kl...} = 0.265$

Therefore, only those values of $r_{ij.kl...}$ greater than 0.265 are retained in the results listed as Table IX. Most of the observations made in discussing the m_{ij} hold for the $r_{ij.kl...}$. However, note that longitudinal cyclic stick position, engine torque pressure, and mean normal load factor show no significant correlation with any of the five vibration variables. Furthermore, oscillatory cyclic stick forces do not correlate with any of the selected input variables to a significant level. The strongest relationships are:

Oscillatory Copilot Vertical Acceleration	-	Lateral Cyclic Stick Position
Oscillatory Main Rotor Pitch Link Axial Force	-	Maximum Mean Normal Load, Advance Ratio
Oscillatory Main Rotor Chordwise Bending Moment, Station 135	-	Collective Stick Position, Advance Ratio

MULTIPLE CORRELATION COEFFICIENTS

The coefficient of multiple correlation is computed and interpreted in a manner similar to the simple correlation coefficient. However, the standard error of estimate used is derived from the multiple regression equation. The interpretation of the coefficient of multiple correlation is most clear when it is given in terms of the coefficient of multiple determination, which is just its square. If x_i is the dependent variable and x_j, x_k, ... are the independent variables, the coefficient of multiple determination can be expressed as

$$R^2_{i.jkl...} = \frac{\text{associated variation}}{\text{total variation}}$$

Thus $R^2_{i.jkl...}$ is a measure of the usefulness of the regression plane for estimating purposes (Reference 8).

Coefficients of determination were calculated using program JRSW03 (see Appendix I) for the variable combinations considered previously. This program is capable of computing $R^2_{1.2}$, $R^2_{1.23}$, etc. That is, the ratio of variation of x_1 associated with x_2 to the total variation of x_1 is computed first, then the ratio of the variation in x_1 associated with x_2 and x_3 to the total variation in x_1, and so on through the specified list of input variables. Further, the variables are taken in the order of their contribution to the coefficient of multiple determination. These cumulative coefficients of determination are listed in Table X.

The relationships indicated by the multiple correlation coefficients are essentially the same as those found by use of the partial correlation coefficients except for the role of pitch rate. The maximum contribution of pitch rate to any $R^2_{i.jkl...}$

is 3 percent when it is taken with the oscillatory copilot vertical acceleration. The strong relationships previously noted appear again, and the weakness of correlation with cyclic stick forces persists.

OBSERVATIONS ON THE STATISTICAL ANALYSIS OF FLIGHT TEST DATA

Several factors can be considered to enhance and extend the analysis of flight test data by statistical methods for the purpose of discovering or determining relationships among variables. A primary consideration is the connection between the test plan and performance and the analytical objectives. The design-of-experiment concept indicates a critical relationship when statistical methods are to be applied to the data. A change in objectives generally requires a change in the test plan and new objectives stated after the fact may not be achieved.

Data acquisition is part of the general test plan and performance, but is sufficiently important to deserve further discussion. At the present time, flight test data recorded on magnetic tape in a format accessible to data processing programs is essential for extensive statistical analysis. Control over identification and accuracy cannot otherwise be maintained.

Better methods for analyzing data should be used. Multiple linear regression analysis as employed in this study may yield improved information with a broader data base. Possibilities of polynomial or functional linear analysis should be explored. Statistical methods can be used with data from the entire flight spectrum to clarify relationships between variables and to determine the reliability of test information.

SIMULATED MANEUVERS

Helicopter maneuverability can be studied from the point of view of several disciplines and for various reasons. One approach is to study a large body of flight-test data in order to determine the significant variables affecting maneuverability, as has been done in this effort. Another approach would be to simulate maneuvers on a computer and to examine the interdependency of the variables in the calculated maneuvers. The simulations can use a simplified analytical model, such as those based on the concept of energy maneuverability (References 9 through 12), or a complex model, such as that of the Rotorcraft Flight Simulation Program C81 (References 13 and 14). The C81 analytical model has been used to simulate high-g maneuvers to supplement the flight test maneuver data. A description of the program inputs and sample level flight correlation cases are given in Appendix II.

A series of fixed-collective symmetric pullups has been simulated to determine the thrust levels at which certain maneuver limiting phenomena occur. The pullups were simulated at seven different advance ratios using the same helicopter configuration. At a given advance ratio, different maximum mean normal load factors were achieved by varying the rate at which the longitudinal cyclic stick position was changed.

The AH-1G configuration chosen for this study had a gross weight of 7477 pounds, an aft center of gravity and no wing stores. The inertia properties of this configuration are well known and the rotor loads computed for the lightweight configurations compare favorably with those measured in flight (see Appendix II, flights 34-A and 280-A). The center-of-gravity waterline was taken at 68.0 inches for the symmetric pullups because it was the value used for the simulation of flights 277 and 280. In addition, contractor experience with symmetric pullup simulations has shown that the highest values of C_T/σ are reached with the light gross weight, aft center-of-gravity configuration.

The entry conditions for the seven sets of maneuvers are given in Table XI. Operational fixed-collective maneuvers are entered by diving from level flight cruise at a power setting of approximately 34 psi. This corresponds to a level flight cruise speed of about 132 knots (μ = 0.30) and a collective stick position of 27 percent for the configuration used in this study. For true airspeeds in excess of 132 knots, a rate of sink was chosen that gave about the same collective stick position. An autorotational (zero main rotor horsepower) entry was used for airspeeds less than 132 knots. (It is noted in Table XI

that a small amount of engine horsepower remained even at zero root collective for the autorotational entry maneuvers. The horsepower required, though, was effectively zero.)

FIXED COLLECTIVE SYMMETRIC PULLUPS

The maneuver simulations were conducted to determine the value of C_T/σ at which the onset of retreating blade stall occurs, as a function of advance ratio. In addition, the simulation data were used to establish the thrust levels at which the maximum continuous engine horsepower and steady transmission torque rating were exceeded. The flapping stop and cyclic force feedback limits were found, where the information was available. Finally, a control system fatigue limit (based on the oscillatory pitch link axial force) and the absolute aerodynamic limit were determined.

For teetering rotors, the onset of retreating blade stall is accompanied by a sharp increase in oscillatory main rotor root chordwise bending moments. For a given advance ratio, the thrust level at which retreating blade stall becomes evident is determined from a plot of the oscillatory chordwise bending moment versus C_T/σ. As shown in Figure 9, significant retreating blade stall is signalled by the change in slope ("knee") at a C_T/σ of 0.142. It should be noted that the chordwise bending moment at this point, 100,000 inch-pounds, is well below the structural limits of the blade. For example, a continuous oscillatory load of 335,000 inch-pounds at the root corresponds to to a fatigue life of about one million cycles. The line indicating the onset of retreating blade stall, as defined by the knee in the chordwise bending moment curves for several advance ratios, and the one million cycle fatigue-life line, are given in Figure 10. (The fatigue-life line was determined by extrapolation from the computed loads and the loads were too small at the lower advance ratios to make a valid extrapolation.)

Figure 10 also contains the maximum mean normal load factor points for the 52 symmetric pullups of the flight test data, and the retreating blade stall boundary established by Gustafson (Reference 15). This boundary was determined from a series of level flight tests in a particular helicopter. It was determined that the effects of stall were severe, for that rotor, when the retreating blade tip angle of attack (α_r) exceeded the airfoil stall angle by 4 degrees. The stall band in Figures 10 through 13 assumes that the onset of retreating blade stall in level flight occurs between $\alpha_r = 12°$ and $\alpha_r = 16°$. The incipient stall boundary computed from the simulated autorotational pullups ($0.15 < \mu \leq 0.25$) is below or in this band,

while the power-on C81 maneuvers establish a stall boundary significantly higher than the test data of Gustafson. A small part of this increase is due to the beneficial effects of vehicle pitch rate, as explained by Brown and Schmidt (Reference 16), but it does not account for the entire improvement. Almost all the test points represent maneuvers being flown well into stall. Such highly stalled maneuvers do not cause flying qualities problems with teetering rotors since no hub moments are generated and no pitching or rolling motion is induced by the rotor.

An increase in required horsepower and oscillatory pitch link axial force also occurs at the onset of retreating blade stall, but at slightly different values of C_T/σ. The lines defining the onset of retreating blade stall as determined by these parameters are given in Figures 11 and 12. (There was no sharp increase in the oscillatory pitch link axial force at $\mu = 0.40$.) The retreating blade stall band of Figure 13 is the result of combining the three criteria for the determination of incipient retreating blade stall.

The available shaft horsepower for the AH-1G helicopter is given in Reference 17. This maximum continuous engine horsepower is exceeded for fixed collective symmetric pullups at thrust levels above the line shown in Figure 14. Maneuvers can be flown in excess of the engine horsepower limit, as the additional required power can be acquired from rate-of-sink or deceleration The steady-state transmission torque rating is 18,380 foot-pounds and is exceeded transiently for maneuvers at thrust levels above the line shown in Figure 15.

The flapping stop in the AH-1G helicopter is at ±12 degrees. The stop was not contacted in any of the flight test maneuvers and was encountered only once in the simulated pullups, at $\mu = 0.40$ and $C_T/\sigma = 0.174$.

A cyclic force feedback limit line cannot be predicted from the maneuver simulations because the complex dynamics of the rotating and fixed controls have not been included in the analytical model. The hydraulic boost system was purposely designed to be reversible above a boost tube load of 2220 pounds axial force (Reference 18 is for the AH-1J control system, but the cyclic boost system is identical to that in the AH-1G). Any boost tube load in excess of 2220 pounds will cause vibration of the flight control system to alert the pilot that the severity of the maneuver should be decreased.

The oscillatory pitch link axial force has been used to define the onset of retreating blade stall. It is also used to determine a fatigue life maneuver limitation, as the fatigue lives of all components of the rotating control system and the blade

grip are given in terms of this parameter (Reference 19). Of these components, the rotating swashplate (swashplate outer ring) has the lowest reduced endurance limit, with a life of 9806 hours under a continuous oscillatory pitch link load of 1431 pounds. The thrust levels at which this value is exceeded transiently are above the line given in Figure 16. (The pitch link load line between μ = 0.15 and 0.30 was established by extrapolation, as the computed pitch link loads at these advance ratios did not reach 1431 pounds.) During a maneuver at a C_T/σ above this level, the pitch link load will exceed 1431 pounds for only a few cycles, doing a very small amount of fatigue damage, so maneuvers can be flown past this fatigue-life line. Figure 16 also includes an estimated cyclic force feedback limit, based on the assumption that a 2220-pound oscillatory pitch link axial force would cause feedback. This estimated limit is not given at the lower values of advance ratio as extrapolation from the low computed loads would be unreliable.

The maximum lift capability of the rotor establishes the absolute aerodynamic limit. This limit has been determined for fixed-collective symmetric pullups by increasing the severity of the simulated maneuver until no further gain in maximum mean normal load was achieved. The limit line generated by this procedure is given in Figure 17. Duhon (Reference 5) has computed an absolute aerodynamic limit with no restrictions on the maneuver type or control displacements, and this limit band is also shown in Figure 17. These data show that allowing collective motion significantly improves the low speed maximum C_T/σ capability of the helicopter. This is reasonable, as cyclic-only motion in hover will give no significant increase in normal load factor.

ABSOLUTE AERODYNAMIC LIMIT CONTOUR PLOTS

The absolute aerodynamic limit is reached when the rotor is operating at the highest average C_L (which is $6C_T/\sigma$ - Reference 20). For the fixed collective symmetric pullups simulated, the average C_L at the absolute aerodynamic limit, Figure 17, is as follows:

Advance Ratio	C_L
0.15	0.58
0.20	0.70
0.25	0.83
0.30	0.95
0.325	0.99
0.35	1.06
0.40	1.17

The maximum average C_L observed in the flight test symmetric maneuvers is about 1.01 over the whole range of advance ratios.

To get these high values of C_L with the amount of cyclic pitch involved in the simulated maneuvers, the rotor blade elements will have to be operating at values of c_ℓ greater than C_L over a significant portion of the disc. Computer generated contour plots of c_ℓ have been used to determine the proportion of the rotor disc in which high values of c_ℓ are obtained. Angle-of-attack contour plots were also used to determine the amount of stall associated with the high value of c_ℓ.

Contour plots for the unaccelerated entry condition (C_T/σ = 0.057, C_L = 0.40) were used to establish the baseline data for each advance ratio. High values of c_ℓ (>1.0) are observed over about five percent of the disc area just outside the reverse flow region (Figure 18) for the autorotational entries, centered along an azimuth of 240 to 250 degrees. Reference to angle-of-attack contour plots (Figure 19) shows that there is a very small region of stall (α>12.0 degrees) at the edge of the reverse flow region at azimuth angles between 240 and 300 degrees. The contour plots for the power-on entry conditions show very small regions of high c_ℓ within the reverse flow region and no regions of stall, as the angle of attack over the whole disc is less than 9 degrees and it is less than 6 degrees on the advancing side.

At the absolute aerodynamic limit (i.e., at the time of maximum mean normal load factor) for the autorotational pullups, the region of high lift coefficients has shifted aft (centered along an axis at 360 degrees) and grown slightly larger (Figure 20). The lift coefficients are significantly larger over the whole disc. The angle-of-attack contour plots (Figure 21) show a large increase in the stalled area on the disc. In trim, the stalled area was less than 5 percent of the disc area, while at the absolute aerodynamic limit, between 15 percent (μ = 0.15) and 25 percent (μ = 0.25) of the disc area was stalled.

Larger regions of high lift coefficients exist at the absolute aerodynamic limit for the power-on maneuvers (Figure 22), with the blade operating at values of c_ℓ >1.0 over 20 to 25 percent of the disc. The coefficient of lift has increased by a value of approximately 0.5 over the whole rotor disc, compared with the values in unaccelerated flight. The angle-of-attack contour plots (Figure 23) give additional information, as the stall angle is exceeded over at least 30 percent of the disc

area. The maximum value of C_T/σ observed for the simulated maneuvers was 0.196 at $\mu = 0.40$. The angle-of-attack contour plot for this condition (Figure 23d) shows that the blade is stalled over 65 percent of the disc. There are large regions in which the angle of attack is very large, indicating deep stall. Therefore, 0.196 is about the maximum value of C_T/σ that can be achieved by this rotor.

STATISTICAL ANALYSIS OF C81 DATA

The simulated fixed-collective symmetric pullups provide a data base of 64 maneuvers for statistical analysis. The values of 14 variables at the time of occurrence of maximum mean normal load were analyzed in the same manner as the flight test data. Corresponding C81 variables are available for seven of the nine basic flight test variables investigated. The oscillatory normal load factor from C81 replaces the measured oscillatory copilot vertical acceleration, and stick forces are not computed. The matrix of simple correlation coefficients for these variables is given in Table XII. This matrix corresponds to the one for test data given in Table VI.

The strongest relationships indicated by these coefficients are:

Oscillatory CG Vertical Acceleration with Oscillatory Main Rotor Chordwise Bending Moment

Oscillatory Main Rotor Pitch Link Axial Force with Δ(Lateral Cyclic Stick Position), Engine Torque Pressure, and Oscillatory Main Rotor Chordwise Bending Moment

Mean Normal Load Factor with Δ(Cyclic Stick Positions)

The Student-t test has been applied to the correlation coefficients. For 64 observations, there is a 95-percent probability that the value of the correlation coefficient is significantly different from zero if its magnitude is greater than 0.20. Table XIII gives the correlation coefficients greater than this value relating oscillatory variables to control positions, engine torque pressure, maximum mean normal load factor, fuselage angular rates, and advance ratio. These results may be compared to those given in Table VII. The C81 data show much stronger correlation of oscillatory variables with change in cyclic stick position at the time of maximum g. Also the yaw rate is only weakly correlated with these oscillatory variables. The coefficients are generally much larger than those for the test values in Table VII.

Multiple regression analysis was carried out for the C81 data in the same manner as for the test data. For partial correlation, there is 95-percent certainty that the value of the coefficient is significantly different from zero if its magnitude is greater than 0.265. The partial correlation coefficients exceeding 0.265, which were computed for the variables previously considered in Table IX are given in Table XIV. The results show that the role of engine torque pressure is much greater than was indicated by the simple correlation coefficients. The following relationships predominate:

Oscillatory CG Vertical Acceleration with Engine Torque Pressure, Pitch Rate, and Roll Rate

Oscillatory Main Rotor Pitch Link Axial Force with Engine Torque Pressure and Advance Ratio

Oscillatory Main Rotor Chordwise Bending Moment with Engine Torque Pressure, Roll Rate, and Δ(Longitudinal Cyclic Stick Position)

Cumulative coefficients of determination were computed for the oscillatory variables. Results are shown in Table XV for the four most effective independent variables and for the entire group. These figures indicate substantially the same connections as listed for the partial correlation coefficient results. Again the levels of correlation are much higher for the C81 data than for corresponding quantities from the flight test data. Here 80 percent or more of the variation in the oscillatory variables is associated with variations in the listed independent variables.

Higher values of correlation coefficients were expected from the C81 data than from the test data since the computer program is based on many functional relationships. However, the variables used in the multiple regression analysis are not the entire set which influences results. For instance, the remaining 17 percent (or less) variation in fuselage vibration may involve variations in fuselage attitude relative to the flight path. Further, the various nonlinear effects may bias the analysis, even over a relatively limited speed range.

SIMULATION OF FLIGHT TEST MANEUVERS

Maneuvers similar to the three most severe maneuvers in the AH-1G flight test data have been simulated with C81. The type of maneuver, aircraft configuration and entry conditions are given in Table XVI. For the autorotational pullups (counters 775 and 840), the collective and longitudinal cyclic motions were input and the lateral cyclic and pedal were controlled by the C81 autopilot. All control motions were input for the left rolling pullout maneuver of counter 740.

The first 1.5 seconds of the flight test record for counter 775 consists of unaccelerated autorotational flight, so this portion of the maneuver was not included in the simulation to conserve computer time. The flight test and simulated time histories for this maneuver are given in Figure 24. The normal load factor traces are identical until the time of maximum normal load factor. The simulated maneuver came close to the flight test value of maximum normal load factor, but could not quite reach it. The shapes of the two time histories are similar through the high-g portion of the maneuver.

The pitch attitude trace shows that the simulated aircraft and flight test article were not at exactly the same entry condition for the maneuver. As the simulation progressed, the two traces are very close together and both show an almost zero pitch rate at the time of maximum mean normal load factor. The flight test longitudinal cyclic position given in the figure is the sum of both the cyclic stick and longitudinal cyclic SCAS actuator position. The C81 simulation did not use the SCAS option in the program, so the only longitudinal control input is from the cyclic stick, and it is seen that the longitudinal control motions agree quite well over the latter portion of the maneuver.

The zero-horsepower-required condition of autorotation was not reached, as a small amount of horsepower required was indicated at the collective setting which gave a rate-of-sink similar to that recorded in flight. (The pressure altitude was recorded by photopanel and the scatter in the data is due to vibration.) The C81 collective stick position is lower than that measured in flight, but C81 has always predicted lower collective settings, as discussed in Appendix II. What is important here is that the required horsepower is effectively zero and the rate of sink is about the same as that measured in flight, so that the actual entry condition has been closely simulated. Also, the change in collective between 4.35 seconds and 4.8 seconds is about the same for the flight test and simulated maneuvers.

The true airspeed trace shows that the aircraft deceleration has been matched well. Unfortunately, the recorded data do not provide accurate rotor rpm data, so there is no way to determine if the rotor deceleration in the simulation matches that of the flight test maneuver.

The oscillatory main rotor pitch link axial force computed by C81 is greater than that measured throughout the maneuver, but the time histories have the same shape. The computed oscillatory chordwise and beamwise bending moments at station 135 reach their peak values at the same time as the measured loads, and are somewhat greater than the flight test loads. The

low chordwise and beamwise bending moments at the beginning of the simulated maneuver are due, in part, to the difference in the entry conditions. The small discrepancies between the time histories throughout the remainder of the maneuver are probably due to differences in the rotor dynamics and aerodynamics.

Total lift coefficient and angle-of-attack contour plots were generated during the simulation of this maneuver. During the autorotational entry, the blades are operating at high lift coefficients over approximately 5 percent of the disc, in an area outside the reverse flow region, between the azimuths of 150 and 360 degrees (Figure 25). A very small region of stall exists, centered outside the reverse flow region at an azimuth of 270 degrees. At the time of maximum mean normal load, the coefficient of lift is in excess of 1.0 over approximately 15 percent of the rotor disc, and angles of attack in excess of the static stall angle occur over one-third of the disc (Figure 26).

The time histories for the autorotational pullup of counter 840 are given in Figure 27. The first six-tenths of one second of the flight test record corresponds to unaccelerated flight, which was not simulated. The computed mean normal load factor trace follows the measured time history well. The initial jump in the measured data seen between 1 and 1-1/2 seconds appears to be due to a gust, as it is not accompanied by a high pitch rate or a spike in the measured rotor loads (which would be expected if the cg acceleration had been caused by an increase in rotor normal force). The simulated maneuver achieves the same maximum mean normal load factor as the test maneuver, but it is reached a little earlier than in flight. The high mean normal load factor could not be sustained for as long a time in the simulation as it was in flight, but the normal load factor does not decrease as rapidly as in the test data.

The computed pitch attitude time history agrees favorably with the test data through the middle of the maneuver. Again, the aircraft trimmed in a slightly less nose down attitude in the C81 than in flight. The computed pitch attitude increases at a greater rate than the measured pitch angle at and past the time of maximum mean normal load factor. This high pitch rate could not be arrested, even though the forward stick motion initiated at 3 seconds was at a higher rate than the measured rate.

The collective stick position for the autorotational entry condition in C81 gives the same rate of sink as that measured in flight and essentially zero horsepower. The photopanel data show the engine to be operating in flight idle, so the measured collective stick position of 14 percent may be in

error. The true airspeed time histories show the simulated aircraft to be slowing at a slightly greater rate than the actual aircraft.

The oscillatory pitch link axial force trace coincides with the measured time history until the beginning of the collective flare. The two traces are similar through the maximum mean normal load factor portion of the maneuver, although the computed pitch link load reaches a higher value at a later time.

The computed oscillatory chordwise and beamwise bending moment time histories do not match the flight test data, and the maximum computed loads are somewhat greater than those measured. The large dip in the computed time histories at 3.35 seconds is unusual, but reflects a small drop in the measured chordwise load and a sharp drop in the beamwise bending moment at 3.3 seconds.

Rotor aerodynamic contour plots were generated for this maneuver also. During the unaccelerated autorotational entry condition, total lift coefficients in excess of 1.0 are observed over approximately 10 percent of the disc in a crescent shaped area almost completely surrounding the reverse flow region (Figure 28). Stall is observed over approximately 5 percent of the disc area, just outside the reverse flow region at an azimuth of 270 degrees.

At the time of maximum mean normal load factor, values of c_ℓ greater than one are obtained over about one-quarter of the disc, while the blade is operating in stall over at least three-quarters of the disc (Figure 29). The low lift coefficients observed between the azimuths of 270 and 360 degrees are accompanied by very large angles of attack, indicating that the rotor is operating "on the backside of the lift curve" in this region.

The time histories for the left rolling pullout maneuver (flight 116, counter 740) are presented in Figure 30. The pilot card notes that this was a coordinated turn, and the mean lateral acceleration was held to ±0.1 g throughout the simulation. The computed mean normal load factor and roll attitude traces follow the measured time histories very well. More left cyclic is required to trim the simulated helicopter in the entry condition than was measured, but the lateral cyclic stick motion generally follows the motion recorded for the test maneuver. The measured and computed longitudinal cyclic stick position time histories agree quite well. The calculated rate of sink matches that measured in flight reasonably well and the true airspeed trace shows that the deceleration in the simulation was similar to that of the flight test maneuver.

The computed oscillatory pitch link axial force is in good agreement with the measured load for most of the maneuver and is lower during the peak-g portion of the maneuver. Correlation between the computed and measured oscillatory chordwise bending moments is generally good, although the dip in the computed time history at 2.5 seconds is not reflected in the test data. This dip also occurs in the oscillatory beamwise bending moment time history, and coincides with the decreasing roll rate. These discrepancies are most likely due to differences in the way the maneuver was flown, and it is possible that simulated left turn was more coordinated than the flight test maneuver.

The contour plots at the entry of the maneuver (Figure 31) show a small region of high lift coefficients and no stall. At the time of maximum mean normal load factor, the blade is operating at high lift coefficients over about 25 percent of the disc and stall is observed over 70 percent of the disc area (Figure 32).

MANEUVER LIMITING MECHANISMS

The designer needs to understand the phenomena occurring during high-g maneuvers so that ways may be found to improve maneuverability. Cyclic force feedback and maximum aerodynamic thrust capability have already been discussed in detail. The mechanisms of these and five other phenomena have been investigated and are presented here.

The maximum normal load factor achievable in a symmetric pullup can be influenced by the way the maneuver is terminated. If the pullup ends with a pushover, the pilot will start recovery early. This avoids a low-g pushover, with its loss of control effectiveness. Higher normal load factors can be attained in the pullup if it is ended by a right roll similar to a wingover maneuver (Reference 3).

Excessive cockpit vibrations can restrict the crew's ability to read the instruments and control the aircraft. High vibration levels are an indication of stall. The statistical analysis of the C81 data shows a strong correlation between oscillatory normal load factor and chordwise bending moments, which are also a good indication of stall. The highest oscillatory copilot vertical vibration observed in the test data occurred during a banked turn maneuver (counter 7, flight 10) at a maximum mean normal load factor of 1.39 g. The copilot vertical acceleration for this maneuver was harmonically analyzed and the predominant components are at even harmonics, indicating that the forcing functions are even harmonic vertical hub shears and odd harmonic inplane hub shears.

Rotor stall is not the only cause of high cockpit vibrations, as banked turns at load factors greater than 1.39 g experienced less vibration. The harmonic analysis of the copilot vertical vibration and blade bending moments showed high frequency components which are associated with the rotor intersecting its own wake. The occurrence of wake crossing is dependent on the airspeed and fuselage and rotor angular rates and is not entirely repeatable. This aerodynamic effect cannot be modified, but a vibration isolation system, such as pylon nodalization, can postpone the onset of cockpit vibration to higher normal load factors.

Transient engine torque pressure surges as large as 15 psi may be encountered during maneuvers initiated at high power settings. Livingston (Reference 21) has shown that the engine torque pressure will tend to increase whenever:

- the rotor pitch rate is negative
- the rotor roll rate is negative, or
- the cyclic stick moves forward

The largest engine torque pressure surge, and the largest value of engine torque pressure, was observed during the roll reversal maneuver of counter 820, flight 118. The time histories of several parameters of this maneuver are given in Figure 33. (The engine torque pressure was recorded photographically, and the photopanel record was 0.3 second longer than the oscillograph record for this maneuver.) Rotor pitch and roll rate data are unavailable but can be deduced from the slopes of the fuselage angular rate traces. The rotor roll rate is negative between about 0.9 and 4.5 seconds. The positive pitch rate, which tends to decrease engine torque pressure, is overcome by the negative roll rate, and the surge begins at about 2 seconds. The examples used in Reference 21 show that there is a time lag of approximately 1 second between the beginning of a negative angular rate or forward stick motion and the beginning of the torque surge. Therefore, the sharp forward cyclic motion at about 3.6 seconds, in addition to the preceding negative roll rate, is the cause of the large torque pressure surge beginning at 4.6 seconds.

In several of the structural demonstration flight test maneuvers (Reference 4), the maximum mean normal load factor achieved was restricted by a limit imposed on the collective pitch change rate. The control system hydraulic fluid flow rate was intentionally regulated to a maximum of 1.2 gallons/minute. (The cyclic controls have the same flow rate limit, but there is no indication in the flight test data that cyclic rate limiting was encountered.) This corresponds to a collective pitch angle rate of 29.5 degrees/second and a collective stick rate of 123 percent/second. This limitation was incorporated in the control system design to avoid overstressing the rotor by the rapid buildup in loads accompanying a sharp collective input.

Cyclic and collective control force feedback is an additional control system design feature intended to warn the pilot when a structural limit is being approached. The main rotor oscillatory pitch link axial force required to cause force feedback is about 2220 pounds. The rotating swashplate has a fatigue life of 10^6 cycles at a continuous oscillatory pitch link load of about 2150 pounds (Reference 19), which is close to the control force feedback load limit. It was noted during the C81 simulation of the fixed collective symmetric pullups that the continuous oscillatory main rotor root chordwise bending moment corresponding to a fatigue life of 10^6 cycles was attained at the thrust levels at which the oscillatory main rotor pitch link axial force reached 2220 pounds. Maneuvers can be flown which cause loads in excess of the 10^6 cycles fatigue life, but the life of the rotor and rotating control system will be decreased in proportion to the time spent at high loads.

The absolute aerodynamic limit is reached when large portions of the rotor are operating in stall. Figure 17 shows that the limit is reached at different thrust levels for different types of maneuvers, with low-speed, fixed-collective symmetric pullups reaching the limit at lower values of C_T/σ than the collective moving maneuvers used by Duhon (Reference 5). The angle-of-attack contour plots for the autorotational pullup maneuver of counter 840 and the fixed collective symmetric pullup at μ = 0.40 and C_T/σ = 0.196 are reproduced in Figure 34. The static stall angle is exceeded over at least 90 percent of the rotor disc for the maneuver of counter 840 and at least 70 percent of the disc for the fixed collective symmetric pullup. Deep stall (α>30 degrees) is observed over 15 to 20 percent of the disc area.

SUMMARY AND CONCLUSIONS

One-hundred-thirty-two AH-1G high-g maneuver records have been examined to evaluate more than thirty performance and oscillatory load parameters. Simple and multiple linear regression analysis of the data was performed, but the interrelationships among the variables could not be determined due to the generally low correlation coefficients. A series of high-g maneuvers was simulated with C81 to supplement the test data, and a set of parameters corresponding to the flight test variables was statistically analyzed. The correlation coefficients had sufficient range to show which variables were strongly related. No new mechanisms were revealed, but the results generally agreed with prevailing theory.

The computed data were also used to determine the point of slope changes in plots of horsepower and oscillatory loads variables versus C_T/σ. This information was then converted into contour lines on C_T/σ versus μ plots to indicate incipient stall, fatigue life levels, engine and transmission rating boundaries, control feedback warning, and the absolute aerodynamic limit. This limit was investigated by the use of rotor aerodynamic contour plots, which showed that very large regions of deep stall exist on the rotor disc.

Three additional maneuvers, similar to the most severe maneuvers in the test data, were simulated with C81. Comparison between the measured and computed time histories of performance and oscillatory load data showed excellent correlation. Rotor aerodynamic contour plots for these maneuvers again showed large regions of stall.

Evaluation of the computed and measured data has shown that engine torque pressure surge and the absolute aerodynamic limit are the only phenomena which limit the maximum normal load factor. Control force feedback has been designed into the aircraft to force the pilot to limit maneuvers to load levels that will not decrease the useful life of the vehicle. Cockpit vibration has been found to restrict some maneuvers, but no clear cause-effect relationship was discernable in the data, and the problem can be alleviated in future aircraft by a vibration isolation system, such as pylon nodalization. High-g symmetric maneuvers may be limited by degradation of control effectiveness at low load factors during the recovery, but this restriction can be removed by modifying the recovery technique.

Several conclusions can be reached with regard to future studies of high-g maneuvers. The accuracy and consistency of flight path information should be improved and main rotor flapping

and blade feathering angles should be recorded. The aircraft configurations and instrumentation data should be documented in greater detail, and the data should be recorded on magnetic tape to facilitate data handling. In accordance with the principles of experimental design, the purposes and objectives of the tests should be known and stated before the program is conducted. These objectives will then become the basis for a test program designed to facilitate the statistical analysis of the data.

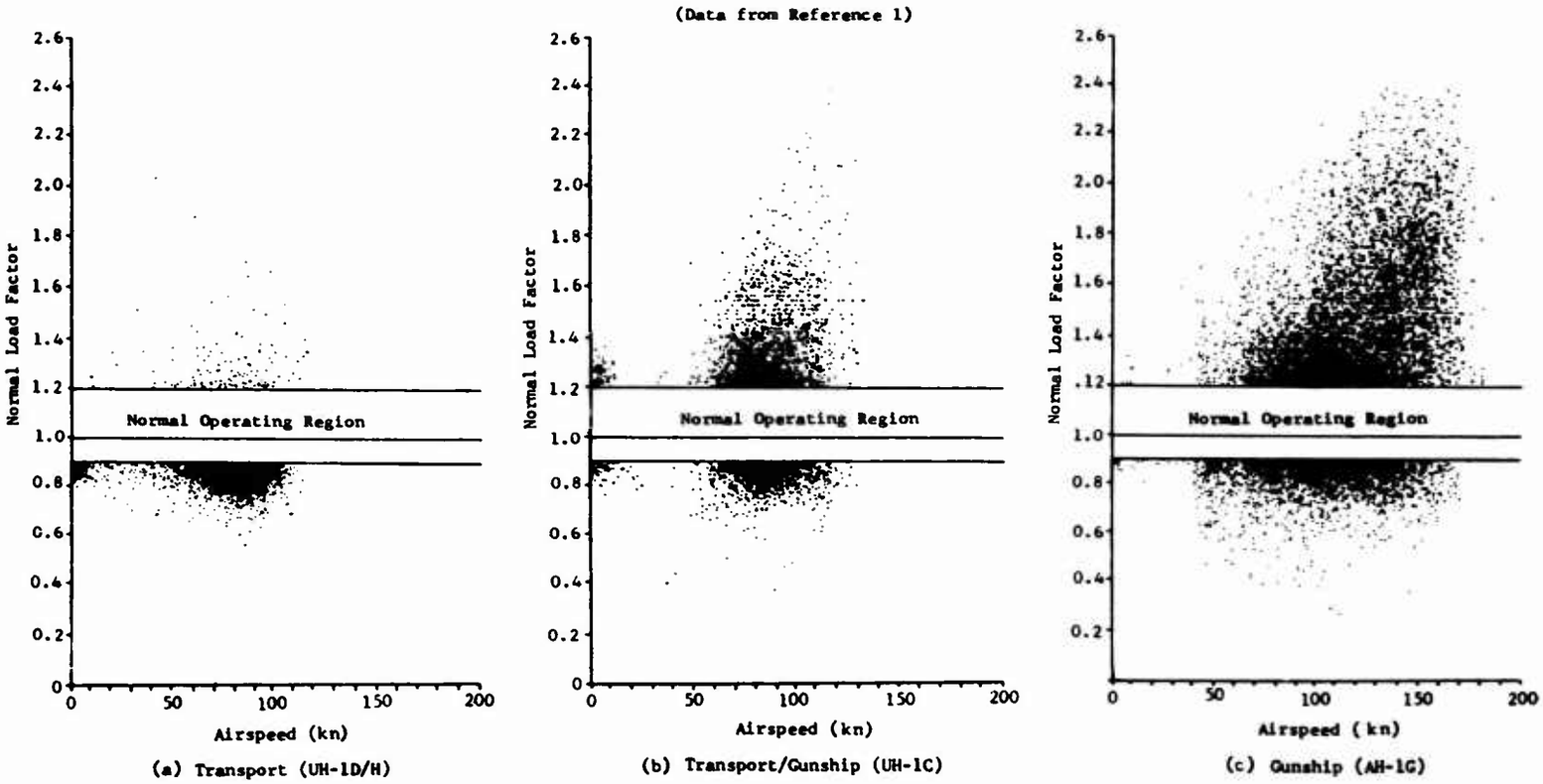

Figure 1. Southeast Asia Operational Flight Envelopes for Three Mission Types.

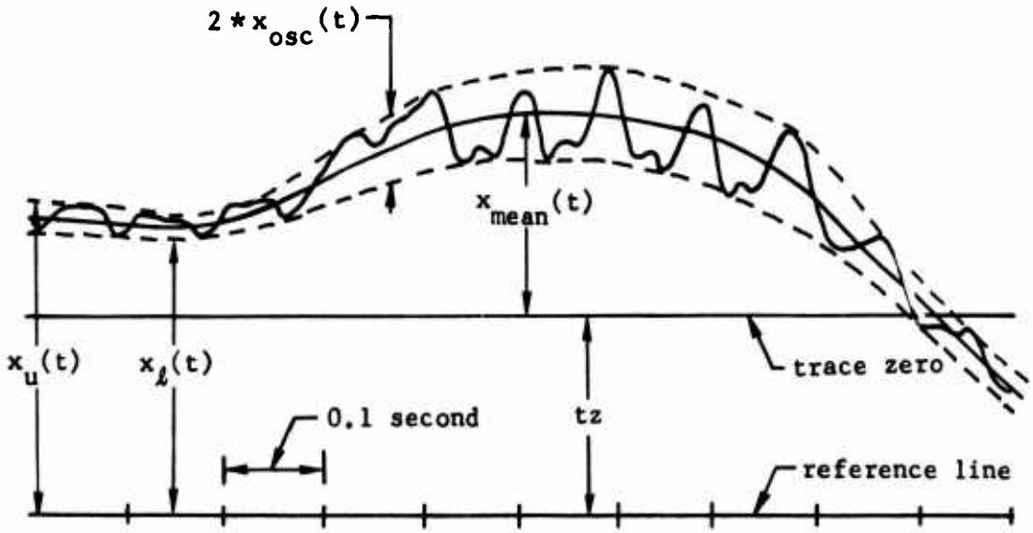

$$x_{mean}(t) = \left(\frac{x_u(t) - x_\ell(t)}{2} - tz \right) * \left(\text{calibration constant} \right) + \left(\text{value of trace zero} \right)$$

$$x_{osc}(t) = \left(\left| \frac{x_u(t) - x_\ell(t)}{2} \right| \right) * \left(\text{calibration constant} \right)$$

Figure 2. Method of Data Reduction.

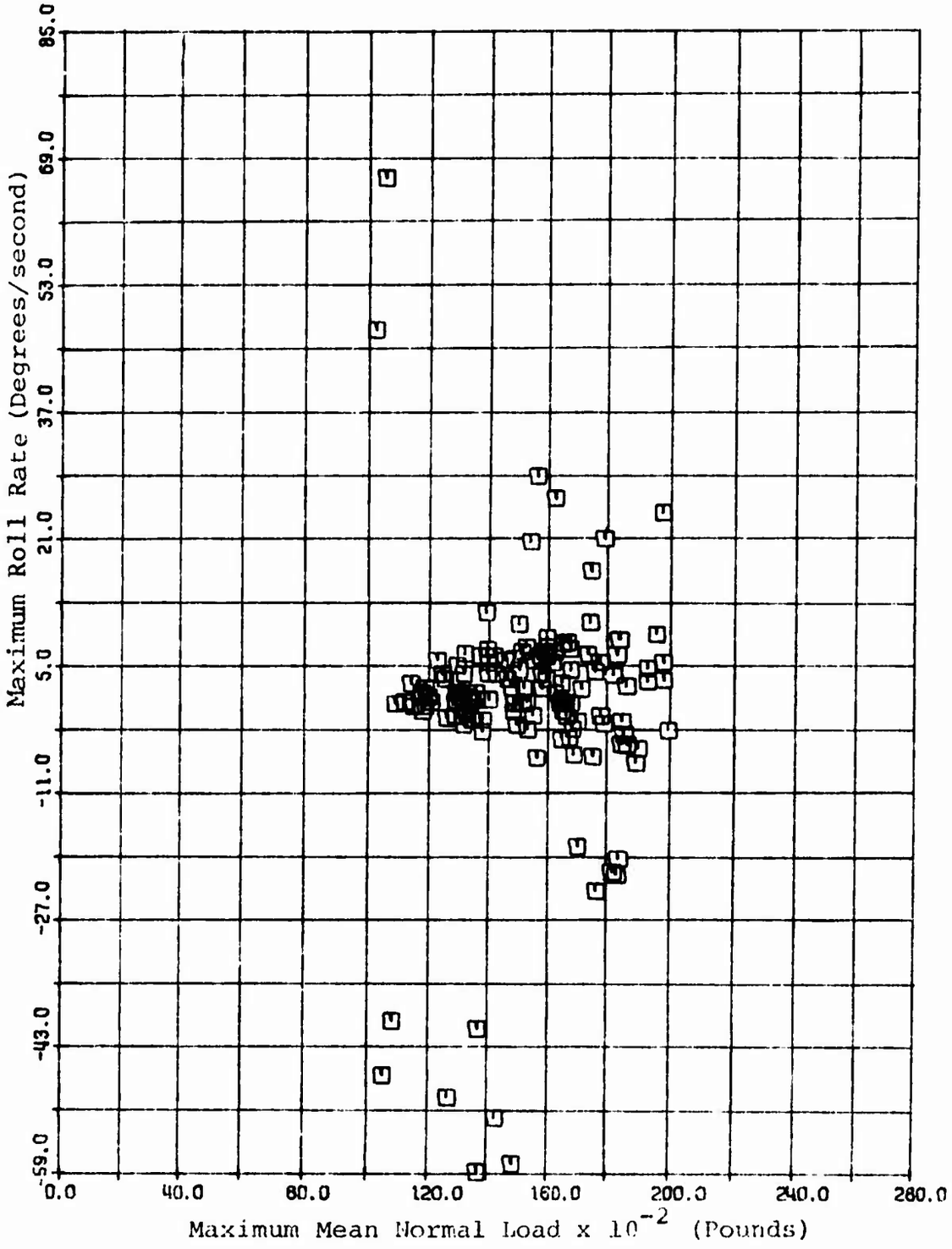

Figure 3. Scatter Diagram, Maximum Roll Rate Versus Maximum Mean Normal Load.

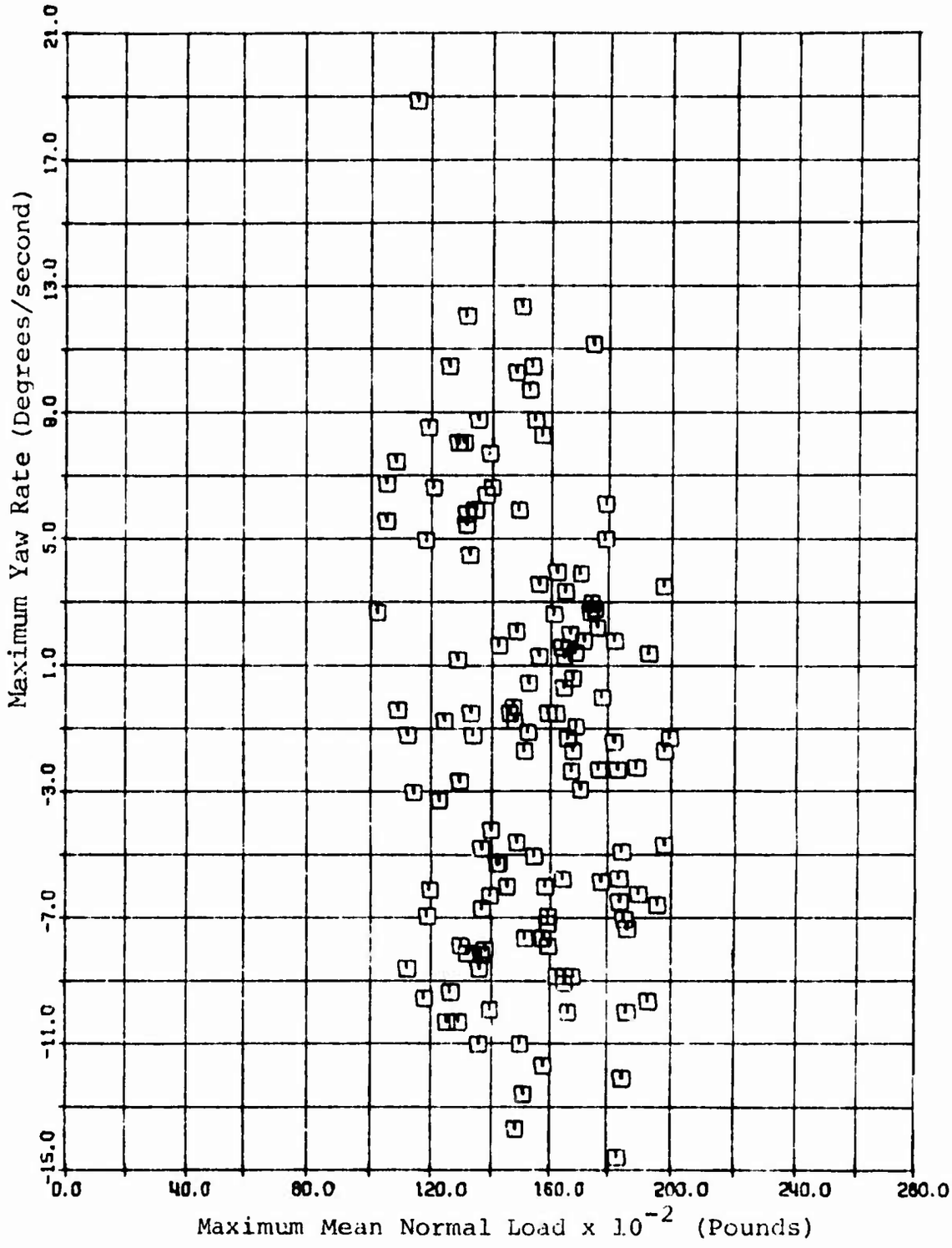

Figure 4. Scatter Diagram, Maximum Yaw Rate Versus Maximum Mean Normal Load.

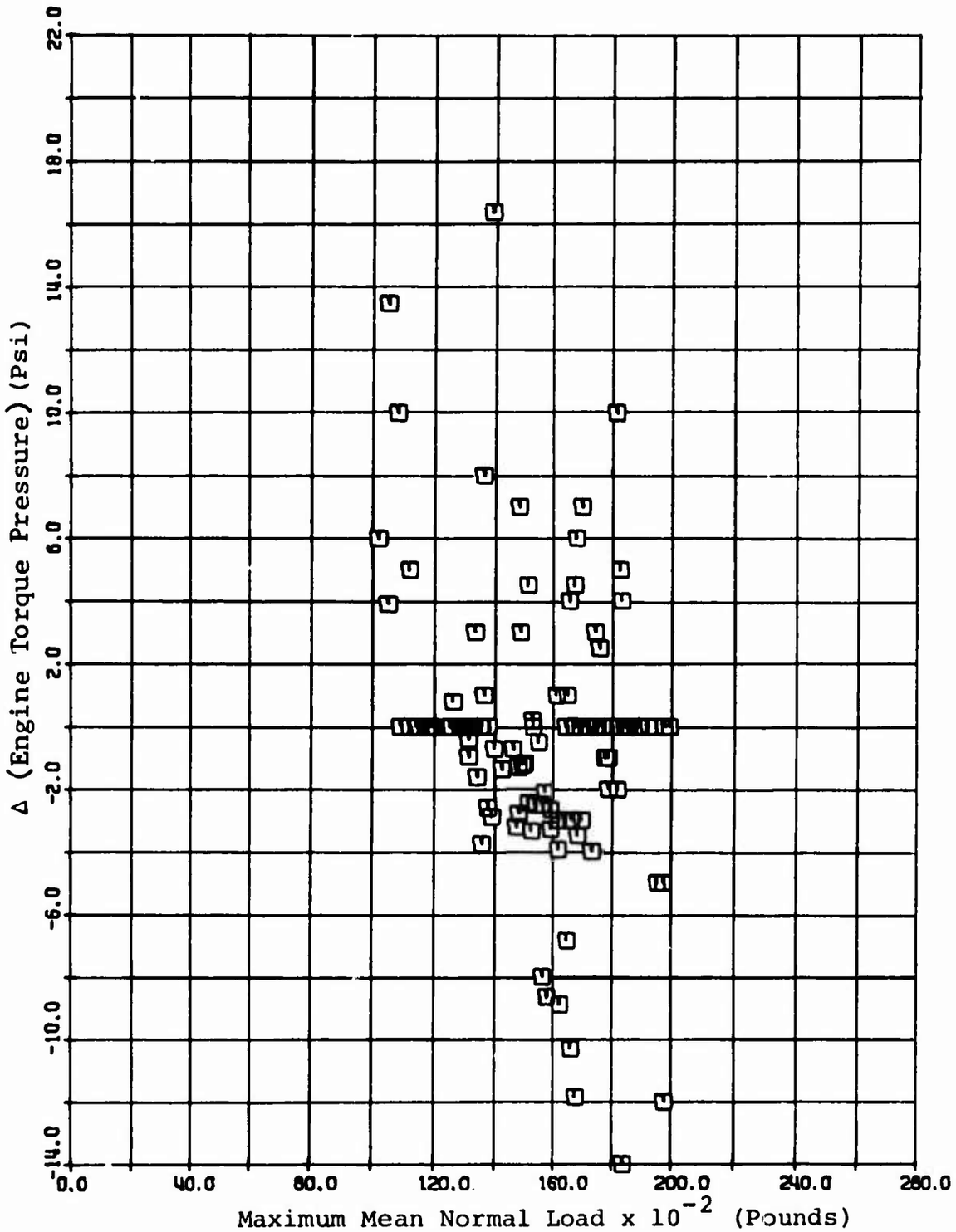

Figure 5. Scatter Diagram, Δ(Engine Torque Pressure) Versus Maximum Mean Normal Load.

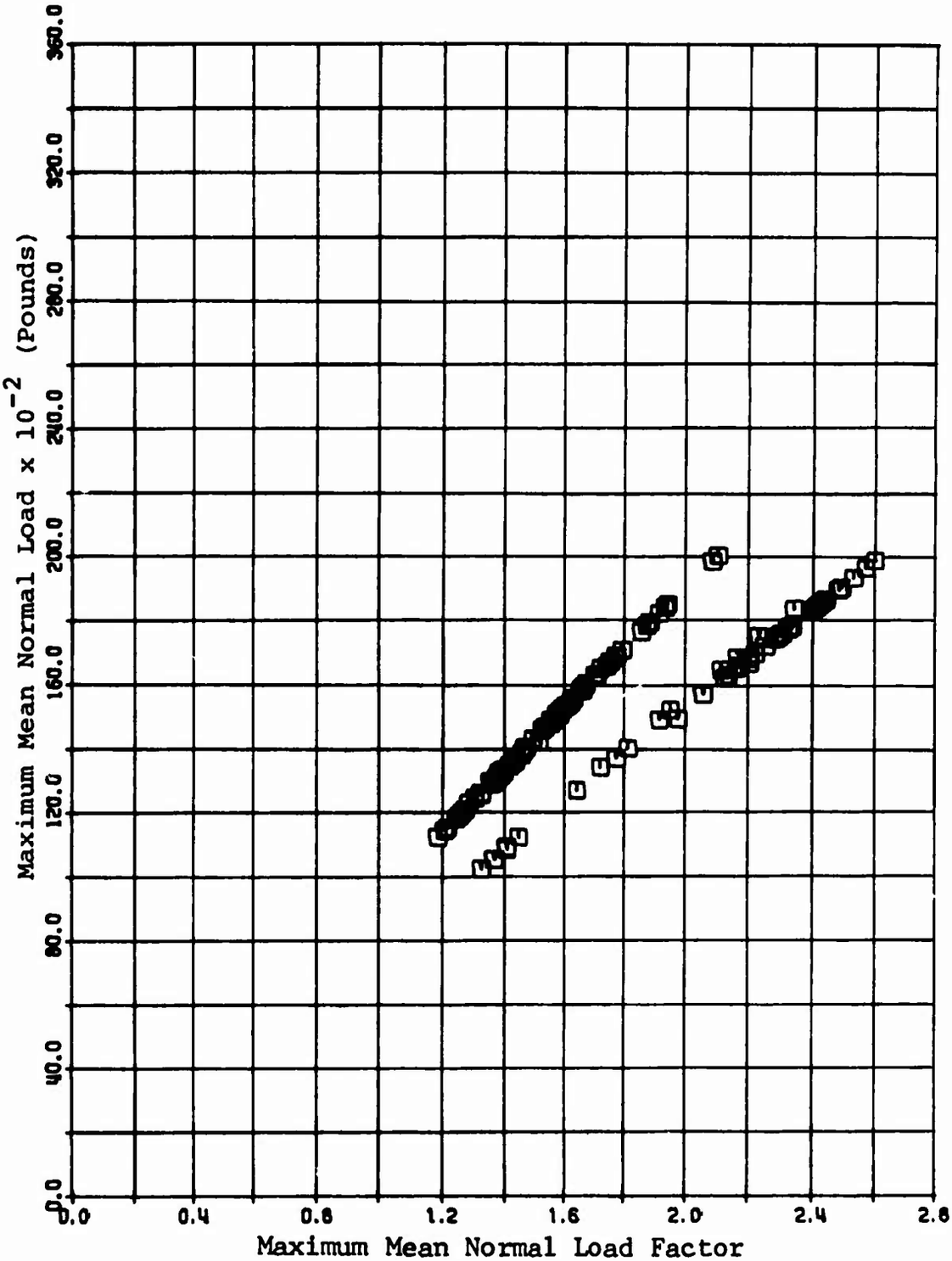

Figure 6. Scatter Diagram, Maximum Mean Normal Load Versus Maximum Mean Normal Load Factor.

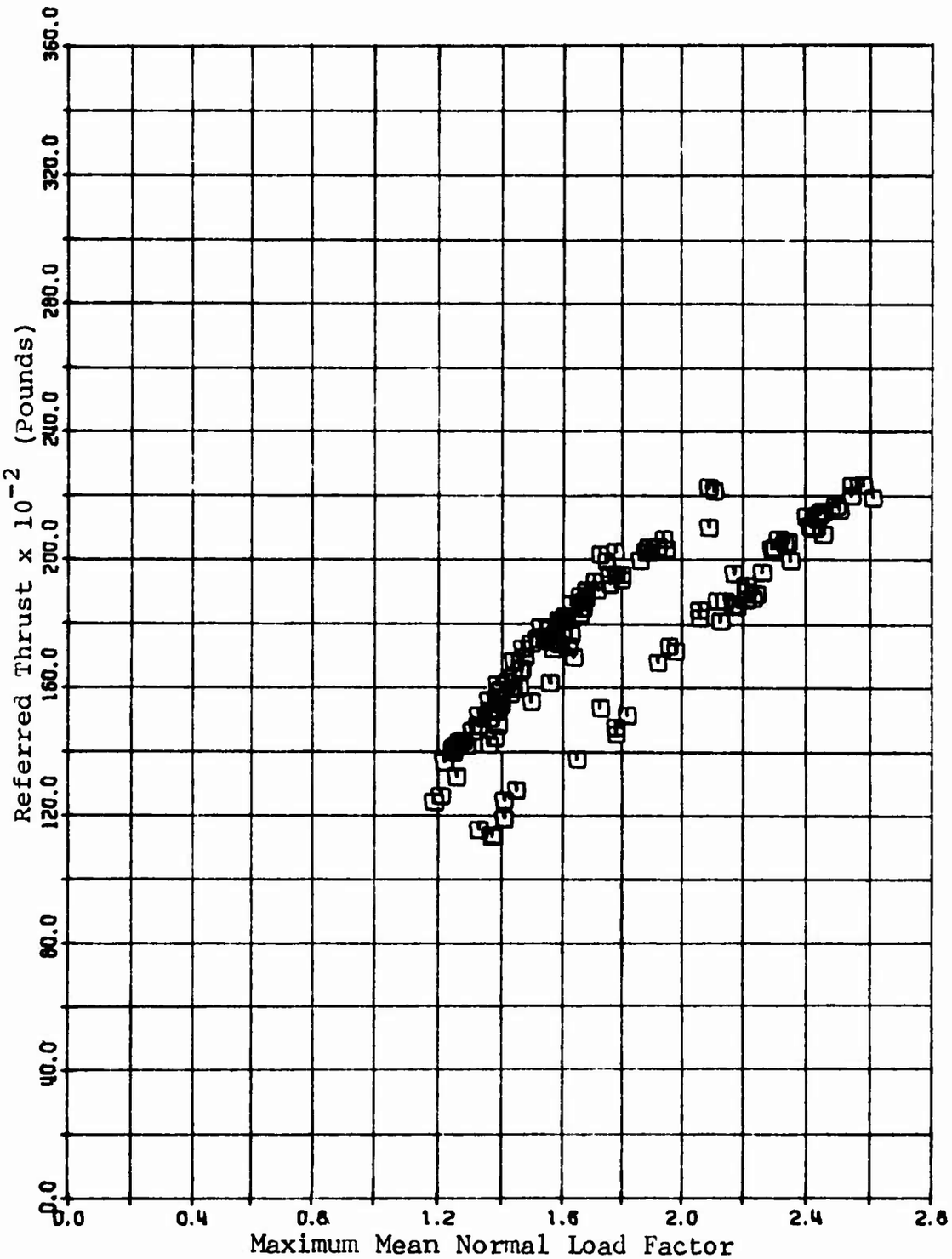

Figure 7. Scatter Diagram, Referred Thrust Versus Maximum Mean Normal Load Factor.

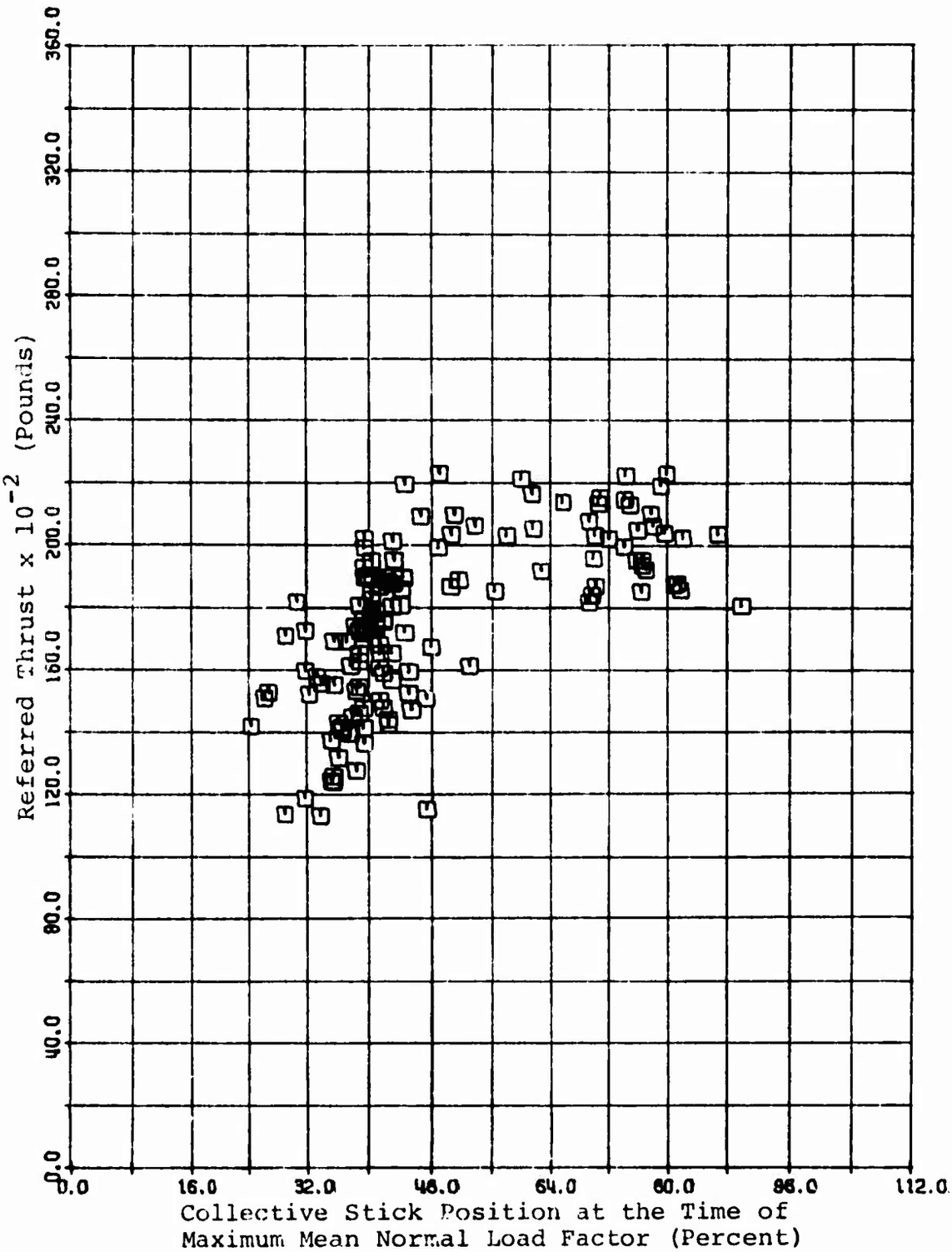

Figure 8. Scatter Diagram, Referred Thrust Versus Collective Stick Position at the Time of Maximum Mean Normal Load Factor.

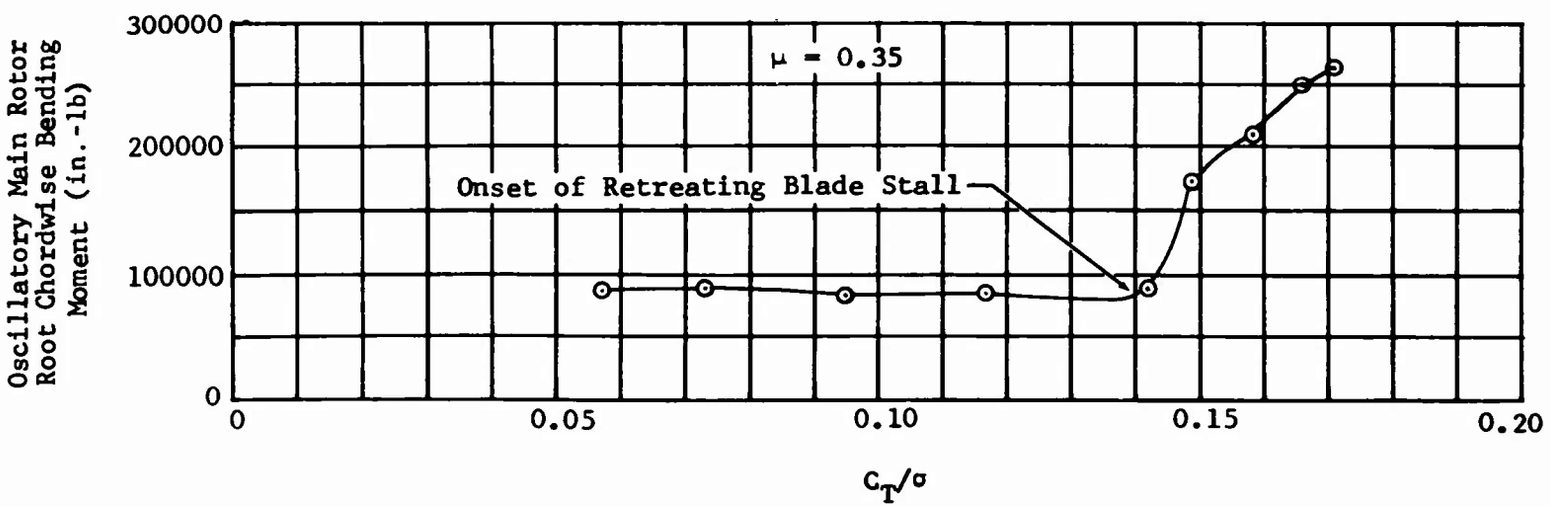

Figure 9. Method of Determining Retreating Blade Stall Limit at a Constant Advance Ratio.

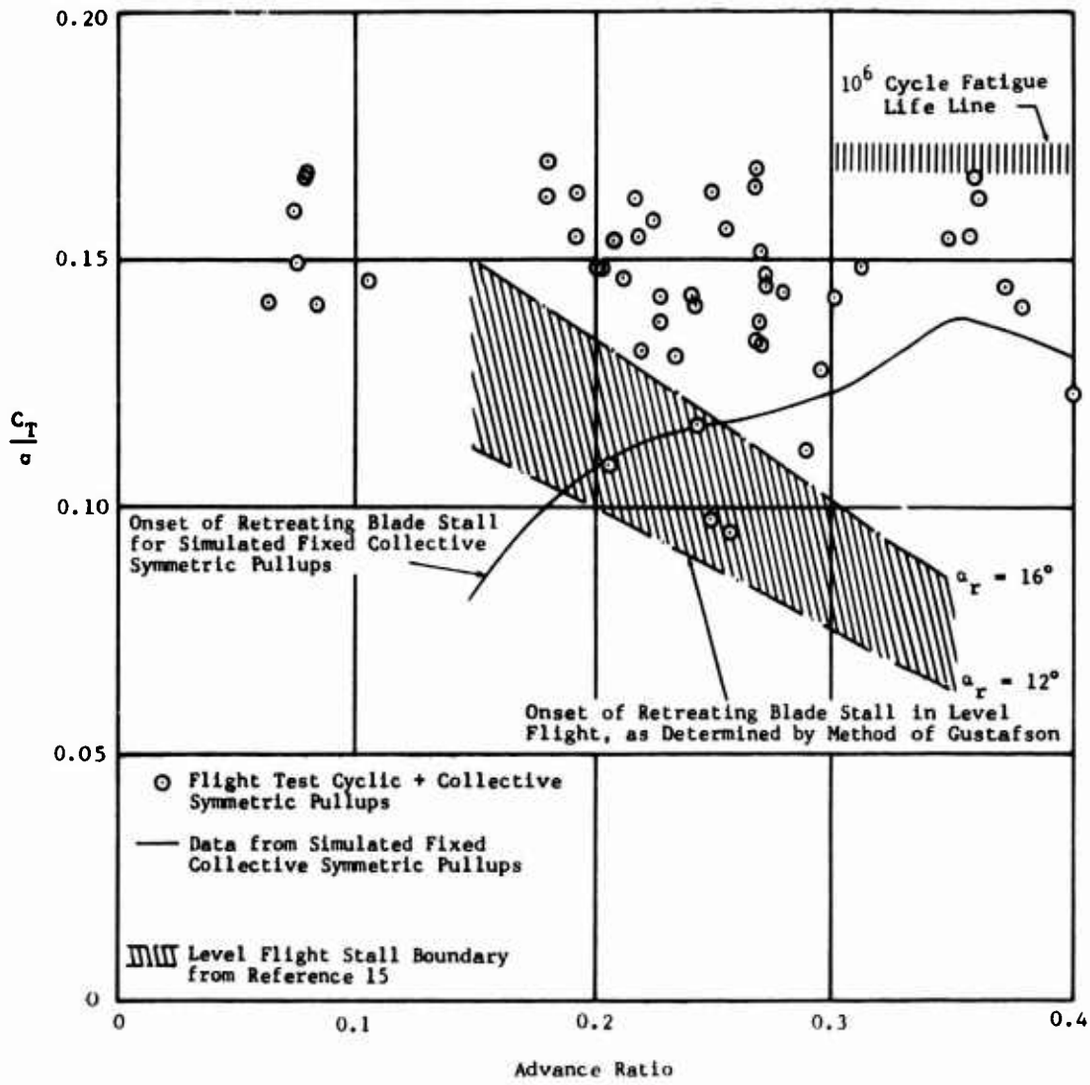

Figure 10. Onset of Retreating Blade Stall for Fixed Collective Symmetric Pullups as Determined From Oscillatory Main Rotor Root Chordwise Bending Moment Data and as Determined by the Method of Gustafson, With Flight Test Maneuver Points.

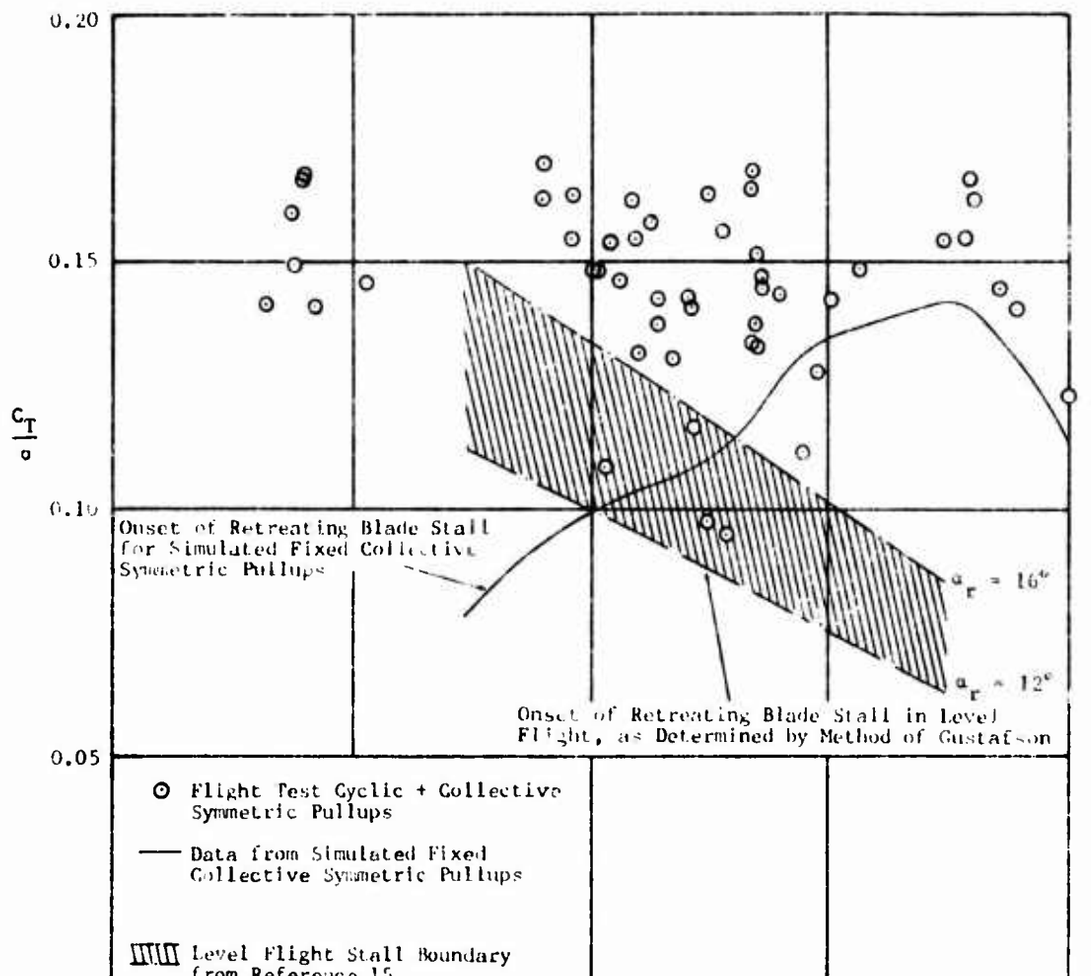

Figure 11. Onset of Retreating Blade Stall for Fixed Collective Symmetric Pullups as Determined From Engine Shaft Horsepower Data and as Determined by the Method of Gustafson, With Flight Test Maneuver Points.

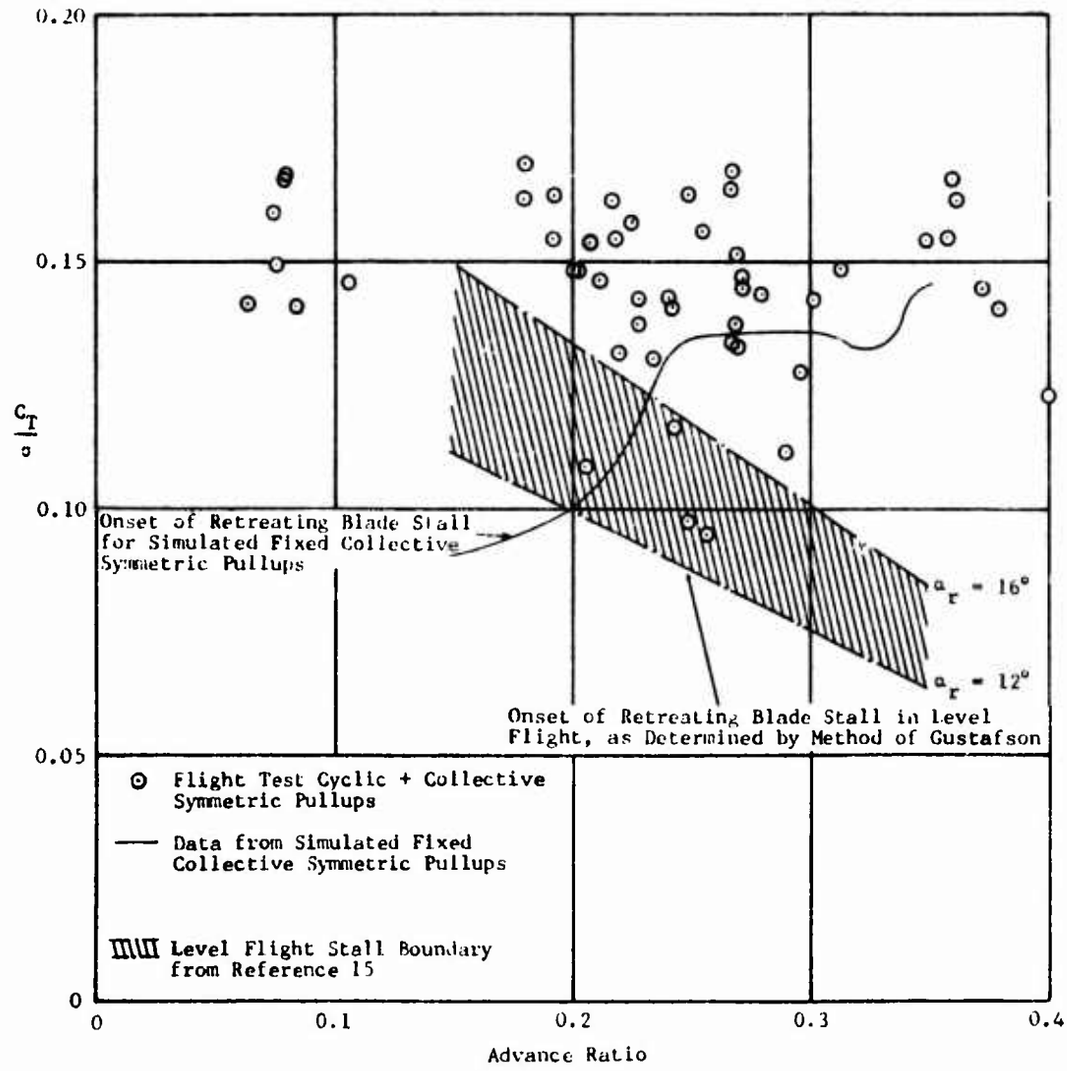

Figure 12. Onset of Retreating Blade Stall for Fixed Collective Symmetric Pullups as Determined From Oscillatory Main Rotor Pitch Link Axial Force Data and as Determined by the Method of Gustafson, With Flight Test Maneuver Points.

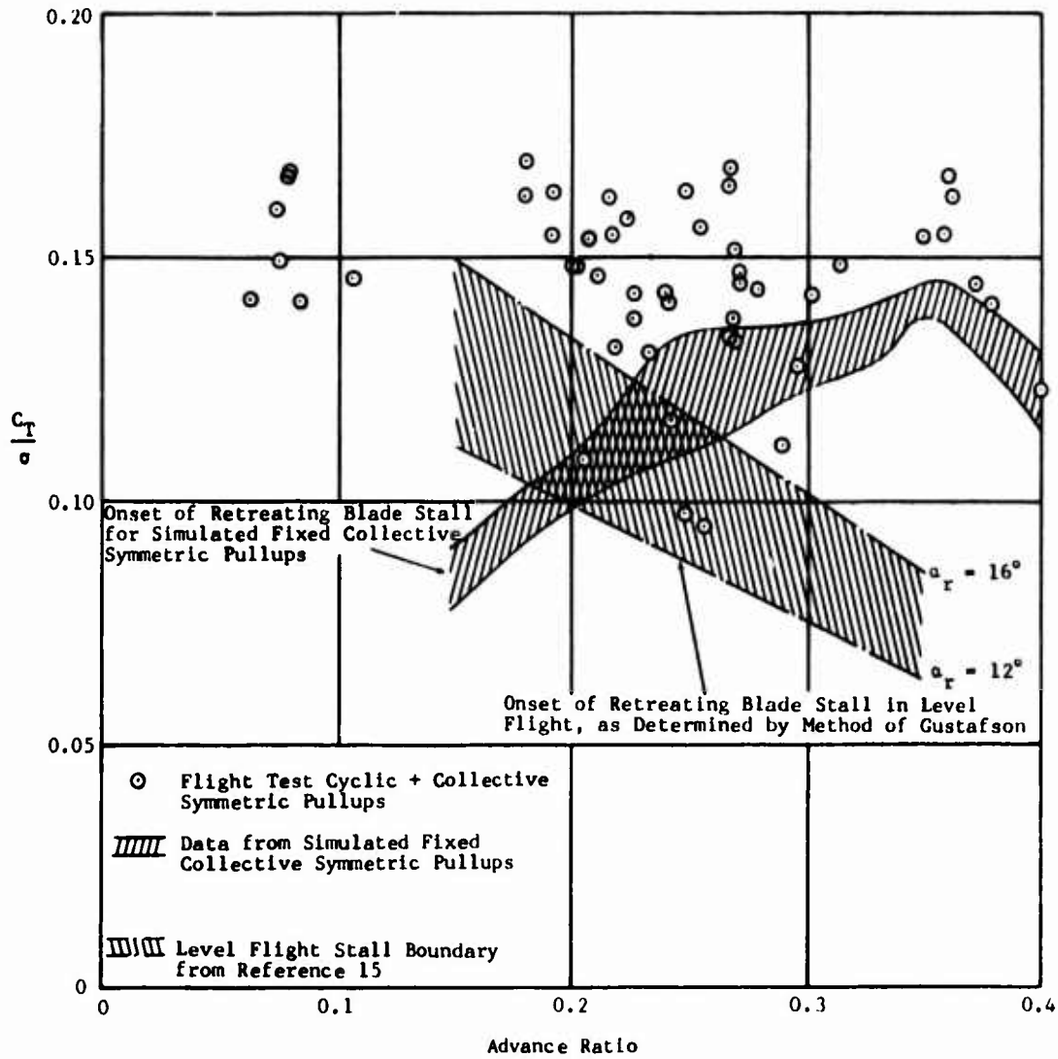

Figure 13. Onset of Retreating Blade Stall for Fixed Collective Symmetric Pullups as Determined by Combination of the Three Parameters and by the Method of Gustafson, With Flight Test Maneuver Points.

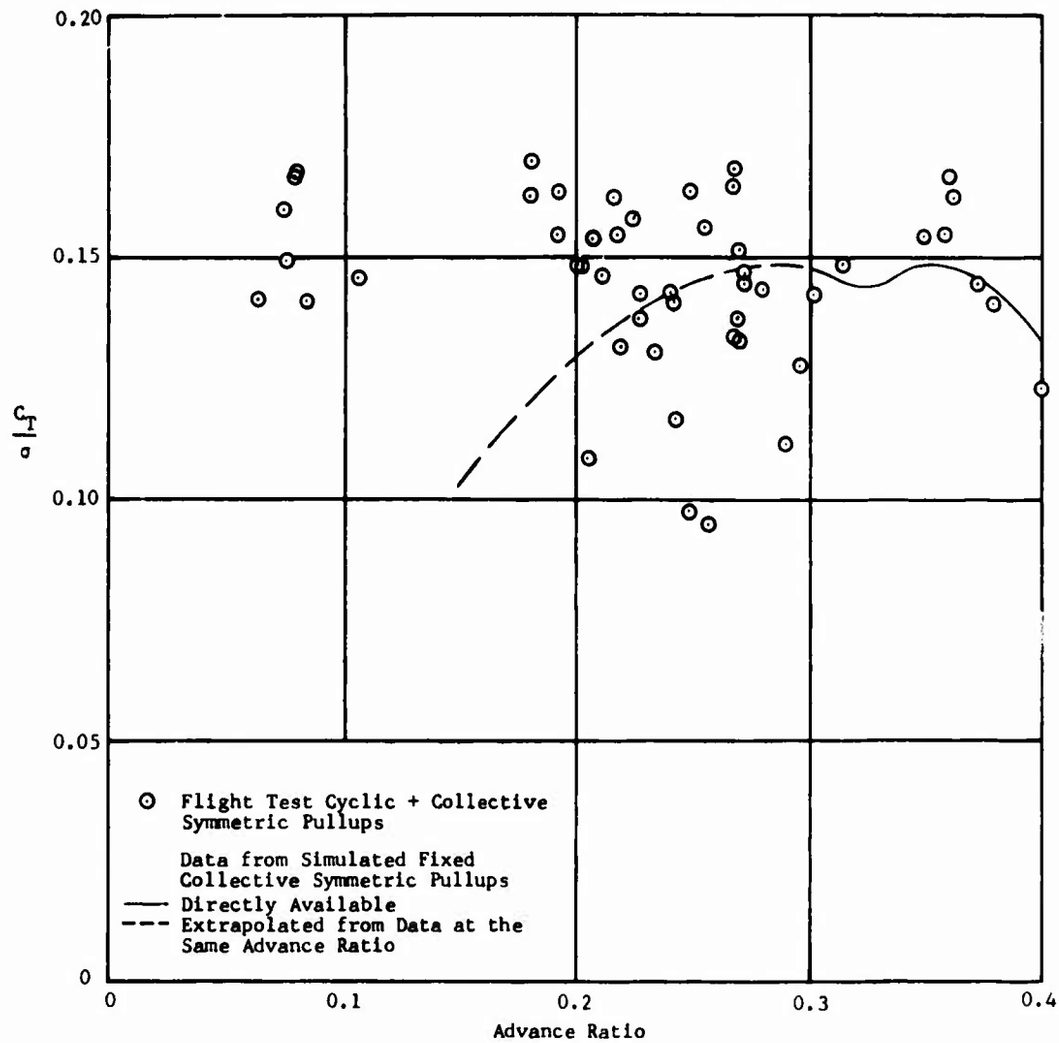

Figure 14. Maximum Continuous Engine Horsepower Line for Fixed Collective Symmetric Pullups, With Flight Test Maneuver Points.

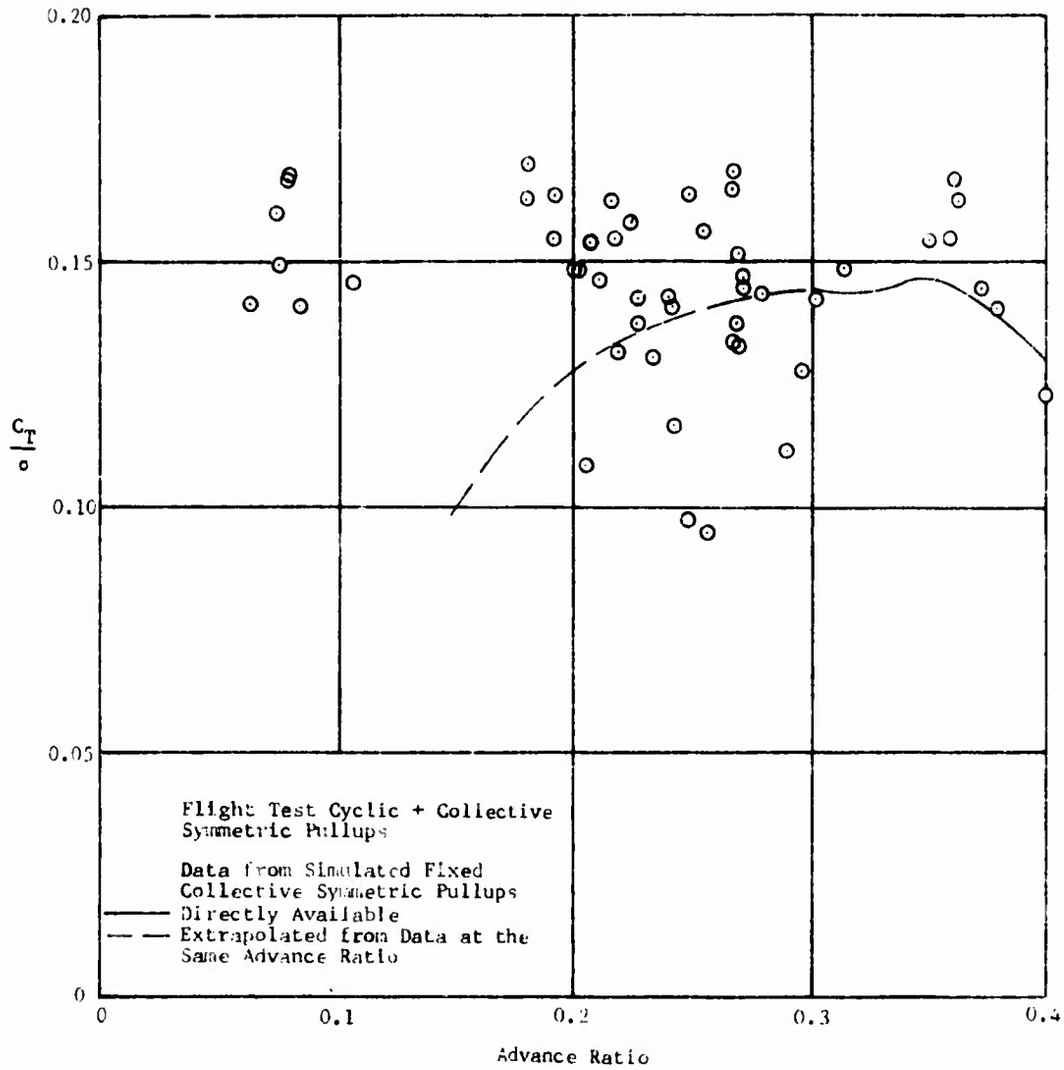

Figure 15. Steady Transmission Torque Rating Line for Fixed Collective Symmetric Pullups, With Flight Test Maneuver Points.

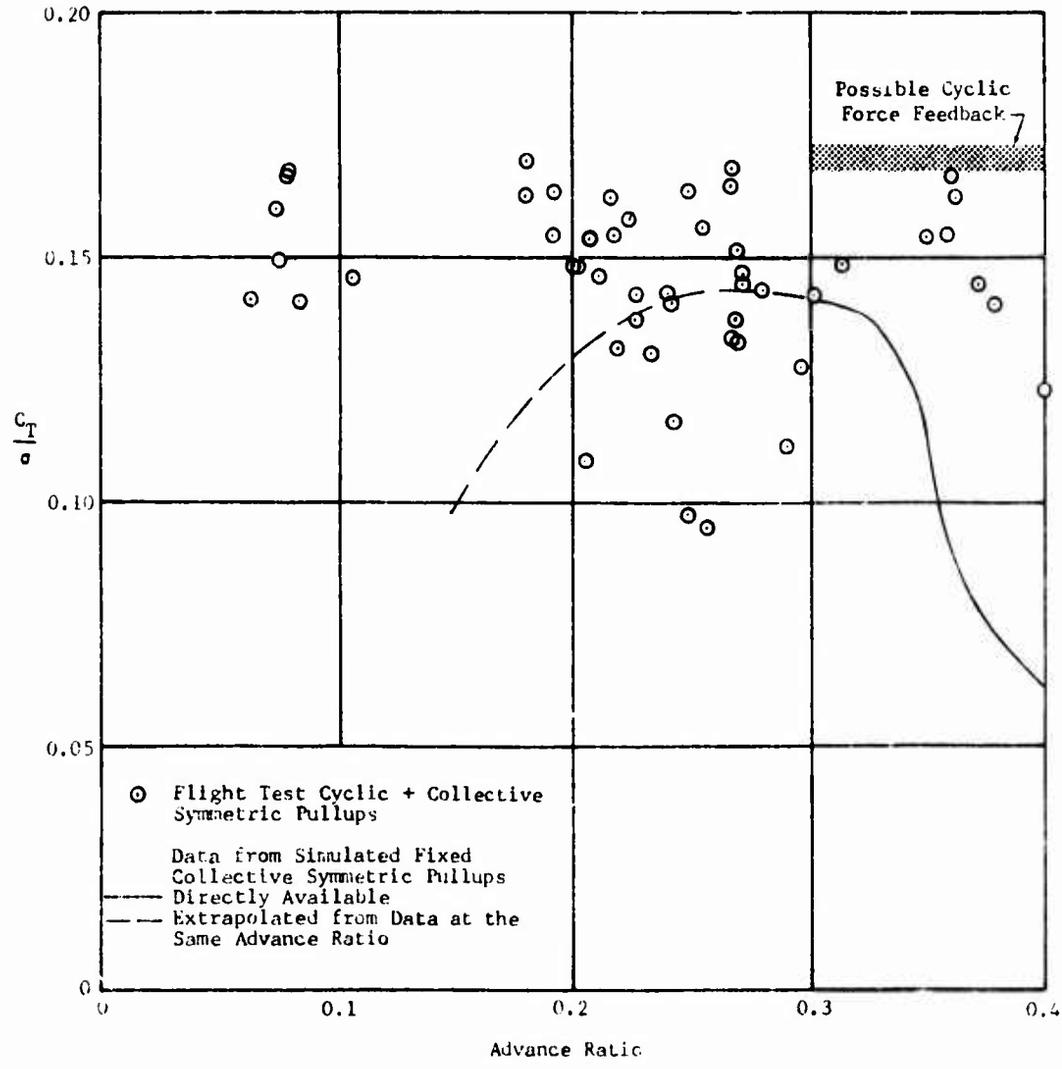

Figure 16. Rotating Swashplate 9806-Hour Fatigue Life Line for Fixed Collective Symmetric Pullups, With Flight Test Maneuver Points.

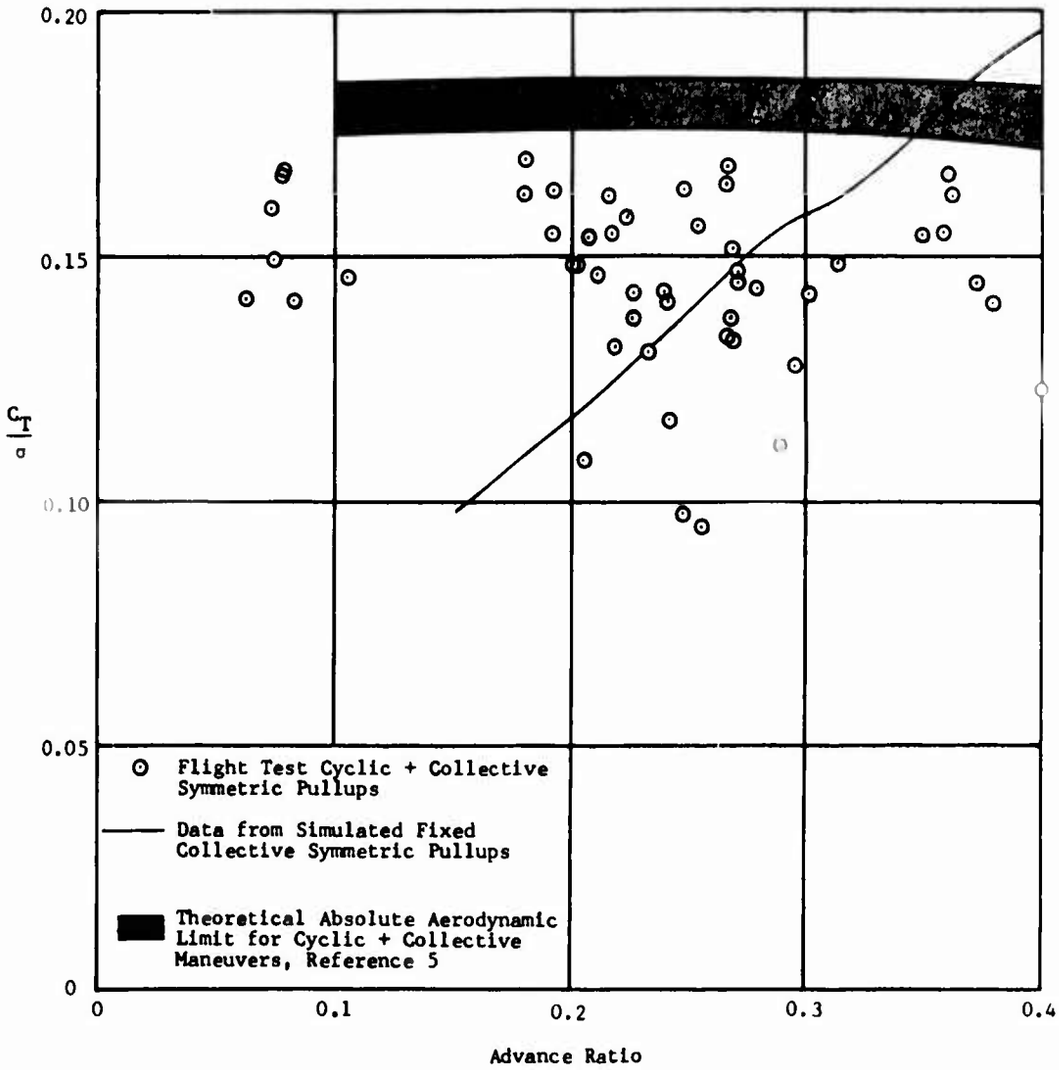

Figure 17. Absolute Aerodynamic Limit Line for Fixed Collective Symmetric Pullups, With Flight Test Maneuver Points.

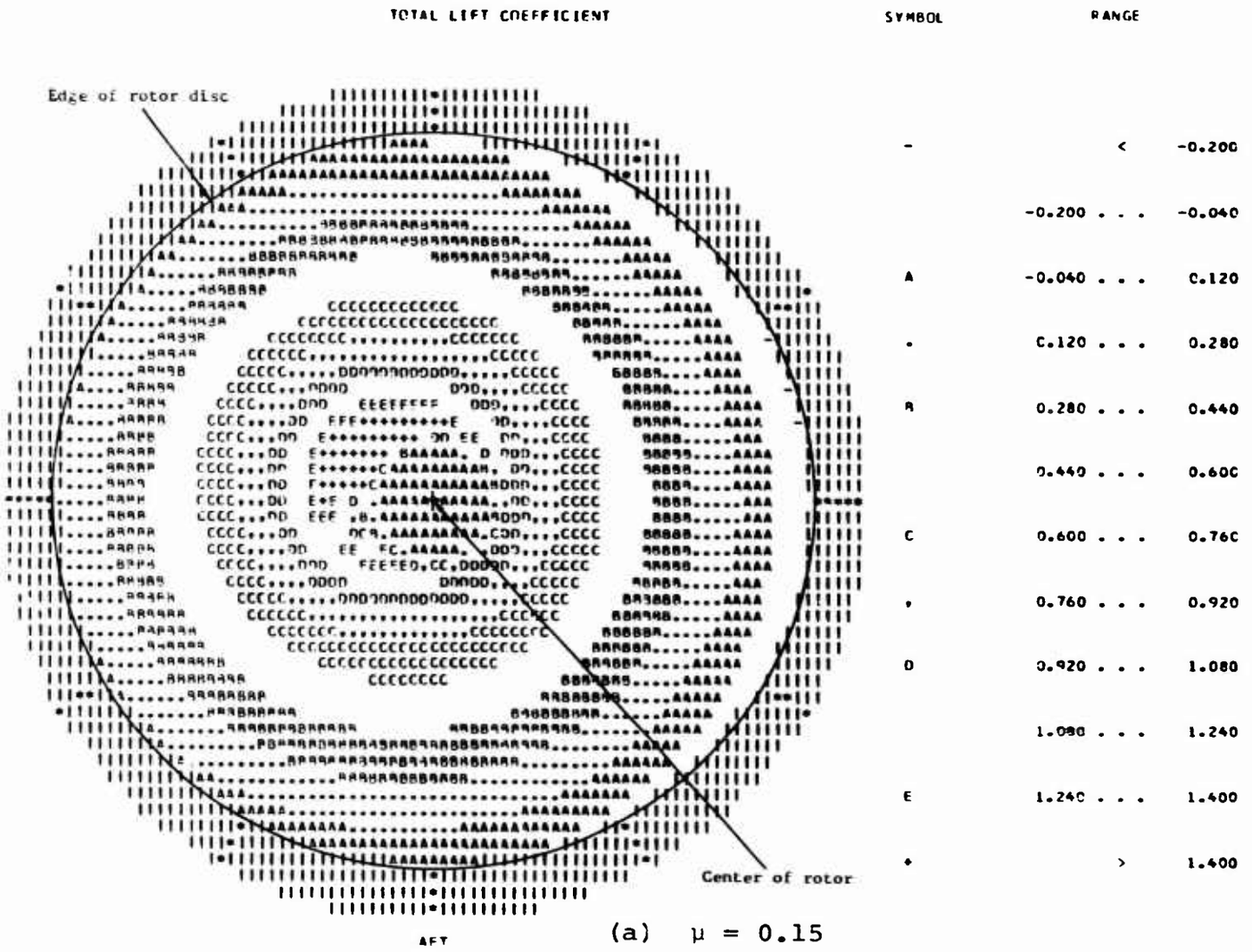

(a) $\mu = 0.15$

Figure 18. Total Lift Coefficient Contour Plots for Autorotational Entry Conditions.

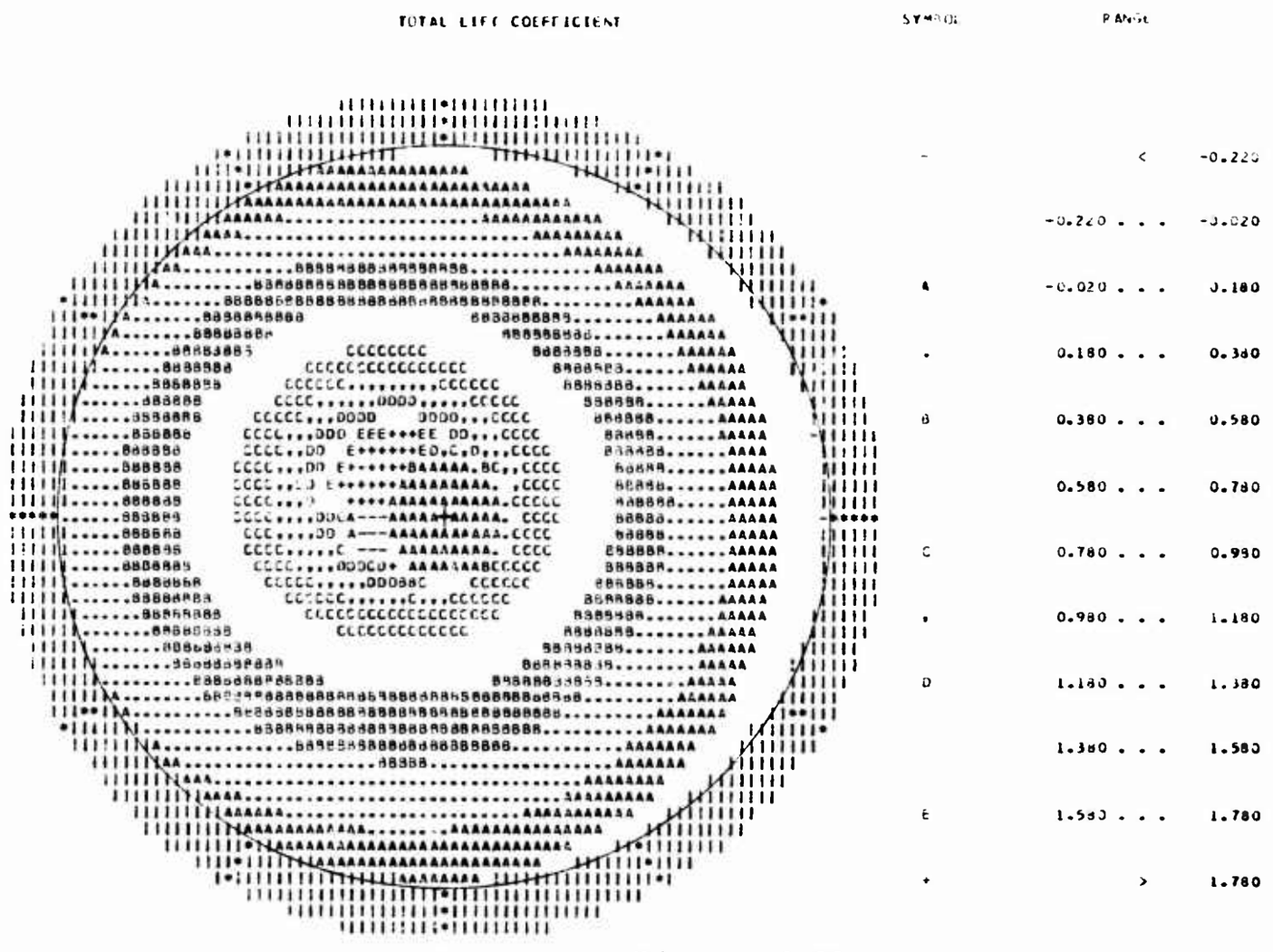

(b) $\mu = 0.20$

Figure 18. Continued.

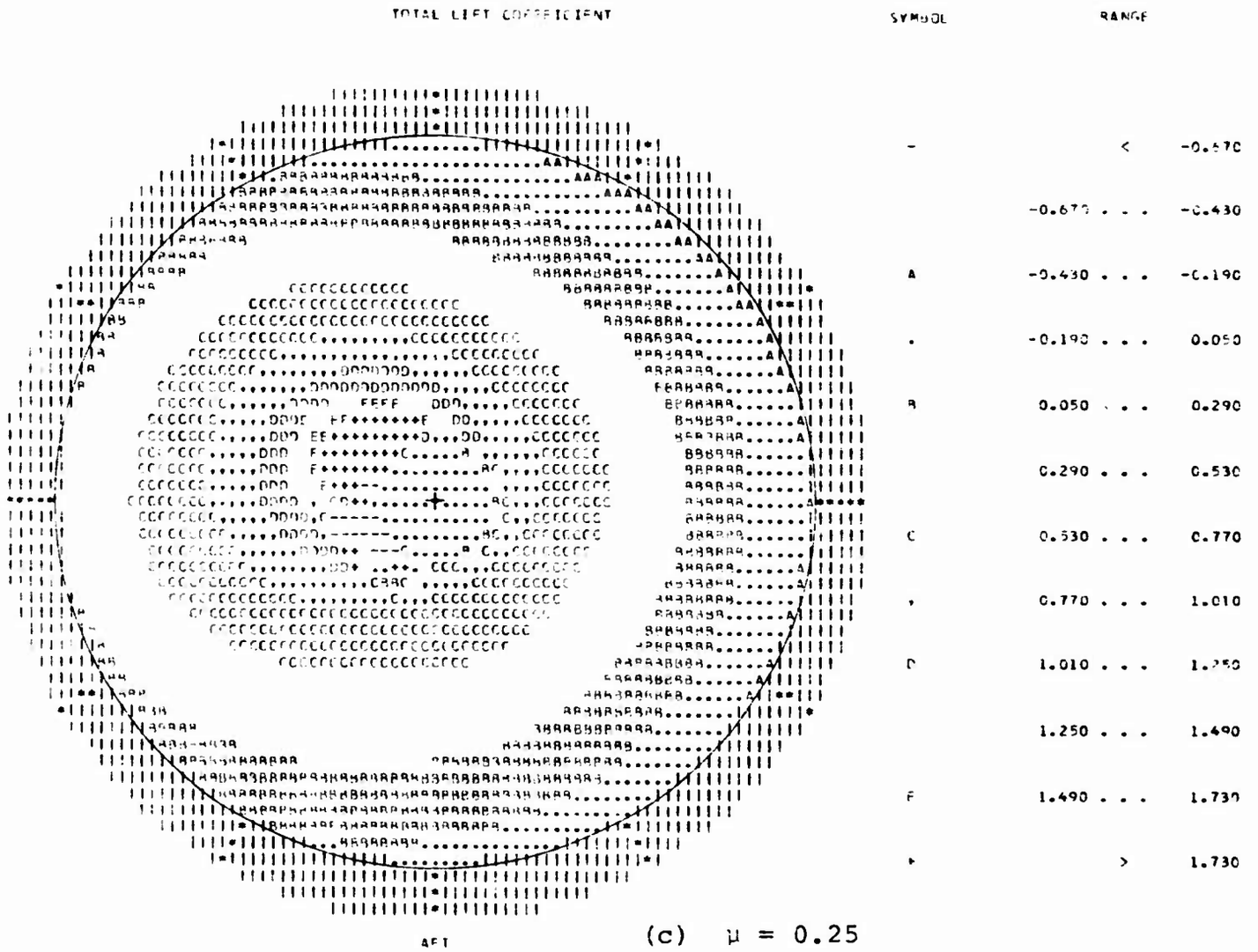

(c) $\mu = 0.25$

Figure 19. Concluded.

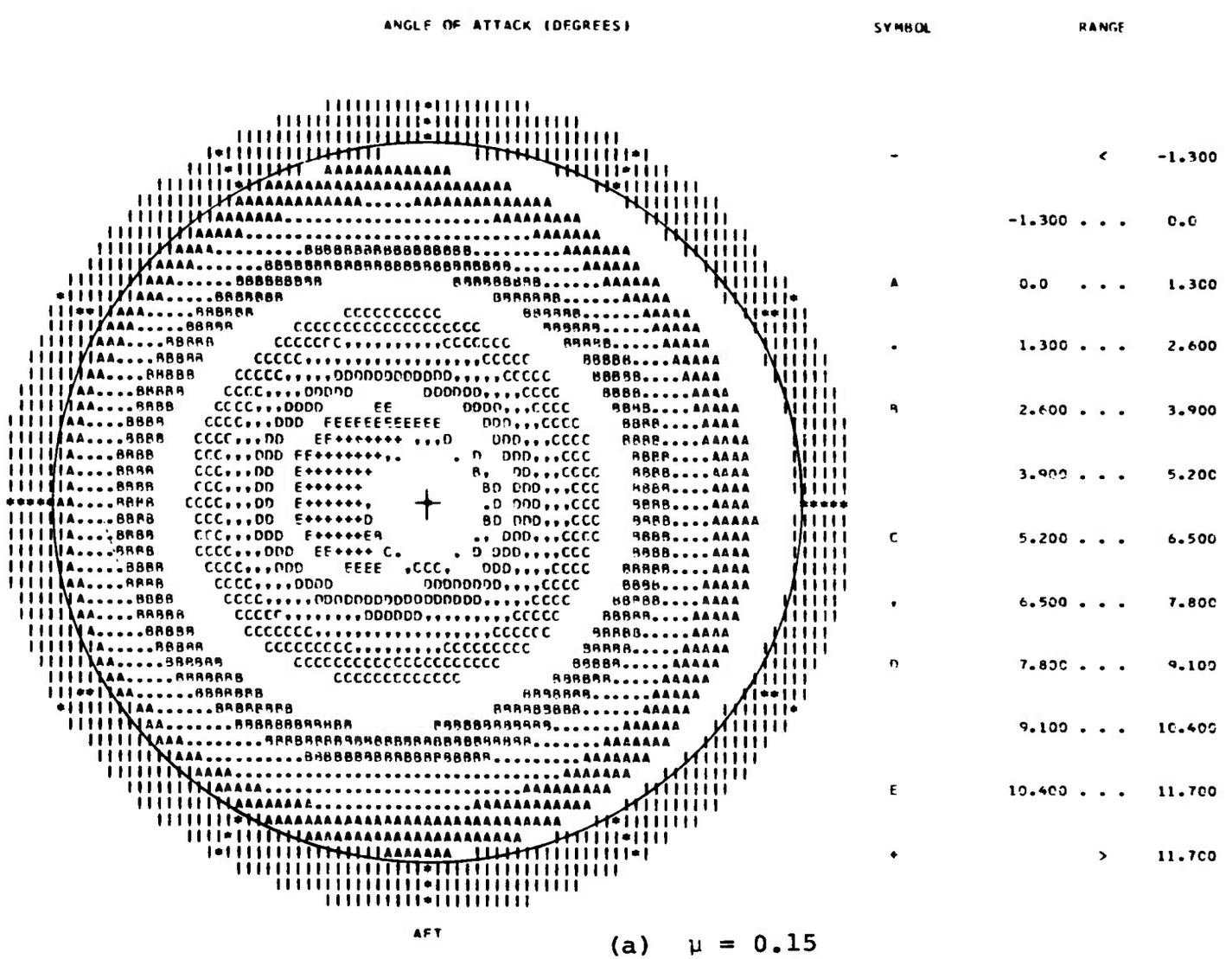

(a) $\mu = 0.15$

Figure 19. Angle-of-Attack Contour Plots for Autorotational Entry Conditions.

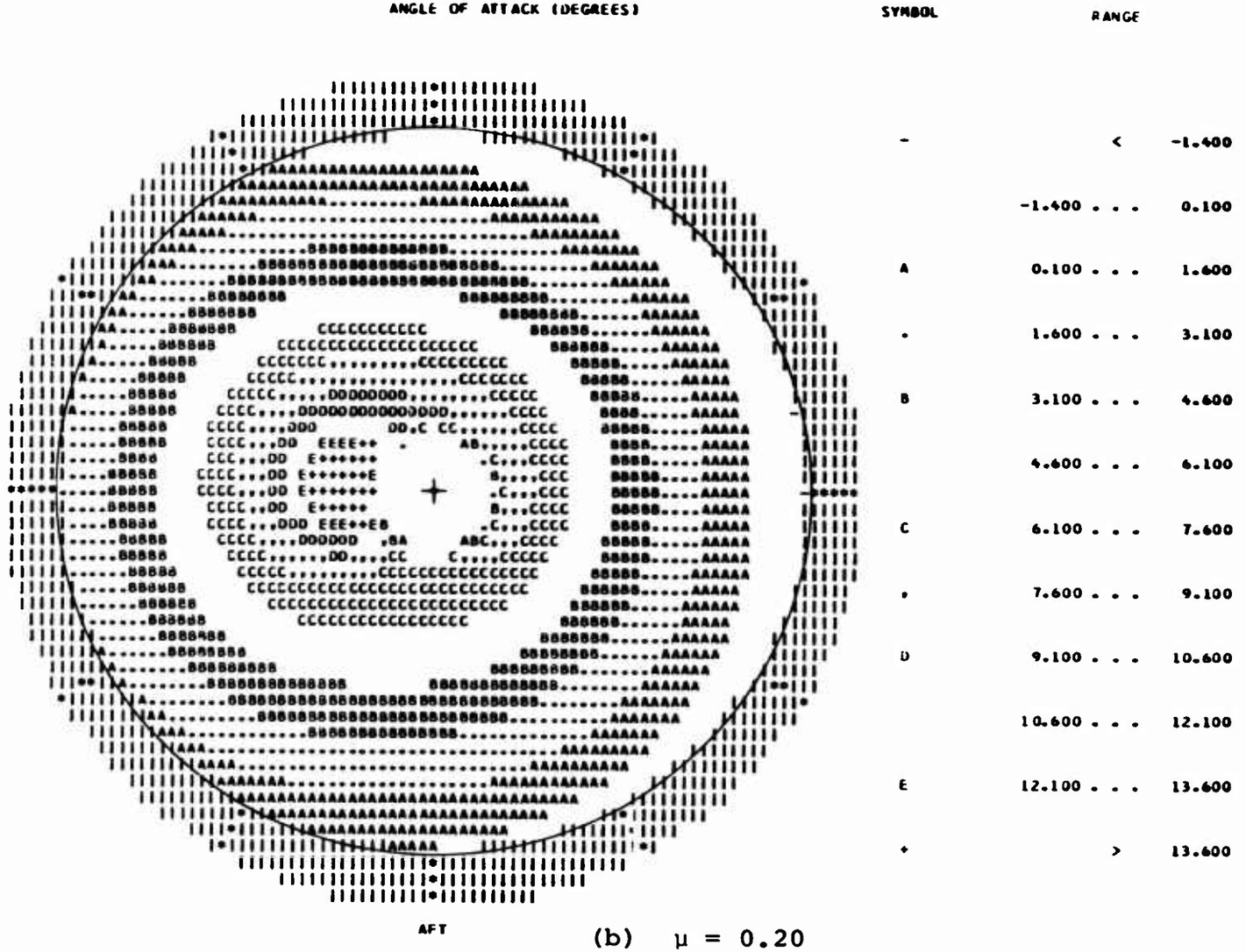

(b) $\mu = 0.20$

Figure 19. Continued.

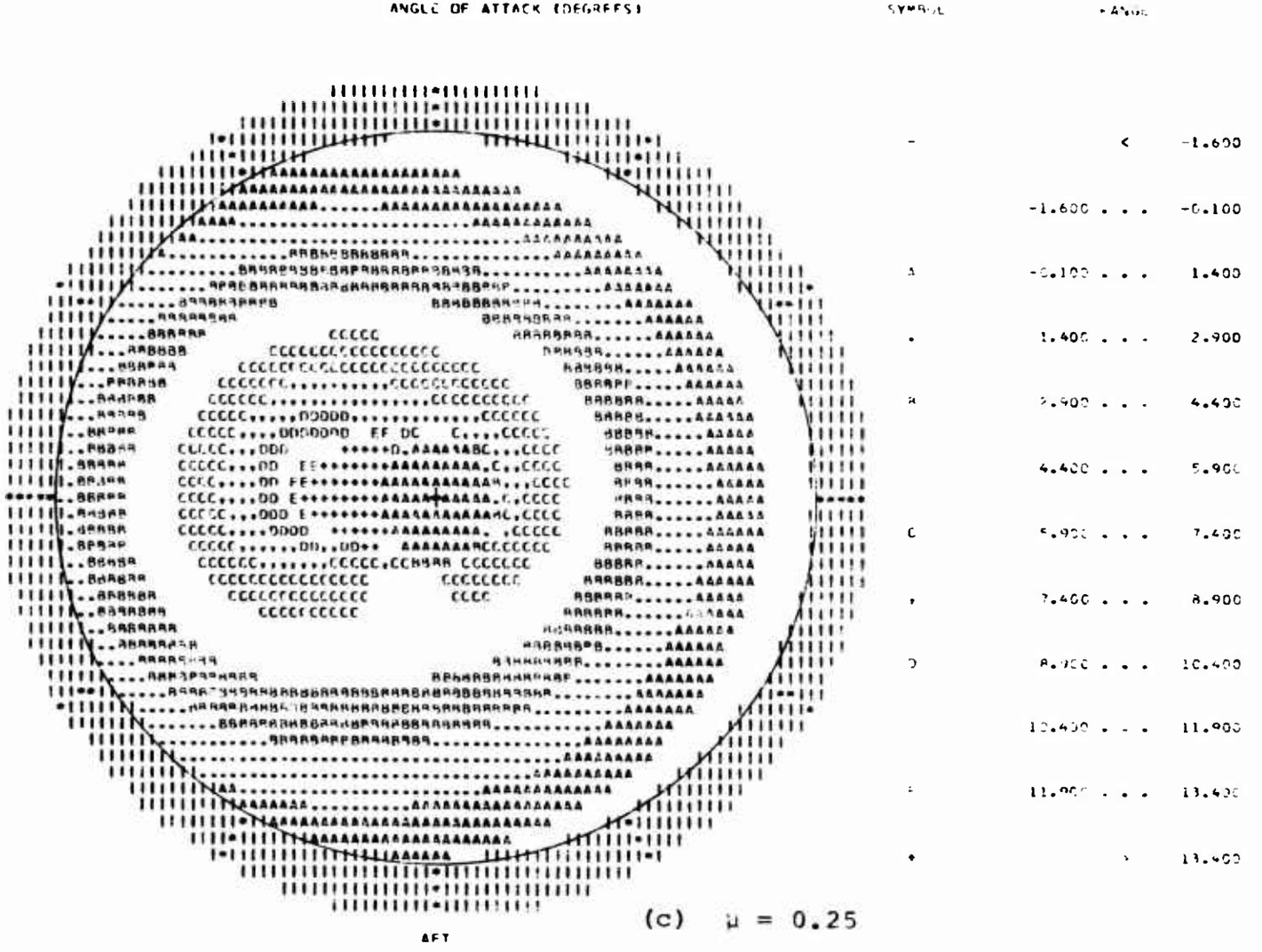

Figure 19. Concluded.

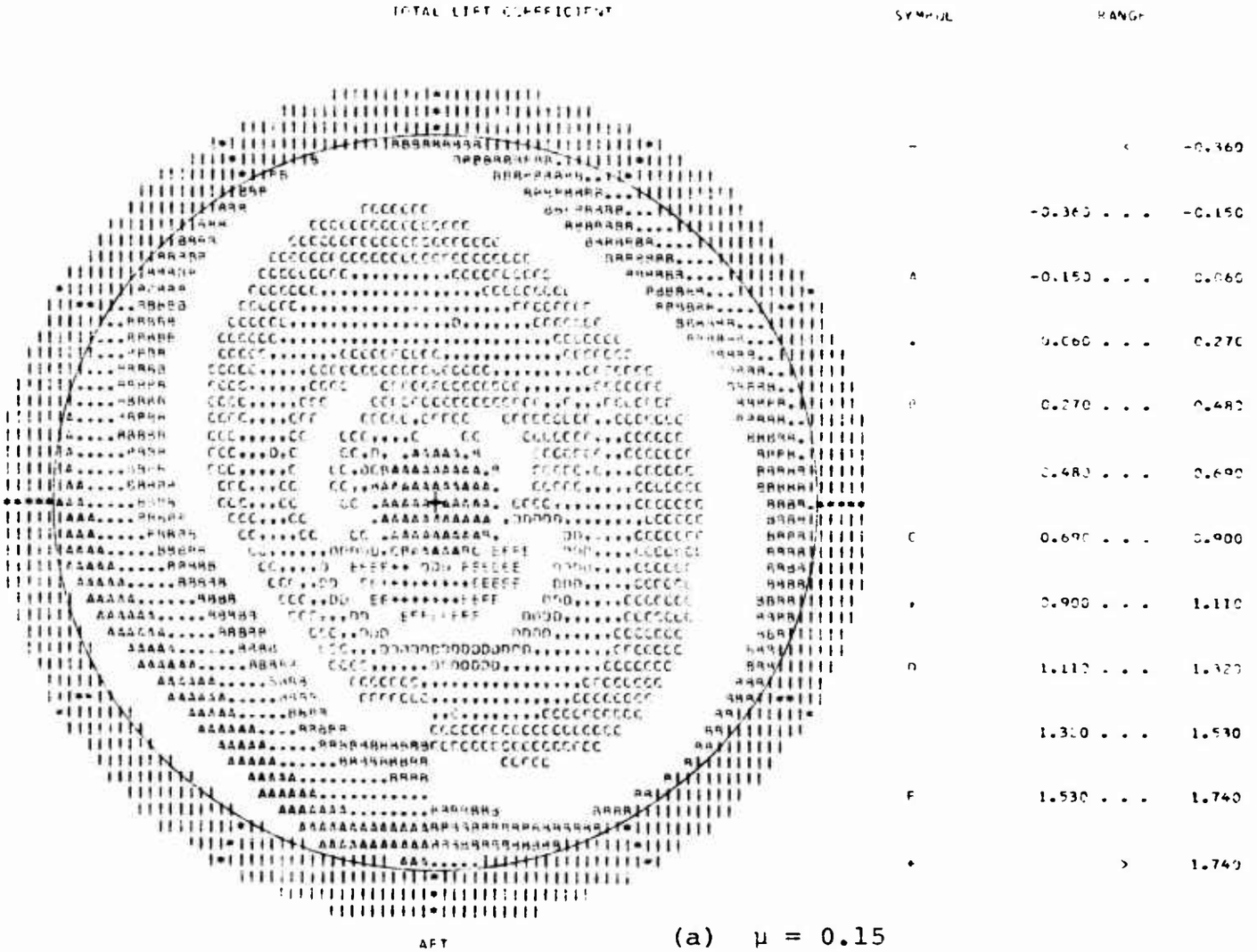

(a) $\mu = 0.15$

Figure 20. Total Lift Coefficient Contour Plots at the Time of Maximum Mean Normal Load Factor for the Autorotational Pullups.

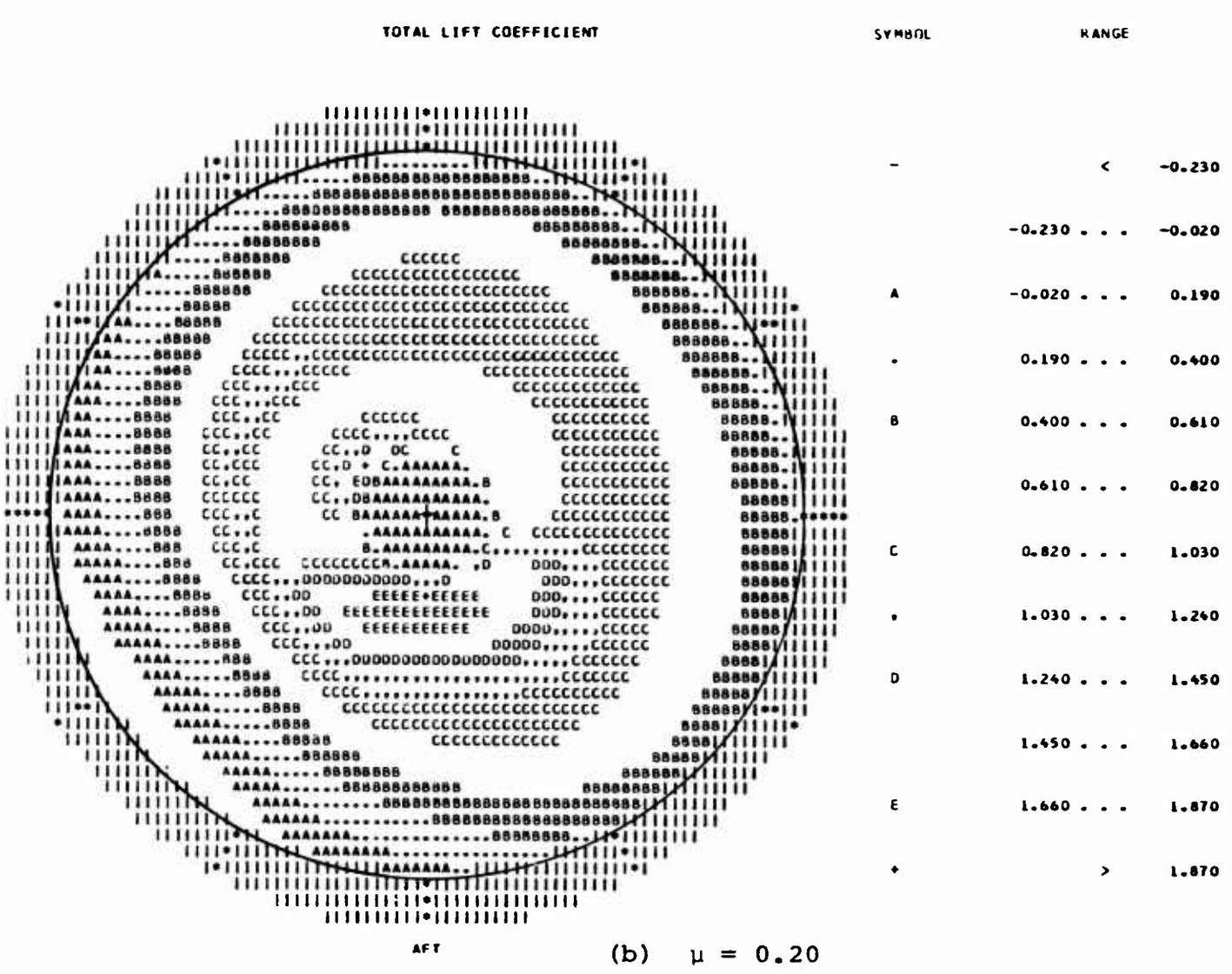

(b) $\mu = 0.20$

Figure 20. Continued.

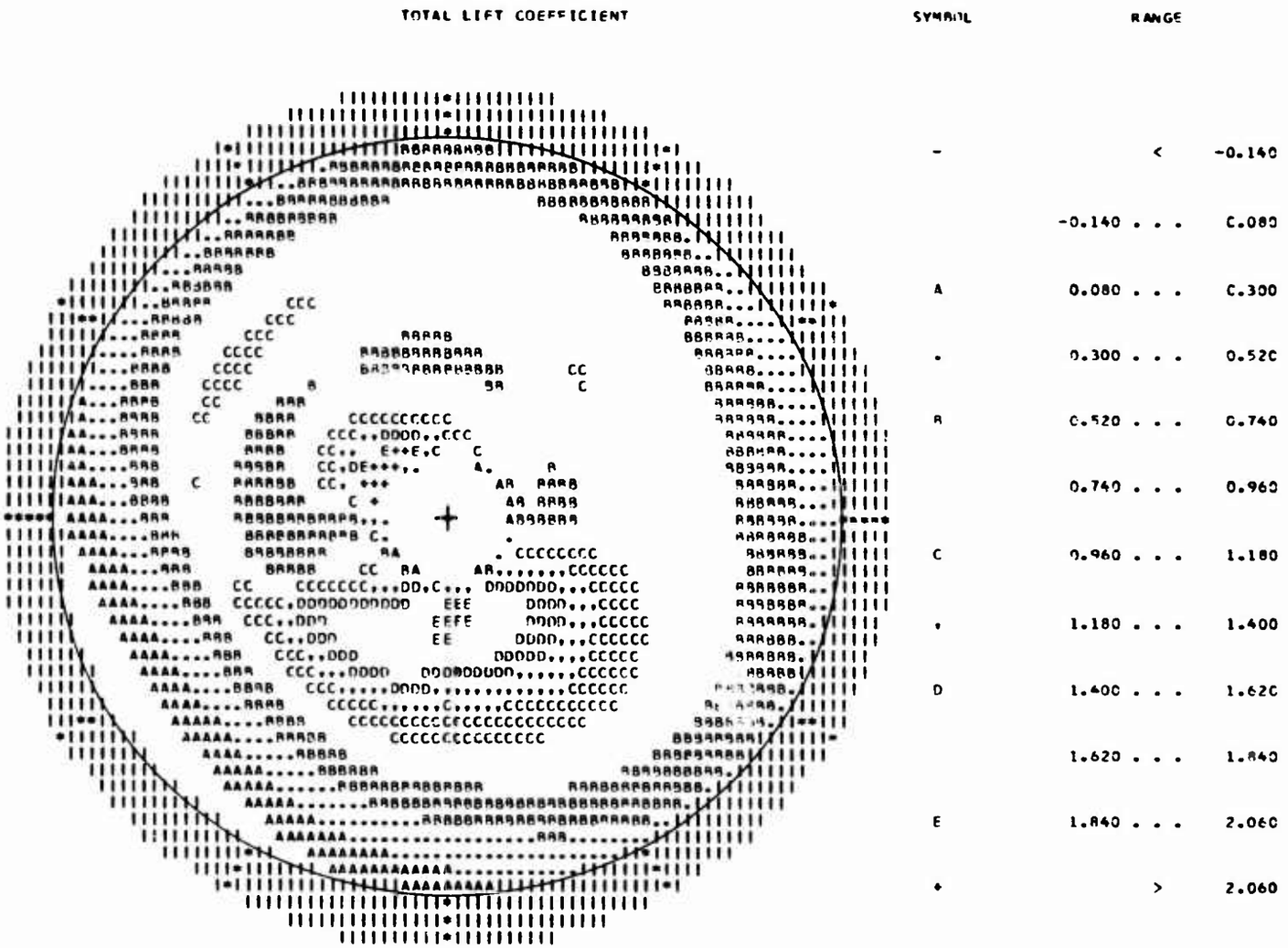

(c) $\mu = 0.25$

Figure 20. Concluded.

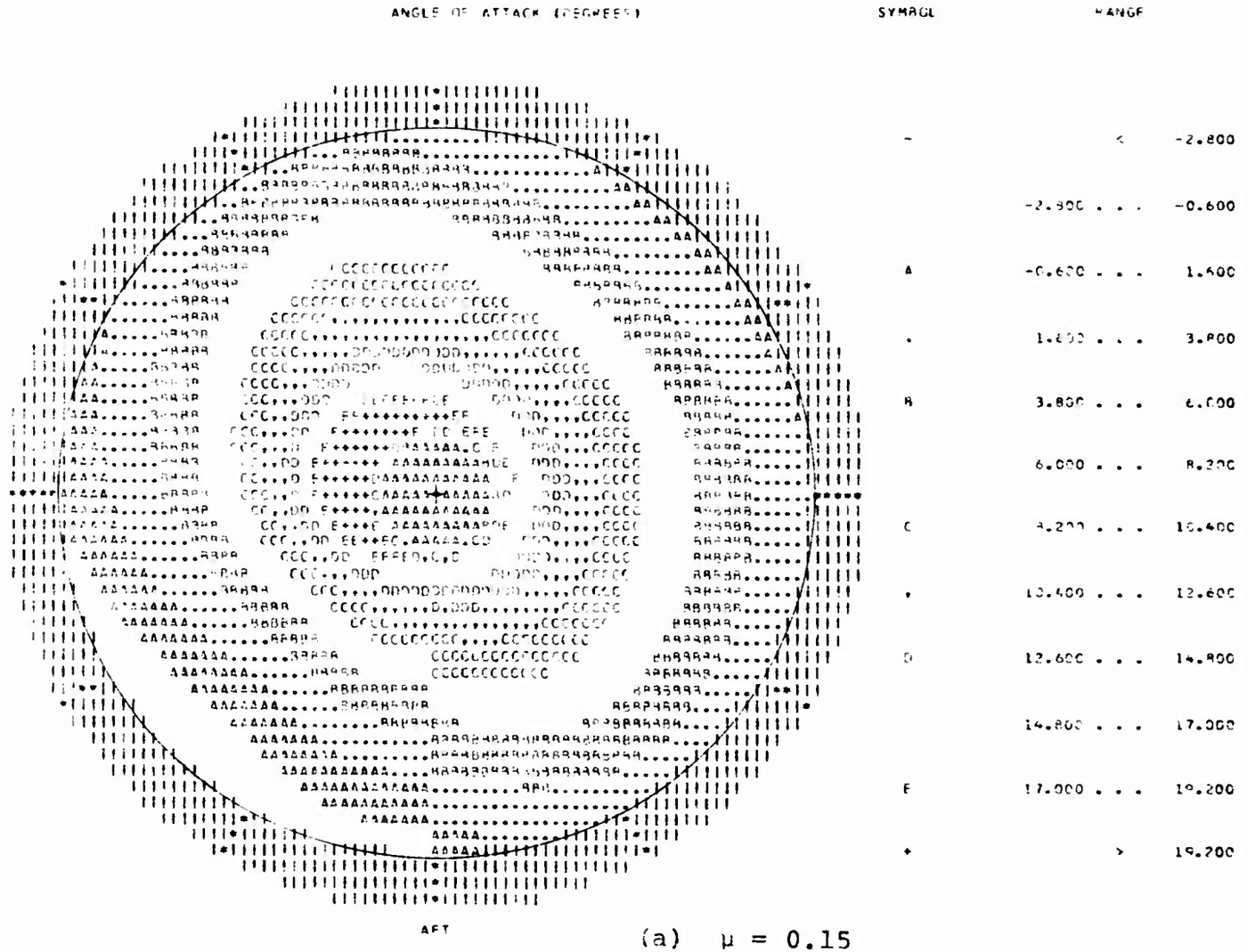

(a) $\mu = 0.15$

Figure 21. Angle-of-Attack Contour Plots at the Time of Maximum Mean Normal Load Factor for the Autorotational Pullups.

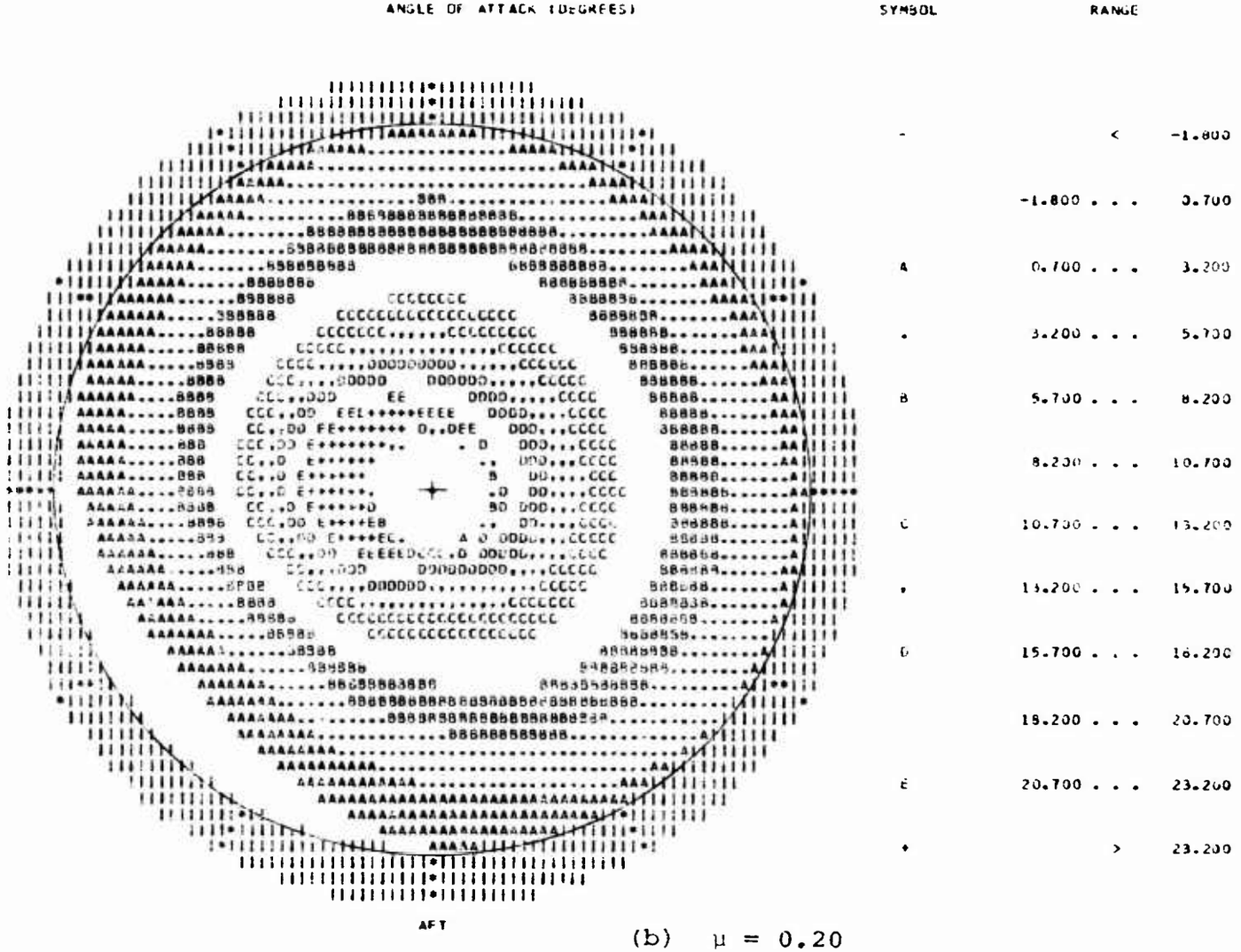

(b) $\mu = 0.20$

Figure 21. Continued.

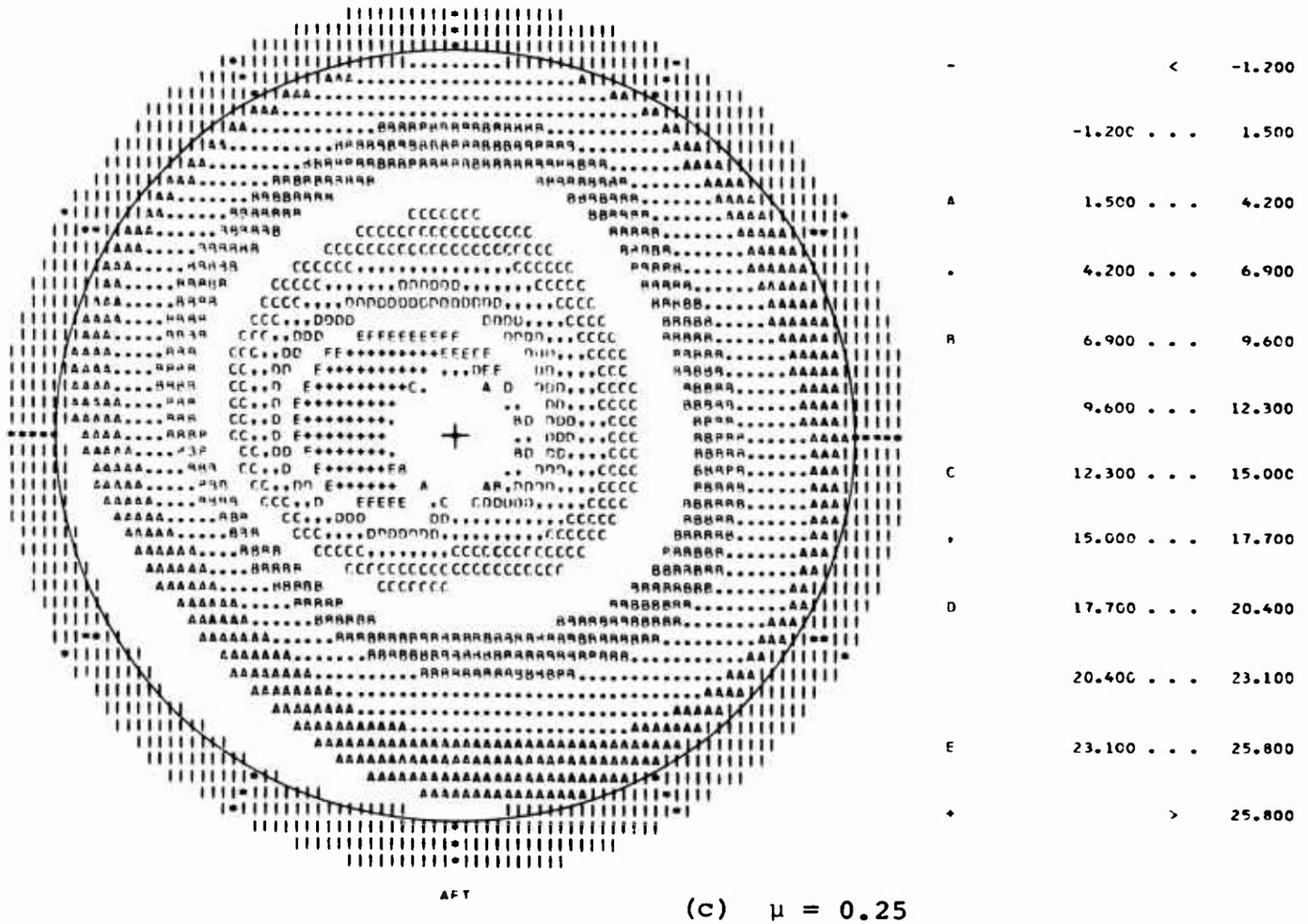

(c) $\mu = 0.25$

Figure 21. Concluded.

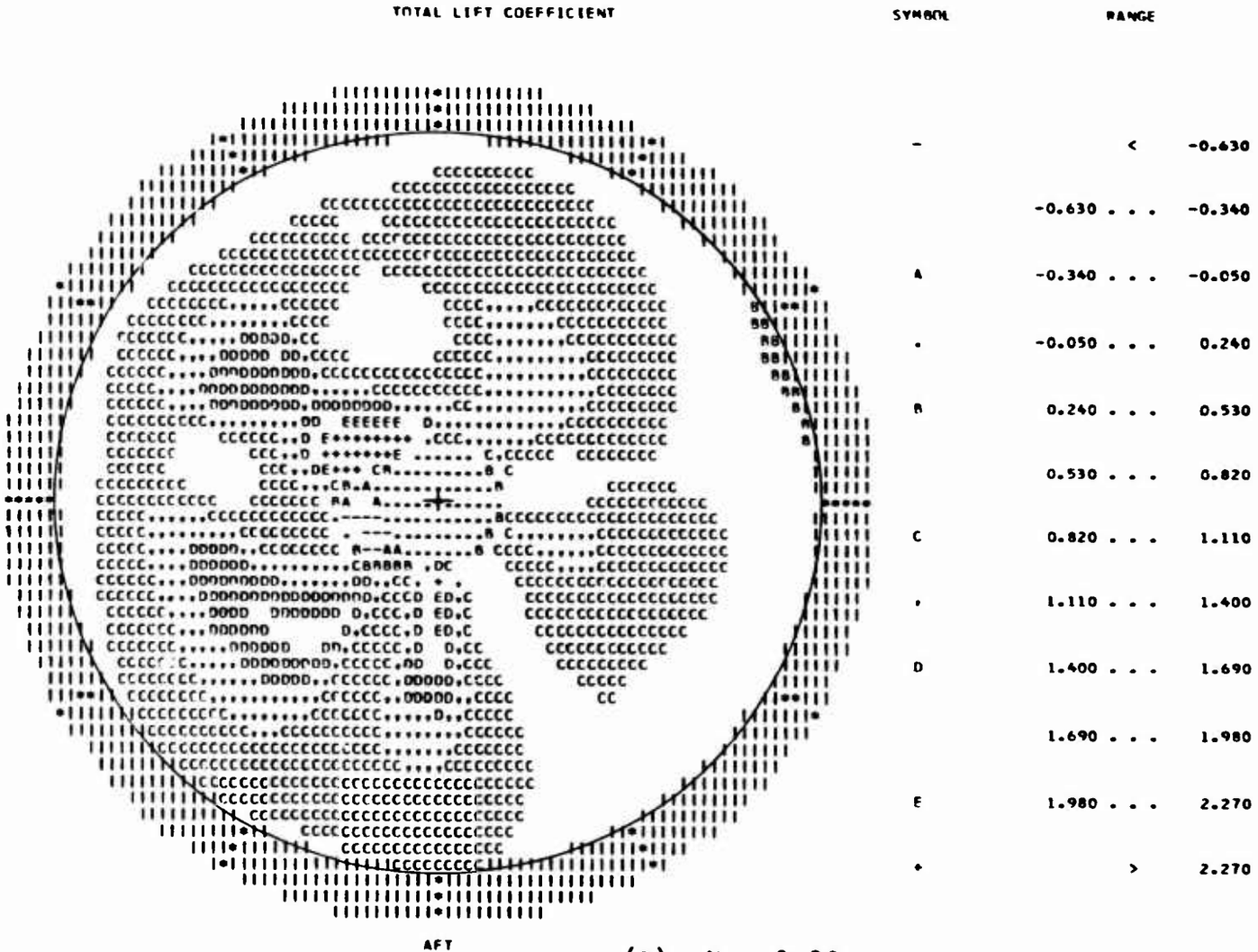

(a) $\mu = 0.30$

Figure 22. Total Lift Coefficient Contour Plots at the Time of Maximum Mean Normal Load Factor for the Power-On Pullups.

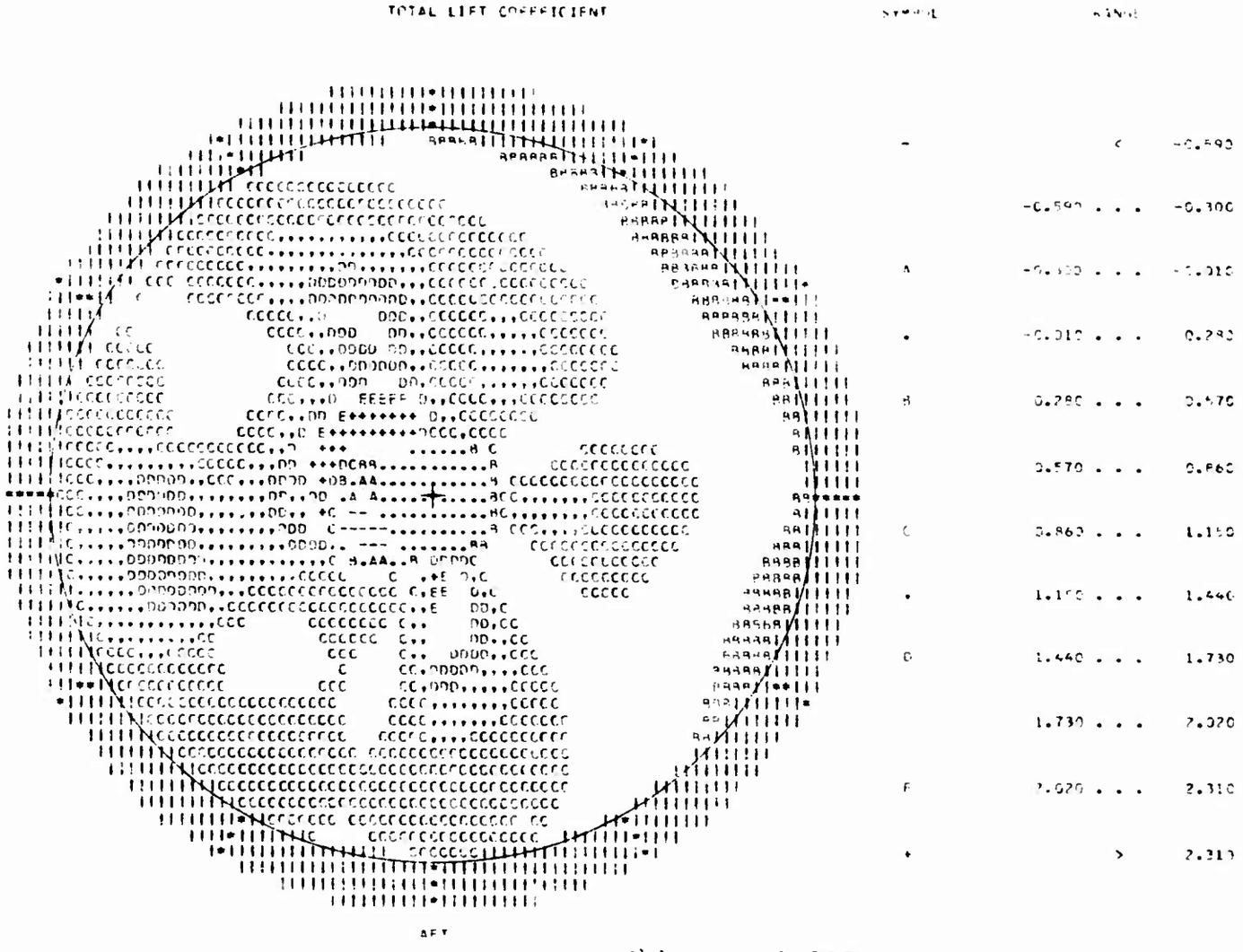

(b) $\mu = 0.325$

Figure 22. Continued.

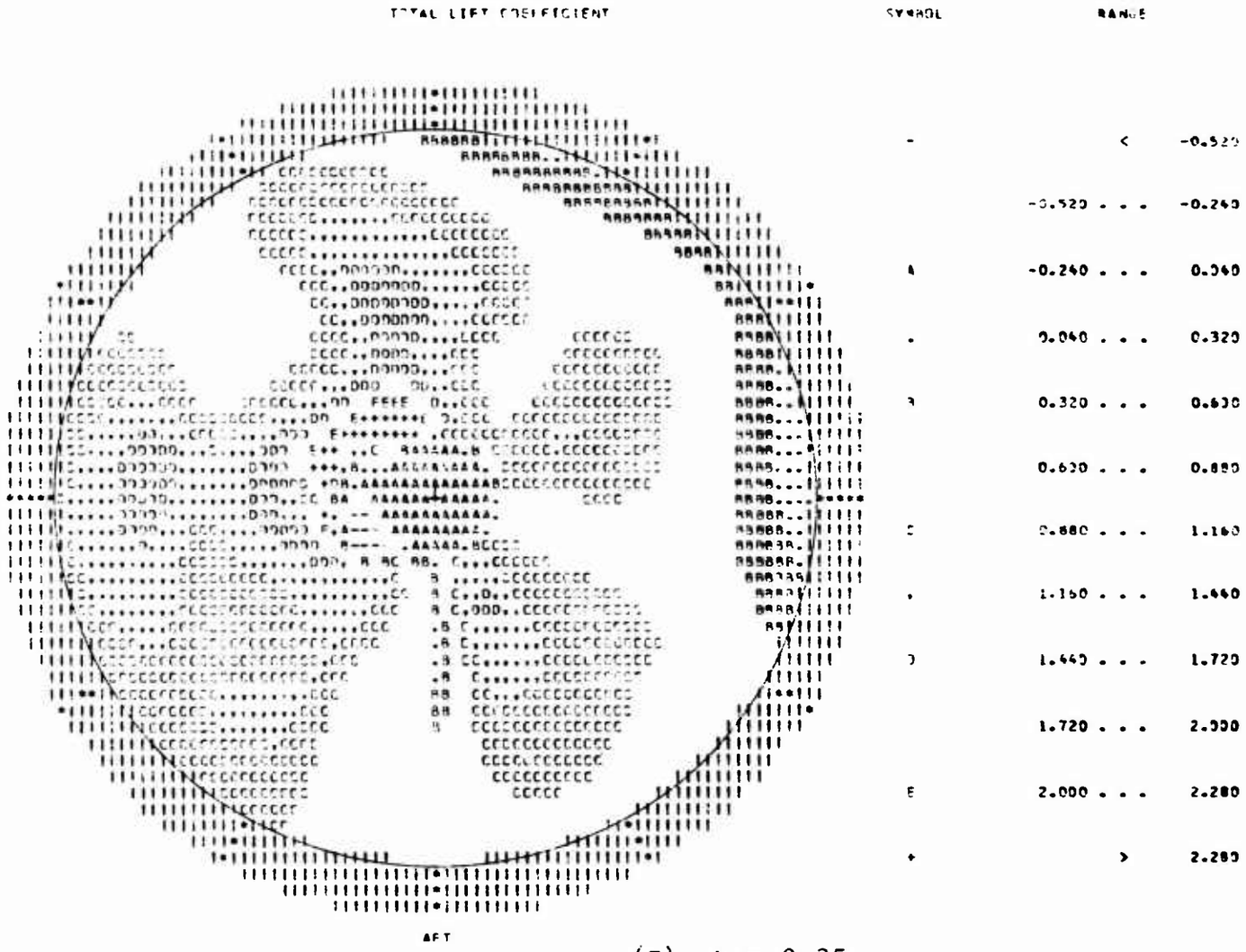

(c) $\mu = 0.35$

Figure 22. Continued.

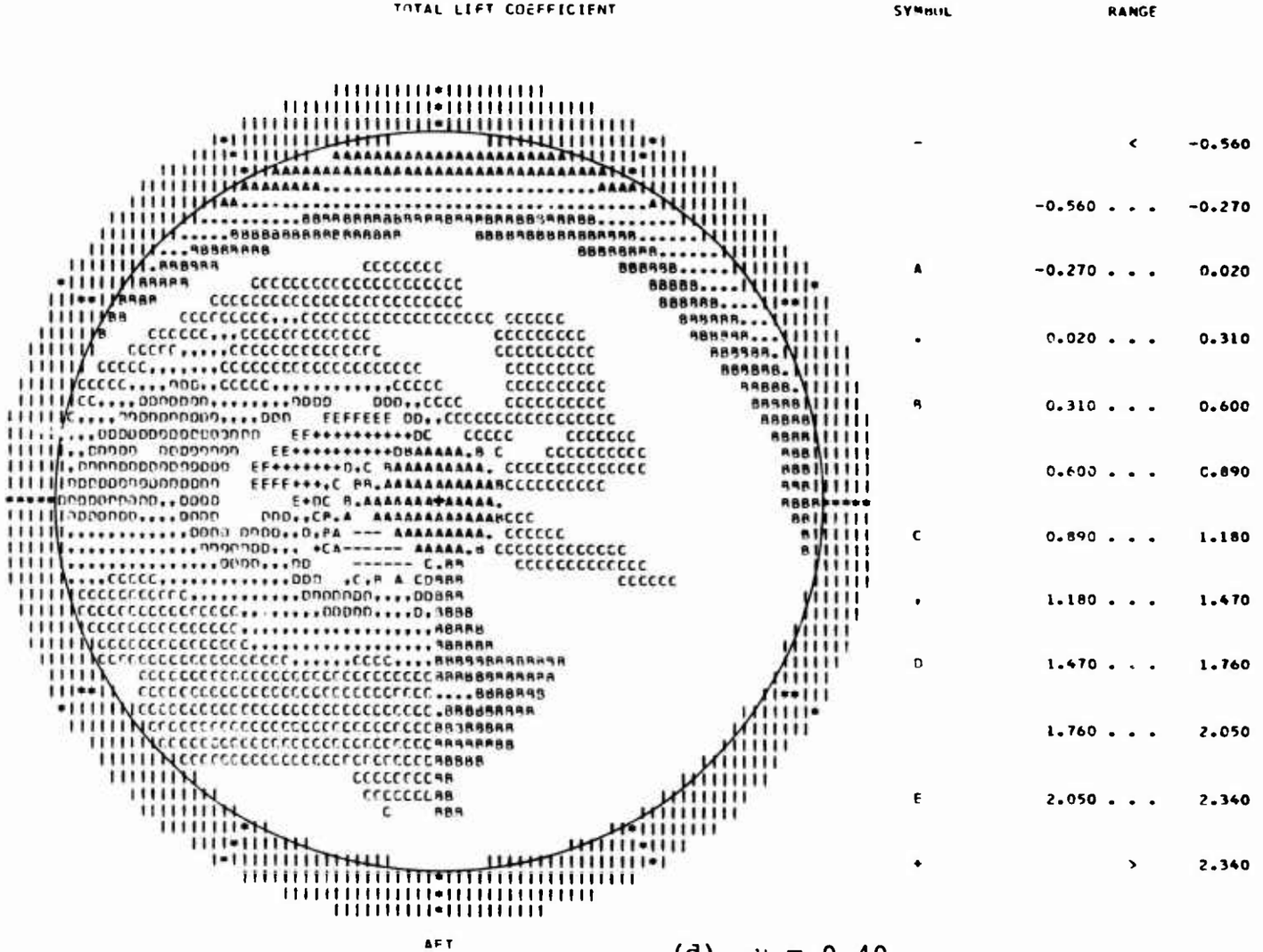

(d) $\mu = 0.40$

Figure 22. Concluded.

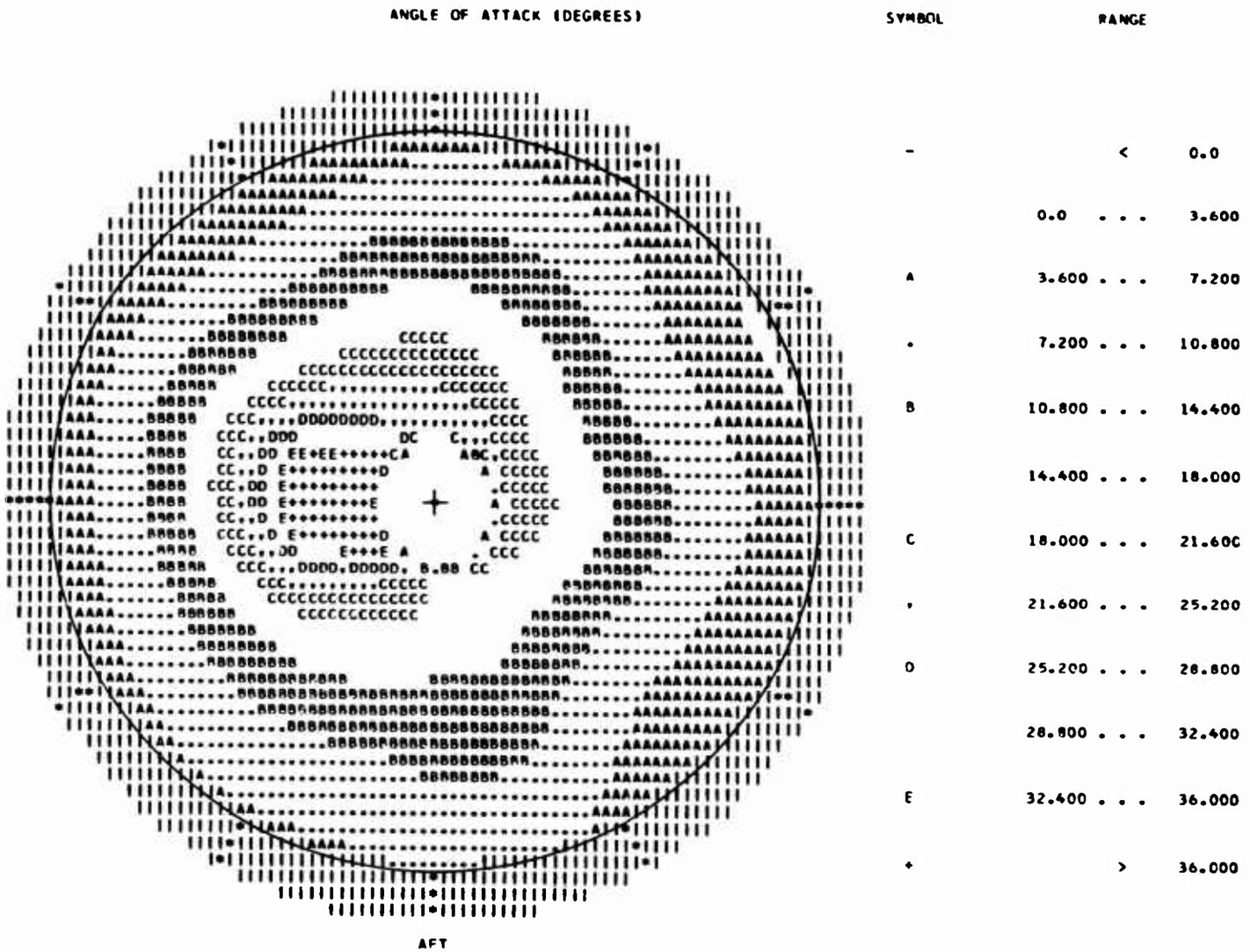

(a) $\mu = 0.30$

Figure 23. Angle-of-Attack Contour Plots at the time of Maximum Mean Normal Load Factor for the Power-On Pullups.

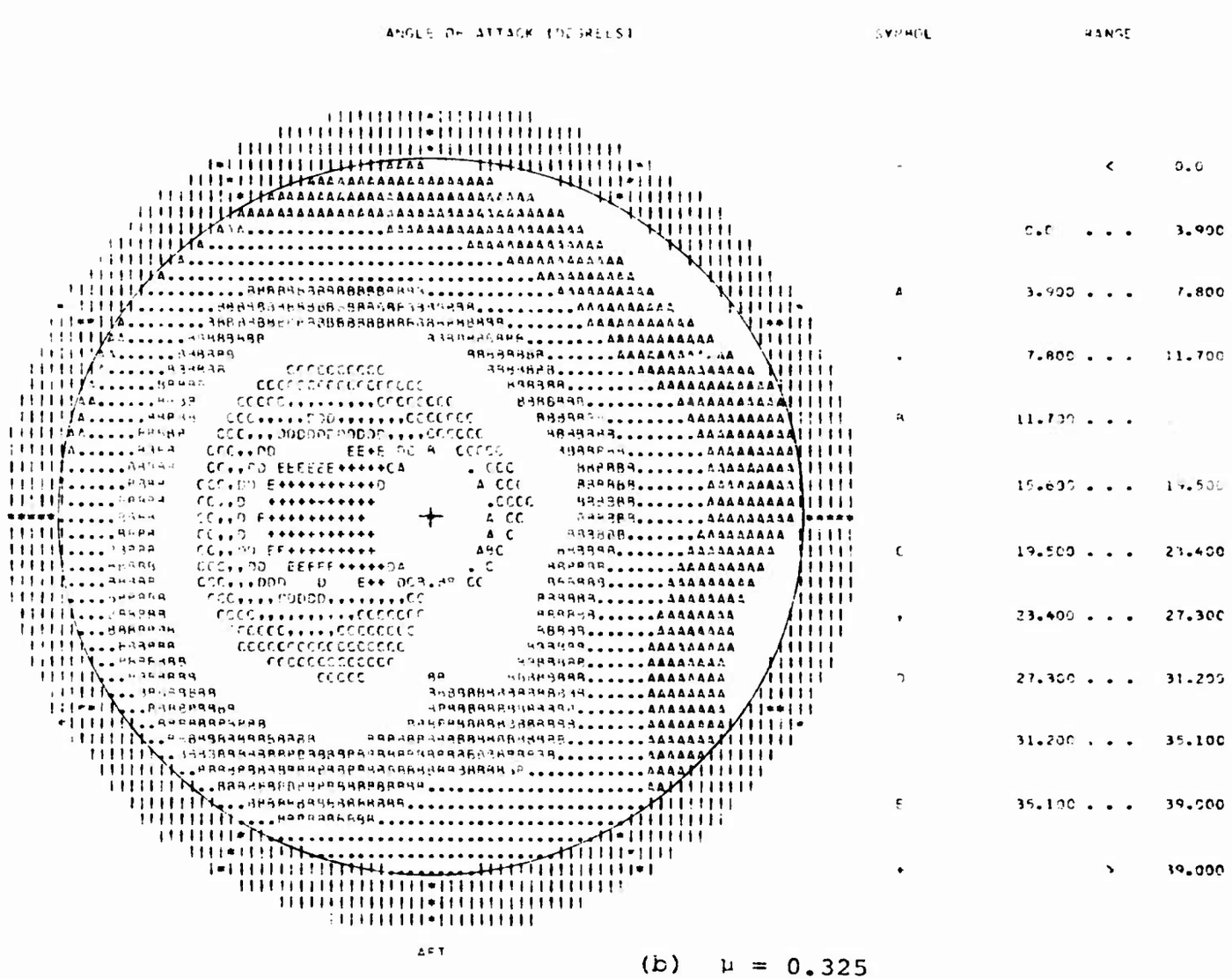

(b) $\mu = 0.325$

Figure 23. Continued.

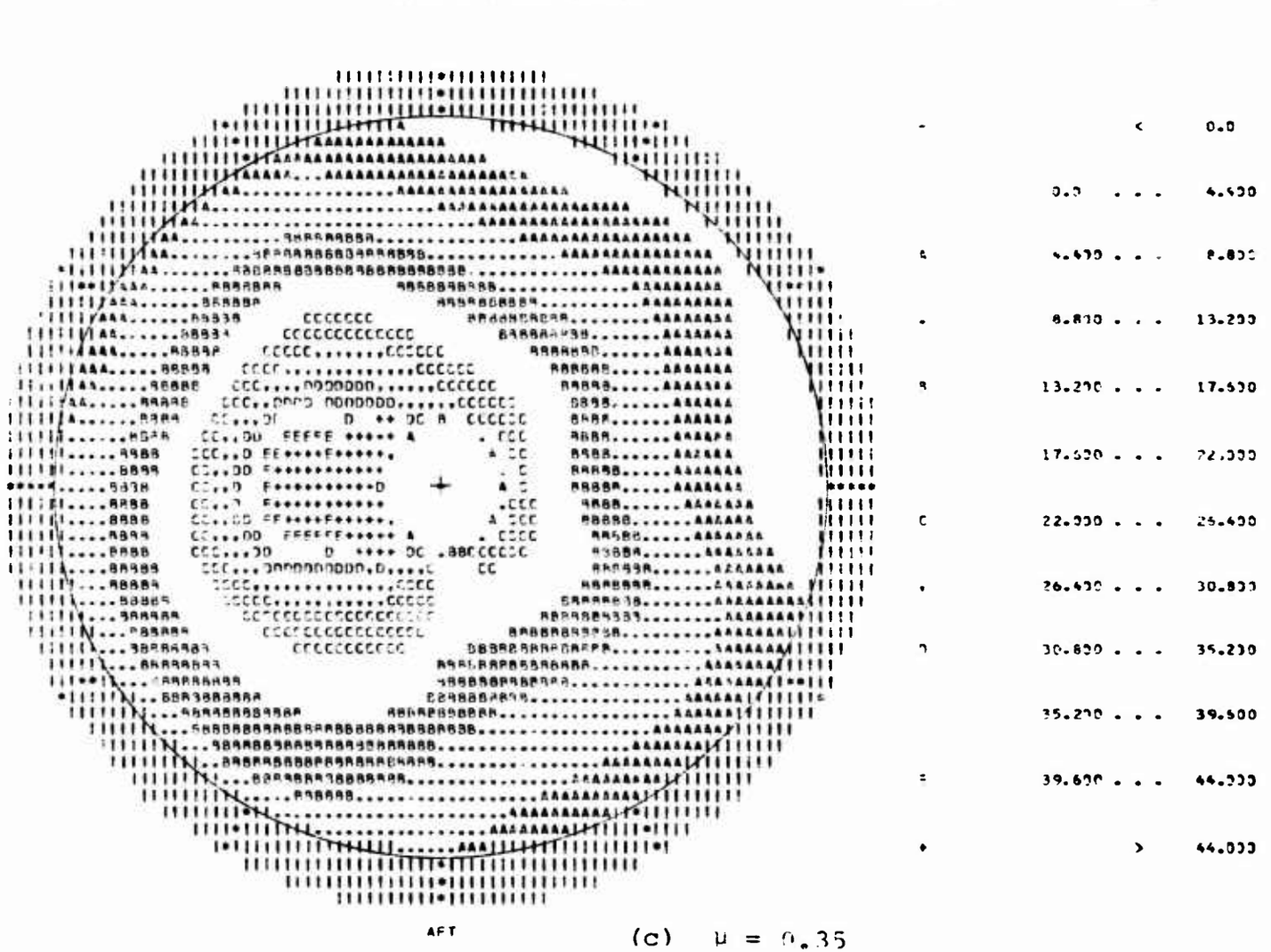

(c) $\mu = 0.35$

Figure 23. Continued.

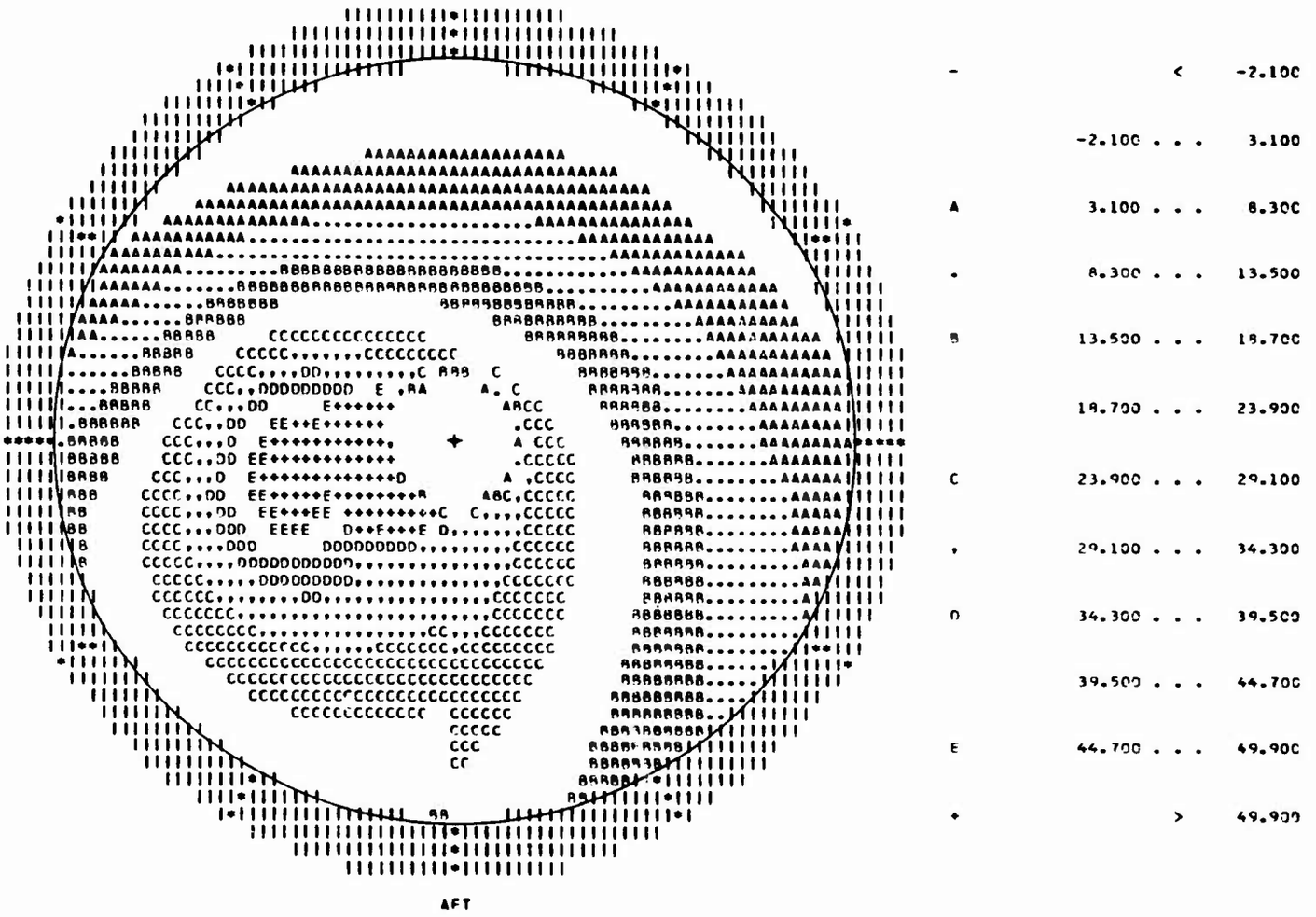

(d) $\mu = 0.40$

Figure 23. Concluded.

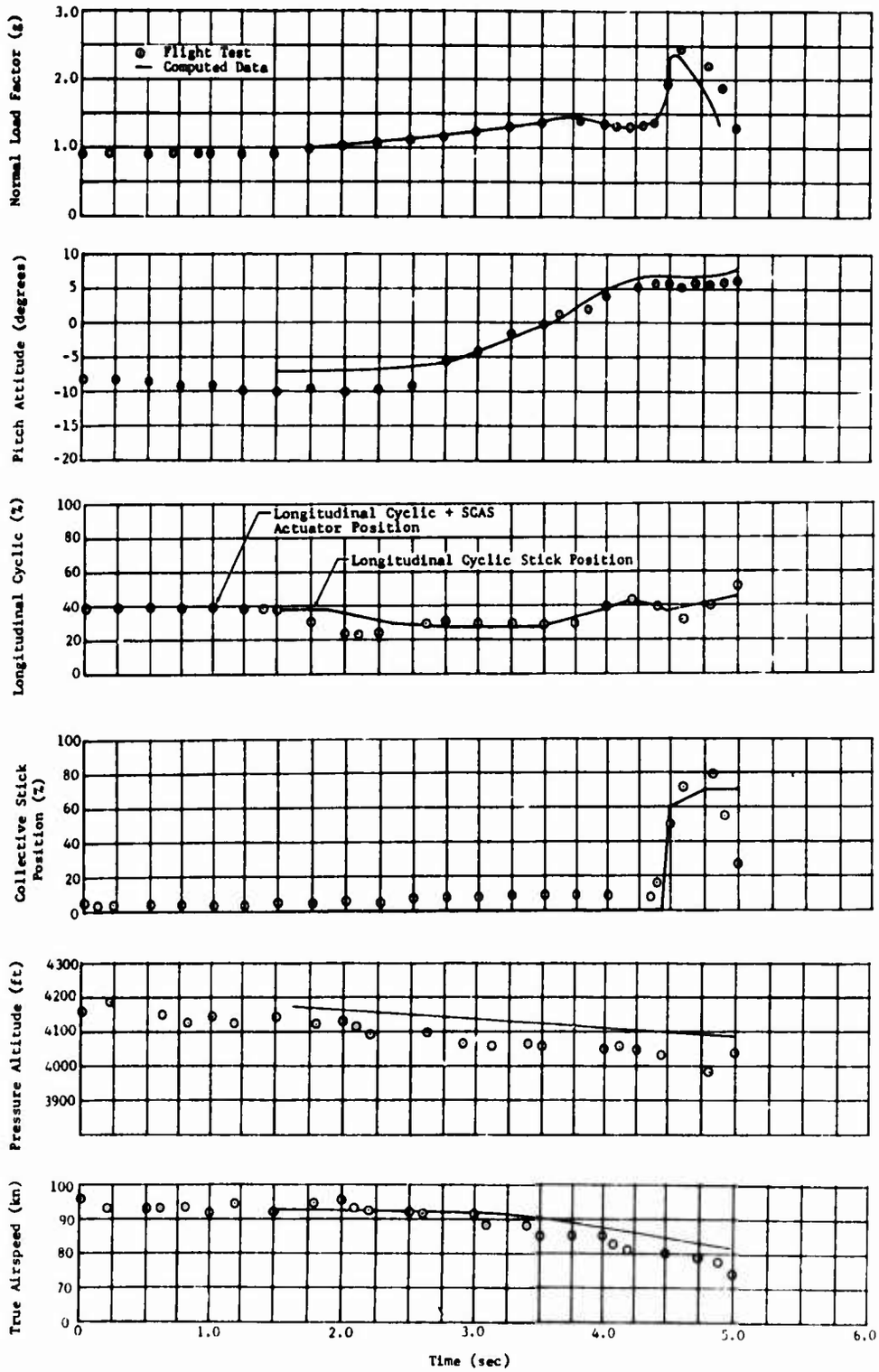

Figure 24. Time Histories of Symmetric Pullup From Autorotation, Counter 775.

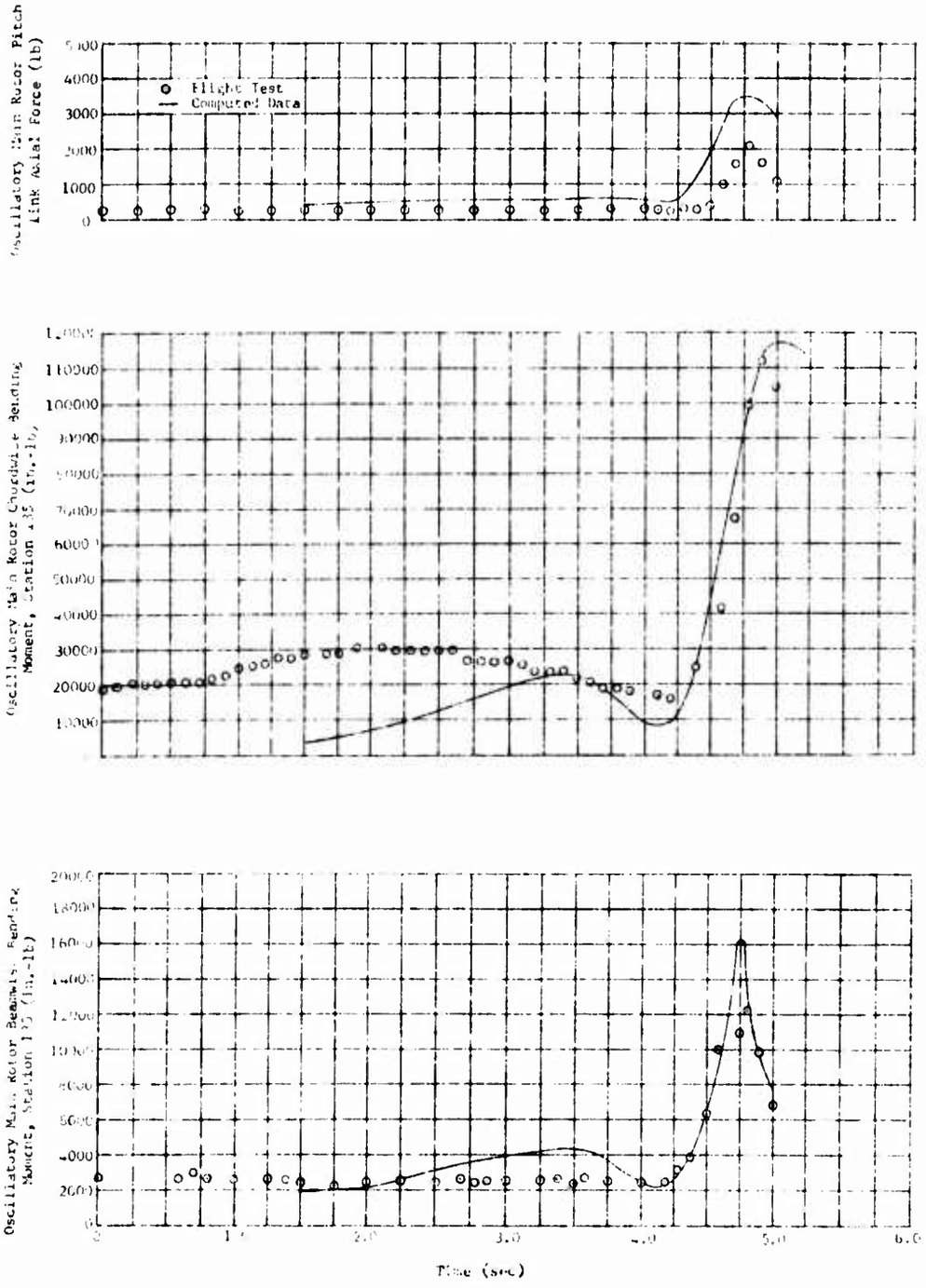

Figure 24. Concluded.

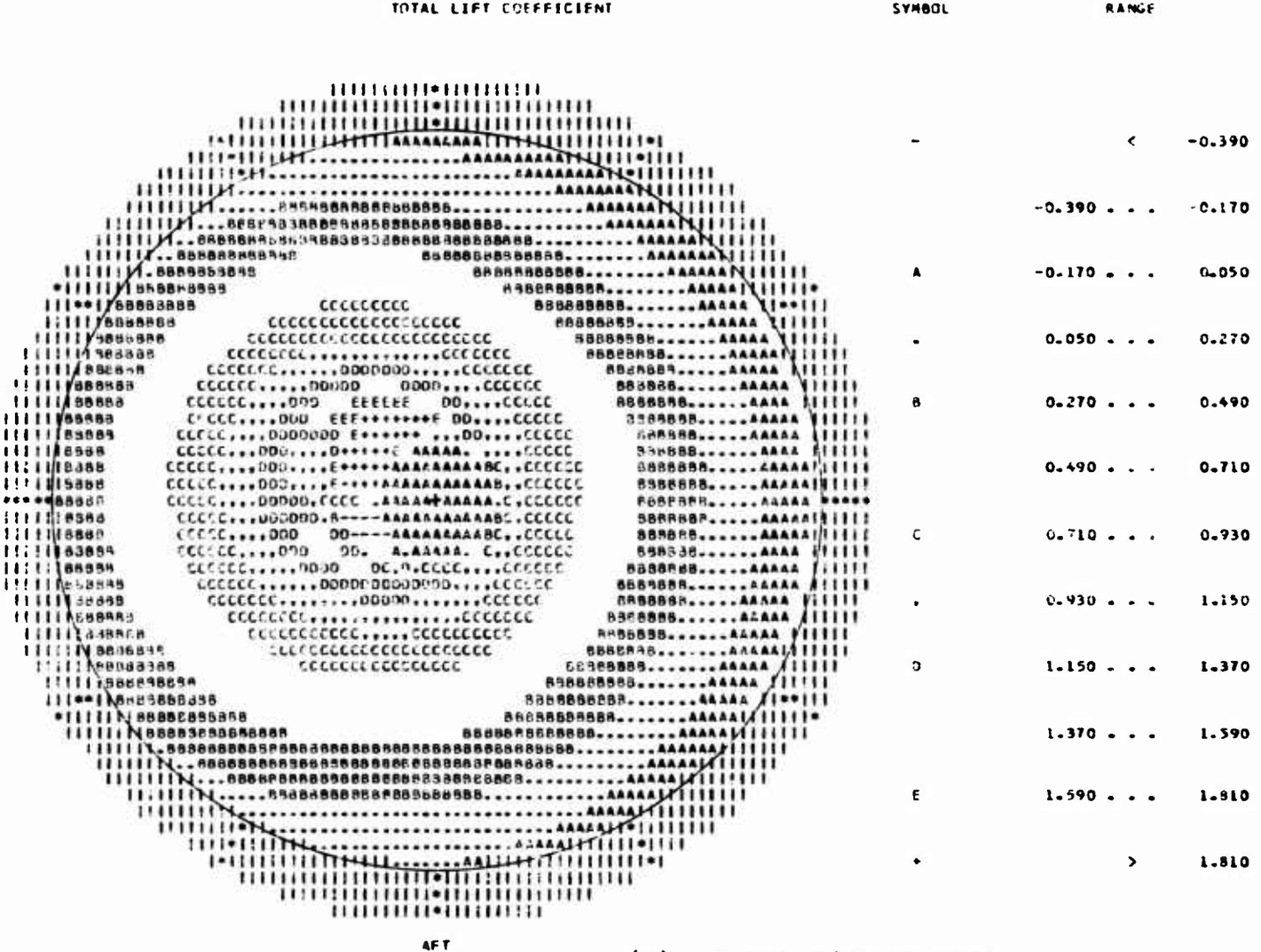

(a) Total Lift Coefficient

Figure 25. Contour Plots at the Time of Entry for the Autorotational Pullup of Counter 775.

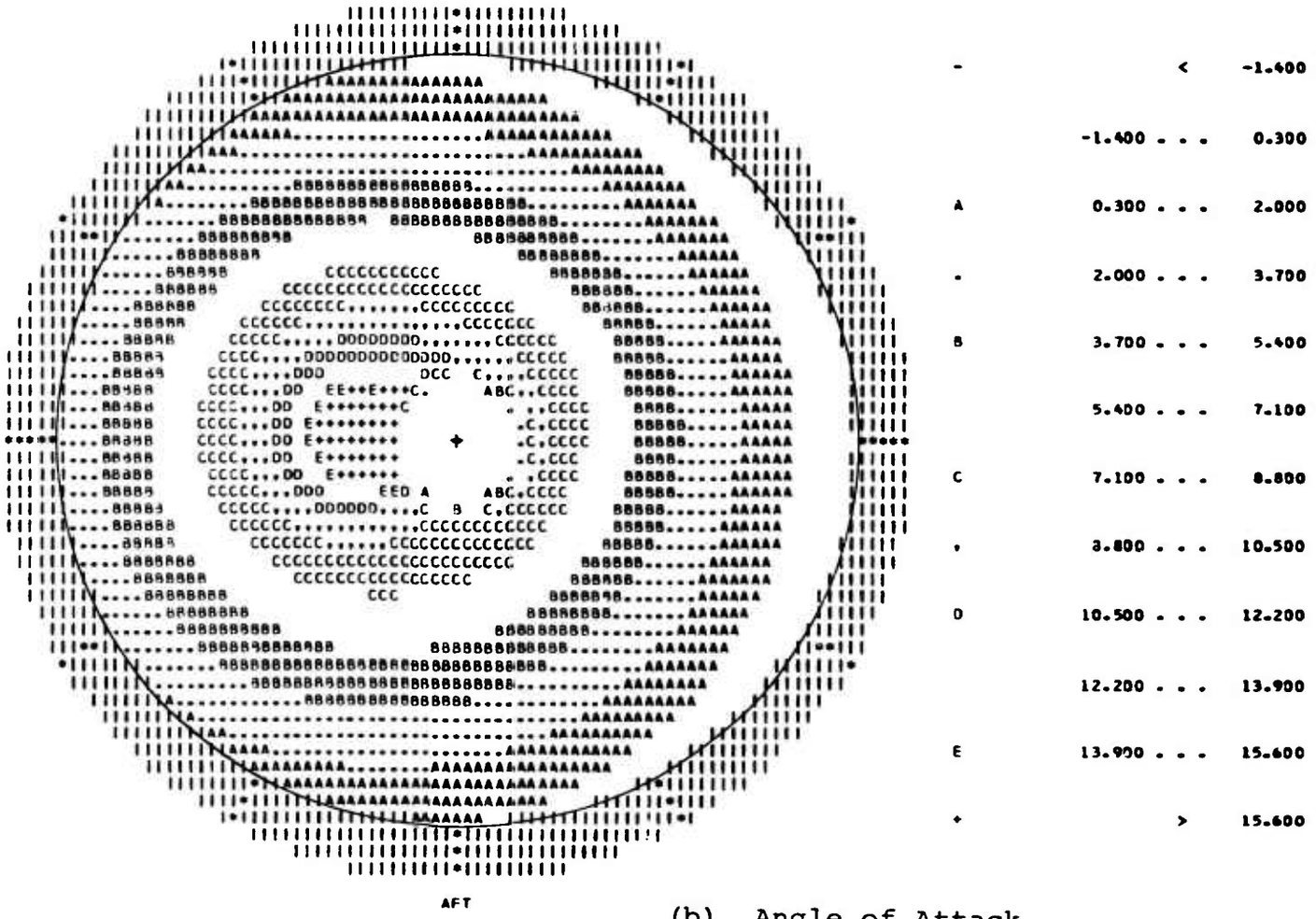

(b) Angle of Attack

Figure 25. Concluded.

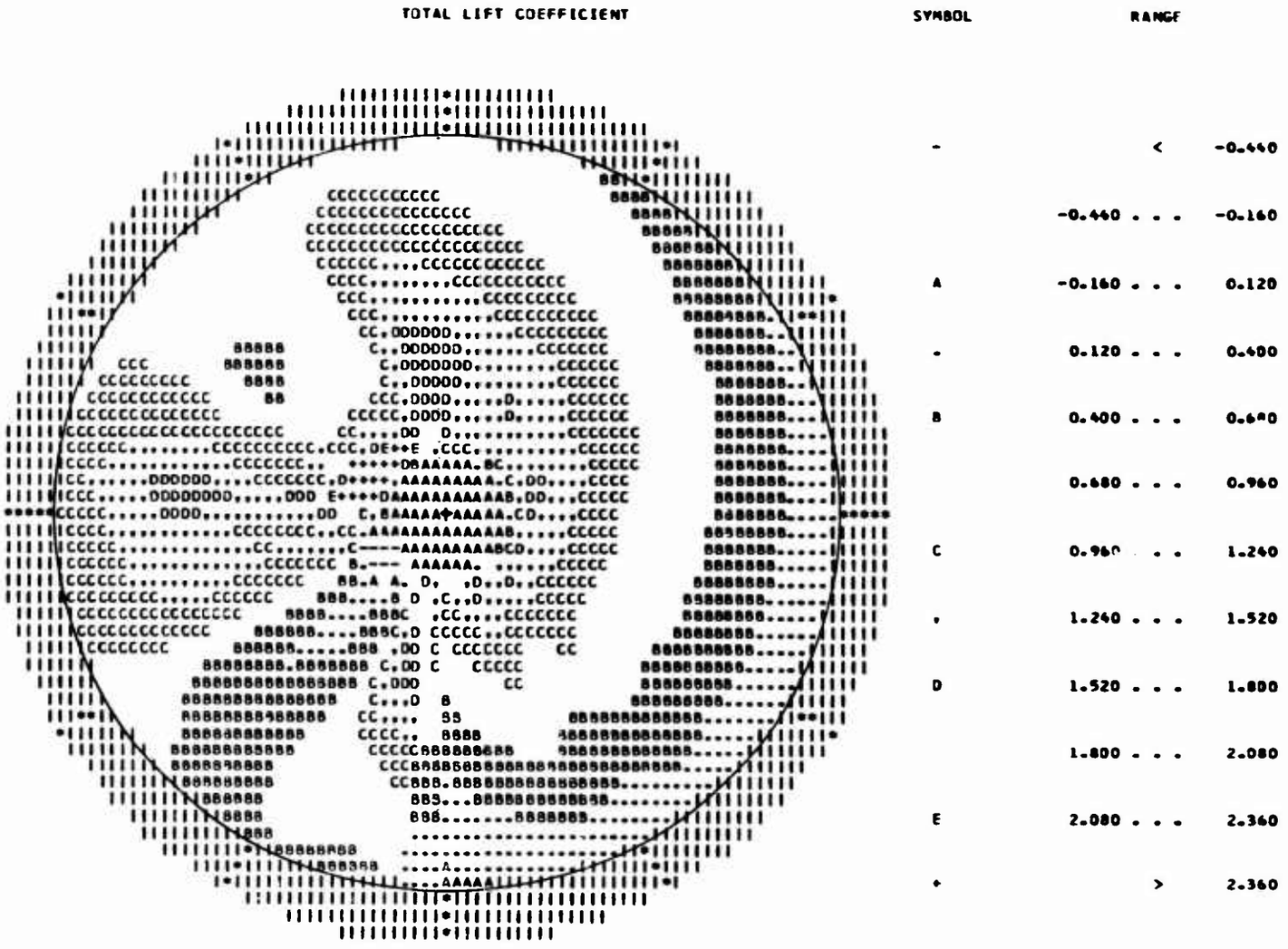

(a) Total Lift Coefficient

Figure 26. Contour Plots at the Time of Maximum Mean Normal Load Factor for the Autorotational Pullup of Counter 775.

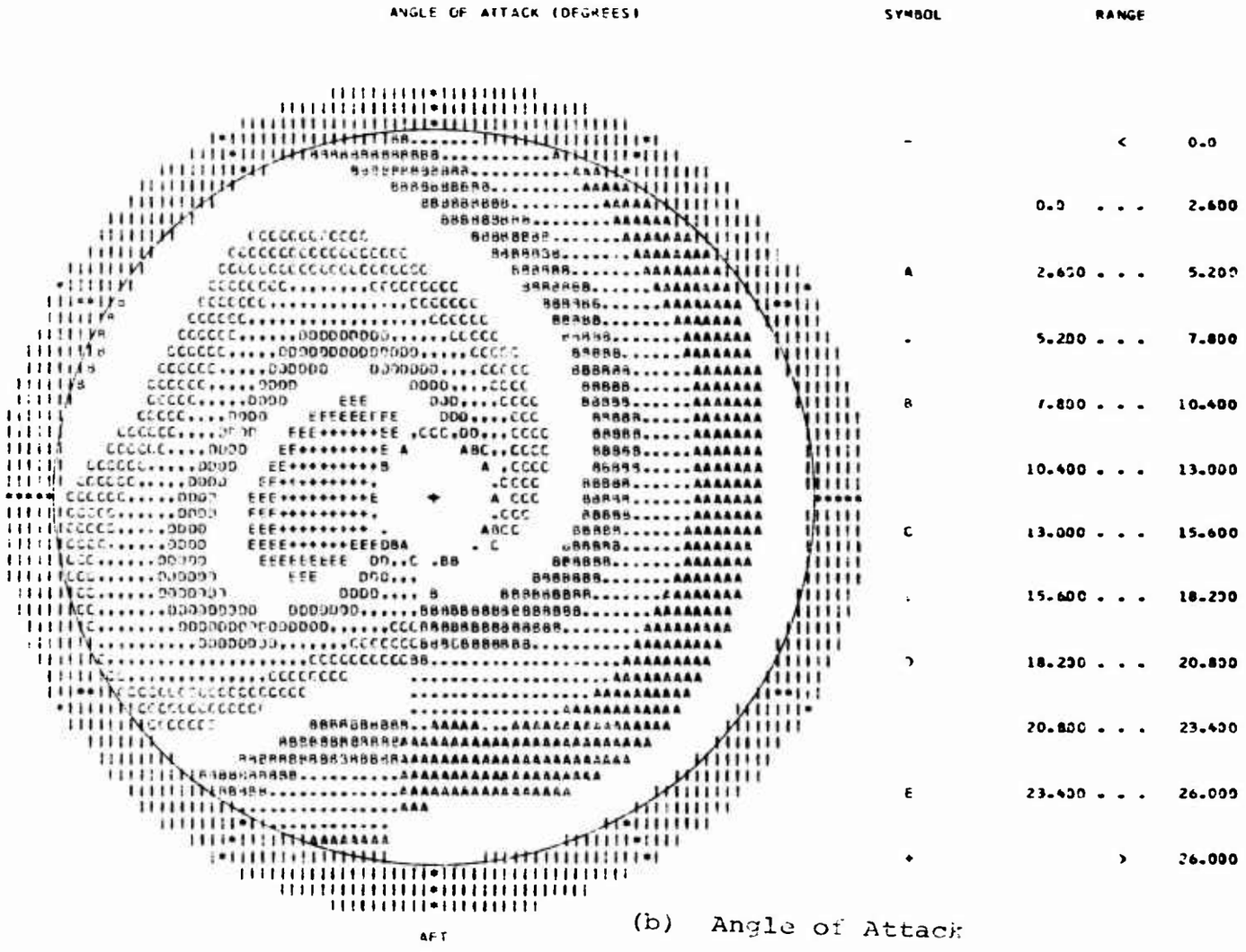

(b) Angle of Attack

Figure 26. Concluded.

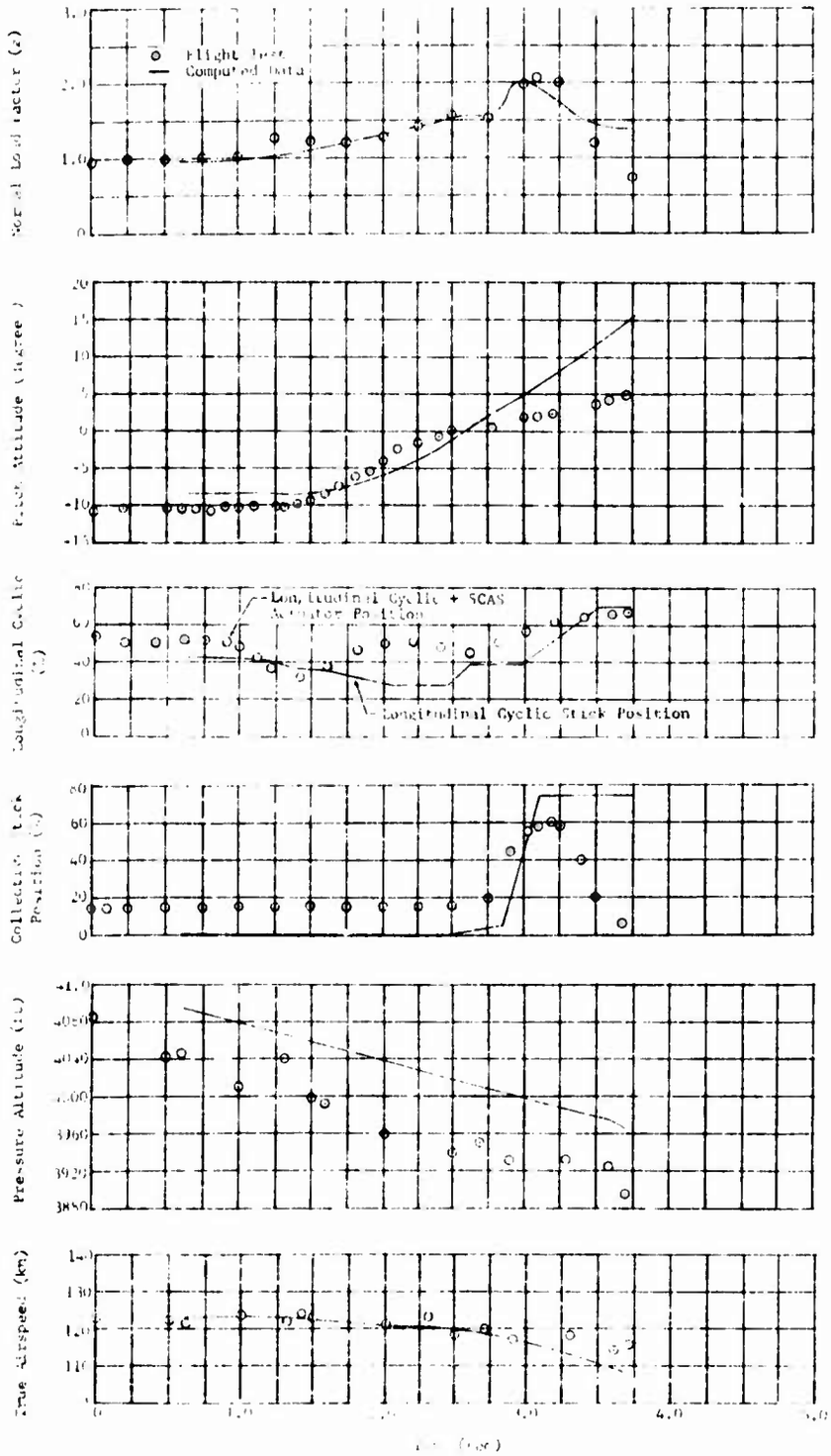

Figure 27. Time Histories of Symmetric Pullup From Autorotation, Counter 840.

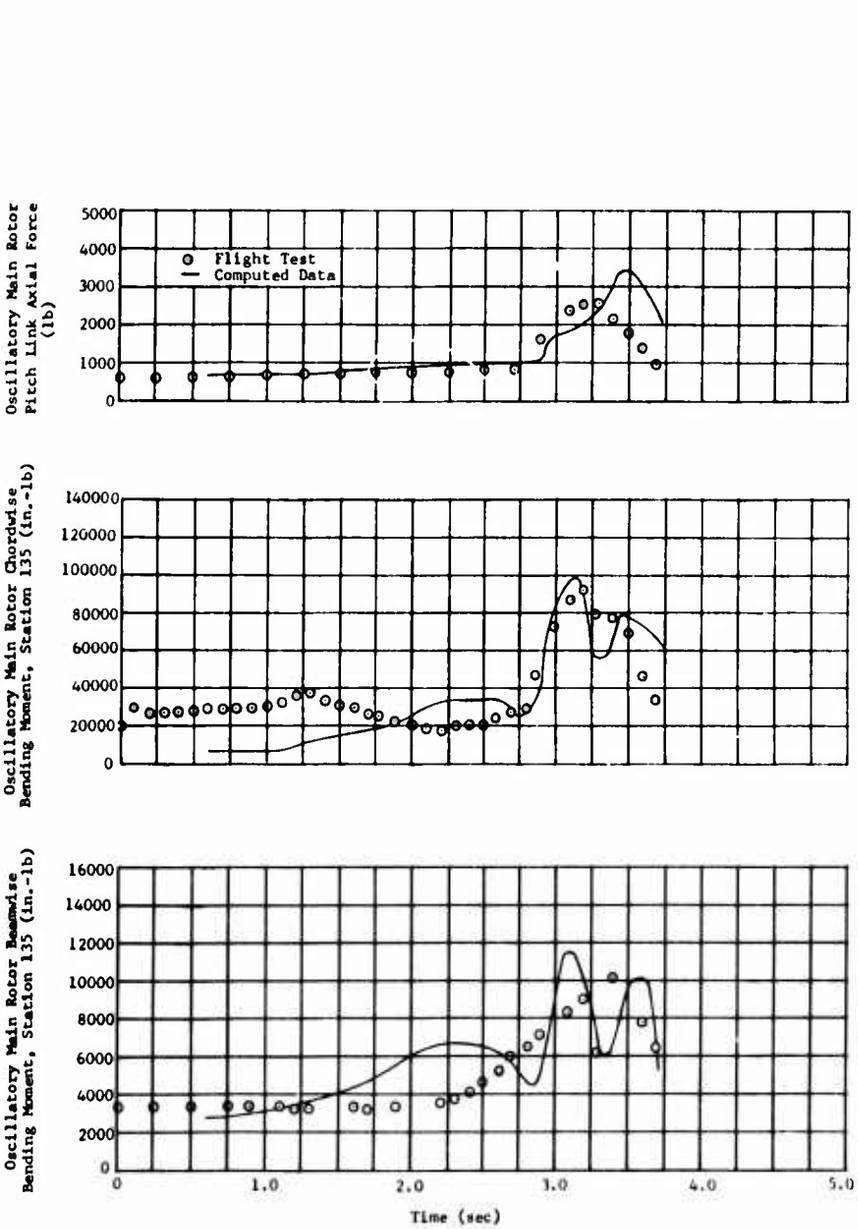

Figure 27. Concluded.

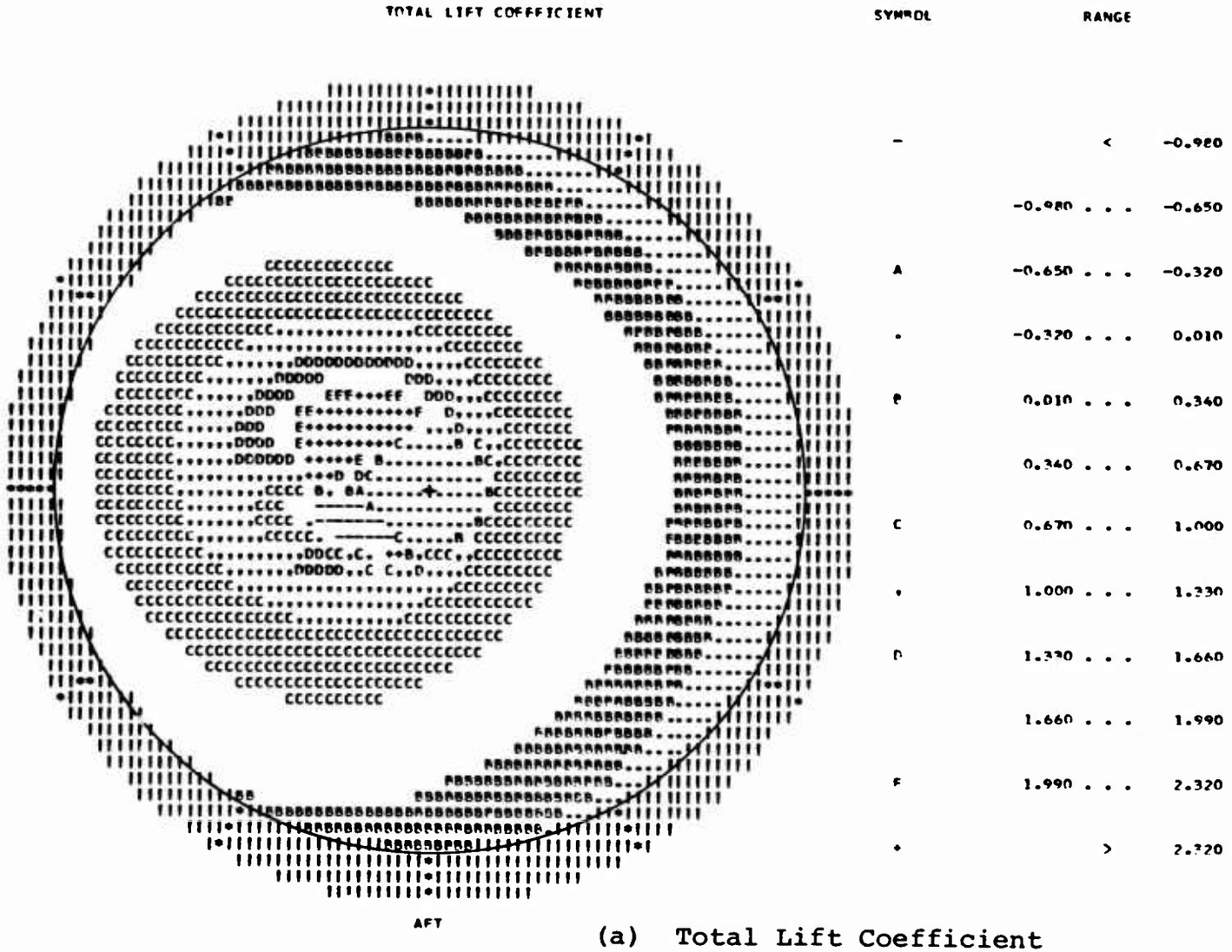

(a) Total Lift Coefficient

Figure 28. Contour Plots at the Time of Entry for the Autorotational Pullup of Counter 840.

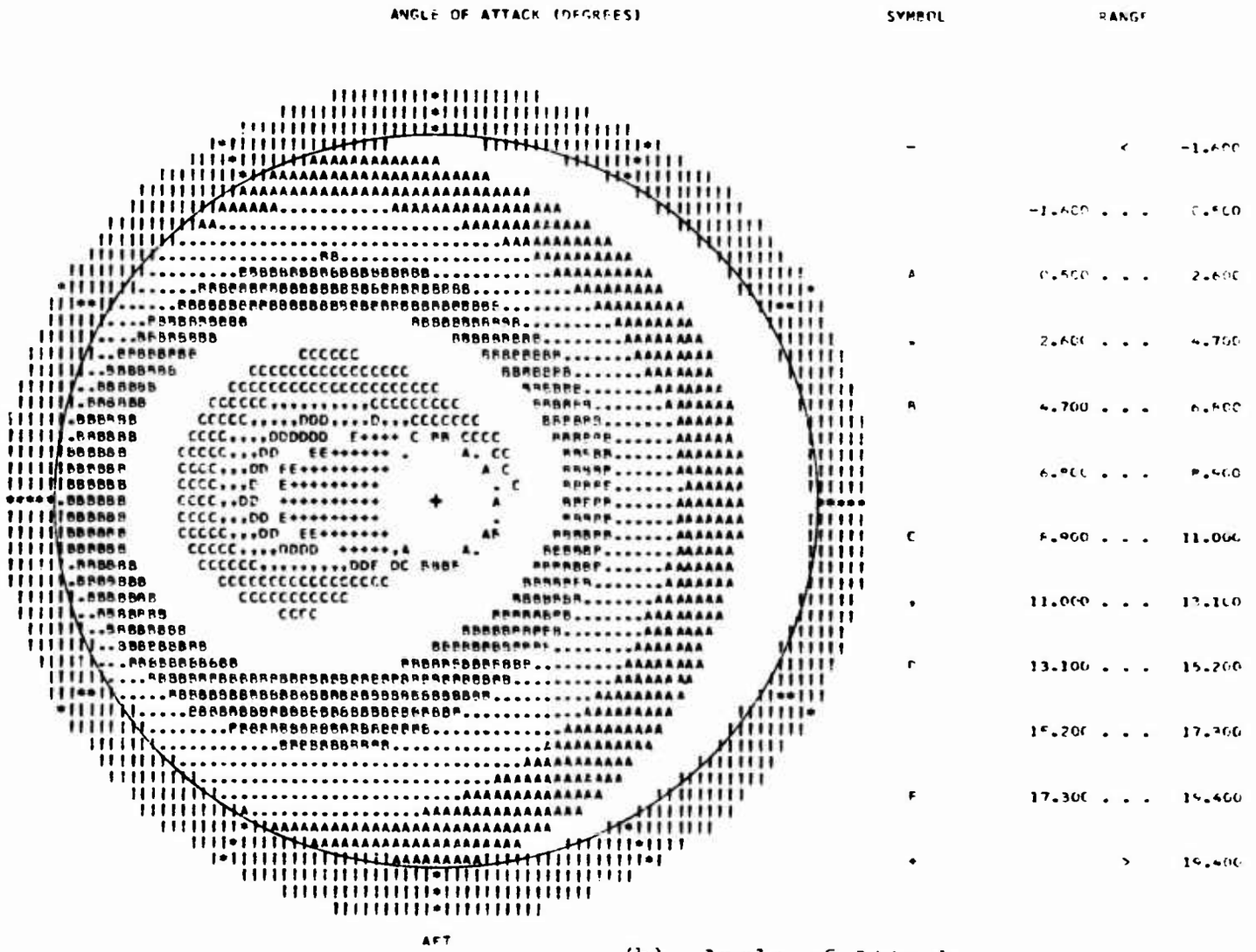

(b) Angle of Attack

Figure 28. Concluded.

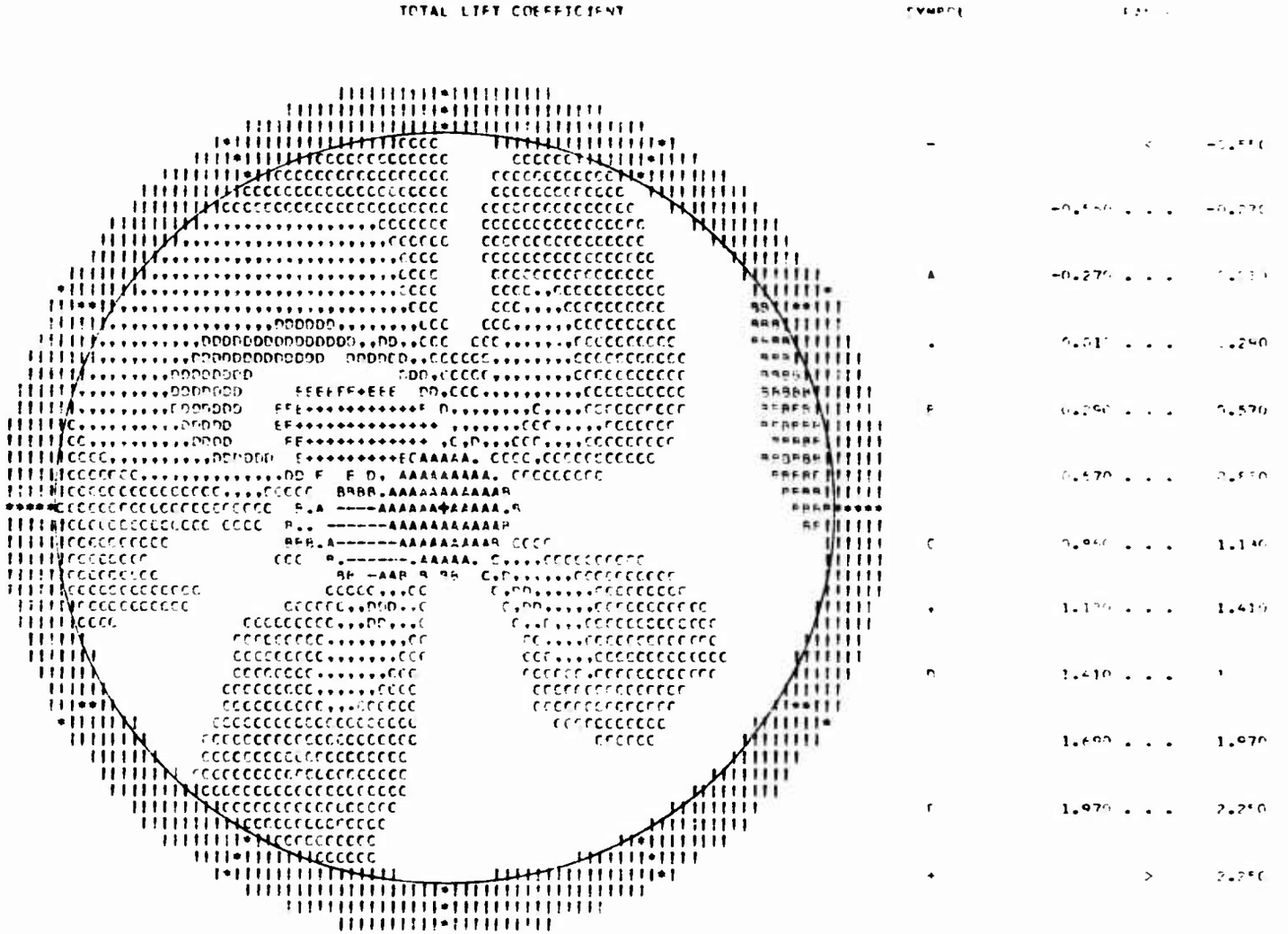

(a) Total Lift Coefficient

Figure 29. Contour Plots at the Time of Maximum Mean Normal Load Factor for the Autorotational Pullup Counter 840.

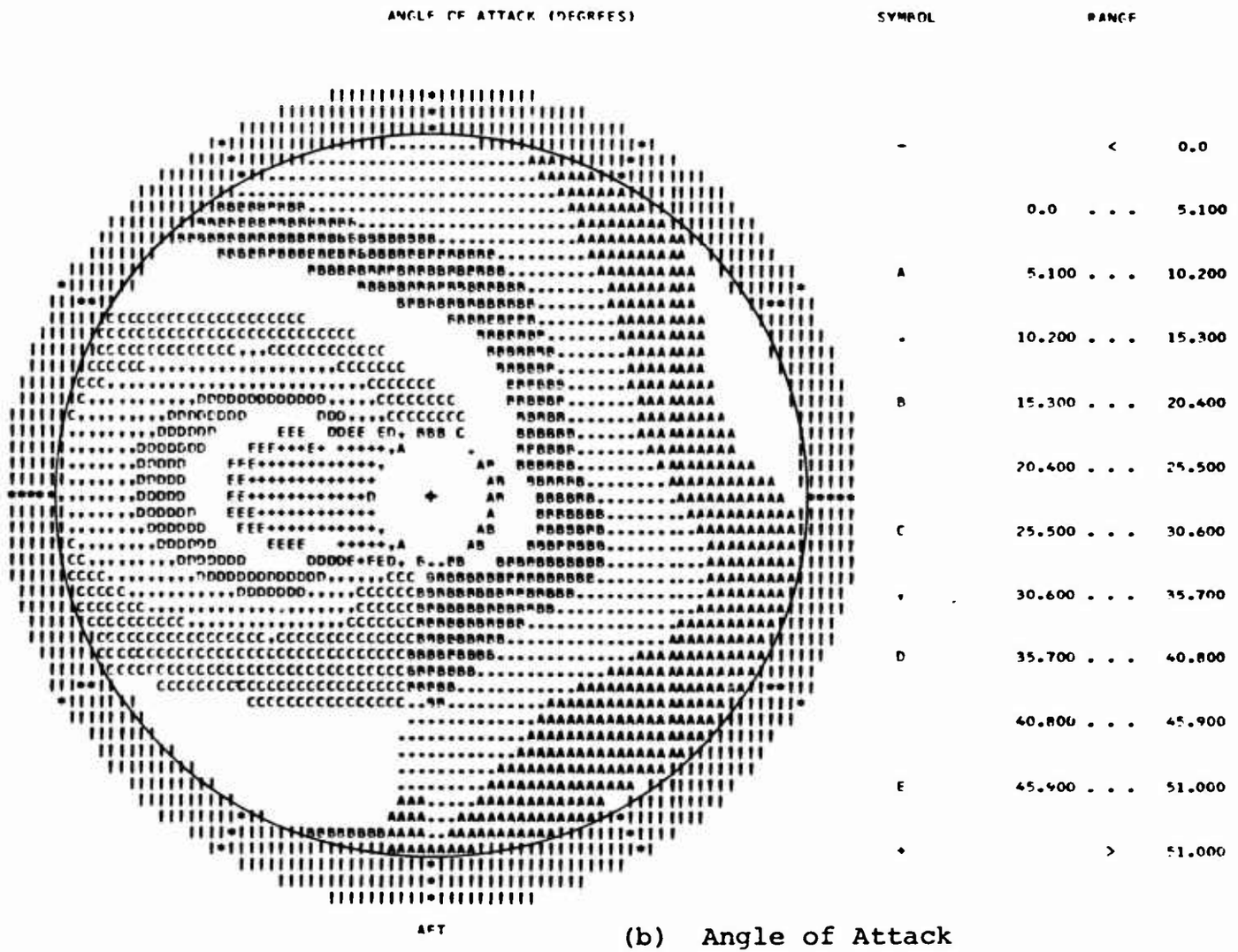

(b) Angle of Attack

Figure 29. Concluded.

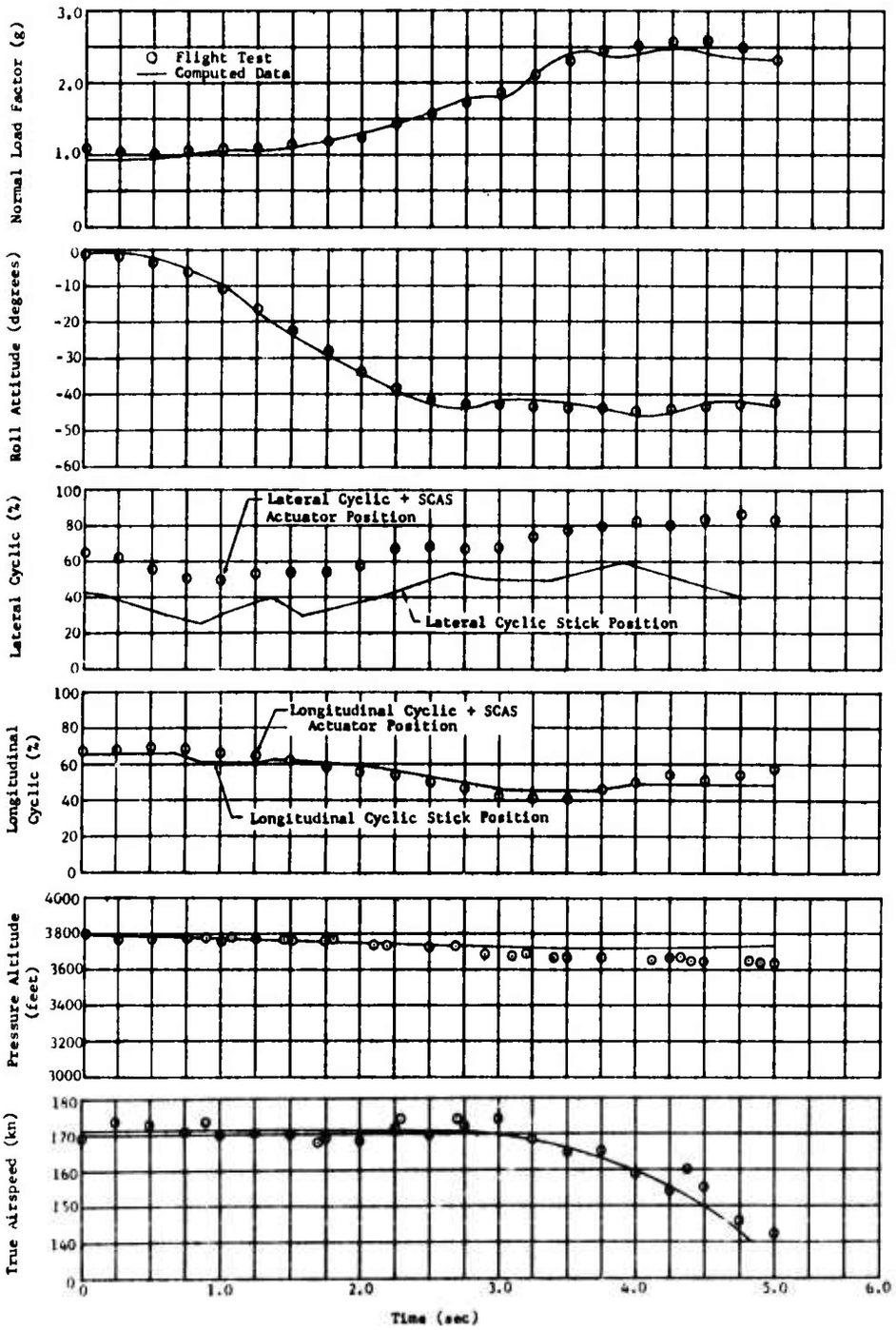

Figure 30. Time Histories of Left Rolling Pullout, Counter 740.

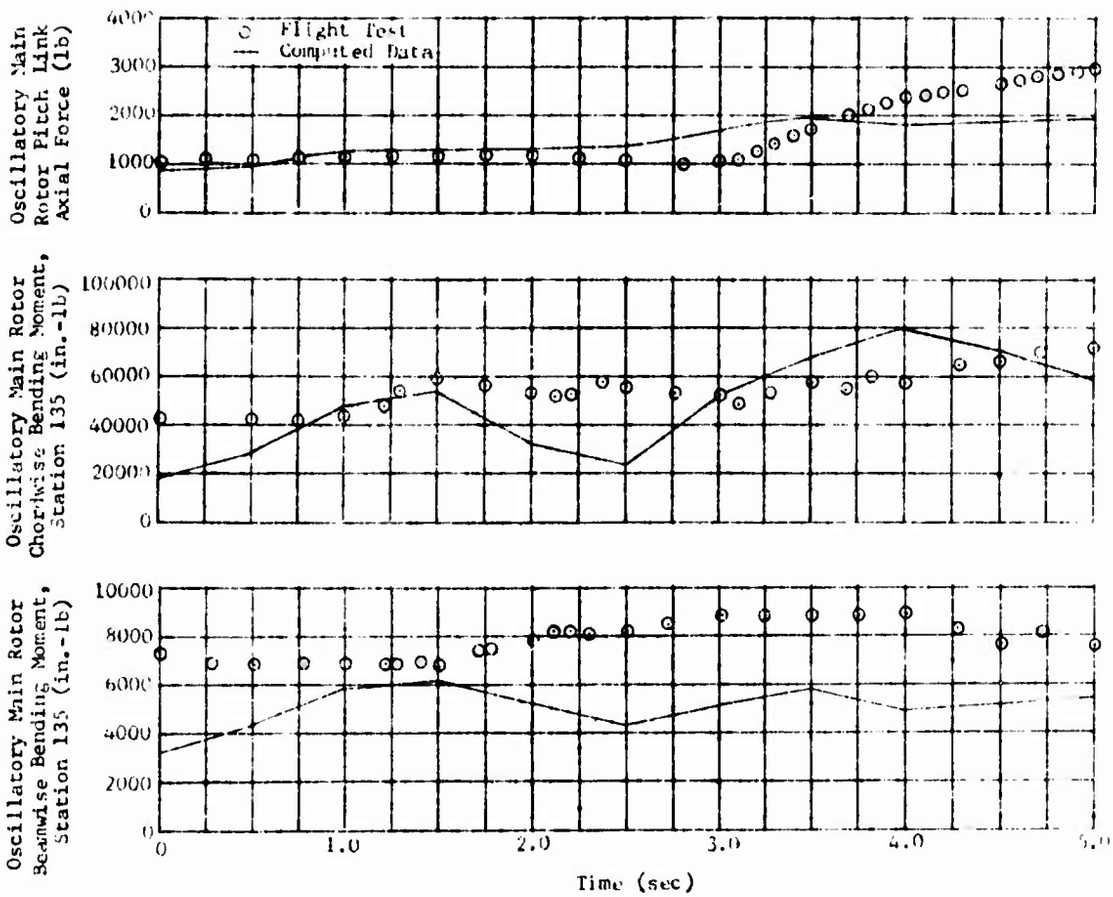

Figure 30. Concluded.

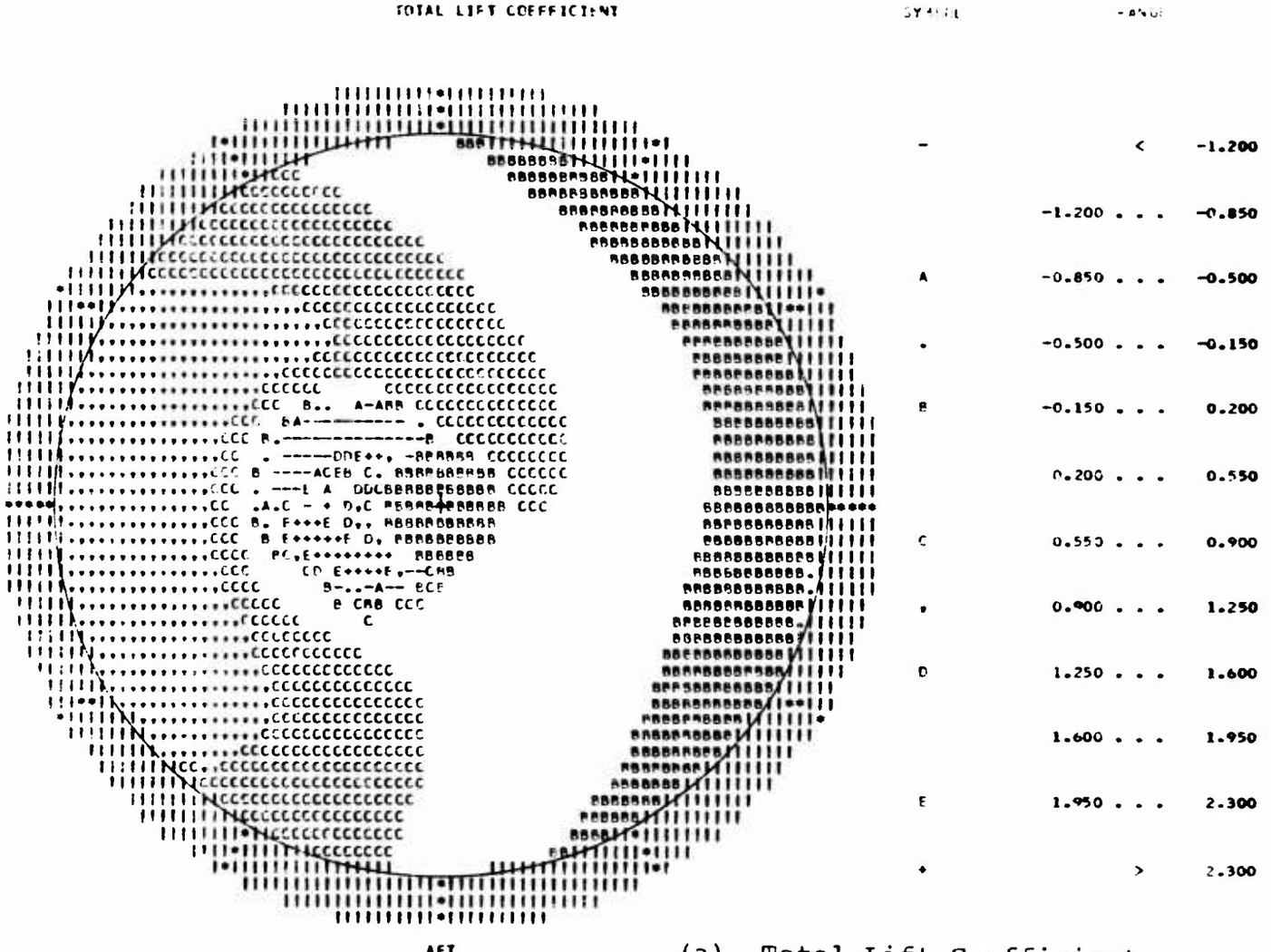

(a) Total Lift Coefficient

Figure 31. Contour Plots at the Time of Entry for the Left Rolling Pullout of Counter 740.

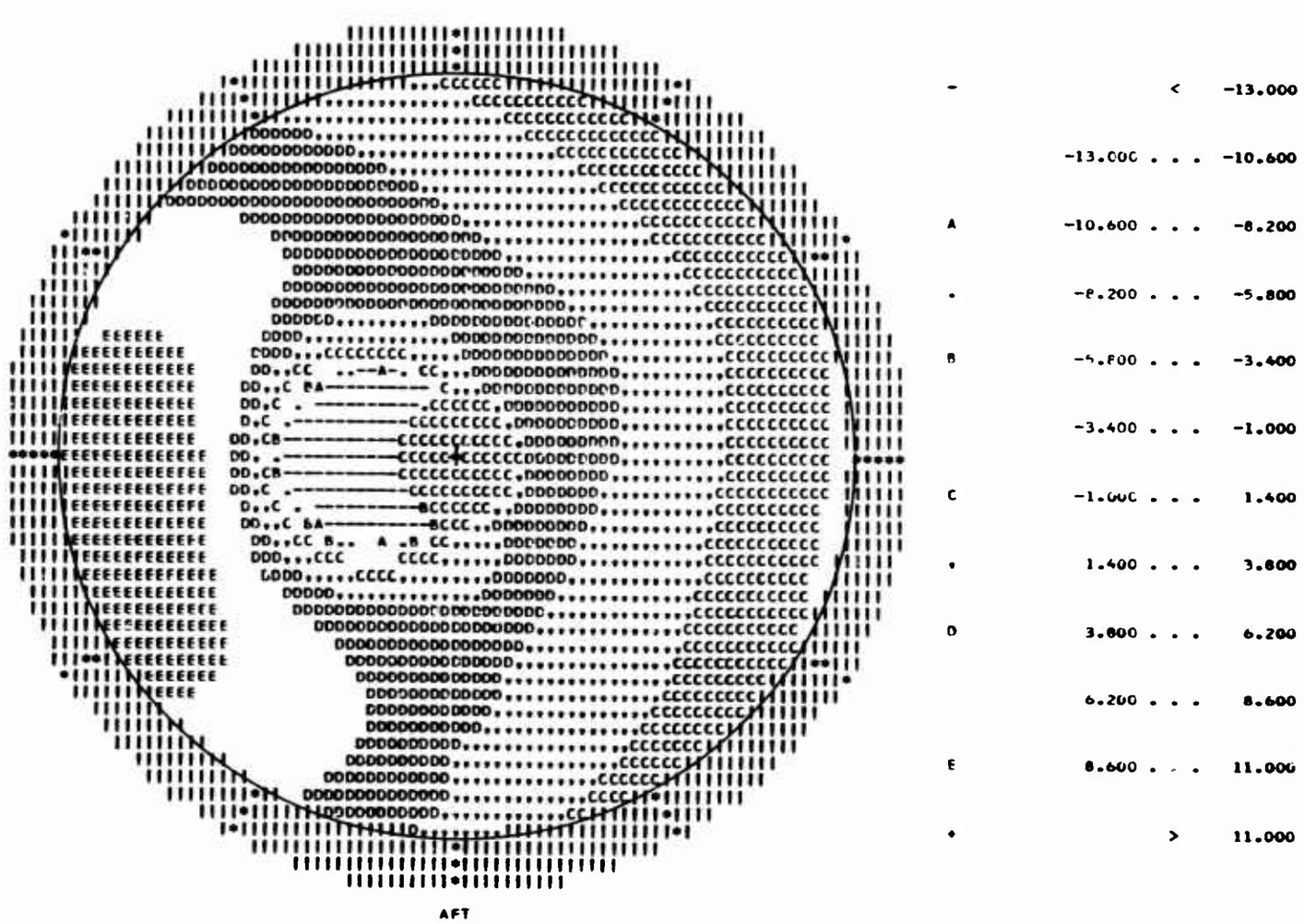

(b) Angle of Attack

Figure 31. Concluded.

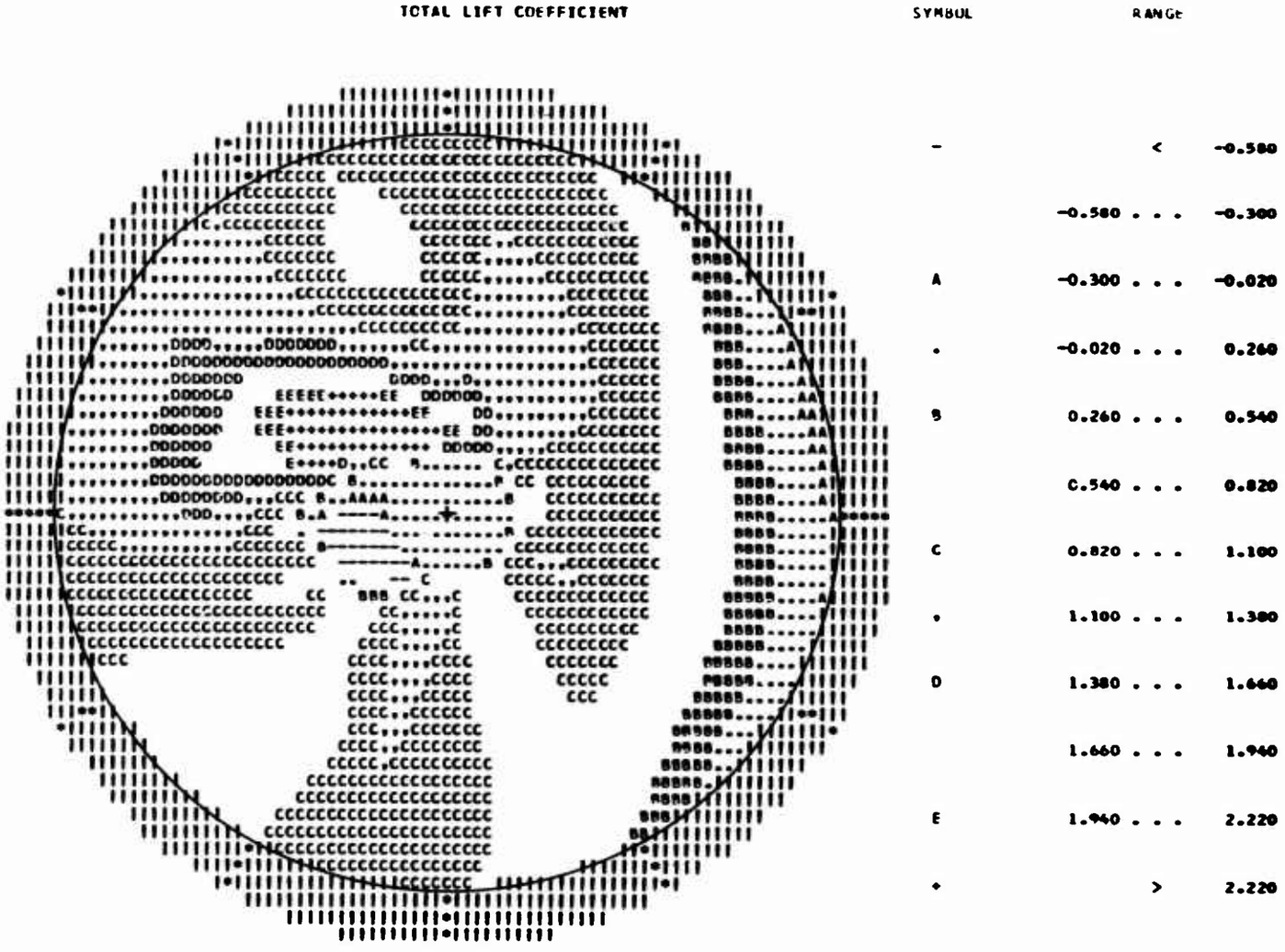

(a) Total Lift Coefficient

Figure 32. Contour Plots at the Time of Maximum Mean Normal Load Factor for the Left Rolling Pullout of Counter 740.

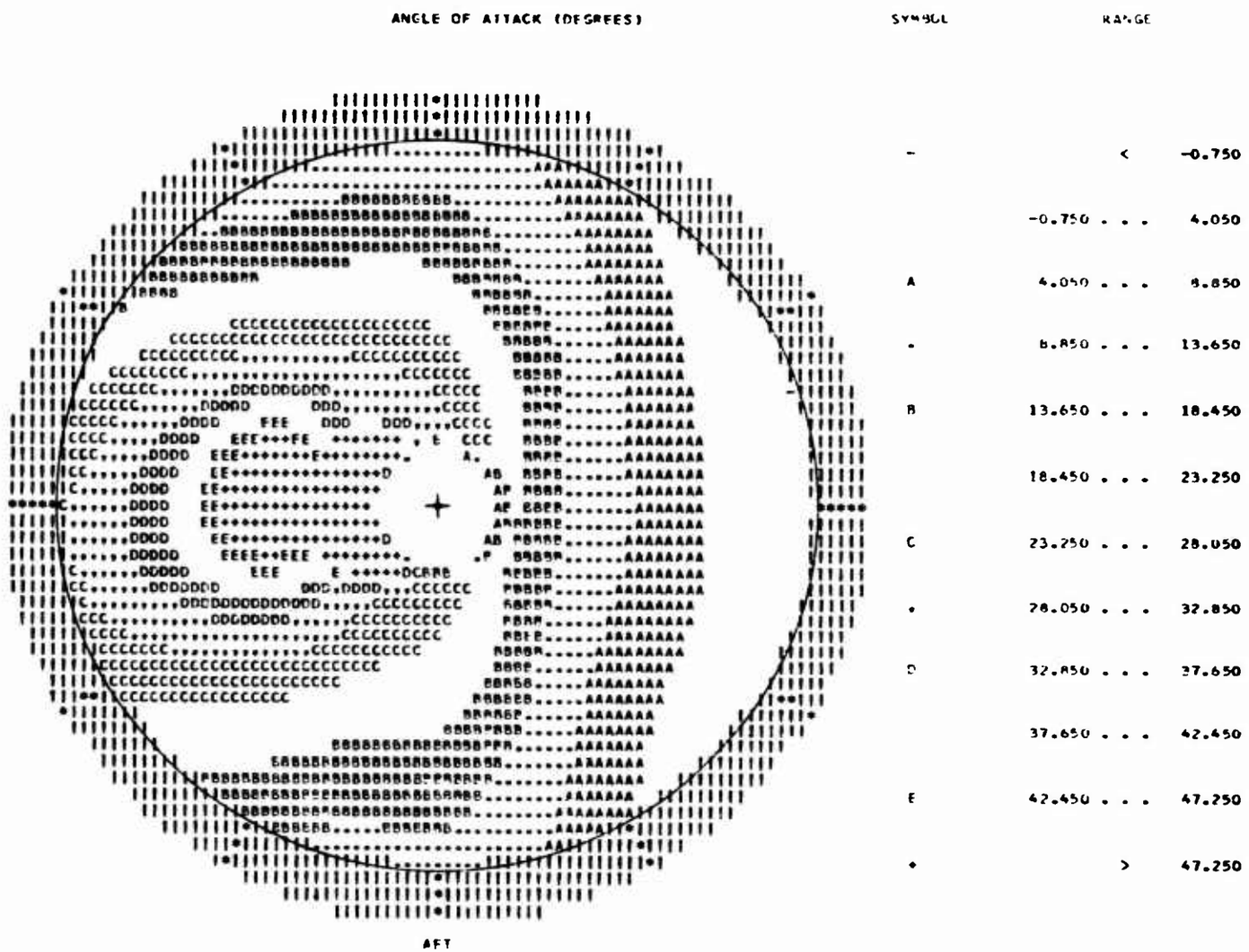

(b) Angle of Attack

Figure 32. Concluded.

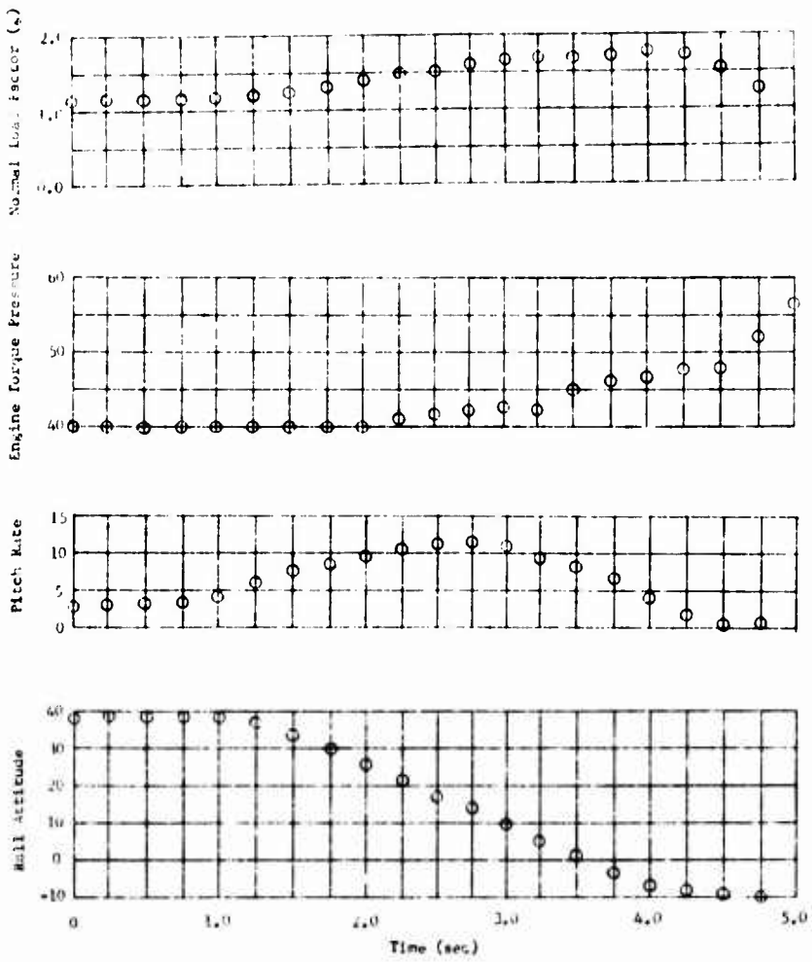

Figure 33. Time Histories of Maneuver Showing Engine Torque Pressure Surge, Flight 118, Counter 820.

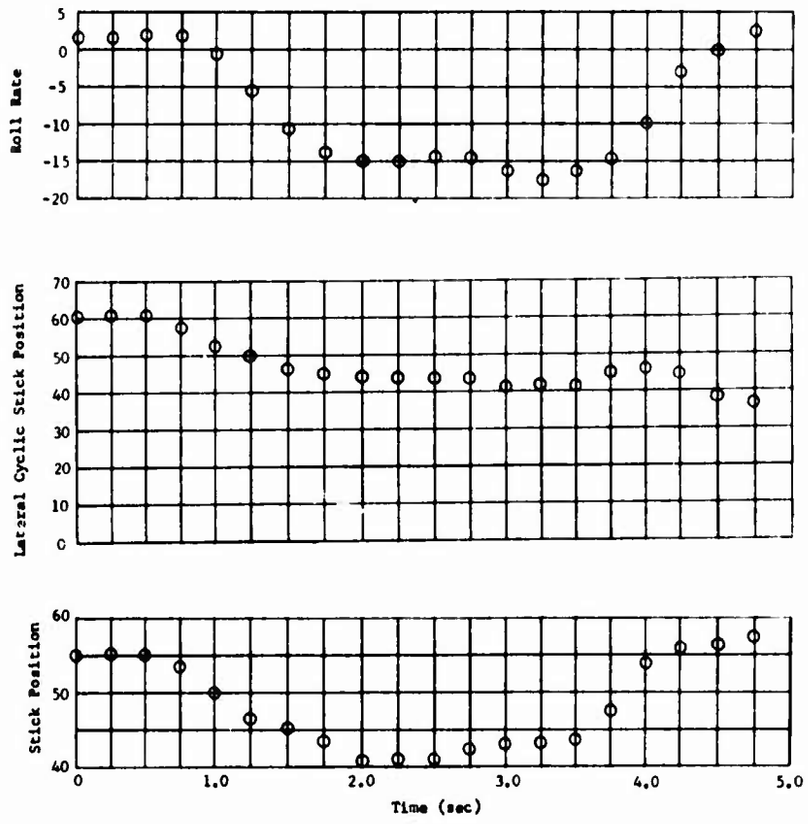

Figure 33. Concluded.

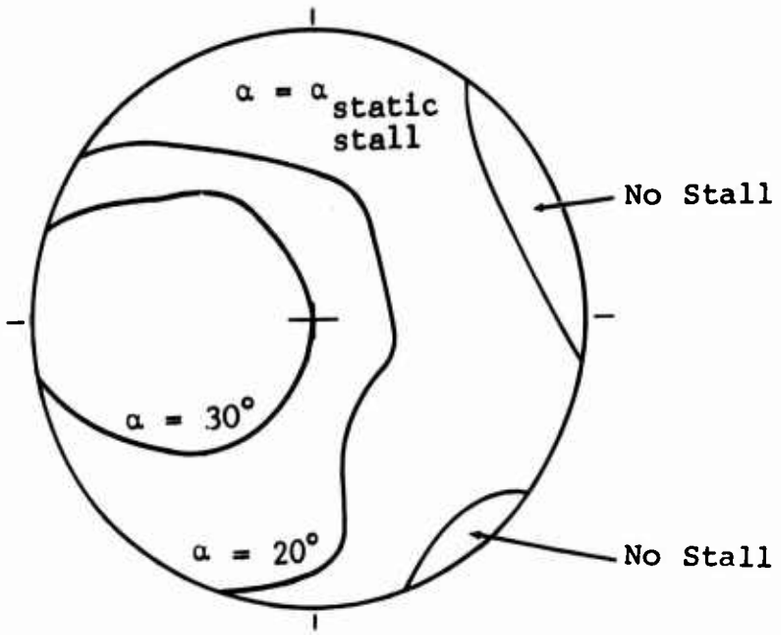

(a) Stall Contour Lines at the Time of Maximum Mean Normal Load Factor for the Simulated Autorotational Pullup of Flight 119, Counter 840. $\mu = 0.277$, $C_T/\sigma = 0.148$

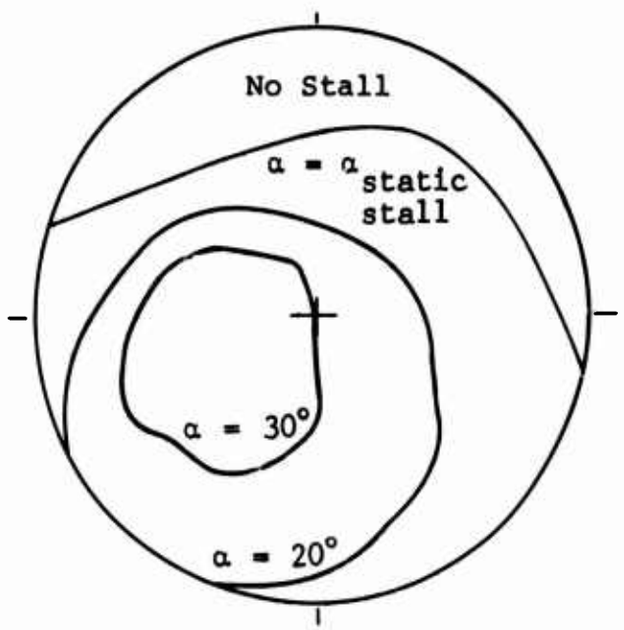

(b) Stall Contour Lines at the Time of Maximum Mean Normal Load Factor for a Fixed Collective Symmetric Pullup. $\mu = 0.40$, $C_T/\sigma = 0.196$

Figure 34. Contour Plots Showing Stalled Regions on Rotor.

TABLE I. MANEUVER TYPES REPRESENTED IN TEST DATA	
Type	Number of Maneuvers
Banked Turns:	
Constant Airspeed, Constant Altitude	13
Constant Airspeed, Varying Altitude	31
Varying Airspeed, Constant Altitude	14
Varying Airspeed, Varying Altitude	13
Rolling Pullups	9
Symmetric Pullups (Power On)	34
Symmetric Pullups from Autorotation	18

TABLE II. FLIGHT TEST VARIABLES EXAMINED
Normal Load Factor
Airspeed*
Pressure Altitude*
Fuselage Angle of Attack**
Pitch Attitude
Pitch Rate
Roll Attitude
Roll Rate
Fuselage Sideslip Angle**
Yaw Attitude
Yaw Rate
Collective Stick Position
Longitudinal Cyclic Stick Position
Longitudinal Cyclic Stick Force**
Lateral Cyclic Stick Position
Lateral Cyclic Stick Force**
Pedal Position
Engine Torque Pressure*
Copilot Vertical Acceleration
Main Rotor Pitch Link Axial Force
Main Rotor Chordwise Bending Moment, Station 135
*Data for these variables recorded from photopanel for the Bell Helicopter Company tests.
**These quantities not measured during Bell Helicopter Company tests.

TABLE III. MAXIMUM VALUES OBSERVED FOR PRIMARY VARIABLES

Variable	Maximum Value Observed
Mean Normal Load Factor	2.61 g
Mean Pitch Rate	21.8 deg/s
Mean Roll Rate	-58.8 deg/s, 66.8 deg/s*
Collective Stick Position	89.9%
Longitudinal Cyclic Stick Position	79.2%
Oscillatory Longitudinal Cyclic Stick Force	6.58 lb
Lateral Cyclic Stick Position	38.6%, 74.7%*
Oscillatory Lateral Cyclic Stick Force	3.50 lb
Mean Engine Torque Pressure	59.0 psi
Oscillatory Copilot Vertical Acceleration	1.34 g
Oscillatory Main Rotor Pitch Link Axial Force	3010 lb
Oscillatory Main Rotor Chordwise Bending Moment, Station 135	145,000 in.-lb

*Extreme excursions from neutral position. The smaller value corresponds to a left bank angle, the higher to a right bank angle.

TABLE IV. SUMMARY OF MANEUVERS

Flight Number	Oscillograph Counter	Measured Maximum Mean Normal Load Factor	Comments
5	11	1.19	1.3 g on pilot card
	13	1.25	1.4 g on pilot card
	14	1.33	
	15	1.37	
	16	1.44	
	21	1.21	1.35 g on pilot card
	23	1.26	1.35 g on pilot card
	25	1.38	
	28	1.22	1.35 g on pilot card
	29	1.27	1.40 g on pilot card
	36	1.25	1.35 g on pilot card
	37	1.28	1.50 g on pilot card
	38	1.26	1.40 g on pilot card
6			Engine Torque Pressure is negative for all counters in Flight 6.
	5	1.39	
	6	1.47	
	8	1.58	
	9	1.36	
	10	1.44	
	11	1.68	
	17	1.52	
	18	1.50	
	19	1.67	
	21	1.53	
	22	1.68	
	23	1.66	
	25	1.47	
	26	1.63	
	27	1.73	
	30	1.59	
	31	1.56	
	32	1.29	1.7 g on pilot card
7	18	1.60	
	21	1.67	
8	7	1.72	
	8	1.67	
	9	1.76	

TABLE IV. - Continued

Flight Number	Oscillo-graph Counter	Measured Maximum Mean Normal Load Factor	Comments
9	18	1.46	
	19	1.44	
	20	1.75	
	21	1.78	
10	7	1.39	
	9	1.47	
	11	1.36	
	12	1.48	
	13	1.42	
	14	1.40	
	15	1.58	
	16	1.33	
	17	1.39	
11	7	1.39	
	14	1.64	
	16	1.43	
	17	1.38	
	18	1.46	
	19	1.62	
	21	1.63	
	22	1.59	
	23	1.57	
22			Copilot Vertical Acceleration, Main Rotor Pitch Link Axial Force and Chordwise Bending Moment (Station 135) unavailable for all counters of Flight 22. In addition, the following variables are unavailable for the individual counters:
	5	1.54	Lateral Cyclic Stick Force
	6	1.66	Lateral Cyclic Stick Force
	7	1.40	Engine Torque Pressure
	8	1.50	
	9	1.56	
	10	1.31	Engine Torque Pressure
	12	1.71	
	13	1.71	Longitudinal Cyclic Stick Force

TABLE IV. - Continued

Flight Number	Oscillograph Counter	Measured Maximum Mean Normal Load Factor	Comments
	14	1.68	Longitudinal Cyclic Stick Force
	15	1.61	
111-A			Longitudinal Cyclic Stick Force, Lateral Cyclic Stick Force, Fuselage Angle of Attack and Fuselage Sideslip Angle unavailable for the remaining counters
	336	2.35	
	337	2.24	
112-B	496	1.98	
	497	2.21	
	498	2.17	
112-C	520	1.41	
	521	1.45	
	522	1.73	
	523	1.96	
	524	1.92	
	525	2.12	
113	596	1.41	
	597	1.37	
	598	1.37	
	599	1.66	
	600	1.33	
	601	1.82	
	602	1.78	
	603	1.78	
114-B	635	2.13	
	636	2.18	
	637	2.21	
	638	2.23	
116-A	723	2.06	
	724	2.30	
	725	2.29	
	726	2.40	
	727	2.28	

TABLE IV. - Concluded

Flight Number	Oscillo-graph Counter	Measured Maximum Mean Normal Load Factor	Comments
116-B	737	2.33	
	738	2.14	
	739	2.06	
	740	2.59	
	741	2.43	
117-A	772	2.44	
	773	2.45	
	774	2.43	
	775	2.46	
117-B	785	2.45	
	786	2.49	
	787	2.34	
	789	2.50	
	790	2.21	
118	814	1.80	
	815	1.76	
	816	1.78	
	817	1.88	
	818	1.89	
	819	1.86	
	820	1.80	
	821	1.94	
	822	1.92	
	823	1.89	
	824	2.09	
	825	1.56	
119	838	1.95	
	839	1.36	Main Rotor Pitch Link Axial Force not available
	840	2.06	
	841	2.07	
120-A	879	2.17	
	881	2.26	
	882	2.17	Main Rotor Pitch Link Axial Force not available
	883	2.54	
	884	2.61	
	885	2.41	

TABLE V. MEAN VALUES AND STANDARD DEVIATIONS OF THE FLIGHT TEST VARIABLES

Variable Number	Variable	Mean Value	Standard Deviation	Units
1	Maximum Mean Normal Load	15307.4	2389.8	lb
2	Oscillatory Copilot Vertical Acceleration at the time of Maximum Mean Normal Load	0.524	0.234	g
3	Maximum Oscillatory Copilot Vertical Acceleration	0.615	0.217	g
4	Oscillatory Main Rotor Pitch Link Axial Force at the time of Maximum Mean Normal Load	1635.8	598.3	lb
5	Maximum Oscillatory Main Rotor Pitch Link Axial Force	1809.7	613.5	lb
6	Longitudinal Cyclic Stick Position at the time of Maximum Mean Normal Load	53.5	12.9	%
7	Δ(Longitudinal Cyclic Stick Position)*	2.1	12.5	%
8	Lateral Cyclic Stick Position at the time of Maximum Mean Normal Load	55.2	7.9	%
9	Δ(Lateral Cyclic Stick Position)	0.45	5.9	%
10	Engine Torque Pressure at the time of Maximum Mean Normal Load	31.7	15.0	psi
11	Maximum Engine Torque Pressure	35.4	16.1	psi

*Δ( ) indicates the difference between the value at the time of maximum mean normal load and the value at the beginning of the maneuver.

TABLE V. - Continued

Variable Number	Variable	Mean Value	Standard Deviation	Units
12	Δ(Engine Torque Pressure)	-.28	4.5	psi
13	Oscillatory Main Rotor Chordwise Bending Moment, Station 135, at the time of Maximum Mean Normal Load	59031.6	25406.0	in.-lb
14	Maximum Main Rotor Oscillatory Chordwise Bending Moment, Station 135	69645.1	28363.0	in.-lb
15	Oscillatory Longitudinal Cyclic Stick Force at the time of Maximum Mean Normal Load	2.21	1.76	lb
16	Maximum Oscillatory Longitudinal Cyclic Stick Force	2.56	1.61	lb
17	Oscillatory Lateral Cyclic Stick Force at the time of Maximum Mean Normal Load	1.87	0.54	lb
18	Maximum Oscillatory Lateral Cyclic Stick Force	2.15	0.50	lb
19	Gross Weight	8816.9	892.8	lb
20	Outside Air Temperature	11.8	4.2	deg C
21	Pressure Altitude at the time of Maximum Mean Normal Load	4120.8	958.4	ft
22	Collective Stick Position at the time of Maximum Mean Normal Load	49.5	16.2	%

TABLE V. - Concluded

Variable Number	Variable	Mean Value	Standard Deviation	Units
23	Calibrated Airspeed at the time of Maximum Mean Normal Load	96.8	29.4	kn
24	Density Ratio at the time of Maximum Mean Normal Load	0.87	0.03	-
25	Pitch Rate at the time of Maximum Mean Normal Load	8.4	4.9	deg/s
26	Maximum Pitch Rate	10.7	5.5	deg/s
27	Roll Rate at the time of Maximum Mean Normal Load	-0.26	9.43	deg/s
28	Maximum Roll Rate	0.37	15.60	deg/s
29	Yaw Rate at the time of Maximum Mean Normal Load	-0.99	5.85	deg/s
30	Maximum Yaw Rate	-1.17	6.64	deg/s
31	Speed of Sound at the time of Maximum Mean Normal Load	111.0	8.3	ft/s
32	Referred Thrust {(Maximum Mean Normal Load)/(Density Ratio)}	17604.0	2682.4	lb
33	Disc Loading (C_T/σ) at the time of Maximum Mean Normal Load	0.134	0.020	-
34	Advance Ratio at the time of Maximum Mean Normal Load	0.129	0.039	-
35	Maximum Normal Load Factor	1.76	0.39	g

TABLE VI. SIMPLE CORRELATION COEFFICIENT MATRIX FOR THE NINE BASE VARIABLES

	Oscillatory Co-pilot Vertical Acceleration*	Oscillatory Main Rotor Pitch Link Axial Force*	Δ(Longitudinal Cyclic Stick Position)	Δ(Lateral Cyclic Stick Position)	Engine Torque Pressure*	Oscillatory Main Rotor Chordwise Bending Moment, Station 135	Oscillatory Longitudinal Cyclic Stick Force*	Oscillatory Lateral Cyclic Stick Force*	Mean Normal Load Factor*
Oscillatory Co-pilot Vertical Acceleration*	1.00	0.06	0.09	-0.08	0.45	0.07	-0.10	0.37	-0.35
Oscillatory Main Rotor Pitch Link Axial Force*	0.06	1.00	-0.28	-0.12	-0.07	0.44	0.36	-0.03	0.49
Δ(Longitudinal Cyclic Stick Position)	0.09	-0.28	1.00	0.20	0.06	-0.19	-0.15	0.08	-0.16
Δ(Lateral Cyclic Stick Position)	-0.08	-0.12	0.20	1.00	0.07	-0.22	-0.06	-0.07	-0.15
Engine Torque Pressure*	0.45	-0.07	0.06	0.07	1.00	0.07	-0.14	0.14	-0.56
Oscillatory Main Rotor Chordwise Bending Moment Station 135*	0.07	0.44	-0.19	-0.22	0.07	1.00	0.33	-0.02	0.42
Oscillatory Longitudinal Cyclic Stick Force*	-0.10	0.36	-0.15	-0.06	-0.14	0.33	1.00	-0.41	0.43
Oscillatory Lateral Cyclic Stick Force*	0.37	-0.03	0.08	-0.07	0.14	-0.02	-0.41	1.00	-0.23
Maximum Mean Normal Load Factor	-0.35	0.49	-0.16	-0.15	-0.56	0.42	0.43	-0.23	1.00

*At the time of maximum mean normal load.

TABLE VII. SIMPLE CORRELATION COEFFICIENTS FOR OSCILLATING LOADS AT THE TIME OF MAXIMUM MEAN NORMAL LOAD, WHICH ARE SIGNIFICANTLY DIFFERENT FROM ZERO WITH 95 PERCENT CONFIDENCE

	Independent Variable									
Dependent Variable	Longitudinal Cyclic Stick Position	Lateral Cyclic Stick Position	Engine Torque Pressure	Collective Stick Position	Pitch Rate	Roll Rate	Yaw Rate	Referred Thrust	Advance Ratio	Mean Normal Load Factor
Oscillatory Copilot Vertical Acceleration	0.50	-0.54	0.45	-0.26	0.31	-	-	-	0.21	-0.35
Main Rotor Pitch Link Axial Force	-	0.18	-	0.46	-	-	-	0.61	0.30	0.49
Oscillatory Main Rotor Chordwise Bending Moment, Sta 135	-	-	-	0.61	-	-0.16	-	0.36	0.35	0.42
Oscillatory Longitudinal Cyclic Stick Force	-	0.33	-	0.37	-0.28	-	-	0.30	0.32	0.43
Oscillatory Lateral Cyclic Stick Force	0.21	-0.28	-	-0.21	0.17	-	-	-	-	-0.23

Dashes indicate $|r_{ij}| < 0.15$ and is therefore not significantly different from zero with 95 percent confidence.

TABLE VIII. COEFFICIENTS OF PARTIAL REGRESSION FOR OSCILLATING LOADS AT THE TIME OF MAXIMUM MEAN NORMAL LOAD, WHICH ARE SIGNIFICANTLY DIFFERENT FROM ZERO WITH 95 PERCENT CONFIDENCE

	Independent Variable									
Dependent Variable	Longitudinal Cyclic Stick Position	Lateral Cyclic Stick Position	Engine Torque Pressure	Collective Stick Position	Pitch Rate	Roll Rate	Yaw Rate	Referred Thrust	Advance Ratio	Mean Normal Load Factor
Oscillatory Copilot Vertical Acceleration	0.19	-0.52	-0.22	-	0.17	-	-	0.15	0.22	-0.18
Main Rotor Pitch Link Axial Force	-0.24	-	0.14	-	-0.31	-	-	0.88	0.39	-0.34
Oscillatory Main Rotor Chordwise Bending Moment, Sta 135	-	-0.40	-	0.69	-	-	-	-0.18	0.45	0.18
Oscillatory Longitudinal Cyclic Stick Force	-0.18	-	0.30	-	-0.35	-	-	0.17	0.29	0.21
Oscillatory Lateral Cyclic Stick Force	-	-0.29	-0.30	-	-	-	-	-	-	-0.23

Dashes indicate $|m_{ij}| < 0.15$ and is therefore not significantly different from zero with 95 percent confidence.

TABLE IX. PARTIAL CORRELATION COEFFICIENTS FOR OSCILLATING LOADS AT THE TIME OF MAXIMUM MEAN NORMAL LOAD, WHICH ARE SIGNIFICANTLY DIFFERENT FROM ZERO WITH 95 PERCENT CONFIDENCE

	Independent Variable									
Dependent Variable	Longitudinal Cyclic Stick Position	Lateral Cyclic Stick Position	Engine Torque Pressure	Collective Stick Position	Pitch Rate	Roll Rate	Yaw Rate	Referred Thrust	Advance Ratio	Mean Normal Load Factor
Oscillatory Copilot Vertical Acceleration	-	-0.35	-	-	-	-	-	-	-	-
Main Rotor Pitch Link Axial Force	-	-	-	-	-0.29	-	-	0.46	0.32	-
Oscillatory Main Rotor Chordwise Bending Moment, Sta 135	-	-0.33	-	0.59	-	-	-	-	0.40	-
Oscillatory Longitudinal Cyclic Stick Force	-	-	-	-	-0.29	-	-	-	-	-
Oscillatory Lateral Cyclic Stick Force	-	-	-	-	-	-	-	-	-	-

Dashes indicate $|r_{ij.kl...}| < 0.265$ and is therefore not significantly different from zero with 95 percent confidence.

TABLE X. CUMULATIVE COEFFICIENTS OF DETERMINATION FOR OSCILLATING LOADS AT THE TIME OF MAXIMUM MEAN NORMAL LOAD

Dependent Variable	Independent Variable	Cumulative Coefficient of Determination
Oscillatory Copilot Vertical Acceleration	Lateral Cyclic Stick Position	0.29
	Longitudinal Cyclic Stick Position	0.36
	Pitch Rate	0.39
	Referred Thrust	0.40
	Roll Rate	0.40
	Advance Ratio	0.41
	Engine Torque Pressure	0.42
	Mean Normal Load Factor	0.42
	Yaw Rate	0.42
	Collective Stick Position	0.42
Oscillatory Main Rotor Pitch Link Axial Force	Referred Thrust	0.37
	Advance Ratio	0.45
	Pitch Rate	0.47
	Engine Torque Pressure	0.50
	Roll Rate	0.50
	Longitudinal Cyclic Stick Position	0.50
	Mean Normal Load Factor	0.51
	Lateral Cyclic Stick Position	0.52
	Collective Stick Position	0.52
	Yaw Rate	0.52
Oscillatory Main Rotor Chordwise Bending Moment, Station 135	Collective Stick Position	0.37
	Advance Ratio	0.49
	Lateral Cyclic Stick Position	0.55
	Longitudinal Cyclic Stick Position	0.59
	Yaw Rate	0.60
	Roll Rate	0.61
	Pitch Rate	0.61
	Engine Torque Pressure	0.61
	Referred Thrust	0.62
	Mean Normal Load Factor	0.62

TABLE X. - Concluded

Dependent Variable	Independent Variable	Cumulative Coefficient of Determination
Longitudinal Cyclic Stick Force	Mean Normal Load Factor	0.19
	Advance Ratio	0.27
	Pitch Rate	0.32
	Engine Torque Pressure	0.34
	Longitudinal Cyclic Stick Position	0.35
	Yaw Rate	0.36
	Referred Thrust	0.36
	Roll Rate	0.36
	Collective Stick Position	0.37
Lateral Cyclic Stick Force	Lateral Cyclic Stick Position	0.08
	Yaw Rate	0.10
	Collective Stick Position	0.11
	Engine Torque Pressure	0.12
	Longitudinal Cyclic Stick Position	0.13
	Pitch Rate	0.14
	Roll Rate	0.15
	Mean Normal Load Factor	0.15
	Referred Thrust	0.16
	Advance Ratio	0.16

TABLE XI. ENTRY CONDITIONS FOR FIXED COLLECTIVE SYMMETRIC PULLUPS

Advance Ratio	True Airspeed (kn)	Ground Speed (kn)	Rate of Sink (ft/s)	Collective Stick Position (%)	Engine Horsepower	Entry Condition
0.150	66.29	65.06	21.5	0.03	75.4	Autorotation*
0.200	88.39	86.33	22.8	0.03	111.5	
0.250	110.47	109.22	28.0	0.12	183.2	
0.300	132.58	132.58	0.0	27.14	784.6	Level Flight
0.325	143.63	143.59	6.5	28.40	851.3	Power-on Dive
0.350	154.89	154.35	17.0	28.58	896.9	
0.400	177.01	174.93	45.7	28.51	1023.4	

*Some residual horsepower is calculated even though the collective stick is at its lowest position. This small amount of horsepower is effectively zero.

TABLE XII. SIMPLE CORRELATION COEFFICIENT MATRIX FOR SEVEN BASIC VARIABLES - C81 DATA

Variable	Oscillatory Normal Load Factor	Oscillatory Main Rotor Pitch Link Axial Force	Δ(Longitudinal Cyclic Stick Position)	Δ(Lateral Cyclic Stick Position)	Engine Torque Pressure	Oscillatory Main Rotor Chordwise Bending Moment Station 135	Maximum Mean Normal Load Factor
Oscillatory Normal Load Factor	1.00	0.64	-0.69	0.51	0.58	0.81	0.68
Oscillatory Main Rotor Pitch Link Axial Force	0.64	1.00	-0.42	0.87	0.81	0.80	0.78
Δ(Longitudinal Cyclic Stick Position)	-0.69	-0.	.00	-0.39	-0.16	-0.65	-0.81
Δ(Lateral Cyclic Stick Position)	0.51	0.87	-0.39	1.00	0.71	0.62	0.80
Engine Torque Pressure	0.58	0.81	-0.16	0.71	1.00	0.71	0.50
Oscillatory Main Rotor Chordwise Bending Moment, Station 135	0.81	0.80	-0.65	0.62	0.71	1.00	0.73
Maximum Mean Normal Load Factor	0.68	0.78	-0.81	0.80	0.50	0.73	1.00

TABLE XIII. SIMPLE CORRELATION COEFFICIENTS GREATER THAN 0.20 FOR OSCILLATING LOADS AT THE TIME OF MAXIMUM MEAN NORMAL LOAD FACTOR - C81 DATA

	Independent Variables										
Dependent Variable	Longitudinal Cyclic Stick Position	Δ(Longitudinal Cyclic Stick Position)	Lateral Cyclic Stick Position	Δ(Lateral Cyclic Stick Position)	Engine Torque Pressure	Pitch Rate	Roll Rate	Yaw Rate	Main Rotor Collective Pitch	Advance Ratio	Maximum Mean Normal Load
Oscillatory Normal Load Factor	-0.32	-0.69	-	0.51	0.58	0.74	-0.64	-0.30	0.36	0.32	0.68
Oscillatory Main Rotor Pitch Link Axial Force	-	-0.42	-	0.87	0.81	0.44	-0.80	-0.44	0.77	0.81	0.77
Oscillatory Main Rotor Chordwise Bending Moment Station 135	-	-0.65	-	0.62	0.71	0.66	-0.74	-0.42	0.58	0.58	0.73

Dashes indicate $|r_{ij}| < 0.20$ and is therefore not significantly different from zero with 95 percent confidence.

TABLE XIV. PARTIAL CORRELATION COEFFICIENTS GREATER THAN 0.265 FOR OSCILLATING LOADS AT THE TIME OF MAXIMUM MEAN NORMAL LOAD FACTOR - C81 DATA

	Independent Variables										
Dependent Variable	Longitudinal Cyclic Stick Position	Δ(Longitudinal Cyclic Stick Position)	Lateral Cyclic Stick Position	Δ(Latsral Cyclic Stick Position)	Engine Torque Pressure	Pitch Rate	Roll Rate	Yaw Rate	Main Rotor Collective Pitch	Advance Ratio	Maximum Mean Normal Load
Oscillatory Normal Load Factor	-	-	-	-	0.50	0.40	-0.40	-	-	-	-
Oscillatory Main Rotor Pitch Link Axial Force	-	-	-	-	0.50	-	-	-	-	0.40	-
Oscillatory Main Rotor Chordwise Bending Moment Station 135	-	-0.41	-	-	0.54	-	-0.45	-	-	-	-

Dashes indicate $|r_{ij.kl...}| < 0.265$ and is therefore not significantly different from zero with 95 percent confidence.

TABLE XV. CUMULATIVE COEFFICIENTS OF DETERMINATION - C81 DATA

Dependent Variable	Independent Variable	Cumulative Coefficient of Determination
Oscillatory Normal Load Factor	Pitch Rate	0.55
	Engine Torque Pressure	0.73
	Maximum Mean Normal Load	0.75
	Roll Rate	0.80
	+ Others	0.83
Oscillatory Main Rotor Pitch Link Axial Force	Δ(Lateral Cyclic Stick Position)	0.76
	Engine Torque Pressure	0.83
	Maximum Mean Normal Load	0.86
	Advance Ratio	0.89
	+ Others	0.91
Oscillatory Main Rotor Chordwise Bending Moment Station 135	Roll Rate	0.55
	Pitch Rate	0.68
	Engine Torque Pressure	0.80
	Δ(Longitudinal Cyclic Stick Position)	0.84
	+ Others	0.88

TABLE XVI. HELICOPTER CONFIGURATION AND ENTRY CONDITIONS FOR SIMULATED FLIGHT TEST MANEUVERS

	Counter 775	Counter 840	Counter 740
Maneuver Type	Symmetric Pullup	Symmetric Pullup	Rolling Pullout
Gross Weight (lb)	7599	9479	7599
Center of Gravity Station Line (in.)	190.75	192.59	190.75
Number of Stores	0	4	0
Entry Condition	Autorotation	Autorotation	Power-on Dive
Advance Ratio	0.209	0.271	0.385
True Airspeed (kn)	93.7	123.0	171.0
Ground Speed (kn)	92.3	120.08	170.3
Rate of Sink (ft/s)	27.5	45.0	26.0
Pressure Altitude (ft)	-	-	2800
OAT (°F)	-	-	66
Collective Stick Position (%)	0.77	0.35	31.3
Engine Horsepower	11.6	50.9	906.1

LITERATURE CITED

1. Spencer, J. L., MEASURED FLIGHT PROFILES FROM UH-1C, UH-1D/H, and AH-1G HELICOPTERS OPERATING IN SOUTHEAST ASIA, Report 204-100-061, Bell Helicopter Company, Fort Worth, Texas, November 15, 1971.

2. Giessler, F. J., Braun, J. F., and Alexander, W. T., COLLECTION AND ANALYSIS OF HELICOPTER COMBAT FLIGHT LOADS DATA FROM AH-1G HELICOPTERS IN SOUTHEAST ASIA, presented at the 26th Annual National Forum of the American Helicopter Society, Washington, D. C., June, 1970.

3. Lewis, R. B., et al., ENGINEERING FLIGHT TEST AH-1G HELICOPTER (HUEY COBRA) MANEUVERING LIMITATIONS FINAL REPORT, USAASTA Project No. 69-11, U. S. Army Aviation Systems Test Activity, Edwards Air Force Base, California, March 1971.

4. Spencer, J. L., RESULTS OF PHASE A STRUCTURAL DEMONSTRATION FLIGHT TEST OF THE AH-1G HELICOPTER, Report 209-099-040, Bell Helicopter Company, Fort Worth, Texas, March 11, 1968.

5. Duhon, J. M., SUBSTANTIATION OF MAXIMUM ROTOR LIFT CAPABILITY, Report 209-099-066, Bell Helicopter Company, Fort Worth, Texas, May 11, 1966.

6. Glass, M. E., Kidd, D. L., and Norvell, J. P., AH-1G DESIGN AND OPERATIONAL FLIGHT LOADS STUDY, USAAMRDL Technical Report 73-41, U. S. Army Air Mobility Research and Development Laboratory, Fort Eustis, Virginia, January 1974, AD775838.

7. Hoel, P. G., INTRODUCTION TO MATHEMATICAL STATISTICS, John Wiley and Sons, New York, 1947.

8. Richmond, S. B., STATISTICAL ANALYSIS, Second Edition, The Ronald Press Company, New York, 1964.

9. Wood, T. L., A TECHNIQUE FOR COMPUTING THE MANEUVERING FLIGHT TRAJECTORIES OF HELICOPTERS, Report 299-099-472, Bell Helicopter Company, Fort Worth, Texas, March 6, 1970.

10. Wood, T. L., and Livingston, C. L., AN ENERGY METHOD FOR PREDICTION OF HELICOPTER MANEUVERABILITY, Report 299-099-557, Bell Helicopter Company, Fort Worth, Texas, December 28, 1971.

LITERATURE CITED - Continued

11. Wells, C. D., and Wood, T. L., MANEUVERABILITY-THEORY AND APPLICATION, presented at the 28th Annual National Forum of the American Helicopter Society, Washington, D. C., May 1972.

12. Wood, T. L., Ford, D. G., and Brigman, G. H., MANEUVER CRITERIA EVALUATION PROGRAM, USAAMRDL Technical Report 74-32, U. S. Army Air Mobility Research and Development Laboratory, Fort Eustis, Virginia, June 1974, AD782209.

13. Bennett, R. L., ROTOR SYSTEM DESIGN AND EVALUATION USING A GENERAL PURPOSE HELICOPTER FLIGHT SIMULATION PROGRAM, AGARD Conference Proceeding 122, Specialists Meeting on Helicopter Rotor Loads Prediction Methods, August 1973.

14. Davis, J. M., et al., ROTORCRAFT FLIGHT SIMULATION WITH AEROELASTIC ROTOR AND IMPROVED AERODYNAMIC REPRESENTATIONS, USAAMRDL Technical Report 74-10A, B, C, U. S. Army Air Mobility Research and Development Laboratory, Fort Eustis, Virginia, June 1974, AD782854, 782756, 782841.

15. Gustafson, F. B., and Myers, G. C., Jr., STALLING OF HELICOPTER BLADES, Technical Note 1083, National Advisory Committee for Aeronautics, Washington, D. C., June 1946.

16. Brown, E. L., and Schmidt, P. S., THE EFFECT OF HELICOPTER PITCHING VELOCITY ON ROTOR LIFT CAPABILITY, Journal of the American Helicopter Society, Volume 8, Number 4, October 1963.

17. Walker, T. L., AH-1G SUBSTANTIATING DATA REPORT, ARMY S/N 66-15246 through 66-15357, PART I, STANDARD AIRCRAFT CHARACTERISTICS, CHARTS FY1966, PHASE B DATA BASIS, Report 209-099-156, Bell Helicopter Company, Fort Worth, Texas, July 15, 1968.

18. Greer, W. W., AH-1J HELICOPTER HYDRAULIC SYSTEM DESIGN REPORT, Report 209-099-181, Bell Helicopter Company, Fort Worth, Texas, January 9, 1969.

19. Seibel, J. K., FATIGUE LIFE SUBSTANTIATION OF DYNAMIC COMPONENTS OF THE AH-1G HELICOPTER, Report 209-099-064, Bell Helicopter Company, Fort Worth, Texas, June 17, 1968.

20. Gessow, A., and Myers, G. C., Jr., AERODYNAMICS OF THE HELICOPTER. Frederick Ungar Publishing Company, New York, 1967.

LITERATURE CITED - Concluded

21. Livingston, C. L., and Murphy, M. R., FLYING QUALITIES CONSIDERATIONS IN THE DESIGN AND DEVELOPMENT OF THE HUEY COBRA, Journal of the American Helicopter Society, Volume 14, Number 1, January 1969.

22. Anon., ENGINEERING DESIGN HANDBOOK, EXPERIMENTAL STATISTICS, SECTION 1, BASIC CONCEPTS AND ANALYSIS OF MEASUREMENT DATA, ACMP 706-110, Headquarters, U. S. Army Materiel Command, 1969.

23. Wani, J. K., PROBABILITY AND STATISTICAL INFERENCE, Appleton-Century Crofts, New York, 1971.

24. Anon., SYSTEM/360 SCIENTIFIC SUBROUTINE PACKAGE, Version III, Programmer's Manual, IBM Manual GH20-0205-4, International Business Machine Corporation, White Plains, New York, 1968.

25. Clinard, R. L., STRUCTURAL ANALYSIS OF 540-011-100-13 HUB AND BLADE ASSEMBLY FOR THE MODEL 209/AH-1J, UH-1C, UH-1E, AH-1G, UH-1L, TH-1L, UH-1M, HH-1K HELICOPTERS, Report 209-099-174, Bell Helicopter Company, Fort Worth, Texas, May 26, 1969.

26. Oldenbuttel, R. H., A LOW SPEED WIND TUNNEL TEST OF THE .125 SCALE BELL HELICOPTER MODEL 209 INVESTIGATING AERODYNAMIC CHARACTERISTICS, Report LSWT269, LTV Aerospace Corporation, Vought Aeronautics Division, Dallas, Texas, May 23, 1968.

27. Wettengell, W. O., MODEL AH-1G NONFIRING LOAD LEVEL SURVEY, Report 209-099-041, Bell Helicopter Company, Fort Worth, Texas, May 20, 1967.

28. Adaska, W. W., QUALIFICATION LOAD LEVEL SURVEY FOR IMPROVED MAIN ROTOR BLADES ON THE MODEL AH-1G HELICOPTER P.I.P. TASK NO. UH/AH-8-69, Report 209-099-305, Bell Helicopter Company, Fort Worth, Texas, June 5, 1970.

29. Finnestead, R. L., et al., ENGINEERING FLIGHT TEST AH-1G HELICOPTER (HUEY COBRA), PHASE D, PART 2, PERFORMANCE, FINAL REPORT, USAASTA Project No. 66-06, U. S. Army Aviation Test Activity, Edwards Air Force Base, California, April 1970.

APPENDIX I
STATISTICAL ANALYSIS

The classical techniques of linear regression analysis and statistical inference are presented in detail in works such as References 7, 8, 22, and 23. The discussion given here is intended to describe the modifications required to analyze a body of data containing incomplete sets of observations. The description includes an explanation of the quantities computed in Bell Helicopter Company Program JRSW03. This program is based on IBM Scientific Subroutine Package (SSP) program STEPR, and SSP subroutine MISR (Reference 24).

Given a sample containing m observations of n variables, and representing each variable as

$$x_{ij}; \quad i=1,2,\ldots,m; j=1,2,\ldots,n$$

The mean value, $\bar{x}_j$, of the j^{th} variable is defined as

$$\bar{x}_j = \frac{\sum_{i=1}^{m} x_{ij}}{M_j}$$

where M_j is the total number of values observed for the j^{th} variable ($M_j \leq m$). No value is entered in the summation for those values of i for which x_{ij} is unavailable. Defining the deviation as

$$d_{ij} = x_{ij} - \bar{x}_j$$

with $d_{ij} = 0$ when x_{ij} is unavailable, the standard deviation of the sample, s_j, is

$$s_j = \sqrt{\frac{\sum_{i=1}^{m} (d_{ij})^2}{M_j}}$$

When the sample is large, the standard deviation of the population, σ_j, can be estimated from s_j as follows:

$$\sigma_j = s_j \sqrt{\frac{M_j}{M_j - 1}}$$

JRSW03 prints out this estimate for the standard deviation and uses it throughout the calculations.

The correlation coefficient for the k^{th} and p^{th} variables, r_{kp}, is computed as

$$r_{kp} = \frac{\sum_{i=1}^{m} d_{ik}\, d_{ip}}{\sqrt{(M_k-1)(M_p-1)}\,\sigma_k\,\sigma_p}$$

No value is entered in the summation for a given value of i if the value of x_{ik} or x_{ip} is unavailable.

If the matrix of the simple correlation coefficients, r_{kp}, is $\bar{R}$, its determinant is R, and R_{kp} is the cofactor of r_{kp}, then the multiple correlation coefficient of the i^{th} variable, with respect to all other variables is

$$R_{i.jkl...} = \sqrt{1 - \frac{R}{R_{ii}}}$$

If only one dependent and one independent variable are analyzed at a time, the multiple correlation coefficient is equal to the absolute value of the correlation coefficient for that pair of variables, i.e.,

$$R_{i.j} = |r_{ij}|$$

If more than one independent variable is introduced in the analysis, the degrees of freedom of the data are reduced. JRSW03 is capable of correcting the multiple correlation coefficient for this reduction and prints out an adjusted multiple correlation coefficient. With only one independent variable, the two quantities are the same.

The standard error of estimate is

$$\sqrt{\frac{(1-R^2_{i.jkl...})(M_j-1)\sigma_j^{\,2}}{N}}$$

The denominator in this expression, N, is the total number of observations reduced by the number of independent variables introduced, q, plus one,

$$N = M_j - (q+1)$$

A regression hyper-plane can be determined for any sample containing three or more variables. If any two variables (x_{ik}, x_{ip}; i-1, 2,...m) are taken at a time, a regression line can be determined in the plane formed by the two variables. The regression line is the least squares curve fit line, and its slope (m_{kp}, the regression coefficient) and intercept (b_k) are computed as

$$m_{kp} = r_{kp}\left(\frac{\sigma_k}{\sigma_p}\right) \qquad b_k = -m_{kp}\,\bar{x}_p + \bar{x}_k$$

The standard error of the regression coefficient is equal to the square root of the cross product of the deviations of the independent and dependent variables, divided by the number of observations for which both variables are available. If $M_j < M_k$, then the standard error of the regression coefficient is

$$\frac{1}{M_j}\sqrt{\sum_{i=1}^{m} d_{ij}\,d_{ik}}$$

The square of the multiple correlation coefficient is the proportion of the variation of the dependent variable explained by the variation of the independent variables. The variation remaining in the dependent variable is the total variation reduced by $R^2_{i.jkl...}$. The variation, or variance, is σ_j^2 and the sum of the squares of the deviation is $(M_j-1)\sigma_j^2$. JRSW03 computes the amount by which the sum of the squares has been reduced and prints it out as the "sum of squares reduced in this step." This term is equal to

$$R^2_{i.jkl...}(M_j-1)\sigma_j^2$$

while the "proportion reduced in this step" is $R^2_{i.jkl...}$. If more independent variables are introduced in another step, then the "sum of the squares reduced in this step" and "proportion reduced in this step" are quantities based on only the independent variables introduced in that step. The "cumulative sum of the squares reduced" and the "cumulative proportion reduced" are based on all the independent variables introduced through that step.

The computed t-value is

$$t_{comp} = \frac{|r_{kp}|\sqrt{M_j-2}}{\sqrt{1-r_{kp}^2}}$$

and is used to determine the significance of the sample correlation coefficient as a measure of the population correlation coefficient.

APPENDIX II
CALIBRATION OF C81 INPUT DATA

The Rotorcraft Flight Simulation Program C81 has been under development for the past decade. The latest version of this program, AGAJ7402, was used throughout this project. A description of the analysis incorporated in the program and an input guide are in Reference 14. The purpose of this appendix is to discuss the inputs that were used and to show the correlation between experimental data and the results of the C81 simulation.

INPUT DATA

A listing of the inputs to the program for the AH-1G is given in Table XVII. The inputs control the program options used in the analysis, provide the physical parameters of the helicopter and describe the desired flight conditions. Since the values of the majority of the inputs can be determined in a straightforward manner, the discussion will be limited to the derivation of those variables which are peculiar to the AGAJ7402 version of the program or which were changed to enhance the calibration between computed and experimental data.

Logic Control Variables

The inputs in the Program Logic Group and Iteration Logic Group govern the operation of the program. The user determines the mathematical representation of the helicopter that he wants and the different types of analysis to be applied to this model and sets the values in the two logic groups accordingly. The first 14 entries in the Program Logic Group control which input groups are read by the program. For the AH-1G model, the nonzero or activated read options are:

Variable	Input Groups to be Read
IPL(2) = 1	1 Airfoil Data Table
IPL(3) = 5	5 Mode Shapes
IPL(6) = 2	2 Rotor Airfoil Aerodynamic Subgroups
IPL(9) = -1	Wing Group (without control linkages)
IPL(10) = 3	3 Stabilizing Surface Groups (with control linkages)

In addition, if the configuration being simulated has external stores, the value of IPL(12) is set equal to the number of stores and that number of Stores Subgroups is input. (See Table XVIII for a listing of the Stores Group for 4 empty XM-159 rocket pods.)

The next ten values of the Program Logic Group control the use of options in the mathematical analysis. The options selected are:

Variable	Option
IPL(16) = 1	Yaw angle is held constant in trim
IPL(18) = 1	Main rotor steady-state aerodynamics are computed according to Rotor Airfoil Aerodynamic Subgroup 1, and the airfoil has a constant section root to tip
IPL(19) = 2	Tail rotor steady-state aerodynamics are computed according to Rotor Airfoil Aerodynamic Subgroup 2, and the airfoil has a constant section root to tip
IPL(20) = -1	Bell unsteady aerodynamics model is used for main rotor
IPL(21) = 1	Time variant rotor analysis is used for main rotor

The simulation of the left rolling pullout maneuver (counter 740, flight 116-B) had to be initiated with a fully time-variant trim. For this case, IPL(22) was set to 2.

Additional output is selected by setting the values of IPL(25) and IPL(26) to 1. This latter selection yields the optional trim page which contains the nondimensional flight parameters, such as C_T/σ.

The Iteration Logic Group contains inputs which are used in, and control, the numerical solution procedure. XIT(1) sets the maximum number of iterations allowed to trim the helicopter. The value of 41 was selected so that a partial derivative matrix would be available from the last iteration should a trim condition not be reached in 41 iterations. The azimuth increment for the time-variant trim procedure, XIT(2), was input as 10 degrees to satisfy the Runge-Kutta stability requirement of at least 10 cycles of the highest harmonic per rotor revolution. The next 12 entries in this group (XIT(3) through XIT(14)) are inputs to numerical dampers which govern the stability of the numerical procedure. The values used have been found to give good results.

The last seven inputs to the Iteration Logic Group are the allowable errors for the trim procedure. At the end of each trim iteration, the net forces and moments on the aircraft center of gravity and the flapping moments on both rotors are computed. For a trimmed flight condition, these net forces and moments should be zero, but this is almost impossible to achieve because the solution process is numerical. In C81, the aircraft is considered trimmed if the absolute values of the net forces and moments are less than the values input for the allowable errors. The allowable errors used for this study give solutions very close to trim with a moderate number of iterations.

Physical Parameters of the Helicopter

The majority of the inputs to the program provide a physical description of the helicopter. The inputs are made in separate groups for each of the major components of the aircraft. The groups will be discussed in the order in which they are input.

CLCD5474 is the rotor airfoil aerodynamic table. The table entries for moderate angles of attack for Mach numbers between 0.3 and 0.8 were determined from wind-tunnel test data for a two-dimensional 540 rotor airfoil section (9.33 percent symmetric). The values at extreme angles of attack and Mach numbers of zero and one are those of an NACA 0012 and intermediate values were determined by fairing the 540 values into the 0012 values. The resulting airfoil table is given in Table XIX.

MODE540A contains the information necessary to compute the main rotor dynamic response. The constituents of this group are the mass, ρI_x and ρI_y distributions, and the five main rotor mode shapes. The frequency, damping ratio, and mode type indicator for each mode are also input in this group. C81 prints out all these data, plus several computed properties such as bending moment coefficients, as given in Table XX.

The mode shapes and their natural frequencies are computed by the Myklestad program (DF1758). The inputs used to generate the 540 rotor mode shapes are given in Table XXI. The blade stiffness, I_{BB} and I_{CC} distributions have been determined analytically. Three-hundred-twenty-four is the nominal main rotor operating rpm and 16 degrees root collective pitch angle was chosen because it was a representative value for the flights to be simulated. The control system stiffness is the measured static value.

The mass distribution input to the Myklestad program differs from the one input to C81. The latter is the mass distribution for the blade as given in Reference 25, while the former is the

one which gives the best match of beam and chord natural frequencies when compared with the results of ground runup tests. The dynamic pylon model in C81 was not used and the inplane hub impedance was simulated in the Myklestad program by inputting a value for HSOFT. The value of $-6.5/(10^6$ lb) gives a first inplane natural frequency of 1.507 per rev which agrees with the value determined in the ground runup tests. The blade shear center distribution is not known and was accordingly input as zero. Since the airfoil section is structurally symmetric, the beamwise cg offset is zero. The inplane cg offset also differs from that given in Reference 25, but in conjunction with the input mass distribution, control system stiffness and GJ distribution, gives a good match of blade torsional response, as determined by the computed natural frequency and the C81 computed pitch link loads.

The Myklestad program computes natural frequencies and mode shapes for three different sets of hub boundary conditions, as follows:

Mode Type	Hub Boundary Conditions		
	Out-of-Plane	Inplane	Torsion
Cyclic	Cantilevered	Pinned	Cantilevered
Collective	Pinned	Cantilevered	Cantilevered
Scissor	Cantilevered	Cantilevered	Cantilevered

As pointed out by Bennett (Reference 13), the proper modes to use for a teetering rotor are a mix of cyclic and collective modes. For the current study, the first three cyclic modes and the first and third collective modes were selected. The second out-of-plane collective mode was excluded because it is very similar in frequency and deflections to the second out-of-plane cyclic mode and its inclusion changes the computed beam and chord bending moments to a great extent. Either the cyclic or collective torsion mode can be selected for the torsion mode. Its mode type indicator was changed to independent because the blade will respond torsionally to any integer harmonic forcing function. Also, the damping ratio for this mode was raised from the 0.02 structural damping ratio of the other modes to 0.10 critical to include the damping of the control system.

The mass and aerodynamic properties of the fuselage are given in the Fuselage Group. The mass properties are for the whole aircraft without any external stores, while the aerodynamic properties are for the fuselage alone, i.e., without rotors, wing, stabilizing surfaces, or external stores. The gross weight and center-of-gravity stationline and buttline (XFS(1),

XFS(5), and XFS(7)) are determined by weighing the aircraft while the center-of-gravity waterline and moments and product of inertia are to be calculated using the mass properties of each component of the helicopter. The mass properties in the basic fuselage group used in this analysis are those of the light gross weight, aft cg Huey Cobra. Different configurations were modeled by adding external stores in the stores group or changing the mass properties with an &CHANGE card.

The fuselage aerodynamic properties were computed from wind-tunnel test data (Reference 26) by using computer program AS812A. The fuselage reference center (XFS(2), XFS(3), and XFS(4)) corresponds to the balance reference center used in the wind-tunnel tests.

The first Rotor Airfoil Aerodynamic Subgroup of the Rotor Aerodynamic Group describes the main rotor aerodynamics while the second subgroup gives the tail rotor aerodynamics. The main rotor airfoil table, CLCD5474, is selected by the unitary value of YRR(18) and the yawed flow model is determined by the values of XMR(20), XMR(21), and XMR(28). The remainder of the values in this subgroup supplement the information given in the table, as described in the User's Guide (Reference 14). The tail rotor information in the second subgroup is a direct carryover of the values used in previous versions of the program and represents the tail rotor well.

The Main Rotor Group and Tail Rotor Group give the nonaerodynamic properties of the rotors and all the properties of the rotor mast and pylon. The majority of these values can be determined by direct measurement from detailed drawings of the aircraft. The pylon equivalent flat plate drag areas are estimated and the main rotor hub drag is included in the pylon drag, so the main rotor hub drag coefficient is set to zero. Blade response and bending moments are printed out in maneuver for the segment number input in XMR(15). It should be noted that for printout purposes, segment 20 is the hub, while segment 1 is the hub for the plots. (This can be confusing, thus the program will be modified so that segment 1 is the hub for both printout and plots.)

The geometric and aerodynamic properties of the wing, elevator, and fin are given in the Wing Group and Stabilizing Surface Groups. These properties are either measured or computed in a straightforward manner and require no further discussion.

If the helicopter configuration being simulated has external stores, the Stores Group is included. The data in this group represent four empty XM159 stores. The aerodynamic properties were calculated by assuming that the stores are right circular cylinders and all wing-store interference drag is included in the store drag properties.

The control linkages input in the Controls Group are those reported in Reference 27.

Flight Conditions

The desired flight conditions are input in the Flight Constants Group and, in a maneuver, may be modified by the use of "J-cards" (see section 3.21, Reference 14). The speed inputs (XFC(1) through XFC(3)) are in ground reference and are added vectorally to give the true airspeed. An altitude input (at XFC(4)) less than 1.5 rotor diameters turns on the ground-effect calculations of the program. The next seven inputs (XFC(5) through XFC(11)) give the approximate aircraft attitude and control positions for the initial iteration in the trim procedure. The rotor flapping angles and thrust (XFC(15) through XFC(20)) are also approximations for the initial iteration. (If these values are too far from the trimmed flight values, the program may not converge to a solution in the 41 iterations allowed.) The engine horsepower input (XFC(24)) is 1246 because the program assumes a 9-percent loss, leaving 1134 horsepower available for the rotors, which is the gearbox limit at 6600 engine rpm (XFC(25)). The values of XFC(26) through XFC(28) are used to compute the density ratio and speed of sound for the flight condition, as described in the User's Guide (Reference 14).

COMPARISON OF FLIGHT TEST AND COMPUTED DATA

Four different series of AH-1G level flight tests were simulated with C81 to demonstrate the ability of the mathematical model to represent the helicopter. The aircraft configurations and flight conditions for the four flights are given in Table XXII. Insufficient information was available to determine the waterline location of the center of gravity. Several trial values were used and a value of 60 inches for flights 34 and 40, and 68 inches for flights 277 and 280, were found to give the best overall pitch attitude correlation (Figure 35). The computed pitch attitudes agree very well with the measured values for flights 34, 40, and 277. The measured pitch attitude values for flight 280 show a slight nose-up trend with forward speed which is clearly contradicted by the measured data of the other three flights. The computed pitch attitude data for this flight show the proper trend.

The measured and computed horsepower data agree very well (Figure 36). The horsepower required at high speeds in C81 is somewhat greater than that measured for flights 34 and 40, but it should be noted that the measured horsepower required at $\mu = 0.314$ for flight 40 indicates that the helicopter is most likely in a dive. The fuselage and pylon equivalent flat plate drag areas had to be increased for flight 277 (to 8.7 and 6.7

square feet, respectively) to get the correlation shown. Also, the equivalent flat plate drag area of the pylon had to be increased to 7.4 square feet to get the horsepower correlation shown for flight 280. These changes in drag area for configurations with a forward center of gravity are documented in Reference 29. The additional drag was not necessary for flights 34 and 40, which were flown with the center of gravity further aft. Figures 37 through 40 show the measured and computed control displacements for the four flights. In all cases, the data trends correlate excellently. The discrepancies in absolute displacements can be due to differences between the actual and reported control gearings and lost motion in the control system. Since there is no lost motion between the collective stick and the swashplate in C81, the program is computing a lower collective stick position than that measured in flight.

The oscillatory pitch link axial force is computed by dividing the root torsional bending moment by the pitch horn radius. The comparison between computed and measured oscillatory pitch link axial force is presented in Figure 41. The correlation is excellent for flights 34 and 40 and good for flights 277 and 280. When the estimated breakout friction of the pitch bearings is taken into consideration, the correlation improves for flights 40, 277, and 280, and the loads predicted for flight 34 are over-conservative. The slight downward trend of the computed oscillatory pitch link axial force at $\mu = 0.28$ is unexpected, but the test data show a similar trend.

Correlation between computed and measured oscillatory chordwise bending moments is somewhat hampered by the scatter in the test data. The jump in measured loads in the speed range of 80 to 100 knots (Figure 42) is due to wake crossing which is known to occur at these speeds. This phenomenon cannot yet be simulated in C81 due to the lack of data to input to the wake model. There is still a good deal of scatter in the data in addition to the jump due to wake crossing. The trend of the computed and measured chordwise bending moments agrees quite well for flight 34, and there is a good match of the actual curves for flight 280.

The computed chordwise bending moments for flight 40 agree very well with the measured values at low speeds but increase at a greater rate at high speeds. This discrepancy in slopes would be explained if the aircraft was actually in a dive for the higher speed test points, as was assumed in the discussion of horsepower. In a dive, the rotor has to provide less propulsive force at any given airspeed and will not be as close to stall at the higher speeds, thereby lowering the drag on the rotor blades and the chordwise bending moments.

For flight 277, the computed oscillatory chordwise bending moment, station 60, is within the scatter band of the test data. The loads computed at station 135 and 160 are close to those measured in flight (Figure 43).

The computed oscillatory beamwise bending moments compare favorably with those measured in flight (Figure 44), and the correlation at station 60 for flights 34 and 280 is excellent.

The correlation for the moments at station 60 for flights 40 and 277 is good, and the computed loads at station 160 for all flights follow the trends of the measured data (Figure 45).

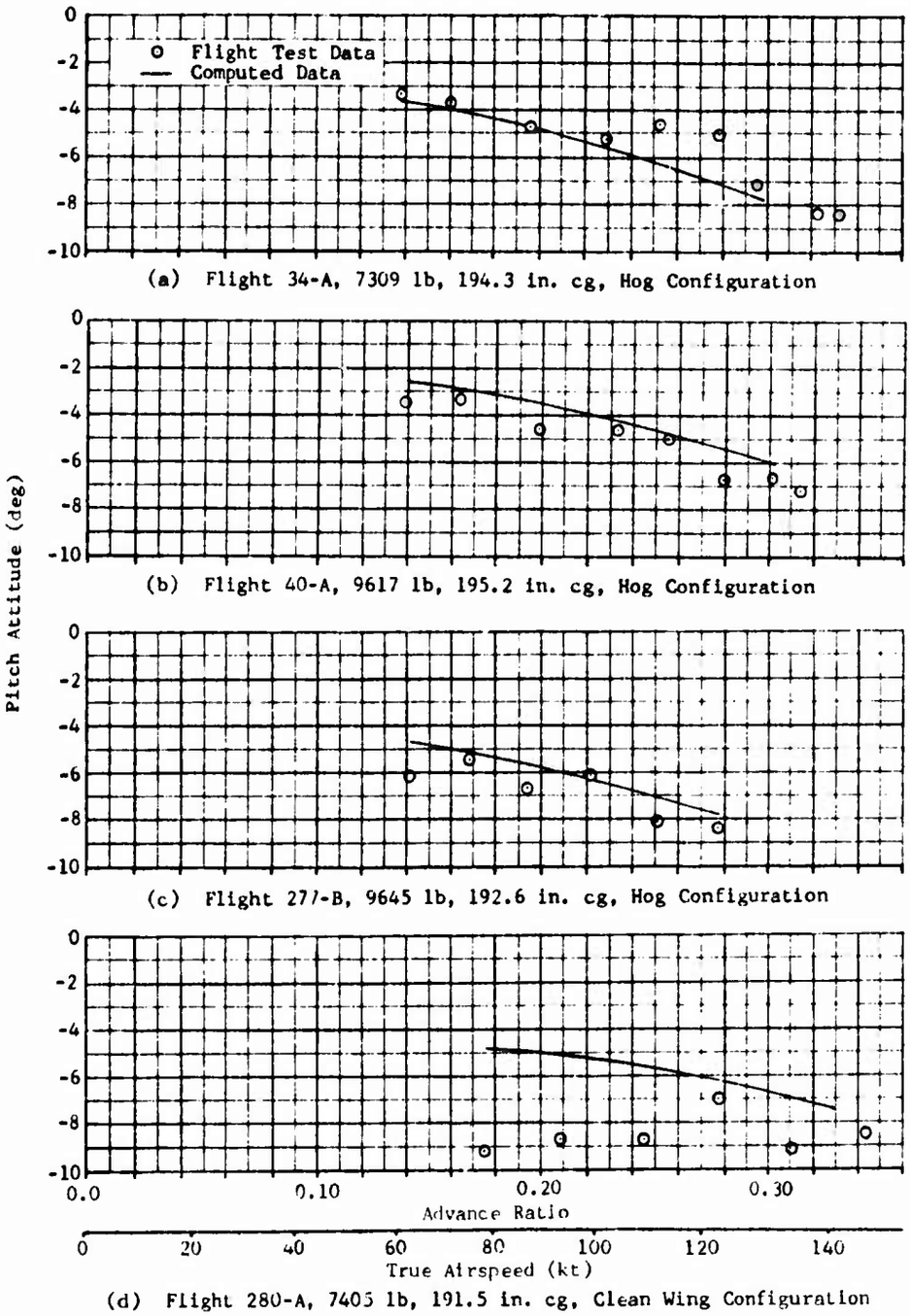

Figure 35. Comparison of Measured and Computed Pitch Attitude.

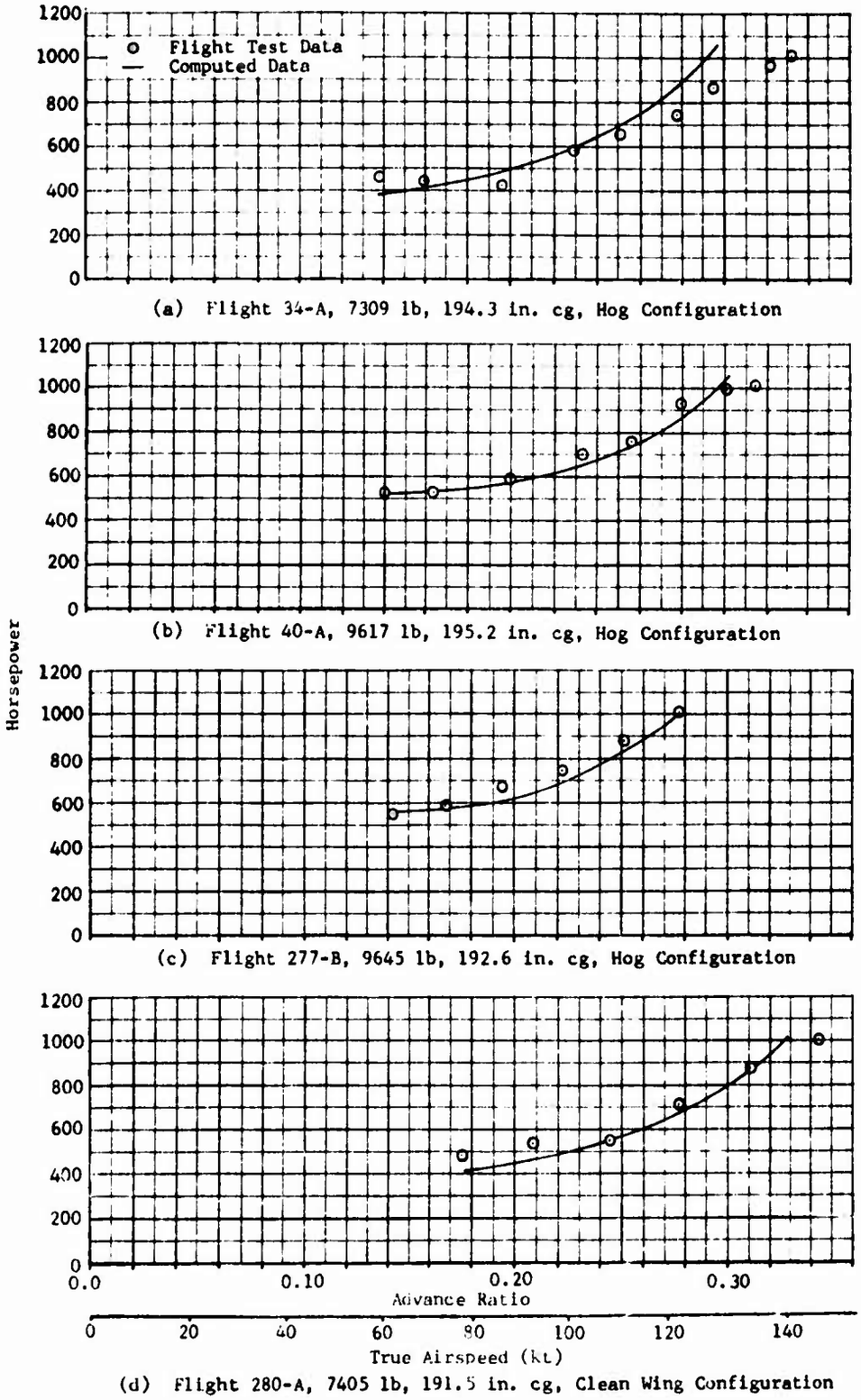

(a) Flight 34-A, 7309 lb, 194.3 in. cg, Hog Configuration

(b) Flight 40-A, 9617 lb, 195.2 in. cg, Hog Configuration

(c) Flight 277-B, 9645 lb, 192.6 in. cg, Hog Configuration

(d) Flight 280-A, 7405 lb, 191.5 in. cg, Clean Wing Configuration

Figure 36. Comparison of Measured and Computed Engine Shaft Horsepower.

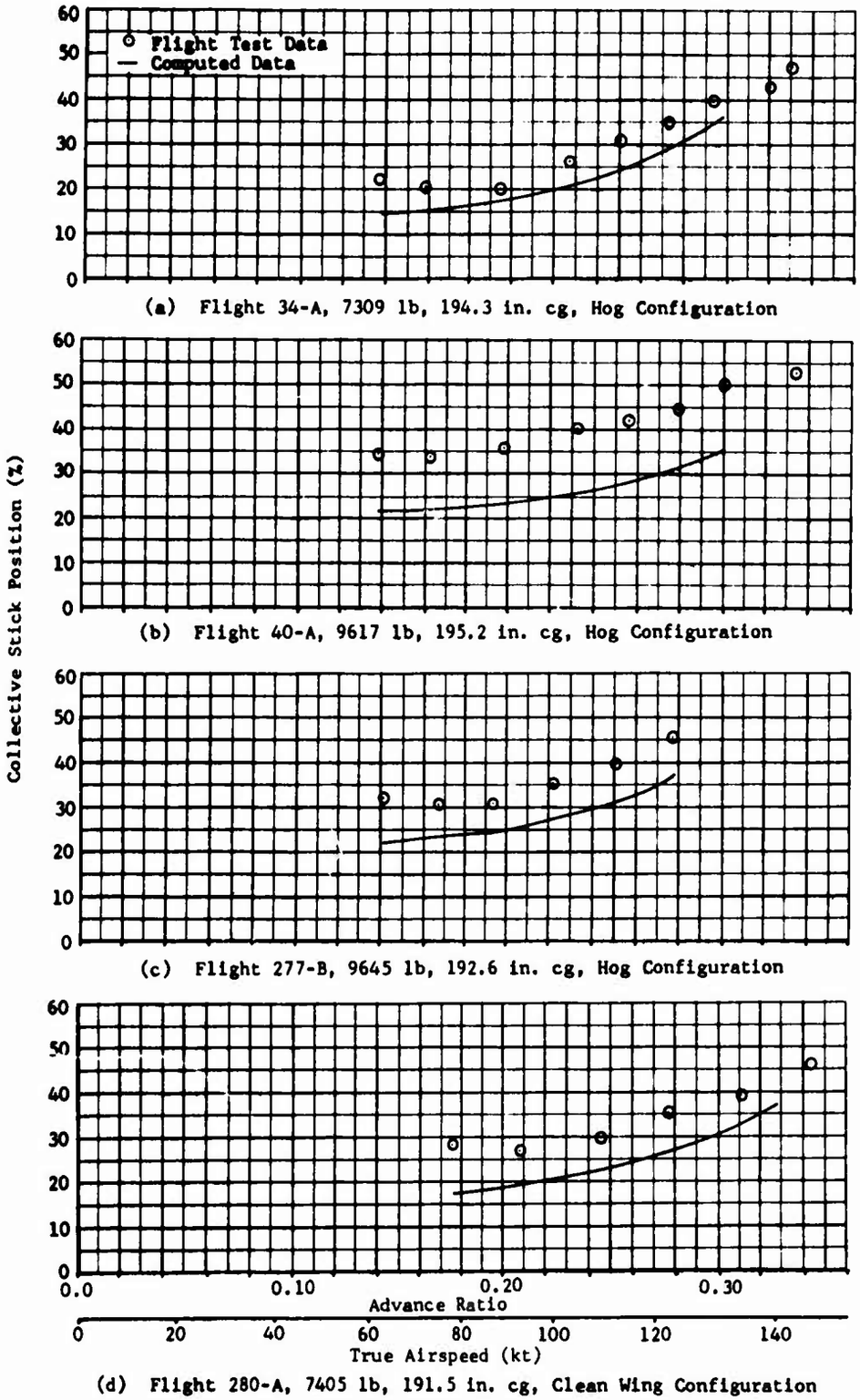

(a) Flight 34-A, 7309 lb, 194.3 in. cg, Hog Configuration

(b) Flight 40-A, 9617 lb, 195.2 in. cg, Hog Configuration

(c) Flight 277-B, 9645 lb, 192.6 in. cg, Hog Configuration

(d) Flight 280-A, 7405 lb, 191.5 in. cg, Clean Wing Configuration

Figure 37. Comparison of Measured and Computed Collective Stick Position.

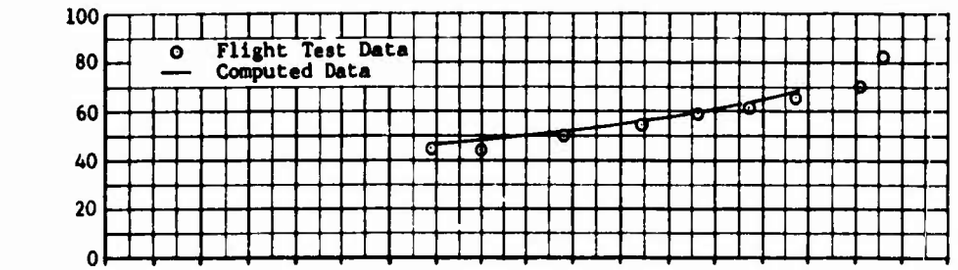

(a) Flight 34-A, 7309 lb, 194.3 in. cg, Hog Configuration

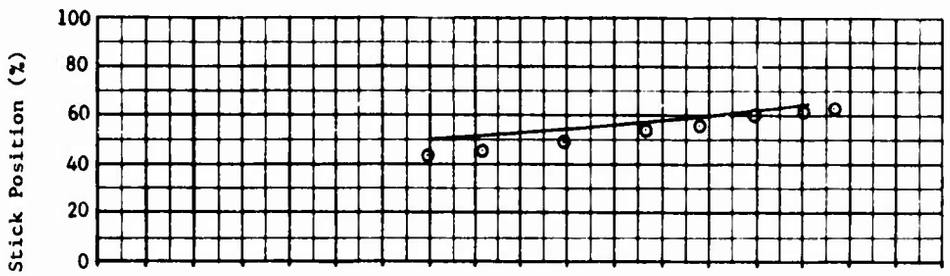

(b) Flight 40-A, 9617 lb, 195.2 in. cg, Hog Configuration

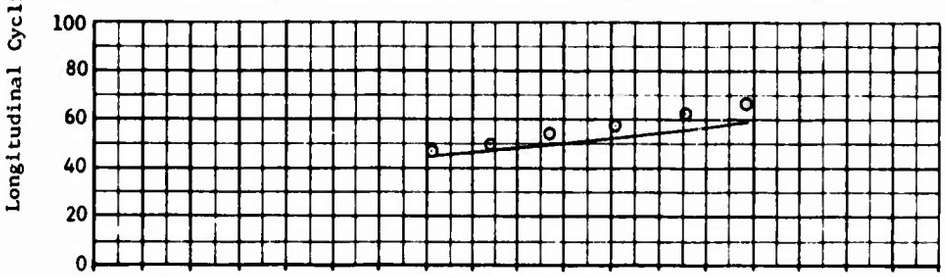

(c) Flight 277-B, 9645 lb, 192.6 in. cg, Hog Configuration

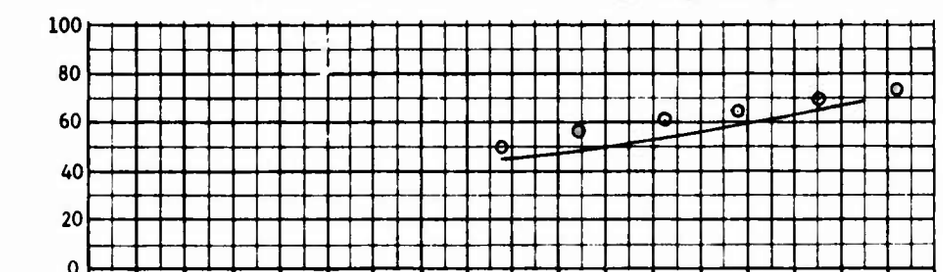

(d) Flight 280-A, 7405 lb, 191.5 in. cg, Clean Wing Configuration

Figure 38. Comparison of Measured and Computed Longitudinal Cyclic Stick Position.

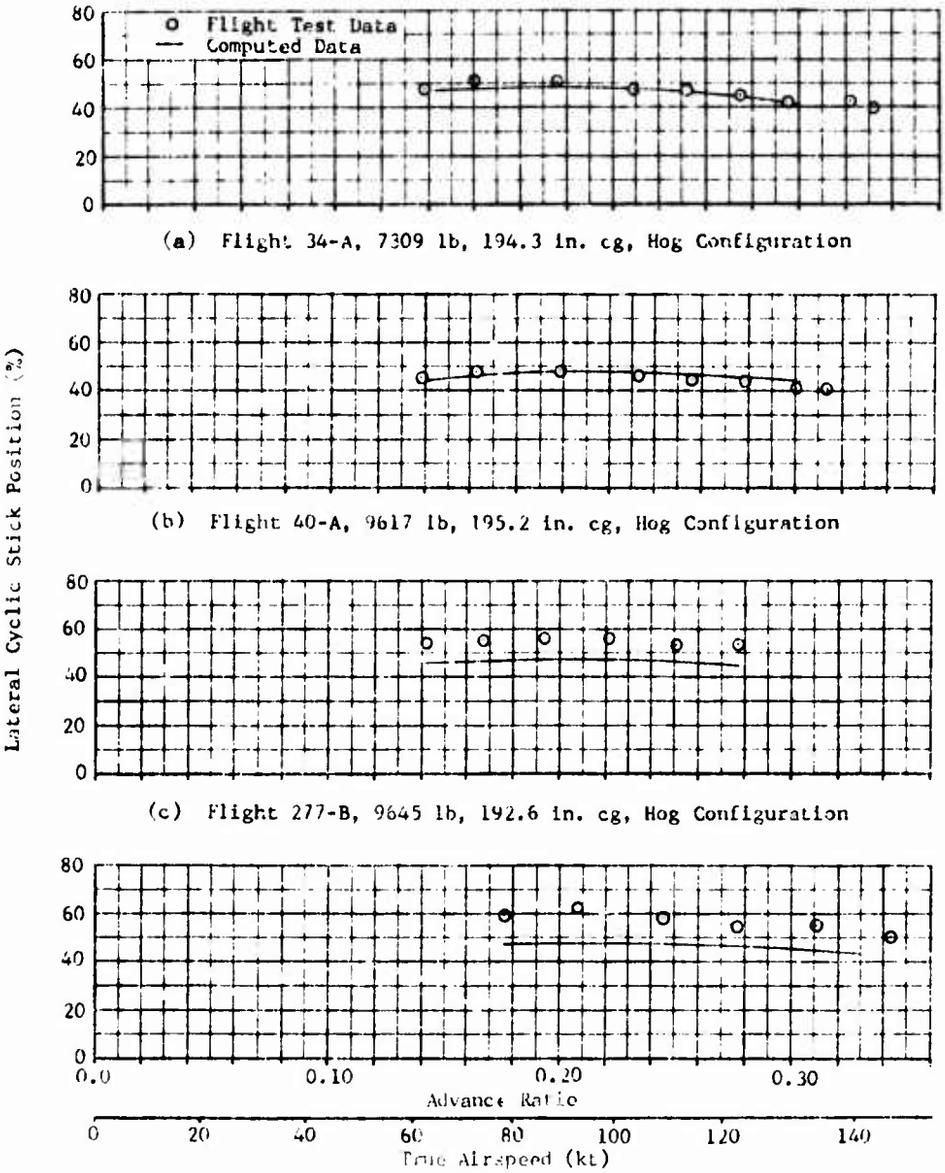

(a) Flight 34-A, 7309 lb, 194.3 in. cg, Hog Configuration

(b) Flight 40-A, 9617 lb, 195.2 in. cg, Hog Configuration

(c) Flight 277-B, 9645 lb, 192.6 in. cg, Hog Configuration

(d) Flight 280-A, 7405 lb, 191.5 in. cg, Clean Wing Configuration

Figure 39. Comparison of Measured and Computed Lateral Cyclic Stick Position.

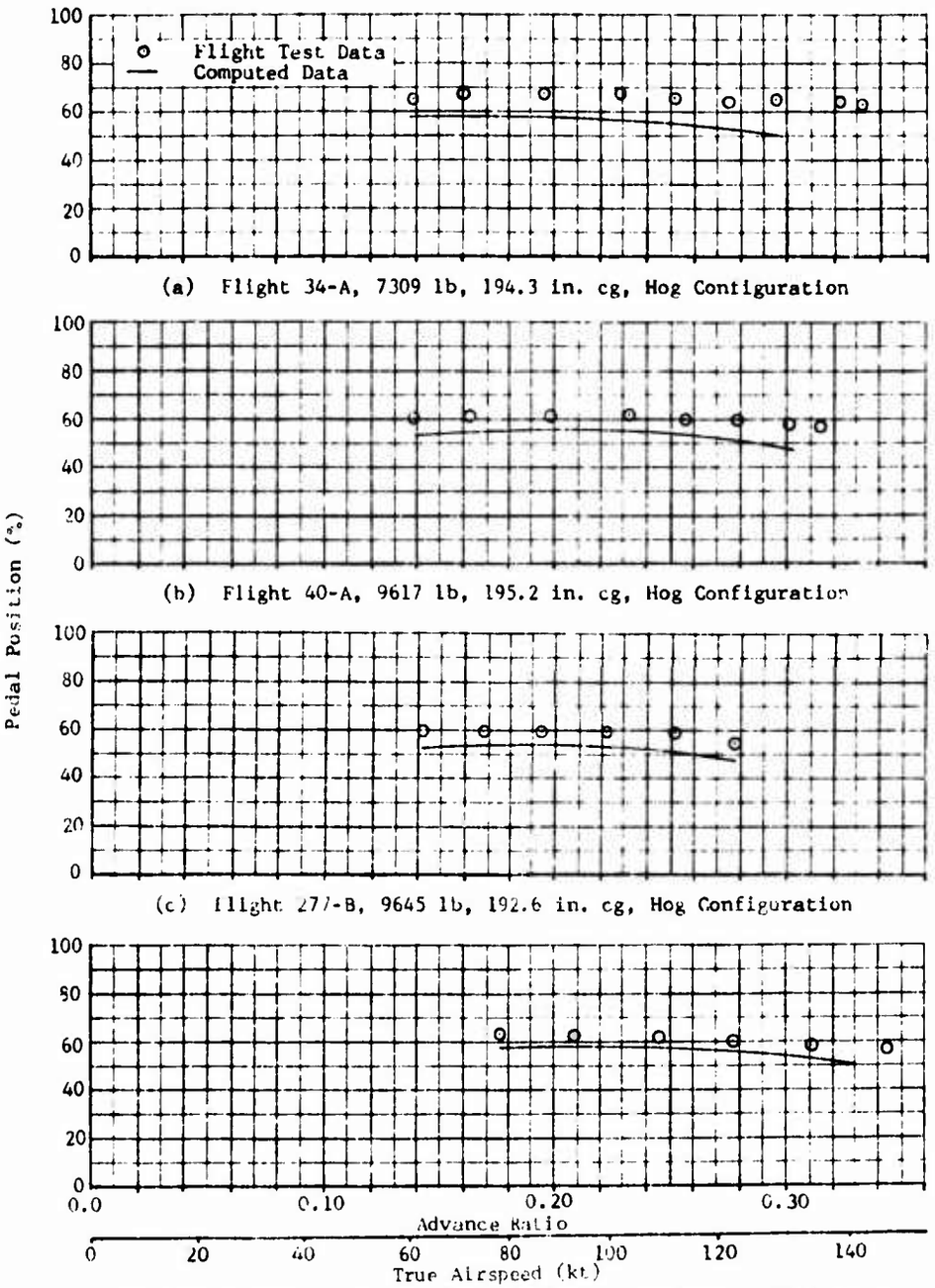

(a) Flight 34-A, 7309 lb, 194.3 in. cg, Hog Configuration

(b) Flight 40-A, 9617 lb, 195.2 in. cg, Hog Configuration

(c) Flight 277-B, 9645 lb, 192.6 in. cg, Hog Configuration

(d) Flight 280-A, 7405 lb, 191.5 in. cg, Clean Wing Configuration

Figure 40. Comparison of Measured and Computed Pedal Position.

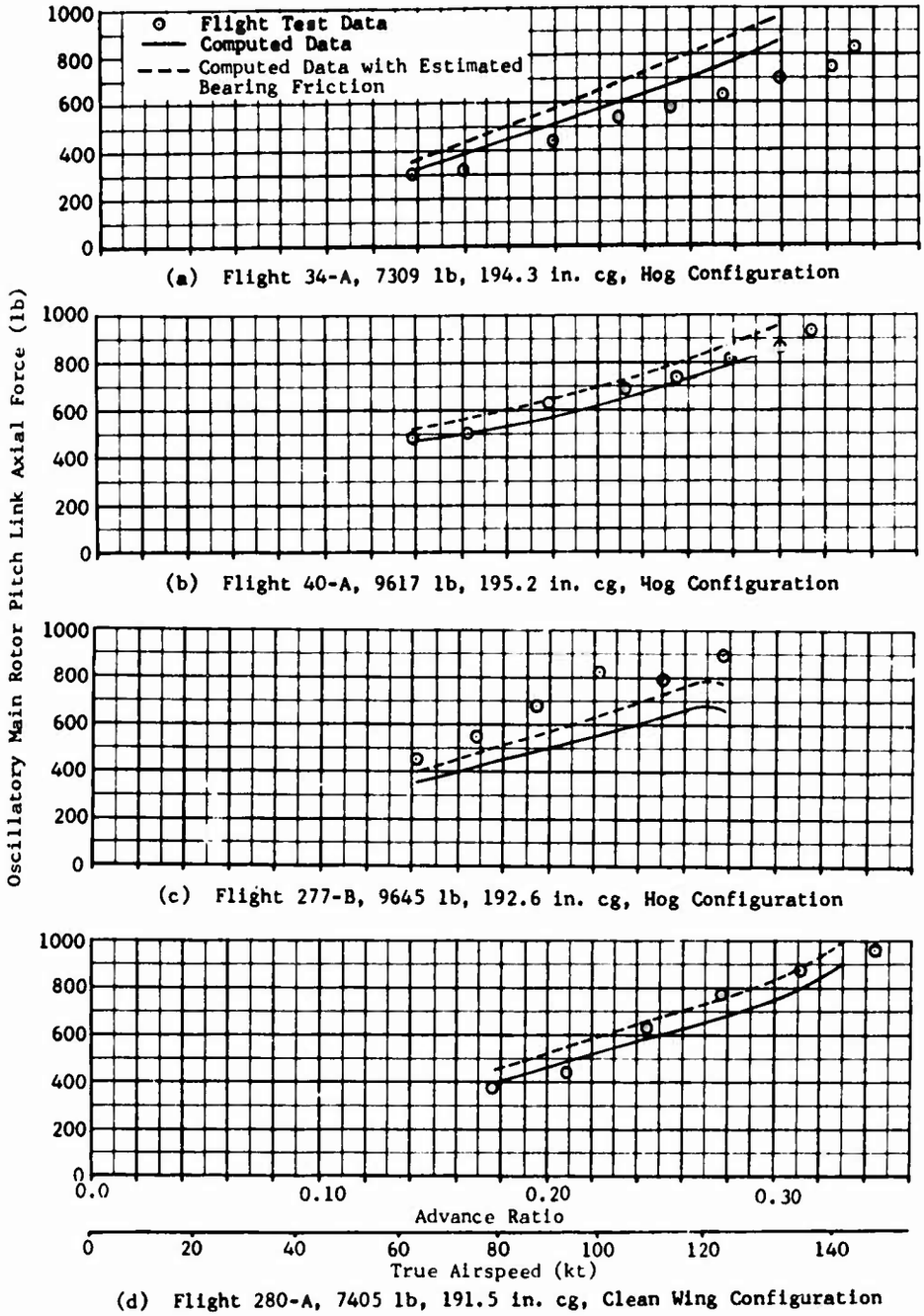

Figure 41. Comparison of Measured and Computed Oscillatory Main Rotor Pitch Link Axial Force.

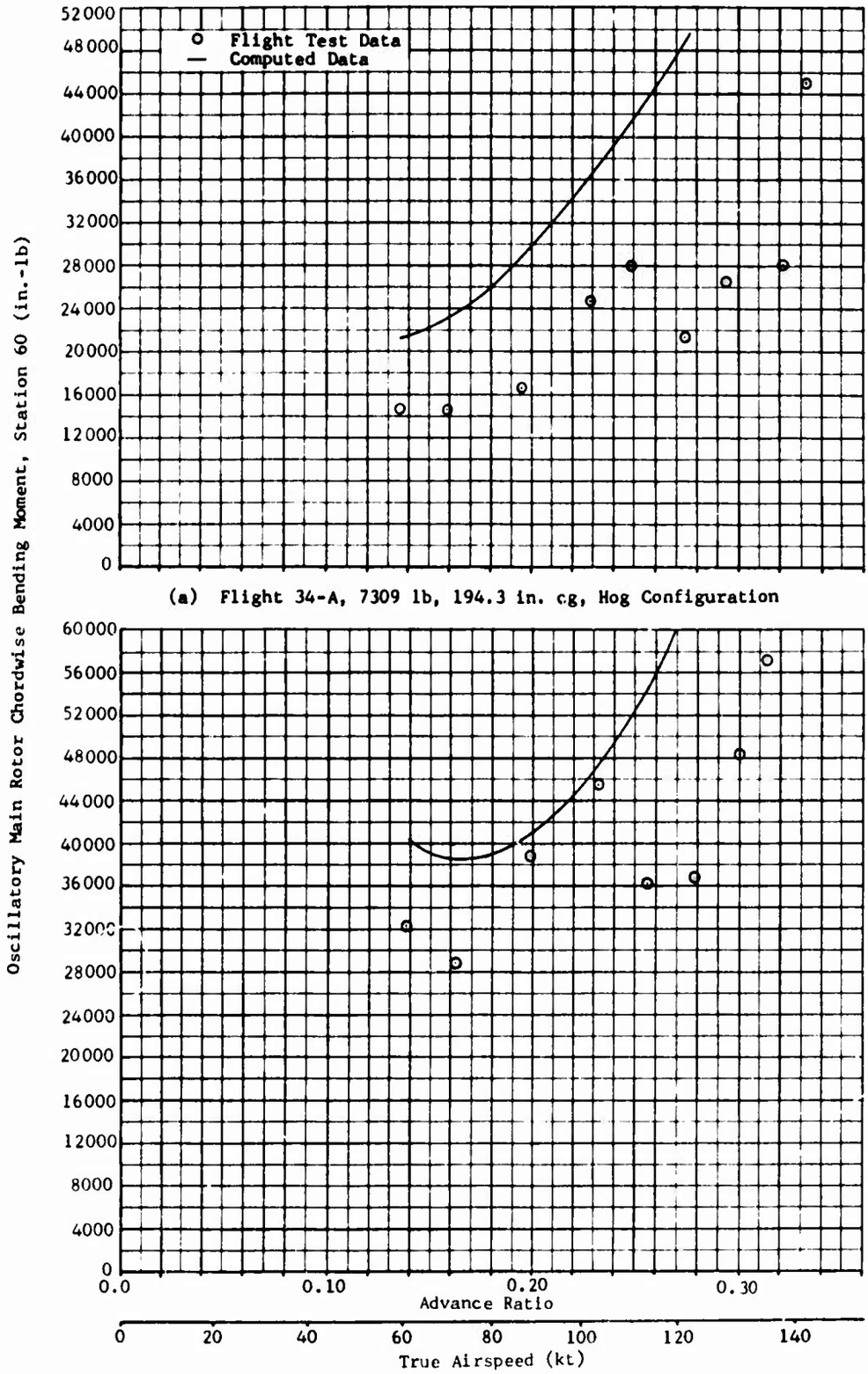

(a) Flight 34-A, 7309 lb, 194.3 in. cg, Hog Configuration

(b) Flight 40-A, 9617 lb, 195.2 in. cg, Hog Configuration

Figure 42. Comparison of Measured and Computed Oscillatory Main Rotor Chordwise Bending Moment, Station 60.

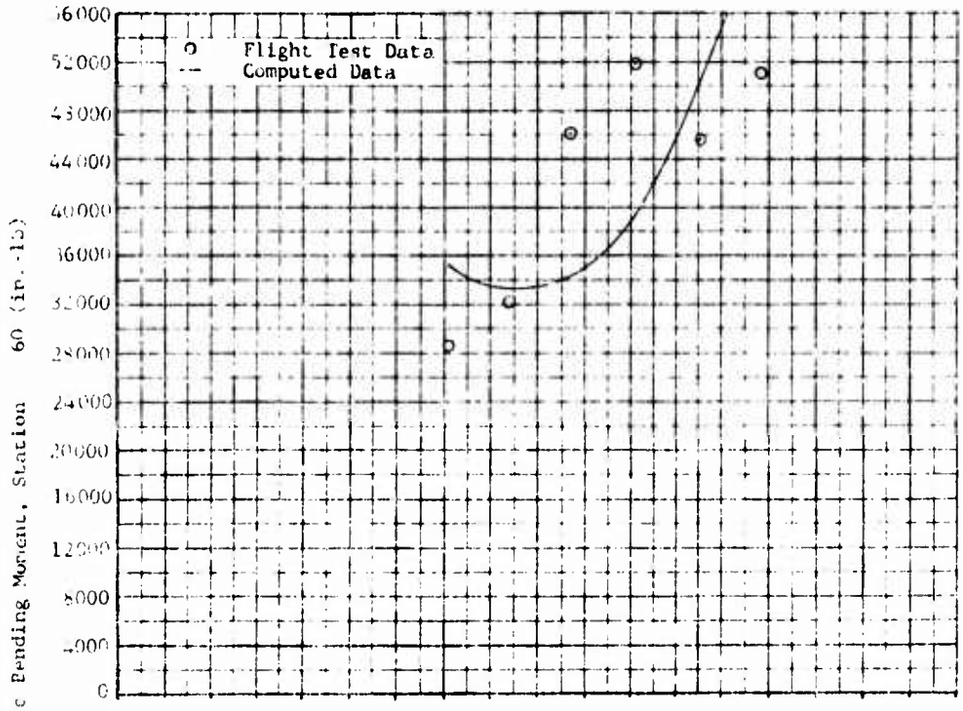

(c) Flight 277-B, 9645 lb, 192.6 in. cg, Hog Configuration

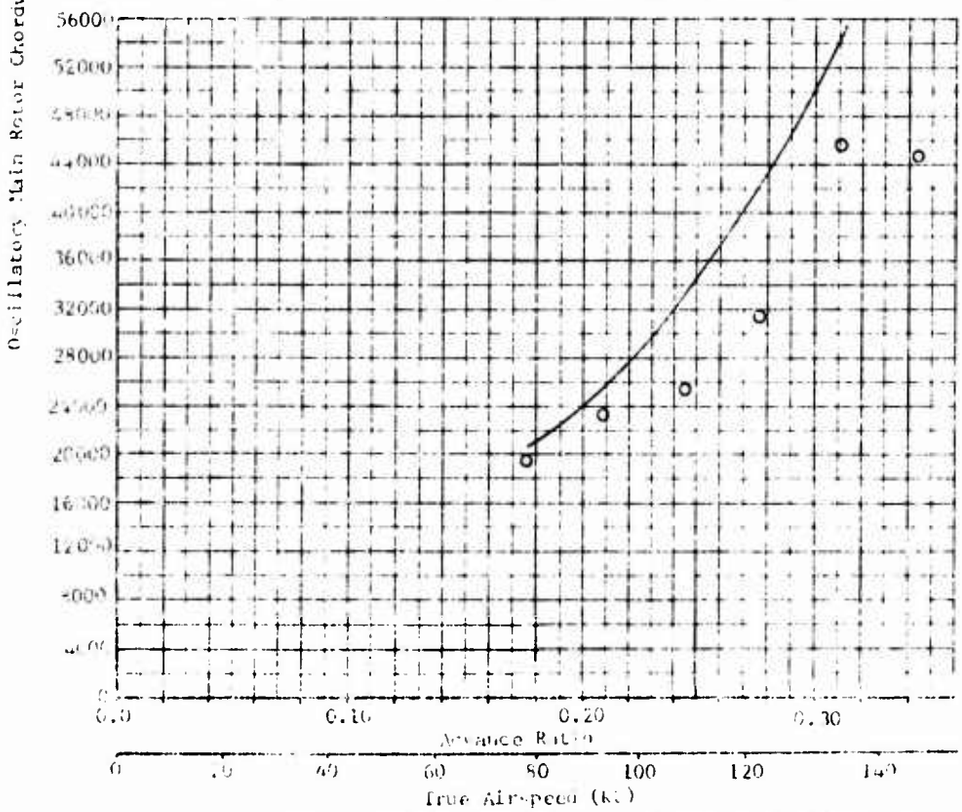

(d) Flight 280-A, 9405 lb, 191.5 in. cg, Clean Wing Configuration

Figure 42. Concluded.

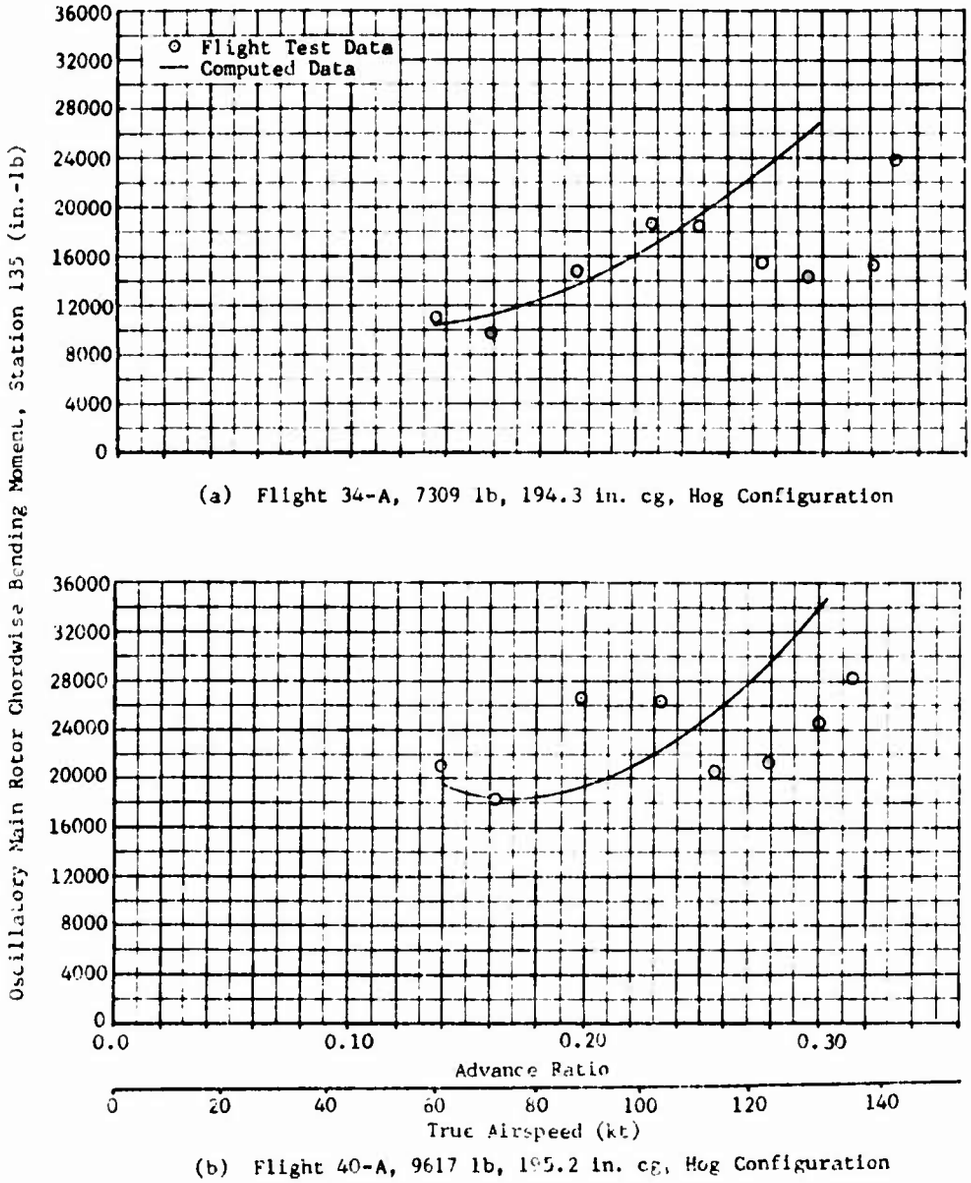

(a) Flight 34-A, 7309 lb, 194.3 in. cg, Hog Configuration

(b) Flight 40-A, 9617 lb, 195.2 in. cg, Hog Configuration

Figure 43. Comparison of Measured and Computed Oscillatory Main Rotor Chordwise Bending Moment, Stations 135 and 160.

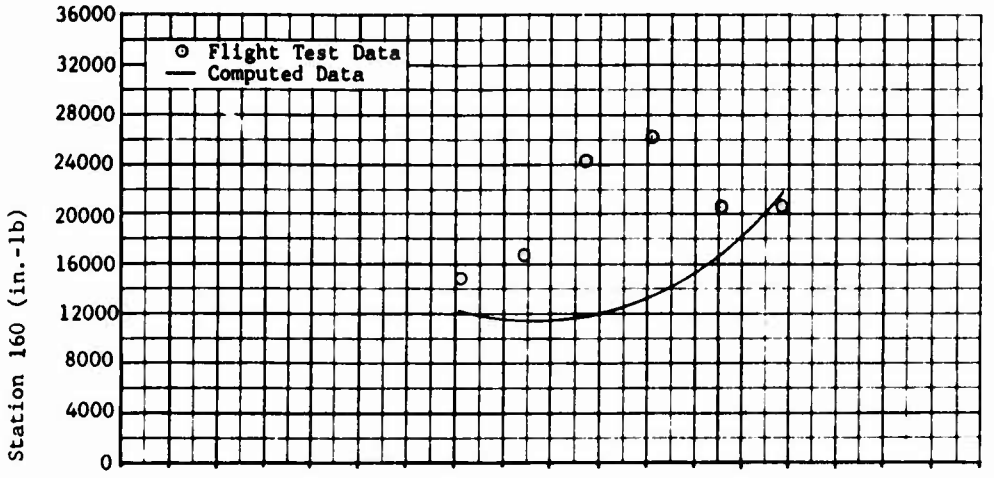

(c) Flight 277-B, 9645 lb, 192.6 in. cg, Hog Configuration

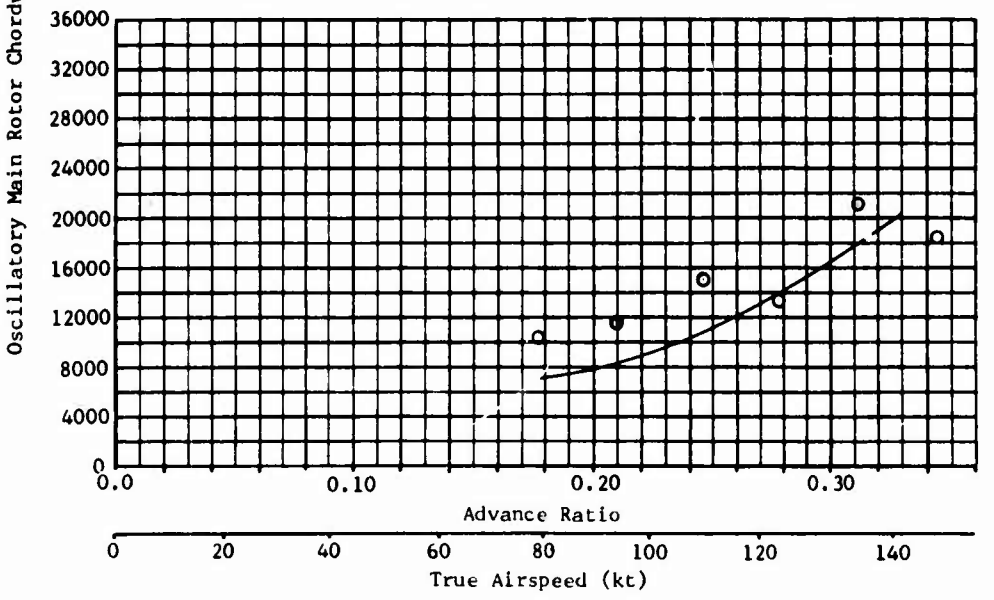

(d) Flight 280-A, 7405 lb, 191.5 in. cg, Clean Wing Configuration

Figure 43. Concluded.

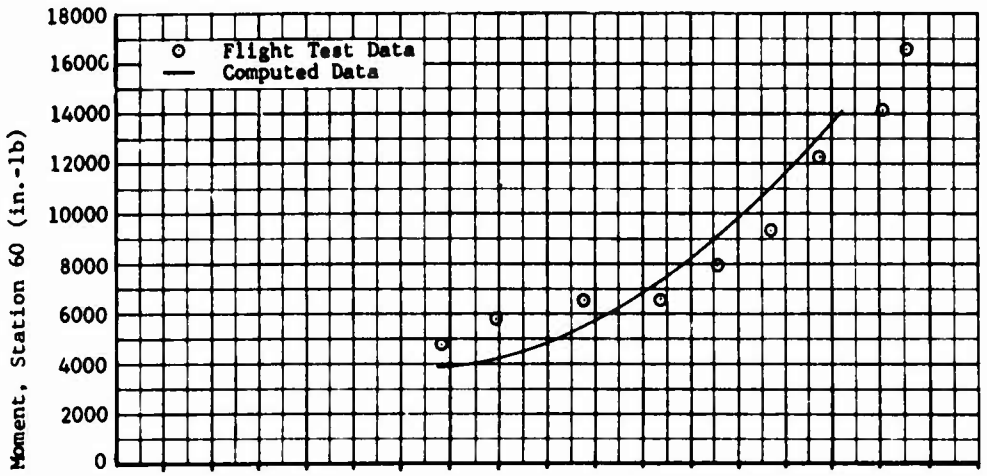

(a) Flight 34-A, 7309 lb, 194.3 in. cg, Hog Configuration

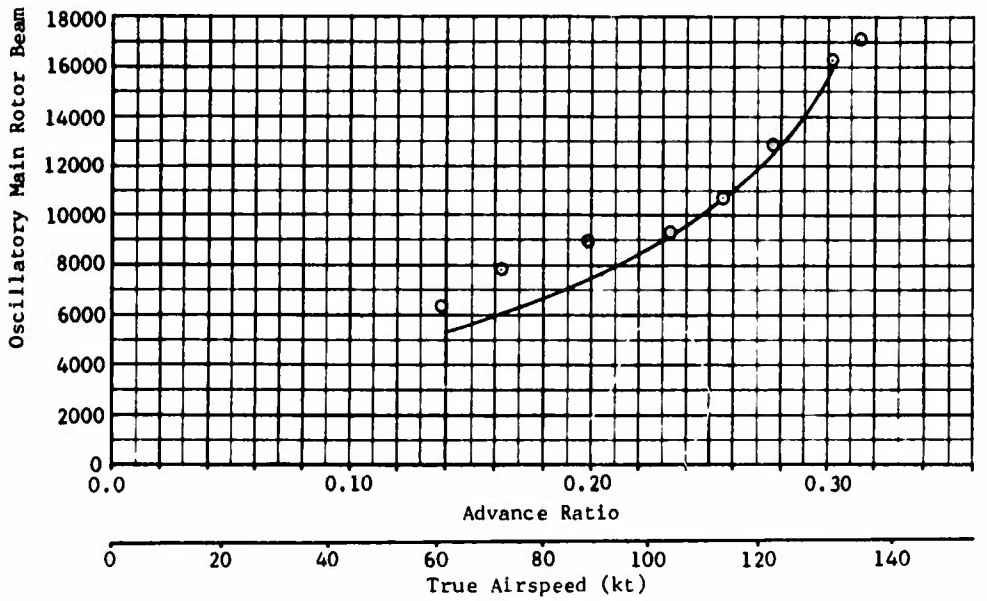

(b) Flight 40-A, 9617 lb, 195.2 in. cg, Hog Configuration

Figure 44. Comparison of Measured and Computed Oscillatory Main Rotor Beam Bending Moment, Station 60.

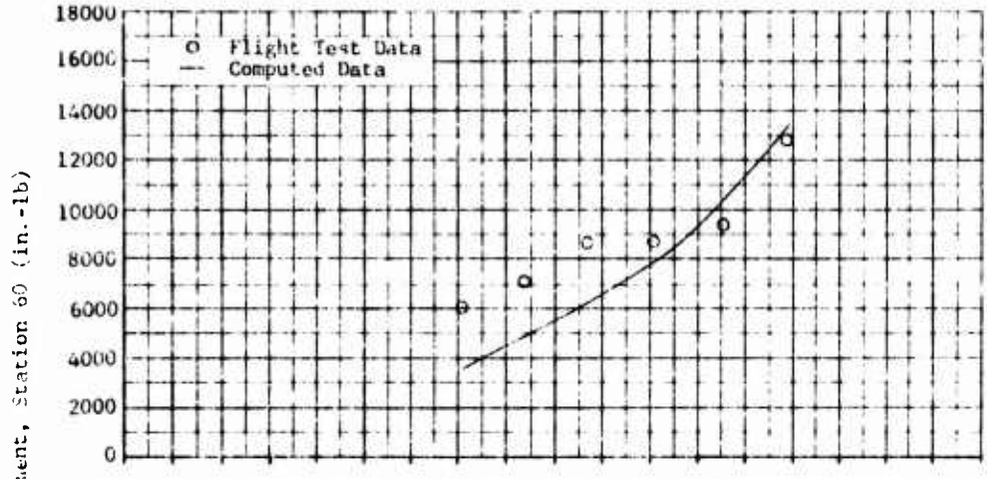

(c) Flight 277-B, 9645 lb, 192.6 in. cg, Hog Configuration

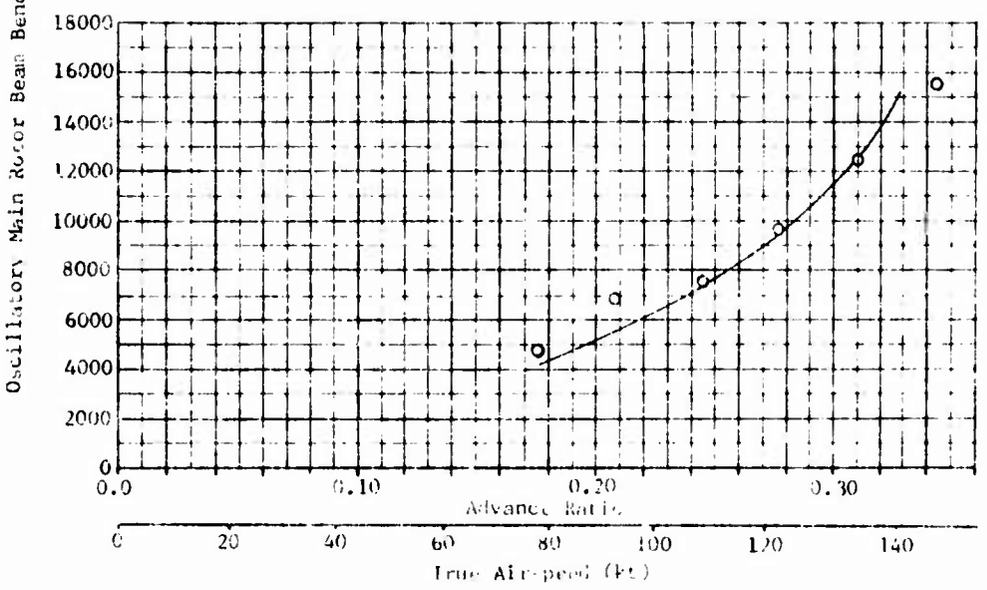

(d) Flight 280-A, 7405 lb, 191.5 in. cg, Clean Wing Configuration

Figure 44. Concluded.

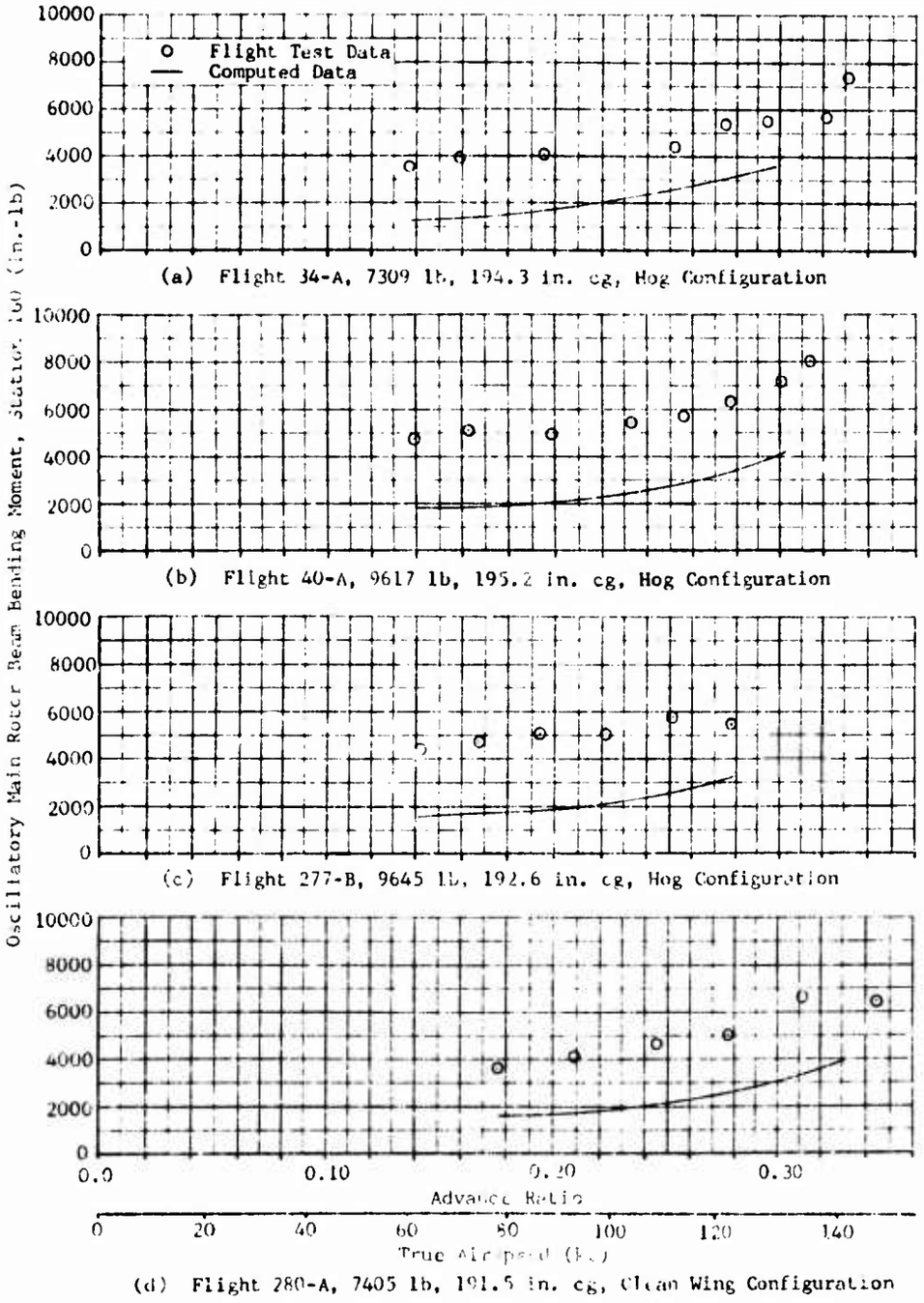

Figure 45. Comparison of Measured and Computed Oscillatory Main Rotor Beam Bending Moment, Station 160.

TABLE XVII. C81 INPUT LISTING FOR AH-1G

```
PLOG209E        J.R. VAN GAASBEEK   (02-02-74)
                MODEL 209 PROGRAM LOGIC GROUP                                   AG

                                PROGRAM LOGIC GROUP
 0    1    5    0    0    2    0    0   -1    3    0    0    0    0
 0    1    0    1    2   -1    1    0    0    0    1    1    0    0
 0    0    0    0    0    0    0    0    0    0    0    0    0    0

CLCD5474            P.Y.HSIEH (1-24-74)
                MODEL 209 M/R AIRFOIL DATA TABLE                                AG

MODE540A            J.R. VAN GAASBEEK   (4-2-74)
                540250    540 BLADE WITH TORSION   HSOFT=-6.5

FLGE209A        J.R. VAN GAASBEEK   (3-22-74)
                CLEAN COBRA FUSELAGE, AFT CG

                                FUSELAGE GROUP
 7477.000        200.0000        0.0             54.00000        200.0000        0.0             68.00000
 2265.000        11880.00         9900.000       580.0000        0.0             0.0             0.0
-4.113799        0.0             0.0             0.0             0.0             0.0            -0.1649200E-01
 0.1794500E-01   0.2739770      -0.1903000E-02    0.7109998E-03   0.9462997E-02  -0.1530000E-03   0.3050000E-03
 5.500000        0.0             156.1000        84.70000        0.0             0.0            -0.2696200E-01
 0.4341300E-01  -0.7022095E-01  -0.1970000E-03    0.5780000E-03   0.1266100E-01   0.1000300E-04   0.6599999E-04
-6.906600        0.0             0.0             0.0             300.0000        0.0             0.4389170
-0.7697695E-01   4.849087        0.1390000E-01  -0.8010000E-02  -0.5651300E-01   0.1731000E-02  -0.3101000E-02
 0.0             11.76000        45.00000        0.3995540       0.4357100E-01   0.4109999E-03  -0.3699999E-04
 1.638453        0.4149800E-01   0.2351000E-02  -0.3571000E-02  -0.2769998E-03   0.2914600E-02  -0.4799999E-04
 0.0            -140.0000        45.00000        0.5549997E-02  -0.2209679      -0.1399700E-01   0.8119999E-03
-4.299999       -0.4806000E-01  -0.4260000E-02   0.3011000E-02  -0.9549999E-04  -0.4042000E-02  -0.2020000E-03
 600.0000        0.0             0.0            -8.757113       0.6939799E-01   0.9264000E-02  -0.1040000E-02
 15.94162        0.1254000E-02  -0.3040000E-02   0.1731300E-01   0.2510000E-02  -0.3025000E-02  -0.1640000E-03

AERO209A    J.R. VAN GAASBEEK (04-05-74) / CARL MATTHYS (04-01-70)
MODEL 209.  MAIN ROTOR IS IN GROUP ONE AND TAIL ROTOR IS IN GROUP TWO.

                                RTR AERODYNAMIC GROUP
 0.8400000       1.270000        1.299999       -0.7000000       0.0             0.0             0.7000000
 0.9499997E-01   0.0             0.4750000E-01   0.0             0.9999998E-02   0.0             0.3000000E-04
 0.4000000E-01   0.3400000       0.8333324E-01   1.000000        0.0             1.000000        0.5000000
 0.0             0.0             0.0             0.0             0.0             0.0             60.00000
 0.0             0.0             0.0             0.0             0.0             0.0             0.0
 0.8400000       1.270000        1.299999       -0.7000000       0.0             0.0             0.7000000
 0.9499997E-01   0.0             0.4750000E-01   0.0             0.9999998E-02   0.0             0.3000000E-04
 0.4000000E-01   0.3400000       0.8999997E-01   0.0             0.0             0.0             0.0
 0.0             0.0             0.0             0.0             0.0             0.0             0.0
 0.0             0.0             0.0             0.0             0.0             0.0             0.0

MNRT209D        J.R. VAN GAASBEEK   (06-22-74)
                MODEL 209 MAIN ROTOR GROUP                                      AG

                                MAIN ROTOR GROUP
 2.000000        4.500000        0.0             22.00000        27.00000       -10.00000        12.00000
 200.0000        0.0             152.6200        475.0000        1411.800        0.4910000E-01   0.0
 17.00000        0.0             10000.00        0.0             0.9700000       0.0             3.400000
 2.750000        0.0             0.0             0.0             0.0             0.0             0.0
 0.0             0.0             0.0             0.0             0.0             0.0             0.0
 0.0             200.0000        0.0             152.6200        3.500000       -0.2500000       0.0
 0.0             0.0             0.0             0.0             0.0             0.0             0.0

TLRT209B        JOHN M. DAVIS   (10-09-73)
 DATA DECK FURNISHED TO USAAMRDL UNDER CONTRACT DAAJ02-72-C-0098

                                TAIL ROTOR GROUP
 2.000000        0.0             0.0             4.250000        8.410000        0.0             11.00000
 520.7000       -14.85000        118.2700        14.96000        1.398000        0.2510000       0.0
 0.0             0.0             10000.00        0.0             0.0             0.0             0.5000000
 1.500000        0.0             30.00000        0.1199999       0.0             0.0             0.2000000
 0.0             0.0             0.0             0.0             0.0             0.0             0.0
 0.0             0.0             0.0             0.0             0.2500000       0.0             0.0
 0.0             0.0             90.00000        0.0             0.0             0.0             0.0

WING209D        J.R. VAN GAASBEEK   (11-30-73)
                MODEL 209 WING GROUP (FIXED SURFACE)                            AG

                                WING GROUP
 27.79999        192.0000        39.00000        62.00000        14.00000        3.500000        11.00000
 3.910000        0.6670000       0.5870000       2.419999        0.0             9.200000        0.0
 0.0             0.0             0.0             0.0             0.0             0.0             0.0
 0.0             0.0             0.0             0.0             0.0             0.0             0.0
 0.5000000       0.5000000       0.0             0.0             0.0             0.0             0.0
 0.0             0.0             0.0             0.0             0.0             0.0             0.0
 0.8400000       1.250000        1.200000        0.0             0.0             0.0             1.099999
 0.1070000       0.0             0.5350000E-01   0.0             0.9999998E-02   0.0             0.3330000E-03
 0.0             0.2000000       0.0             0.0             0.0             0.0             0.0
-0.2000000E-02  -0.9000000E-02   0.8200000       0.0             0.0             0.0             0.0
```

TABLE XVII. - Concluded

STAB209D J.R. VAN GAASBEEK (11-30-73)
MODEL 209 R/H HORIZONTAL STABLIZER AG

STABILIZER NO. 1 GROUP

7.349999	398.5000	22.06999	56.00000	0.7000000	0.0	14.50000
1.490000	1.367000	0.6600000	0.0	0.0	2.000000	0.0
0.0	0.0	0.0	0.0	0.0	0.0	0.0
0.0	0.0	0.0	0.0	0.0	0.0	0.0
1.500000	0.0	0.0	0.0	0.0	0.0	0.0
0.8400000	1.250000	1.200000	0.0	0.0	0.0	1.200000
0.8699995E-01	0.0	0.4350000E-01	0.0	0.7999998E-02	0.0	0.3283999E-03
0.4000000E-01	0.2000000	0.1500000	0.0	0.3320000E-01	0.0	0.0
-0.2000000E-02	-0.9000000E-02	0.8200000	0.6999999E-01	0.0	0.0	0.0
0.0	0.0	0.0	0.8273000	0.1339000	0.0	0.0
0.0	0.0	0.0	0.0	0.0	0.0	0.0

STAB209E J.R. VAN GAASBEEK (11-30-73)
MODEL 209 L/H HORIZONTAL STABLIZER -AG

STABILIZER NO. 2 GROUP

7.349999	398.5000	-22.06999	56.00000	0.7000000	0.0	14.50000
1.490000	1.367000	0.6600000	0.0	0.0	2.000000	0.0
0.0	0.0	0.0	0.0	0.0	0.0	0.0
0.0	0.0	0.0	0.0	0.0	0.0	0.0
1.500000	0.0	0.0	0.0	0.0	0.0	0.0
0.8400000	1.250000	1.200000	0.0	0.0	0.0	1.200000
0.8699995E-01	0.0	0.4350000E-01	0.0	0.7999998E-02	0.0	0.3283999E-03
0.4000000E-01	0.2000000	0.1500000	0.0	0.3320000E-01	0.0	0.0
-0.2000000E-02	-0.9000000E-02	0.8200000	0.6999999E-01	0.0	0.0	0.0
0.0	0.0	0.0	0.8273000	0.1339000	0.0	0.0
0.0	0.0	0.0	0.0	0.0	0.0	0.0

STAB209C JOHN M. DAVIS (10-09-73)
DATA DECK FURNISHED TO USAAMRDL UNDER CONTRACT DAAJ02-72-C-0098

STABILIZER NO. 3 GROUP

18.59999	501.0000	0.0	84.00000	4.500000	90.00000	47.00000
1.559999	0.6670000	0.6400000	0.0	0.9999996E-01	0.0	0.0
0.0	0.0	0.0	0.0	0.0	0.0	0.0
0.0	0.0	0.0	0.0	0.0	0.1799999	0.2000006E-02
0.0	0.0	0.0	0.4000000	-40.00000	-20.00000	0.0
0.8400000	1.250000	1.200000	0.0	0.0	0.0	1.200000
0.9999996E-01	0.0	0.5000000E-01	0.0	0.7999998E-02	0.0	0.1370000E-03
0.4000000E-01	0.2000006	0.1*00000	0.0	0.3320000E-01	0.0	0.0
-0.2000000E-02	-0.9000000F-02	0.8200000	-0.5000000E-01	0.0	0.0	0.0
0.0	0.0	0.0	0.0	0.0	0.0	0.0
0.0	0.0	0.0	0.0	0.0	0.0	0.0

CNTR209D J.R. VAN GAASBEEK (11-30-73)
CONTROLS GROUP FOR SHIP 20002 (66-15246)

CONTROLS GROUP

10.00000	8.500000	21.00000	0.0	0.0	0.0	0.0
12.00000	-13.60000	27.00000	0.0	0.0	0.0	0.0
12.00000	-9.799999	18.00000	0.0	0.0	0.0	0.0
6.500000	-10.00000	30.00000	0.0	0.0	0.0	0.0

ITER209B J.R. VAN GAASBEEK (5-15-74)
ITERATION LIMITS GROUP FOR CONTRACT DAAJ02-73-C-0092

ITERATION GROUP

41.00000	10.00000	2.000000	0.5000000	0.0	0.0	0.3000000
0.2000000	0.2000000	1500.000	500.0000	1.000000	0.9999996E-01	2000.000
50.00000	50.00000	50.00000	100.0000	100.0000	100.0000	10.00000

FLIGHT CONSTANTS GROUP

170.3050	0.0	-26.00000	3800.000	-1.225869	-9.718639	-0.5000000
32.00615	65.91121	42.63089	46.49408	0.0	0.0	0.0
-0.1190000	-1.116400	3.362430	-1.106809	7134.590	356.0999	0.0
0.0	0.0	2000.000	6600.000	1.000000	3800.000	66.00000

TABLE XVIII. C81 INPUT LISTING FOR STORES GROUP

```
                XSTR2048        JAY GUTHRIE (11-30-73) / J.R. VAN GAASBEEK (04-05-74)
                                FOUR EMPTY XM-158 19 ROCKET PODS
152.0000        205.2600        59.65000        48.87000        15.00000        .0              .1000000
1.008000        11.39000        11.39000        .0              .2000000        .0              .0
.0              .0              1.850000        4.000000        4.000000        .0              1.600000
152.0000        198.6200        42.50000        41.71001        15.00000        .0              .1000000
1.008000        11.39000        11.39000        .0              .2000000        .0              .0
.0              .0              1.900000        4.000000        4.000000        .0              1.600000
152.0000        198.6200        -42.50000       41.71001        15.00000        .0              .1000000
1.008000        11.39000        11.39000        .0              .2000000        .0              .0
.0              .0              1.900000        4.000000        4.000000        .0              1.600000
152.0000        205.2600        -59.69000       48.87000        15.00000        .0              .1000000
1.008000        11.39000        11.39000        .0              .2000000        .0              .0
.0              .0              1.850000        4.000000        4.000000        .0              1.600000
```

TABLE XIX. 540 AIRFOIL TABLE USED IN C81

SUPER 540 EXTDSUPER 540 EXTD C81CD DATA TABLES USED
CL

ALPHA/MACH	0.0	0.30000	0.50000	0.60000	0.65000	0.70000	0.75000	0.80000	0.85000	0.90000	1.00000
-180.00000	0.0	0.0	0.0	0.0	0.0	0.0	0.0	0.0	0.0	0.0	0.0
-172.00000	0.78000	0.78000	0.78000	0.78000	0.78000	0.78000	0.78000	0.78000	0.78000	0.78000	0.78000
-161.03003	0.62000	0.62000	0.62000	0.62000	0.62000	0.62000	0.62000	0.62000	0.62000	0.62000	0.62000
-147.00000	1.00000	1.00000	1.00000	1.00000	1.00000	1.00000	1.00000	1.00000	1.00000	1.00000	1.00000
-129.00000	1.00000	1.00000	1.00000	1.00000	1.00000	1.00000	1.00000	1.00000	1.00000	1.00000	1.00000
-49.00000	-1.18000	-1.18000	-1.18000	-1.18000	-1.18000	-1.18000	-1.18000	-1.18000	-1.18000	-1.18000	-1.18000
-39.00000	-1.18000	-1.18000	-1.18000	-1.18000	-1.18000	-1.18000	-1.18000	-1.18000	-1.18000	-1.18000	-1.18000
-21.00000	-0.80000	-0.81300	-0.85000	-0.85000	-0.85000	-0.85000	-0.71500	-0.69000	-0.66400	-0.64000	-0.64100
-18.00000	0.85800	-0.85800	-0.88200	-0.87000	-0.87000	-0.86400	-0.75400	-0.72200	-0.69800	-0.67000	-0.66800
-14.00000	-1.17300	-1.17000	-0.92800	-0.87100	-0.87200	-0.85300	-0.84100	-0.80100	-0.76100	-0.72800	-0.72830
-12.00000	-1.22000	-1.22000	-0.93500	-0.86700	-0.86700	-0.83900	-0.84000	-0.81800	-0.77800	-0.74000	-0.73730
-11.00000	-1.18000	-1.18000	-0.93400	-0.86200	-0.86000	-0.82900	-0.83200	-0.81200	-0.77700	-0.74000	-0.72600
-10.00000	-1.07000	-1.07000	-0.93000	-0.85300	-0.85400	-0.81500	-0.82000	-0.80300	-0.77000	-0.73400	-0.70500
-9.00000	-0.96800	-0.96800	-0.92000	-0.83800	-0.84000	-0.80500	-0.80100	-0.78100	-0.75200	-0.71800	-0.67200
-8.00000	-0.86000	-0.86000	-0.89000	-0.81300	-0.81900	-0.77800	-0.78000	-0.75300	-0.73000	-0.69000	-0.63200
-7.00000	-0.75300	-0.75300	-0.83000	-0.78400	-0.78500	-0.75400	-0.74200	-0.72000	-0.70400	-0.65200	-0.58100
-6.00000	-0.64500	-0.64500	-0.71000	-0.74500	-0.72200	-0.72100	-0.67900	-0.67200	-0.66800	-0.60100	-0.52000
-4.00000	-0.43000	-0.43000	-0.47400	-0.52400	-0.55600	-0.58900	-0.56500	-0.56000	-0.52000	-0.45000	-0.36000
-2.00000	-0.21500	-0.21500	-0.23700	-0.26200	-0.27800	-0.29800	-0.31200	-0.31200	-0.26000	-0.22500	-0.18000
0.0	0.0	0.0	0.0	0.0	0.0	0.0	0.0	0.0	0.0	0.0	0.0
2.00000	0.21500	0.21500	0.23700	0.26200	0.27800	0.29800	0.31200	0.31200	0.26000	0.22500	0.18000
4.00000	0.43000	0.43000	0.47400	0.52400	0.55600	0.58900	0.56500	0.56000	0.52000	0.45000	0.36000
6.00000	0.64500	0.64500	0.71000	0.74500	0.72200	0.72100	0.67900	0.67200	0.66800	0.60100	0.52000
7.00000	0.75300	0.75300	0.83000	0.78400	0.78500	0.75400	0.74200	0.72000	0.70400	0.65200	0.58100
8.00000	0.86000	0.86000	0.89000	0.81300	0.81900	0.77800	0.78000	0.75300	0.73000	0.69000	0.63200
9.00000	0.96800	0.96800	0.92000	0.83800	0.84000	0.80500	0.80100	0.78100	0.75200	0.71800	0.67200
10.00000	1.07500	1.07500	0.93000	0.85300	0.85400	0.81500	0.82000	0.80300	0.77000	0.73400	0.70500
11.00000	1.18400	1.18400	0.93400	0.86200	0.86000	0.82900	0.83200	0.81200	0.77700	0.74000	0.72600
12.00000	1.22000	1.22000	0.93500	0.86700	0.86700	0.83900	0.84000	0.81800	0.77800	0.74000	0.73700
14.00000	1.17200	1.17200	0.92800	0.87100	0.87200	0.85300	0.84100	0.80100	0.76700	0.72800	0.72800
18.00000	0.85800	0.85800	0.88200	0.87000	0.87000	0.86400	0.75400	0.72200	0.69800	0.67000	0.66800
21.00000	0.80000	0.81000	0.85000	0.85000	0.85000	0.85000	0.71500	0.69000	0.66400	0.64000	0.64100
39.00000	1.18000	1.18000	1.18000	1.18000	1.18000	1.18000	1.18000	1.18000	1.18000	1.18000	1.18000
49.00000	1.18000	1.18000	1.18000	1.18000	1.18000	1.18000	1.18000	1.18000	1.18000	1.18000	1.18000
129.00000	-1.00000	-1.00000	-1.00000	-1.00000	-1.00000	-1.00000	-1.00000	-1.00000	-1.00000	-1.00000	-1.00000
147.00000	-1.00000	-1.00000	-1.00000	-1.00000	-1.00000	-1.00000	-1.00000	-1.00000	-1.00000	-1.00000	-1.00000
161.00000	-0.62000	-0.62000	-0.62000	-0.62000	-0.62000	-0.62000	-0.62000	-0.62000	-0.62000	-0.62000	-0.62000
172.50000	-0.78000	-0.78000	-0.78000	-0.78000	-0.78000	-0.78000	-0.78000	-0.78000	-0.78000	-0.78000	-0.78000
180.00000	0.0	0.0	0.0	0.0	0.0	0.0	0.0	0.0	0.0	0.0	0.0

TABLE XIX. - Continued

SUPER 540 EXT'DSUPER 540 EXT'D CLCD DATA TABLES USED
CD

ALPHA/MACH	0.0	0.30000	0.50000	0.60000	0.65000	0.70000	0.75000	0.80000	0.85000	0.90000	1.00000
-180.00000	0.02200	0.02200	0.02200	0.02200	0.02200	0.02200	0.02200	0.02200	0.02200	0.02200	0.02200
-175.00000	0.06200	0.06200	0.06200	0.06200	0.06200	0.06200	0.06200	0.06200	0.06200	0.06200	0.06200
-170.00000	0.13200	0.13200	0.13200	0.13200	0.13200	0.13200	0.13200	0.13200	0.13200	0.13200	0.13200
-165.00000	0.24200	0.24200	0.24200	0.24200	0.24200	0.24200	0.24200	0.24200	0.24200	0.24200	0.24200
-160.00000	0.30200	0.30200	0.30200	0.30200	0.30200	0.30200	0.30200	0.30200	0.30200	0.30200	0.30200
-140.00000	1.04200	1.04200	1.04200	1.04200	1.04200	1.04200	1.04200	1.04200	1.04200	1.04200	1.04200
-120.00000	1.65200	1.65200	1.65200	1.65200	1.65200	1.65200	1.65200	1.65200	1.65200	1.65200	1.65200
-110.00000	1.85200	1.85200	1.85200	1.85200	1.85200	1.85200	1.85200	1.85200	1.85200	1.85200	1.85200
-100.00000	2.00200	2.00200	2.00200	2.00200	2.00200	2.00200	2.00200	2.00200	2.00200	2.00200	2.00200
-90.00000	2.02200	2.02200	2.02200	2.00200	2.00200	2.00200	2.00200	2.00200	2.00200	2.00200	2.00200
-80.00000	1.96200	1.96200	1.96200	1.96200	1.96200	1.96200	1.96200	1.96200	1.96200	1.96200	1.96200
-70.00000	1.84200	1.84200	1.84200	1.84200	1.84200	1.84200	1.84200	1.84200	1.84200	1.84200	1.84200
-60.00000	1.66200	1.66200	1.66200	1.66200	1.66200	1.66200	1.66200	1.66200	1.66200	1.66200	1.66200
-50.00000	1.39200	1.39200	1.39200	1.39200	1.39200	1.39200	1.39200	1.39200	1.39200	1.39200	1.39200
-30.00000	0.60000	0.60000	0.60000	0.60000	0.60000	0.60000	0.60000	0.60000	0.60000	0.60000	0.60000
-28.00000	0.54000	0.54000	0.56300	0.57800	0.57800	0.58100	0.58100	0.58100	0.58100	0.58100	0.58100
-26.00000	0.48000	0.48000	0.52200	0.54500	0.54500	0.54700	0.55800	0.55800	0.55800	0.55800	0.55800
-24.00000	0.42000	0.42000	0.46900	0.50000	0.50200	0.51200	0.52600	0.52600	0.52600	0.52600	0.52600
-22.00000	0.35800	0.35800	0.40900	0.44800	0.46100	0.47200	0.48900	0.49100	0.49100	0.49100	0.49100
-20.00000	0.29900	0.29900	0.35100	0.39600	0.41400	0.43100	0.45100	0.45300	0.45300	0.45300	0.45300
-18.00000	0.24000	0.24000	0.30000	0.34500	0.37000	0.38600	0.40700	0.41400	0.41900	0.41900	0.41900
-16.00000	0.19100	0.19100	0.25300	0.30000	0.32600	0.34100	0.35800	0.36700	0.38100	0.38900	0.38900
-15.00000	0.16700	0.16700	0.23200	0.27500	0.30300	0.31800	0.33300	0.34200	0.36500	0.37200	0.37200
-13.50000	0.13500	0.13500	0.20200	0.24400	0.27100	0.28300	0.29900	0.30900	0.33900	0.35000	0.35100
-12.50000	0.10050	0.10050	0.17500	0.22000	0.24900	0.26100	0.27400	0.28500	0.32100	0.33500	0.33600
-11.50000	0.04600	0.04600	0.14200	0.18800	0.22600	0.23800	0.25100	0.26100	0.30200	0.31900	0.32100
-10.50000	0.02600	0.02600	0.11000	0.15800	0.19500	0.21200	0.22900	0.24000	0.28700	0.30200	0.30500
-9.50000	0.01750	0.01750	0.07800	0.12700	0.16400	0.18800	0.20400	0.21800	0.26900	0.28700	0.29100
-8.50000	0.01250	0.01250	0.04900	0.09600	0.13300	0.16200	0.18000	0.19500	0.25000	0.26900	0.27300
-7.50000	0.01020	0.01020	0.02740	0.06600	0.10200	0.13200	0.15500	0.17100	0.23000	0.25000	0.25700
-6.50000	0.00920	0.00920	0.01240	0.03900	0.07100	0.10200	0.12700	0.14600	0.21000	0.23000	0.23900
-5.50000	0.00850	0.00850	0.01000	0.02230	0.04150	0.07150	0.09850	0.12000	0.18700	0.21100	0.22000	
-4.50000	0.00800	0.00800	0.00920	0.01340	0.02000	0.04300	0.07000	0.10000	0.16600	0.19000	0.19800
-3.50000	0.00790	0.00790	0.00860	0.00890	0.01280	0.02600	0.04500	0.07000	0.14100	0.16600	0.17600
-2.50000	0.00740	0.00740	0.00780	0.00780	0.00930	0.01650	0.02700	0.04200	0.11000	0.14000	0.15000
-1.50000	0.00710	0.00710	0.00710	0.00700	0.00730	0.00980	0.01650	0.02650	0.07000	0.10500	0.12000
-0.50000	0.00680	0.00680	0.00680	0.00670	0.00650	0.00720	0.00890	0.01680	0.05000	0.07200	0.09500
0.0	0.00680	0.00680	0.00670	0.00660	0.00650	0.00680	0.00740	0.01500	0.04500	0.06900	0.09300
0.50000	0.00680	0.00680	0.00680	0.00670	0.00650	0.00720	0.00890	0.01680	0.05000	0.07200	0.09500
1.50000	0.00710	0.00710	0.00710	0.00700	0.00730	0.00980	0.01650	0.02650	0.07000	0.10500	0.12000
2.50000	0.00740	0.00740	0.00780	0.00780	0.00930	0.01650	0.02700	0.04200	0.11000	0.14000	0.15000
3.50000	0.00790	0.00790	0.00860	0.00890	0.01280	0.02600	0.04500	0.07000	0.14100	0.16600	0.17600
4.50000	0.00800	0.00800	0.00920	0.01340	0.02000	0.04300	0.07000	0.10000	0.16600	0.19000	0.19800
5.50000	0.00850	0.00850	0.01000	0.02230	0.04150	0.07150	0.09850	0.12000	0.18700	0.21100	0.22000
6.50000	0.00920	0.00920	0.01240	0.03900	0.07100	0.10200	0.12700	0.14600	0.21000	0.23000	0.23900
7.50000	0.01020	0.01020	0.02740	0.06600	0.10200	0.13200	0.15500	0.17100	0.23000	0.25000	0.25700
8.50000	0.01250	0.01250	0.04900	0.09600	0.13300	0.16200	0.18000	0.19500	0.25000	0.26900	0.27300
9.50000	0.01750	0.01750	0.07800	0.12700	0.16400	0.18800	0.20400	0.21800	0.26900	0.28700	0.29100
10.50000	0.02600	0.02600	0.11000	0.15800	0.19500	0.21200	0.22900	0.24000	0.28700	0.30200	0.30500
11.50000	0.04600	0.04600	0.14200	0.18800	0.22600	0.23800	0.25100	0.26100	0.30200	0.31900	0.32100
12.50000	0.10050	0.10050	0.17500	0.22000	0.24900	0.26100	0.27400	0.28500	0.32100	0.33500	0.33600
13.50000	0.13500	0.13500	0.20200	0.24400	0.27100	0.28300	0.29900	0.30900	0.33900	0.35000	0.35100
15.00000	0.16700	0.16700	0.23200	0.27500	0.30300	0.31800	0.33300	0.34200	0.36500	0.37200	0.37200
16.00000	0.19100	0.19100	0.25300	0.30000	0.32600	0.34100	0.35800	0.36700	0.38100	0.38900	0.38900
18.00000	0.24000	0.24000	0.30000	0.34500	0.37000	0.38600	0.40700	0.41400	0.41900	0.41900	0.41900
20.00000	0.29900	0.29900	0.35100	0.39600	0.41400	0.43100	0.45100	0.45300	0.45300	0.45300	0.45300
22.00000	0.35800	0.35800	0.40900	0.44800	0.46100	0.47200	0.48900	0.49100	0.49100	0.49100	0.49100
24.00000	0.42000	0.42000	0.46900	0.50000	0.50200	0.51200	0.52600	0.52600	0.52600	0.52600	0.52600
26.00000	0.48000	0.48000	0.52200	0.54500	0.54500	0.54700	0.55800	0.55800	0.55800	0.55800	0.55800
28.00000	0.54000	0.54000	0.56300	0.57800	0.57800	0.58100	0.58100	0.58100	0.58100	0.58100	0.58100
30.00000	0.60000	0.60000	0.60000	0.60000	0.60000	0.60000	0.60000	0.60000	0.60000	0.60000	0.60000
50.00000	1.39200	1.39200	1.39200	1.39200	1.39200	1.39200	1.39200	1.39200	1.39200	1.39200	1.39200
60.00000	1.66200	1.66200	1.66200	1.66200	1.66200	1.66200	1.66200	1.66200	1.66200	1.66200	1.66200
70.00000	1.84200	1.84200	1.84200	1.84200	1.84200	1.84200	1.84200	1.84200	1.84200	1.84200	1.84200
80.00000	1.96200	1.96200	1.96200	1.96200	1.96200	1.96200	1.96200	1.96200	1.96200	1.96200	1.96200
90.00000	2.02200	2.02200	2.02200	2.00200	2.00200	2.00200	2.00200	2.00200	2.00200	2.00200	2.00200
100.00000	2.00200	2.00200	2.00200	2.00200	2.00200	2.00200	2.00200	2.00200	2.00200	2.00200	2.00200
110.00000	1.85200	1.85200	1.85200	1.85200	1.85200	1.85200	1.85200	1.85200	1.85200	1.85200	1.85200
120.00000	1.65200	1.65200	1.65200	1.65200	1.65200	1.65200	1.65200	1.65200	1.65200	1.65200	1.65200
140.00000	1.04200	1.04200	1.04200	1.04200	1.04200	1.04200	1.04200	1.04200	1.04200	1.04200	1.04200
160.00000	0.30200	0.30200	0.30200	0.30200	0.30200	0.30200	0.30200	0.30200	0.30200	0.30200	0.30200
165.00000	0.24200	0.24200	0.24200	0.24200	0.24200	0.24200	0.24200	0.24200	0.24200	0.24200	0.24200
170.00000	0.13200	0.13200	0.13200	0.13200	0.13200	0.13200	0.13200	0.13200	0.13200	0.13200	0.13200
175.00000	0.06200	0.06200	0.06200	0.06200	0.06200	0.06200	0.06200	0.06200	0.06200	0.06200	0.06200
180.00000	0.02200	0.02200	0.02200	0.02200	0.02200	0.02200	0.02200	0.02200	0.02200	0.02200	0.02200

TABLE XIX. - Concluded

SUPER 540 EXT'DSUPER 540 EXT'D CLCD DATA TABLES USED
CM

ALPHA/MACH	0.20000	0.30000	0.40000	0.50000	0.60000	0.70000	0.75000	0.80000	0.90000
-180.00000	0.0	0.0	0.0	0.0	0.0	0.0	0.0	0.0	0.0
-170.00000	0.40000	0.40000	0.40000	0.40000	0.40000	0.40000	0.40000	0.40000	0.40000
-165.00000	0.30000	0.30000	0.30000	0.30000	0.30000	0.30000	0.30000	0.30000	0.30000
-160.00000	0.30000	0.30000	0.30000	0.30000	0.30000	0.30000	0.30000	0.30000	0.30000
-135.00000	0.50000	0.50000	0.50000	0.50000	0.50000	0.50000	0.50000	0.50000	0.50000
-90.00000	0.50000	0.50000	0.50000	0.50000	0.50000	0.50000	0.50000	0.50000	0.50000
-30.00000	0.17400	0.19400	0.19600	0.21400	0.23500	0.25000	0.26400	0.27700	0.29800
-23.00000	0.11200	0.11800	0.12800	0.14400	0.15700	0.17100	0.18300	0.20600	0.23200
-16.00000	0.07300	0.07800	0.08600	0.09700	0.10800	0.11700	0.13700	0.17600	0.20000
-15.00000	0.05400	0.06500	0.07300	0.08400	0.09700	0.11100	0.13300	0.17300	0.19500
-14.00000	0.0	0.02700	0.05400	0.06800	0.08600	0.10300	0.12700	0.16700	0.18900
-13.00000	0.0	0.00150	0.02500	0.05000	0.07400	0.09300	0.12200	0.16300	0.18400
-12.00000	0.0	0.0	0.00200	0.03000	0.06000	0.08300	0.11600	0.15700	0.17600
-11.00000	0.0	0.0	-0.00300	0.01400	0.04600	0.07400	0.10800	0.14900	0.17000
-10.00000	0.0	0.0	-0.00200	0.00200	0.03200	0.06500	0.10000	0.14200	0.16300
-9.00000	0.0	0.0	0.0	-0.00300	0.01600	0.05400	0.08900	0.13200	0.15400
-8.00000	0.0	0.0	0.0	-0.00400	0.00500	0.04100	0.08200	0.12300	0.14500
-7.00000	0.0	0.0	0.0	0.0	-0.00400	0.02750	0.07200	0.11250	0.13600
-6.00000	0.0	0.0	0.0	0.0	-0.00300	0.01600	0.06200	0.10000	0.12500
-4.00000	0.0	0.0	0.0	0.0	0.0	0.00500	0.04000	0.07600	0.10200
-3.00000	0.0	0.0	0.0	0.0	0.0	-0.00300	0.02600	0.06650	0.08700
-2.00000	0.0	0.0	0.0	0.0	0.0	0.0	0.01300	0.05300	0.07000
-1.00000	0.0	0.0	0.0	0.0	0.0	0.0	0.00350	0.03300	0.04500
0.0	0.0	0.0	0.0	0.0	0.0	0.0	0.0	0.0	0.0
1.00000	0.0	0.0	0.0	0.0	0.0	0.0	-0.00400	-0.03300	-0.04500
2.00000	0.0	0.0	0.0	0.0	0.0	0.0	-0.01300	-0.05300	-0.07000
3.00000	0.0	0.0	0.0	0.0	0.0	0.00250	-0.02600	-0.06700	-0.08700
4.00000	0.0	0.0	0.0	0.0	0.0	-0.00500	-0.04000	-0.07600	-0.10200
6.00000	0.0	0.0	0.0	0.0	0.00300	-0.01600	-0.06300	-0.10000	-0.12500
7.00000	0.0	0.0	0.0	0.0	0.00400	-0.02800	-0.07200	-0.11300	-0.13600
8.00000	0.0	0.0	0.0	0.00400	-0.00500	-0.04100	-0.08200	-0.12300	-0.14500
9.00000	0.0	0.0	0.0	0.00300	-0.01600	-0.05400	-0.08900	-0.13200	-0.15400
10.00000	0.0	0.0	0.00150	-0.00200	-0.03200	-0.06500	-0.10000	-0.14200	-0.16300
11.00000	0.0	0.0	0.00300	-0.01400	-0.04600	-0.07400	-0.10800	-0.14900	-0.17000
12.00000	0.0	0.0	-0.00200	-0.03000	-0.06000	-0.08300	-0.11600	-0.15700	-0.17600
13.00000	0.0	-0.00200	-0.02500	-0.05000	-0.07400	-0.09300	-0.12200	-0.16300	-0.18400
14.00000	0.0	-0.02700	-0.05400	-0.06800	-0.08600	-0.10300	-0.12700	-0.16700	-0.18900
15.00000	-0.05400	-0.06500	-0.07300	-0.08400	-0.09700	-0.11100	-0.13300	-0.17300	-0.19500
16.00000	-0.07300	-0.07800	-0.08600	-0.09700	-0.10800	-0.11700	-0.13700	-0.17600	-0.20000
23.00000	-0.11200	-0.11800	-0.12800	-0.14400	-0.15700	-0.17100	-0.18300	-0.20600	-0.23200
30.00000	-0.17400	-0.18400	-0.19600	-0.21400	-0.23500	-0.25000	-0.26400	-0.27700	-0.29800
90.00000	-0.50000	-0.50000	-0.50000	-0.50000	-0.50000	-0.50000	-0.50000	-0.50000	-0.50000
135.00000	-0.50000	-0.50000	-0.50000	-0.50000	-0.50000	-0.50000	-0.50000	-0.50000	-0.50000
150.00000	-0.30000	-0.30000	-0.30000	-0.30000	-0.30000	-0.30000	-0.30000	-0.30000	-0.30000
165.00000	-0.30000	-0.30000	-0.30000	-0.30000	-0.30000	-0.30000	-0.30000	-0.30000	-0.30000
170.00000	-0.40000	-0.40000	-0.40000	-0.40000	-0.40000	-0.40000	-0.40000	-0.40000	-0.40000
180.00000	0.0	0.0	0.0	0.0	0.0	0.0	0.0	0.0	0.0

TABLE XX. 540 AEROELASTIC BLADE DATA USED IN C81

MAIN ROTOR AEROELASTIC BLADE DISTRIBUTIONS AND DATA

BLADE STATION NUMBER	WEIGHT (LB/IN)	BEAMWISE INERTIA (IN-LB-SEC**2/IN)	CHORDWISE INERTIA (IN-LB-SEC**2/IN)
1	3.3260	0.0040	0.1685
2	7.6770	0.0040	0.1686
3	7.6520	0.0040	0.1687
4	2.5240	0.0040	0.1682
5	0.9920	0.0020	0.1553
6	0.8010	0.0020	0.106
7	0.7150	0.0010	0.0964
8	0.6910	0.0010	0.0885
9	0.6510	0.0010	0.0825
10	0.6170	0.0010	0.0836
11	0.5810	0.0010	0.0936
12	0.7300	0.0010	0.0840
13	1.2200	0.0020	0.0782
14	1.2200	0.0020	0.0778
15	0.8200	0.0010	0.0719
16	0.5410	0.0010	0.0672
17	0.5410	0.0010	0.0673
18	0.5440	0.0010	0.0674
19	2.0070	0.0010	0.0660
20	2.1180	0.0010	0.0660

TOTAL BLADE WEIGHT = 474.33 LB BLADE TIP WEIGHT = 0.0 LB FLAPPING INERTIA/BLADE = 1485.6 SLUG-FT**2

MAIN ROTOR

	MODE SHAPE FOR MODE 1			MODE SHAPE FOR MODE 2			MODE SHAPE FOR MODE 3		
STA	OUT-OF-PLANE	INPLANE	TORSION	OUT-OF-PLANE	INPLANE	TORSION	OUT-OF-PLANE	INPLANE	TORSION
0	0.0	0.0	0.0	0.0	-0.0695	0.1979	0.0	0.0457	20.1592
1	0.0500	0.0	0.0	-0.0336	-0.0668	0.2282	-0.1417	0.0433	22.9659
2	0.1001	0.0	0.0	-0.0742	-0.0563	0.2572	-0.2468	0.0339	25.6153
3	0.1501	0.0	0.0	-0.1140	-0.0350	0.2816	-0.3480	0.0150	28.0769
4	0.2001	0.0	0.0	-0.1480	0.0	0.2907	-0.4466	0.0	29.1603
5	0.2502	0.0	0.0	-0.1690	0.0300	0.2992	-0.5393	-0.0355	30.5631
6	0.3002	0.0	0.0	-0.1747	0.0729	0.3055	-0.6166	-0.0620	32.1642
7	0.3502	0.0	0.0	-0.1684	0.1219	0.3091	-0.6772	-0.0876	33.8641
8	0.4002	0.0	0.0	-0.1542	0.1757	0.3103	-0.7173	-0.1118	35.5982
9	0.4502	0.0	0.0	-0.1353	0.2332	0.3097	-0.7352	-0.1342	37.4069
10	0.5002	0.0	0.0	-0.1135	0.2940	0.3075	-0.7287	-0.1543	39.2916
11	0.5501	0.0	0.0	-0.0900	0.3574	0.3039	-0.6944	-0.1714	41.2197
12	0.6001	0.0	0.0	-0.0654	0.4232	0.2999	-0.6282	-0.1850	42.9347
13	0.6501	0.0	0.0	-0.0400	0.4911	0.2948	-0.5274	-0.1945	44.4532
14	0.7001	0.0	0.0	-0.0140	0.5607	0.2858	-0.3908	-0.1998	45.8179
15	0.7501	0.0	0.0	0.0124	0.6319	0.2754	-0.2187	-0.2010	46.9612
16	0.8001	0.0	0.0	0.0389	0.7042	0.2681	-0.0146	-0.1987	47.8724
17	0.8501	0.0	0.0	0.0653	0.7775	0.2640	0.2160	-0.1937	48.5751
18	0.9000	0.0	0.0	0.0916	0.8514	0.2638	0.4671	-0.1866	49.0348
19	0.9500	0.0	0.0	0.1178	0.9257	0.2654	0.7310	-0.1783	49.4024
20	1.0000	0.0	0.0	0.1440	1.0000	0.2660	1.0000	-0.1695	49.5103

	MODE SHAPE FOR MODE 4			MODE SHAPE FOR MODE 5			MODE SHAPE FOR MODE 6		
STA	OUT-OF-PLANE	INPLANE	TORSION	OUT-OF-PLANE	INPLANE	TORSION	OUT-OF-PLANE	INPLANE	TORSION
0	0.0	0.0	0.0	0.0	0.0	47.2185	0.0	0.0	0.0
1	0.0229	0.0	0.0	0.0319	0.0115	53.7922	0.0	0.0	0.0
2	0.0678	0.0	0.0	0.0881	0.0229	60.0040	0.0	0.0	0.0
3	0.1134	0.0	0.0	0.1439	0.0340	65.8114	0.0	0.0	0.0
4	0.1598	0.0	0.0	0.1981	0.0446	68.3870	0.0	0.0	0.0
5	0.2075	0.0	0.0	0.2477	0.0540	71.7354	0.0	0.0	0.0
6	0.2569	0.0	0.0	0.2998	0.0615	75.5447	0.0	0.0	0.0
7	0.3075	0.0	0.0	0.3234	0.0670	79.7147	0.0	0.0	0.0
8	0.3591	0.0	0.0	0.3478	0.0703	83.9927	0.0	0.0	0.0
9	0.4112	0.0	0.0	0.3629	0.0716	88.5076	0.0	0.0	0.0
10	0.4639	0.0	0.0	0.3677	0.0707	93.3196	0.0	0.0	0.0
11	0.5169	0.0	0.0	0.3603	0.0674	98.3609	0.0	0.0	0.0
12	0.5700	0.0	0.0	0.3376	0.0611	102.9917	0.0	0.0	0.0
13	0.6234	0.0	-0.1234	0.2961	0.0514	107.0464	0.0	0.0	0.0
14	0.6769	0.0	-0.1652	0.2341	0.0382	110.4936	0.0	0.0	0.0
15	0.7305	0.0	-0.1695	0.1533	0.0219	113.3836	0.0	0.0	0.0
16	0.7843	0.0	-0.1858	0.0580	0.0	115.7613	0.0	0.0	0.0
17	0.8392	0.0	-0.1952	-0.0474	-0.0167	117.6219	0.0	0.0	0.0
18	0.8921	0.0	-0.1967	-0.1598	-0.0377	118.9480	0.0	0.0	0.0
19	0.9460	0.0	-0.1946	-0.2765	-0.0593	119.7372	0.0	0.0	0.0
20	1.0000	0.0	-0.1938	-0.3951	-0.0811	119.9999	0.0	0.0	0.0

MODE NUMBER	1	2	3	4	5
MODE TYPE	RIGID BODY	CYCLIC	CYCLIC	COLLECTIVE	COLLECTIVE
DAMPING RATIO	0.0	0.20000E-01	0.20000E-01	0.20000E-01	0.10000E 00
GENERALIZED INERTIA	0.30779E 01	0.24641E 01	0.43063E 01	0.28328E 01	0.76646E 01
NATURAL FREQUENCY,/REV	0.99900E 00	0.15072E 01	0.27428E 01	0.10619E 01	0.28207 01
CHARACTERISTIC COEFFICIENTS AT BLADE ROOT					
BEAM BENDING MOMENT,FT-LB	-0.15756E 02	-0.27626E 02	0.16429E 03	0.64446E 04	0.31008E 05
CHORD BENDING MOMENT,FT-LB	0.0	0.13670E 06	-0.11483E 06	0.0	0.42035E 04
TORSIONAL MOMENT,FT-LB	0.0	0.16720E 02	0.12559E 05	-0.27786E 01	0.32296E 05
VERTICAL SHEAR,LB	0.55177E 04	-0.19966E 04	-0.24943E 05	0.55094E 04	0.12718E 05
INPLANE SHEAR,LB	0.0	0.10229E 05	-0.64839E 04	0.0	0.30677E 04
MOMENT COEFFICIENTS AT R = 39.60 IN.					
BEAM BENDING MOMENT,FT-LB	-0.35008E 01	-0.80129E 04	0.26260E 05	0.19019E 04	0.10947E 05
CHORD BENDING MOMENT,FT-LB	0.0	0.10439E 06	-0.96890E 05	0.0	-0.30363E 03
TORSIONAL MOMENT,FT-LB	0.0	0.16900E 02	0.12006E 05	-0.27796E 01	0.30881E 05

TABLE XXI. DF1758 INPUTS FOR THE 540 ROTOR

Number of Hub Segments	2.0
VMASS, HMASS, VSOFT, RSOFT	0.0
HSOFT	$-6.5/(10^6$ lb)
Segment Length	13.2 in.
Rotational Frequency	324.0 rpm
Root Collective Pitch	16.0°
Twist	-10.0°
Number of Blades	2.0
Chord	27.0 in.
Control System Stiffness	7.9×10^5 in.-lb/rad

Segment	EIB $X10^{-6}$	EIC $X10^{-6}$	Wt/in.	CG Beam	Offset Chord
1	13.3	4110.0	4.440	0.0	-0.20
2	508.0	1970.0	6.060		-0.20
3	694.0	1750.0	7.240		-0.20
4	256.0	6550.0	2.120		-0.20
5	89.5	4240.0	0.952		-0.36
6	63.1	4050.0	0.761		-0.48
7	50.0	3950.0	0.678		-0.48
8	46.3	3890.0	0.651		-0.52
9	42.0	3640.0	0.611		-0.58
10	37.5	3420.0	0.577		-0.64
11	33.1	3200.0	0.541		-0.68
12	33.0	2990.0	0.690		-0.74
13	35.0	2830.0	1.180		1.02
14	35.0	2620.0	1.180		0.96
15	32.6	2390.0	0.780		-0.94
16	32.3	2200.0	0.501		-0.96
17	32.5	2060.0	0.501		-1.02
18	33.2	2080.0	0.504		-1.04
19	46.4	2260.0	1.670		0.04
20	46.4	2290.0	2.260	0.0	0.04

TABLE XXI. - Concluded

Segment	IBB	ICC	GJ $X10^{-6}$	Shear Center Offset Beam	Chord
1	0.004	0.168	36.00	0.0	0.0
2	0.004	0.168	36.00		
3	0.004	0.168	36.00		
4	0.004	0.168	75.00		
5	0.002	0.155	52.95		
6	0.002	0.106	42.60		
7	0.001	0.096	37.10		
8	0.001	0.088	33.50		
9	0.001	0.082	29.40		
10	0.001	0.083	25.54		
11	0.001	0.093	22.10		
12	0.001	0.083	21.45		
13	0.002	0.075	21.45		
14	0.002	0.075	21.45		
15	0.001	0.070	21.45		
16	0.001	0.066	21.45		
17	0.001	0.066	21.45		
18	0.001	0.066	21.45		
19	0.001	0.066	21.45		
20	0.001	0.066	21.45	0.0	0.0

TABLE XXII. FLIGHT CONDITIONS FOR AH-1G LEVEL FLIGHT DATA

Flight Number	Configuration	Gross Weight	CG Station Line	OAT	Pressure Altitude
34-A*	4 Empty XM-159 Pods	7309	194.3	32.0	2100
40-A*	4 Full XM-159 Pods	9617	195.2	68.0	1200
277-B**	4 Empty XM-159 Pods	9645	192.6	83.0	1200
280-A**	Clean Wing	7405	191.5	73.5	2500

*Reference 27

**Reference 28

APPENDIX III

DATA USED IN STATISTICAL ANALYSIS

The data used in the statistical analysis are provided in this appendix. The data are given by flight number, oscillograph counter and variable number. The following table identifies the variables by variable number. An entry of -.10E+10 was used whenever the value of the variable was not available.

Variable Number	Variable	Units
1	Maximum Mean Normal Load	lb
2	Oscillatory Copilot Vertical Acceleration at the time of Maximum Mean Normal Load	g
3	Maximum Oscillatory Copilot Vertical Acceleration	g
4	Oscillatory Main Rotor Pitch Link Axial Force at the time of Maximum Mean Normal Load	lb
5	Maximum Oscillatory Main Rotor Pitch Link Axial Force	lb
6	Longitudinal Cyclic Stick Position at the time of Maximum Mean Normal Load	%
7	Δ(Longitudinal Cyclic Stick Position)*	%
8	Lateral Cyclic Stick Position at the time of Maximum Mean Normal Load	%
9	Δ(Lateral Cyclic Stick Position)	%
10	Engine Torque Pressure at the time of Maximum Mean Normal Load	psi

*Δ( ) indicates the difference between the value at the time of maximum mean normal load and the value at the beginning of the maneuver.

Variable Number	Variable	Units
11	Maximum Engine Torque Pressure	psi
12	Δ(Engine Torque Pressure)	psi
13	Oscillatory Main Rotor Chordwise Bending Moment, Station 135, at the time of Maximum Mean Normal Load	in.-lb
14	Maximum Main Rotor Oscillatory Chordwise Bending Moment, Station 135	in.-lb
15	Oscillatory Longitudinal Cyclic Stick Force at the time of Maximum Mean Normal Load	lb
16	Maximum Oscillatory Longitudinal Cyclic Stick Force	lb
17	Oscillatory Lateral Cyclic Stick Force at the time of Maximum Mean Normal Load	lb
18	Maximum Oscillatory Lateral Cyclic Stick Force	lb
19	Gross Weight	lb
20	Outside Air Temperature	deg C
21	Pressure Altitude at the time of Maximum Mean Normal Load	ft
22	Collective Stick Position at the time of Maximum Mean Normal Load	%
23	Calibrated Airspeed at the time of Maximum Mean Normal Load	kn
24	Density Ratio at the time of Maximum Mean Normal Load	-
25	Pitch Rate at the time of Maximum Mean Normal Load	deg/s
26	Maximum Pitch Rate	deg/s

Variable Number	Variable	Units
27	Roll Rate at the time of Maximum Mean Normal Load	deg/s
28	Maximum Roll Rate	deg/s
29	Yaw Rate at the time of Maximum Mean Normal Load	deg/s
30	Maximum Yaw Rate	deg/s
31	Speed of Sound at the time of Maximum Mean Normal Load	ft/s
32	Referred Thrust {(Maximum Mean Normal Load) / (Density Ratio)}	lb
33	Disc Loading (C_T/σ) at the time of Maximum Mean Normal Load	-
34	Advance Ratio at the time of Maximum Mean Normal Load	-
35	Maximum Normal Load Factor	g

Flight	Oscillograph Counter	Variable Number 1	2	3	4	5	6
5	11	11251.	.47800	.49900	822.00	877.00	56.800
5	13	11819.	.55100	.56700	794.00	849.00	54.900
5	14	12575.	.64600	.68200	1010.0	1110.0	55.400
5	15	12953.	.67200	.70300	1210.0	1310.0	56.300
5	16	13615.	.77700	.77700	1420.0	1420.0	54.400
5	21	11441.	.47800	.51400	1490.0	1610.0	61.600
5	23	11913.	.57200	.59300	1290.0	1310.0	64.000
5	25	13048.	.54100	.66700	1840.0	1840.0	61.600
5	28	11535.	.52500	.54100	1120.0	1150.0	68.700
5	29	12008.	.57700	.60900	986.00	986.00	68.700
5	36	11819.	.57700	.58800	1070.0	1070.0	67.300
5	37	12102.	.55600	.55600	1230.0	1230.0	60.100
5	38	11913.	.40400	.43000	877.00	904.00	55.800
6	5	13248.	.71900	.74000	1210.0	1230.0	52.500
6	6	14011.	.65100	.65100	1180.0	1230.0	49.600
6	8	15059.	.45700	.46200	986.00	1070.0	42.900
6	9	12962.	.73000	.75100	1340.0	1370.0	59.700
6	10	13725.	.66100	.69800	1780.0	1920.0	57.700
6	11	16312.	.48300	.63000	1640.0	1750.0	54.900
6	17	14214.	.90300	.90300	1620.0	1620.0	65.400
6	18	14297.	.94500	.96100	1590.0	1590.0	63.000
6	19	15917.	.77200	.79800	1840.0	1890.0	62.000
6	21	14582.	.97600	.97600	1590.0	1590.0	63.000
6	22	16012.	.69300	.78200	2140.0	2140.0	60.100
6	23	15821.	.74500	.74500	1750.0	1780.0	60.600
6	25	14011.	.79300	.82400	1920.0	1920.0	71.600
6	26	15536.	.77200	.76630	2270.0	2270.0	68.700
6	27	16489.	.58300	.65100	2990.0	2990.0	68.200
6	30	15154.	.76100	.77700	1670.0	1760.0	55.400
6	31	14968.	.41500	.42500	1150.0	1150.0	46.800
6	32	12295.	.30400	.32500	2470.0	2470.0	76.800
7	18	15234.	.92400	.97100	1840.0	1940.0	64.400
7	21	15995.	.77200	.99200	2080.0	2160.0	66.300
8	7	16292.	.72400	.86600	1920.0	2110.0	54.900
8	8	15818.	.45700	.71900	1640.0	1730.0	47.200
8	9	16671.	.66600	.79300	1940.0	2050.0	51.500
9	18	13404.	.78200	.91300	1370.0	1530.0	56.800
9	19	13615.	.81400	.85600	1260.0	1450.0	57.700
9	20	16546.	.66600	.89200	2080.0	2360.0	60.100
9	21	16930.	.69300	.72400	2440.0	2520.0	57.300
10	7	13183.	1.2400	1.3400	1670.0	1780.0	63.500
10	9	13941.	.62500	.81400	1670.0	1730.0	51.500
11	21	15446.	.33100	.58300	1260.0	1400.0	36.700
11	22	15367.	.46700	.69300	1310.0	1340.0	42.900
11	23	14877.	.45700	.55600	1510.0	1640.0	51.100
10	11	12898.	.73000	.73500	1150.0	1260.0	55.400
10	12	14026.	1.1100	1.1900	1640.0	1640.0	64.400
10	13	13467.	1.1100	1.1400	1530.0	1590.0	63.500
10	14	13279.	1.1400	1.1430	1700.0	1810.0	70.200
10	15	14985.	1.0900	1.1700	1890.0	1890.0	68.200
10	16	12614.	.29900	.32500	986.00	986.00	45.800
10	17	13183.	.30400	.32500	877.00	931.00	44.400
11	7	13172.	1.0400	1.0600	1700.0	1700.0	67.800
11	14	15541.	.91300	.98700	1590.0	1620.0	59.700
11	16	13551.	.69300	.94500	1700.0	1700.0	39.800
11	17	13077.	.56700	.56700	1070.0	1070.0	55.800
11	18	13835.	.44300	.54600	959.00	1150.0	53.900
11	19	15351.	.42000	.48300	1230.0	1340.0	51.500
22	5	14650.	-.10000E+10	-.10000E+10	-.10000E+10	-.10000E+10	77.500
22	6	15792.	-.10000E+10	-.10000E+10	-.10000E+10	-.10000E+10	79.200
22	7	13318.	-.10000E+10	-.10000E+10	-.10000E+10	-.10000E+10	76.400
22	8	14270.	-.10000E+10	-.10000E+10	-.10000E+10	-.10000E+10	67.300
22	9	14440.	-.10000E+10	-.10000E+10	-.10000E+10	-.10000E+10	66.300
22	10	12462.	-.10000E+10	-.10000E+10	-.10000E+10	-.10000E+10	73.000
22	12	15316.	-.10000E+10	-.10000E+10	-.10000E+10	-.10000E+10	71.100
22	13	16267.	-.10000E+10	-.10000E+10	-.10000E+10	-.10000E+10	78.300

Flight	Oscillograph Counter	Variable Number 1	2	3	4	5	6
22	14	15442.	-.10000E+10	-.10000E+10	-.10000E+10	-.10000E+10	75.900
22	15	15415.	-.10000E+10	-.10000E+10	-.10000E+10	-.10000E+10	71.900
112	496	14909.	.36700	.65900	1080.0	1110.0	63.500
112	497	16641.	.66300	.62900	1810.0	2110.0	76.800
112	498	16918.	.59900	.62500	1810.0	1910.0	69.000
112	520	10927.	.27200	.43600	709.00	1200.0	48.100
112	521	11247.	.28100	.46600	857.00	1430.0	47.300
112	522	13427.	.35100	.35100	941.00	940.00	41.200
112	523	15190.	.36800	.36800	1200.0	1370.0	42.400
112	524	14440.	.41700	.45600	1730.0	1780.0	49.600
112	525	16436.	.50400	.53900	2180.0	2240.0	47.300
114	635	16175.	.64200	.64200	1760.0	1880.0	48.000
114	636	16555.	.56800	.64700	1580.0	2030.0	42.700
114	637	16783.	.49800	.67700	1500.0	2030.0	45.300
114	638	16935.	.39800	.66000	1520.0	1530.0	51.900
116	723	15654.	.65000	.67200	2330.0	2330.0	53.700
116	724	17478.	.62800	.62800	2770.0	2850.0	55.500
116	725	17402.	.53600	.60600	2850.0	3010.0	57.900
116	726	18238.	.54400	.58400	2740.0	2980.0	54.100
116	727	17554.	.67600	.83800	2660.0	2660.0	50.800
118	814	17062.	.40500	.40500	1550.0	1890.0	51.500
118	815	16683.	.37400	.37400	1830.0	2040.0	56.600
118	816	16873.	.40100	.42700	1680.0	1920.0	52.000
118	817	17821.	.42700	.46300	1870.0	2100.0	51.700
118	818	17915.	.44100	.51200	1860.0	1860.0	50.400
118	819	17631.	.50300	.66500	2430.0	2610.0	59.200
118	825	14747.	.52100	.60500	2050.0	2150.0	66.700
117	772	18542.	.36600	.48500	1680.0	1680.0	39.200
117	773	18618.	.32200	.47600	929.00	1630.0	38.700
117	774	18456.	.34000	.56000	1760.0	1760.0	39.600
117	775	19304.	.38800	.50700	1010.0	2050.0	33.500
117	785	18618.	.35700	.36200	1660.0	2510.0	45.100
117	786	18922.	.38400	.62600	1960.0	2350.0	43.600
117	787	17782.	.33100	.34400	1690.0	1860.0	46.300
117	789	18994.	.30400	.55600	2020.0	2740.0	44.000
117	790	16774.	.15900	.30400	652.00	880.00	28.700
119	838	18494.	.40800	.40800	-.10000E+10	-.10000E+10	68.100
119	839	12831.	.12600	.17700	-.10000E+10	-.10000E+10	36.300
119	840	20091.	.38100	.39400	2640.0	2830.0	52.100
120	879	16490.	.19000	.26000	-.10000E+10	-.10000E+10	27.600
120	881	17174.	.11000	.45900	-.10000E+10	-.10000E+10	25.700
120	882	16490.	.31800	.52500	-.10000E+10	-.10000E+10	26.700
120	883	19301.	.22500	.65300	-.10000E+10	-.10000E+10	26.200
120	884	19333.	.33100	.59100	-.10000E+10	-.10000E+10	26.000
120	885	18344.	.26900	.64400	-.10000E+10	-.10000E+10	29.700
111	336	18342.	.20500	.43600	685.00	1060.0	21.400
111	337	17483.	.40200	.42300	1060.0	1240.0	24.100
113	596	10849.	.43200	.72400	1240.0	1630.0	36.300
113	597	10541.	.17000	.31000	1140.0	1860.0	35.200
113	598	10541.	.28400	.35400	857.00	1680.0	50.100
113	599	12695.	.29300	.29700	742.00	1550.0	50.600
113	600	10233.	.24900	.39800	1240.0	2140.0	61.900
113	601	14003.	.35800	.36700	1290.0	1450.0	57.900
113	602	13695.	.35800	.35800	1550.0	1550.0	56.800
113	603	13695.	.31000	.38500	1220.0	1580.0	54.200
116	737	17706.	.31000	.69100	2180.0	2300.0	32.400
116	739	16262.	.55400	.62900	2580.0	2790.0	49.100
116	739	15654.	.62900	.63800	2870.0	2950.0	55.800
118	820	17052.	.27600	.62300	1910.0	2270.0	54.200
118	821	18389.	.47200	.58300	1940.0	2050.0	33.600
118	822	18200.	.18200	.59200	2150.0	2380.0	53.800
118	823	17915.	.21800	.43600	2510.0	2640.0	49.300
118	824	18811.	.30700	.39600	2570.0	3000.0	56.000
116	740	19605.	.46100	.53900	2560.0	2950.0	41.400
116	741	19390.	.49300	.57100	2150.0	2400.0	34.200
119	841	19611.	.45600	.52300	2530.0	2820.0	47.300

Flight	Oscillograph Counter	Variable Number 7	8	9	10	11	12
5	11	.0	50.200	.0	37.200	37.300	.0
5	13	-.50000	50.200	.0	38.900	38.900	.0
5	14	.0	48.800	.0	45.100	45.100	.0
5	15	.0	46.400	.0	50.300	50.300	.0
5	16	.0	46.400	.0	49.700	49.700	.0
5	21	.0	51.200	.0	37.800	38.000	.0
5	23	.0	49.730	.0	32.100	32.100	.0
5	25	.0	46.400	.0	48.100	48.100	.0
5	28	.0	48.800	.0	43.300	43.300	.0
5	29	.0	45.400	.0	48.500	48.500	.0
5	36	.0	50.700	.0	39.700	39.700	.0
5	37	.0	50.700	.0	39.400	39.400	.0
5	38	.0	51.200	.0	40.000	40.000	.0
6	5	.0	48.300	.0	-.10000E+10	-.10000E+10	-.10000E+10
6	6	.0	50.700	.0	-.10000E+10	-.10000E+10	-.10000E+10
6	8	.0	55.500	.0	-.10000E+10	-.10000E+10	-.10000E+10
6	9	.0	45.900	.0	-.10000E+10	-.10000E+10	-.10000E+10
6	10	.0	47.300	.0	-.10000E+10	-.10000E+10	-.10000E+10
6	11	.0	50.200	.0	-.10000E+10	-.10000E+10	-.10000E+10
6	17	.0	51.200	.0	-.10000E+10	-.10000E+10	-.10000E+10
6	18	.0	50.700	.0	-.10000E+10	-.10000E+10	-.10000E+10
6	19	.0	55.000	.0	-.10000E+10	-.10000E+10	-.10000E+10
6	21	.0	51.200	.0	-.10000E+10	-.10000E+10	-.10000E+10
6	22	.0	56.400	.0	-.10000E+10	-.10000E+10	-.10000E+10
6	23	.90000	56.400	1.1000	-.10000E+10	-.10000E+10	-.10000E+10
6	25	.0	46.400	.0	-.10000E+10	-.10000E+10	-.10000E+10
6	26	.0	49.200	.0	-.10000E+10	-.10000E+10	-.10000E+10
6	27	.0	55.500	.0	-.10000E+10	-.10000E+10	-.10000E+10
6	30	.0	50.700	.0	-.10000E+10	-.10000E+10	-.10000E+10
6	31	.0	52.100	.0	-.10000E+10	-.10000E+10	-.10000E+10
6	32	.0	54.500	.0	-.10000E+10	-.10000E+10	-.10000E+10
7	14	11.490	48.300	-1.9000	42.200	44.640	-2.4400
7	21	18.790	49.700	-3.3700	39.600	42.900	-3.3300
8	7	24.330	51.200	-7.1400	32.500	41.400	-8.9000
8	8	35.380	49.200	-4.7500	34.400	43.050	-8.6500
8	9	29.210	48.320	-5.7300	32.300	42.600	-10.300
8	18	25.790	47.900	-8.1500	37.300	39.870	-2.5700
8	19	25.250	49.200	-6.2700	37.200	40.950	-3.7500
8	20	21.340	53.600	-.43000	34.700	41.550	-6.8500
8	21	24.790	51.600	-3.8700	29.700	41.550	-11.850
10	7	18.590	40.600	3.8100	46.600	47.300	-.96000
10	9	37.590	44.900	7.1100	42.900	45.780	-2.8800
11	21	42.950	48.900	21.110	42.300	44.790	-2.4900
11	22	34.240	47.800	16.760	43.200	44.360	-1.1600
11	23	34.700	48.300	15.340	42.600	44.790	-2.7900
10	11	.0	51.200	.0	29.300	29.300	.0
10	12	.0	46.800	.0	37.300	38.000	-.70000
10	13	.0	46.800	.0	38.000	39.600	-1.6000
10	14	.0	44.900	.0	46.300	46.300	.0
10	15	.0	44.900	.0	42.900	44.100	-1.2000
10	16	.0	54.900	.0	18.100	18.100	.0
10	17	.0	53.500	.0	16.900	17.300	-.40000
11	7	.0	45.900	.0	45.400	45.400	.0
11	14	.0	51.200	.0	33.700	34.200	-.50000
11	15	.0	49.700	.0	32.100	32.100	.0
11	17	.0	53.100	.0	30.000	30.000	.0
11	19	.0	52.100	.0	29.000	29.000	.0
11	19	.0	54.500	.0	25.500	25.500	.0
22	5	-7.9400	46.800	-1.5300	49.500	50.200	-.70000
22	6	-14.770	50.200	1.3500	47.200	49.300	-2.1000
22	7	-4.9100	49.200	1.4700	-.10000E+10	-.10000E+10	-.10000E+10
22	8	-1.4400	50.700	.10000E-01	39.600	40.950	-1.3500
22	9	-.92000	52.200	.48300	42.800	44.070	-1.2700
22	10	-6.1800	48.200	-.92000	-.10000E+10	-.10000E+10	-.10000E+10
22	12	-1.9000	52.100	-.97000	39.400	42.750	-3.3500
22	13	-21.70	55.500	2.4100	39.40	41.340	-1.9400

Flight	Oscillograph Counter	Variable Number 7	8	9	10	11	12
22	14	-14.13[illegible]	51.600	.92000	41.700	44.360	-2.6600
22	15	-.31[illegible]	48.800	-.92000	31.600	31.800	.20000
112	49[illegible]	12.100	51.900	.60000	36.000	48.000	3.0000
112	497	5.9000	48.900	.50000	40.000	50.000	4.0000
112	498	12.500	50.600	1.4000	39.500	48.000	4.5000
112	520	11.200	63.900	1.2000	30.600	39.800	.0
112	521	11.700	62.700	.30000	31.000	36.000	5.0000
112	522	19.200	63.000	.50000	28.000	31.000	3.0000
112	523	17.200	62.700	.80000	25.500	32.000	4.5000
112	524	19.300	61.600	1.0000	39.000	46.000	7.0000
112	525	22.900	58.700	1.0000	-.10000E+10	-.10000E+10	-.10000E+10
114	635	5.2000	60.700	3.6000	24.000	35.000	1.0000
114	636	10.400	63.300	.60000	27.000	38.000	1.0000
114	637	8.2000	62.300	1.9000	28.000	32.000	.0
114	638	-1.9000	62.200	-1.7000	24.500	28.000	-3.5000
116	723	-15.900	59.600	-1.3000	45.500	50.000	-2.5000
116	724	-12.600	58.100	-1.7000	48.000	49.000	.0
116	725	-9.9300	55.700	-4.4000	42.000	46.000	-4.0000
116	726	-13.300	57.900	-2.1000	46.000	48.000	-2.0000
116	727	-16.600	59.500	-.90000	46.000	44.000	.0
118	814	-5.0000	58.200	-.50000	34.000	49.000	-3.0000
118	815	-.50000	65.500	8.5000	34.000	48.000	-3.0000
118	816	-6.0000	55.700	-3.6000	41.000	49.000	6.0000
118	817	-5.6000	55.100	6.3000	36.000	49.000	-1.0000
118	818	-7.5000	53.700	-6.0000	37.000	49.000	-1.0000
118	819	-9.5000	51.500	-3.1000	52.500	53.000	2.5000
118	825	-6.9000	57.500	1.8000	45.800	53.000	-3.2000
117	772	-3.1000	65.000	-6.3000	4.0000	4.0000	.0
117	773	-2.8000	68.500	-1.4000	4.0000	4.0000	.0
117	774	-1.7000	65.600	-4.3000	2.0000	2.0000	.0
117	775	-8.5000	69.400	-1.0000	2.0000	2.0000	.0
117	785	-3.5000	70.700	-3.9000	2.0000	2.0000	.0
117	786	-5.0000	69.100	-3.1000	2.0000	2.0000	.0
117	787	-1.8100	73.700	1.3000	2.0000	2.0000	.0
117	789	-1.1000	68.100	-3.2000	2.0000	2.0000	.0
117	790	-.30000	65.600	.30000	2.0000	2.0000	.0
119	838	-2.4000	58.200	-1.8000	4.0000	4.0000	.0
119	839	-13.700	65.700	1.6000	4.0000	4.0000	.0
119	840	.40000	72.200	-1.6000	4.0000	4.0000	.0
120	879	.30000	63.600	-1.3000	4.0000	4.0000	.0
120	881	-.30000	62.900	-1.6000	4.0000	4.0000	.0
120	882	.70000	62.800	-2.4000	4.0000	4.0000	.0
120	883	-.60000	64.900	-.60000	4.0000	4.0000	.0
120	884	.60000	64.100	-1.4000	4.0000	4.0000	.0
120	885	.10000	61.700	-.90000	4.0000	4.0000	.0
111	336	36.300	64.200	.50000	36.000	41.000	5.0000
111	337	33.900	63.100	.60000	35.000	38.000	3.0000
113	596	10.200	46.700	19.000	38.000	40.000	10.000
113	597	6.8000	50.000	15.700	39.500	40.000	13.500
113	598	1.9000	63.500	5.3000	34.500	38.400	3.9000
113	599	1.2000	63.800	2.8000	29.200	30.000	.80000
113	600	1.5000	69.300	12.600	42.000	48.000	6.0000
113	601	3.9000	56.300	3.0000	29.600	48.000	16.400
113	602	4.9000	61.100	2.7000	28.000	46.000	8.0000
113	603	2.8000	63.800	6.3000	29.000	42.000	1.0000
116	737	-19.900	45.900	-17.000	30.000	30.000	.0
116	738	-2.8000	64.800	5.2000	28.000	31.000	-3.0000
116	739	2.3000	60.300	3.0000	30.000	38.000	-8.0000
118	820	-1.1000	46.300	-14.600	47.000	57.000	7.0000
118	821	-21.100	38.600	-23.700	49.000	49.000	4.0000
118	822	-6.4000	39.900	-18.500	53.000	59.000	10.000
118	823	-4.8000	74.700	19;600	40;000	44.000	-2.0000
118	824	-4.3000	58.600	5.7000	41.000	46.000	-5.0000
116	740	-23.600	73.500	12.100	34.000	44.000	-5.0000
116	741	-28.100	65.600	3.3000	20.000	38.000	-14.000
119	841	-20.000	69.100	12.200	28.000	41.000	-12.000

Flight	Oscillograph Counter	Variable Number 13	14	15	16	17	18
5	11	21800.	24300.	.89600	.89600	1.1400	1.5200
5	13	23400.	23700.	.67200	1.0100	1.4100	1.6500
5	14	28000.	29800.	.89600	1.0100	1.8700	2.0000
5	15	44300.	44300.	1.0100	1.2300	2.0200	2.3700
5	16	48600.	48900.	1.3400	1.3400	2.2300	2.3500
5	21	40600.	42800.	1.3400	1.5700	1.4000	1.6400
5	23	42400.	44900.	1.6800	2.2400	1.1400	1.5900
5	25	60000.	62100.	1.9000	1.9000	3.3000	3.3000
5	28	42100.	44900.	1.9000	1.9000	1.6300	1.6300
5	29	41200.	43100.	1.4600	1.7900	1.5200	1.5200
5	36	44000.	45500.	1.5700	1.7900	1.3400	1.4600
5	37	44300.	44300.	1.9000	1.9000	1.5600	1.6800
5	38	28600.	29200.	1.1200	1.1200	1.4400	1.4400
6	5	38100.	39100.	1.4600	1.5700	2.1700	2.6500
6	6	40000.	44300.	1.6800	1.7900	1.3200	1.9300
6	8	40600.	44300.	1.2300	1.5700	1.6800	1.8100
6	9	73800.	78600.	2.4600	2.4600	2.9900	2.9900
6	10	52600.	52600.	1.7900	1.7900	1.9300	1.9300
6	11	33800.	40000.	1.5700	1.7900	1.3200	1.9300
6	17	67700.	67700.	2.9100	2.9100	2.0500	2.0500
6	18	70100.	76300.	2.8000	3.1300	2.2900	2.2900
6	19	52300.	52300.	2.3500	2.5700	1.6800	1.9300
6	21	64600.	64900.	2.8000	2.8000	1.8100	1.8100
6	22	52000.	55100.	1.9000	2.0200	1.6800	1.6800
6	23	52000.	52900.	2.2400	2.8000	1.9300	1.9300
6	25	48300.	48300.	2.5700	2.5700	1.8100	1.8100
6	26	64300.	66400.	3.0200	3.3600	1.6800	1.8100
6	27	67400.	74700.	6.5800	6.5800	1.5600	1.6800
6	30	44300.	47700.	1.7900	1.7900	2.2900	2.4100
6	31	24300.	33200.	1.6800	1.6800	1.8100	1.8100
6	32	40600.	40900.	1.5700	1.6800	1.4400	1.8100
7	18	35100.	48000.	3.5800	3.6900	2.1700	2.6500
7	21	23100.	41800.	3.3600	3.6900	1.8100	2.8900
8	7	46800.	68000.	2.1300	3.2500	1.9300	2.9500
9	8	33200.	48900.	1.3400	1.5700	1.6900	2.3100
9	9	55400.	71100.	1.6900	3.5800	1.8100	3.0400
9	18	61800.	71100.	2.3500	3.2500	2.2800	2.3700
9	19	59400.	65800.	2.3500	2.8000	2.0200	2.2500
9	20	54100.	56900.	2.2400	3.2900	1.8900	2.5300
9	21	55400.	65800.	1.9000	2.3500	3.1300	3.5000
10	7	80000.	91400.	4.7600	5.2500	1.6600	1.8100
10	9	50100.	53500.	1.1900	1.6100	1.5800	2.1600
11	21	64300.	70700.	1.1200	2.0200	1.8200	2.1900
11	22	46400.	53500.	1.0100	1.4600	1.8800	2.2600
11	23	44900.	51700.	1.1200	1.7900	1.2000	1.8100
10	11	57200.	57200.	2.2600	2.7600	2.0300	2.1400
10	12	65800.	67700.	3.3100	4.6500	2.5100	2.6300
10	13	69300.	73800.	3.5300	4.8700	2.4000	2.4000
10	14	42400.	47100.	3.1600	3.3900	1.9200	2.1500
10	15	65800.	70100.	4.2300	4.3400	1.6900	2.1700
10	16	32000.	32000.	1.5700	1.5700	1.8000	1.8000
10	17	32000.	32600.	.67200	.89600	1.9200	2.1500
11	7	52300.	52300.	3.0200	3.6500	1.9300	2.2900
11	14	44300.	50800.	3.0200	3.0200	1.6800	1.6800
11	16	49200.	52900.	1.6800	1.6800	1.9300	1.9300
11	17	41500.	45200.	2.2400	2.4600	1.4400	1.6800
11	18	45500.	47100.	2.6900	2.9200	1.5600	2.0700
11	19	41500.	41500.	1.1200	1.5700	1.5600	2.1900
22	5	-.10000E+10	-.10000E+10	4.3800	4.4100	-.10000E+10	-.10000E+10
22	6	-.10000E+10	-.10000E+10	-.10000E+10	-.10000E+10	-.10000E+10	-.10000E+10
22	7	-.10000E+10	-.10000E+10	2.5700	3.1300	2.5500	2.5500
22	8	-.10000E+10	-.10000E+10	2.4600	2.7100	2.2900	2.5300
22	9	-.10000E+10	-.10000E+10	2.9100	4.1700	2.4100	2.6500
22	10	-.10000E+10	-.10000E+10	2.4600	2.4600	1.8700	2.1600
22	12	-.10000E+10	-.10000E+10	4.4100	6.0800	1.4400	2.7700
22	13	-.10000E+10	-.10000E+10	.15600	.49200	2.4100	2.6500

Flight	Oscillograph Counter	Variable Number 13	14	15	16	17	18
22	14	-.10000E+10	-.10000E+10	-.10000E+10	-.10000E+10	2.2900	2.4100
22	15	-.10000E+10	-.10000E+10	3.5200	3.5200	1.5800	1.9500
112	496	39200.	47800.	-.10000E+10	-.10000E+10	-.10000E+10	-.10000E+10
112	497	62000.	62000.	-.10000E+10	-.10000E+10	-.10000E+10	-.10000E+10
112	498	60600.	62000.	-.10000E+10	-.10000E+10	-.10000E+10	-.10000E+10
112	520	39600.	85000.	-.10000E+10	-.10000E+10	-.10000E+10	-.10000E+10
112	521	41000.	87100.	-.10000E+10	-.10000E+10	-.10000E+10	-.10000E+10
112	522	59400.	95800.	-.10000E+10	-.10000E+10	-.10000E+10	-.10000E+10
112	523	58300.	62600.	-.10000E+10	-.10000E+10	-.10000E+10	-.10000E+10
112	524	72000.	81400.	-.10000E+10	-.10000E+10	-.10000E+10	-.10000E+10
112	525	81400.	83500.	-.10000E+10	-.10000E+10	-.10000E+10	-.10000E+10
114	636	.11900E+06	79900.	-.10000E+10	-.10000E+10	-.10000E+10	-.10000E+10
114	636	42100.	62800.	-.10000E+10	-.10000E+10	-.10000E+10	-.10000E+10
114	637	.10400E+06	.14300E+06	-.10000E+10	-.10000E+10	-.10000E+10	-.10000E+10
114	638	.12600E+06	.13900E+06	-.10000E+10	-.10000E+10	-.10000E+10	-.10000E+10
116	723	.11600E+06	.11600E+06	-.10000E+10	-.10000E+10	-.10000E+10	-.10000E+10
116	724	.11500E+06	.11500E+06	-.10000E+10	-.10000E+10	-.10000E+10	-.10000E+10
116	725	99400.	.10100E+06	-.10000E+10	-.10000E+10	-.10000E+10	-.10000E+10
116	726	.11100E+06	.11100E+06	-.10000E+10	-.10000E+10	-.10000E+10	-.10000E+10
116	727	.12500E+06	.12900E+06	-.10000E+10	-.10000E+10	-.10000E+10	-.10000E+10
118	814	52300.	80500.	-.10000E+10	-.10000E+10	-.10000E+10	-.10000E+10
118	815	82600.	86200.	-.10000E+10	-.10000E+10	-.10000E+10	-.10000E+10
118	816	78400.	89000.	-.10000E+10	-.10000E+10	-.10000E+10	-.10000E+10
118	817	73300.	91100.	-.10000E+10	-.10000E+10	-.10000E+10	-.10000E+10
118	818	89700.	89700.	-.10000E+10	-.10000E+10	-.10000E+10	-.10000E+10
118	819	96800.	98200.	-.10000E+10	-.10000E+10	-.10000E+10	-.10000E+10
118	825	44500.	55800.	-.10000E+10	-.10000E+10	-.10000E+10	-.10000E+10
117	772	54200.	67700.	-.10000E+10	-.10000E+10	-.10000E+10	-.10000E+10
117	773	64200.	89100.	-.10000E+10	-.10000E+10	-.10000E+10	-.10000E+10
117	774	72000.	99800.	-.10000E+10	-.10000E+10	-.10000E+10	-.10000E+10
117	775	42100.	.11400E+06	-.10000E+10	-.10000E+10	-.10000E+10	-.10000E+10
117	785	79700.	.10700E+06	-.10000E+10	-.10000E+10	-.10000E+10	-.10000E+10
117	786	63900.	.10900E+06	-.10000E+10	-.10000E+10	-.10000E+10	-.10000E+10
117	787	50400.	93400.	-.10000E+10	-.10000E+10	-.10000E+10	-.10000E+10
117	789	76900.	.11100E+06	-.10000E+10	-.10000E+10	-.10000E+10	-.10000E+10
117	790	43300.	54900.	-.10000E+10	-.10000E+10	-.10000E+10	-.10000E+10
119	833	51400.	51400.	-.10000E+10	-.10000E+10	-.10000E+10	-.10000E+10
119	839	20300.	23100.	-.10000E+10	-.10000E+10	-.10000E+10	-.10000E+10
119	840	75600.	81900.	-.10000E+10	-.10000E+10	-.10000E+10	-.10000E+10
120	879	49200.	49200.	-.10000E+10	-.10000E+10	-.10000E+10	-.10000E+10
120	881	44200.	44200.	-.10000E+10	-.10000E+10	-.10000E+10	-.10000E+10
120	882	46400.	72000.	-.10000E+10	-.10000E+10	-.10000E+10	-.10000E+10
120	883	39200.	41400.	-.10000E+10	-.10000E+10	-.10000E+10	-.10000E+10
120	884	30700.	54900.	-.10000E+10	-.10000E+10	-.10000E+10	-.10000E+10
120	885	47800.	67700.	-.10000E+10	-.10000E+10	-.10000E+10	-.10000E+10
111	336	31400.	31900.	-.10000E+10	-.10000E+10	-.10000E+10	-.10000E+10
111	337	59300.	72800.	-.10000E+10	-.10000E+10	-.10000E+10	-.10000E+10
113	596	74300.	99500.	-.10000E+10	-.10000E+10	-.10000E+10	-.10000E+10
113	597	76400.	95900.	-.10000E+10	-.10000E+10	-.10000E+10	-.10000E+10
113	598	43300.	98800.	-.10000E+10	-.10000E+10	-.10000E+10	-.10000E+10
113	599	33200.	34600.	-.10000E+10	-.10000E+10	-.10000E+10	-.10000E+10
113	600	49700.	.12000E+06	-.10000E+10	-.10000E+10	-.10000E+10	-.10000E+10
113	601	50500.	56200.	-.10000E+10	-.10000E+10	-.10000E+10	-.10000E+10
113	602	61300.	62700.	-.10000E+10	-.10000E+10	-.10000E+10	-.10000E+10
113	603	40400.	40400.	-.10000E+10	-.10000E+10	-.10000E+10	-.10000E+10
116	737	.12300E+06	.13600E+06	-.10000E+10	-.10000E+10	-.10000E+10	-.10000E+10
116	738	.10700E+06	.14500E+06	-.10000E+10	-.10000E+10	-.10000E+10	-.10000E+10
116	739	.11500E+06	.12300E+06	-.10000E+10	-.10000E+10	-.10000E+10	-.10000E+10
118	820	.10500E+06	.11700E+06	-.10000E+10	-.10000E+10	-.10000E+10	-.10000E+10
118	821	89000.	92500.	-.10000E+10	-.10000E+10	-.10000E+10	-.10000E+10
118	822	.11200E+06	.11600E+06	-.10000E+10	-.10000E+10	-.10000E+10	-.10000E+10
118	823	59300.	85500.	-.10000E+10	-.10000E+10	-.10000E+10	-.10000E+10
118	824	70600.	85500.	-.10000E+10	-.10000E+10	-.10000E+10	-.10000E+10
116	740	56500.	74900.	-.10000E+10	-.10000E+10	-.10000E+10	-.10000E+10
116	741	78400.	78400.	-.10000E+10	-.10000E+10	-.10000E+10	-.10000E+10
119	841	53200.	60200.	-.10000E+10	-.10000E+10	-.10000E+10	-.10000E+10

Flight	Oscillograph Counter	Variable Number 19	20	21	22	23	24
5	11	9455.0	10.000	3150.0	35.600	59.200	.90703
5	13	9455.0	10.500	4950.0	37.800	60.100	.84683
5	14	9455.0	10.500	4940.0	42.100	59.100	.85032
5	15	9455.0	10.500	4880.0	45.300	58.500	.84905
5	16	9455.0	10.000	4760.0	45.300	61.700	.85437
5	21	9455.0	11.400	2960.0	35.600	83.600	.90892
5	23	9455.0	11.300	5020.0	39.500	78.000	.84224
5	25	9455.0	11.600	3030.0	42.700	80.500	.90594
5	28	9455.0	12.000	4850.0	39.500	98.300	.84553
5	29	9455.0	11.200	5030.0	42.700	99.800	.84222
5	36	9455.0	11.800	5020.0	36.700	100.00	.84076
5	37	9455.0	11.200	4910.0	36.200	82.300	.84601
5	38	9455.0	11.100	3150.0	36.200	60.000	.90352
6	5	9531.0	12.500	5470.0	41.600	65.600	.82467
6	6	9531.0	12.500	4720.0	41.600	63.300	.84816
6	8	9531.0	12.500	4480.0	42.100	64.900	.85579
6	9	9531.0	12.500	4230.0	41.600	86.400	.86380
6	10	9531.0	12.500	5720.0	41.600	84.600	.81696
6	11	9531.0	12.500	4550.0	43.200	82.000	.85356
6	17	9531.0	12.500	5830.0	41.100	104.00	.81358
6	18	9531.0	12.500	5460.0	41.100	99.000	.82498
6	19	9531.0	12.500	4560.0	41.600	99.800	.85324
6	21	9531.0	12.500	5710.0	41.100	103.00	.81727
6	22	9531.0	12.500	4910.0	40.500	102.00	.84216
6	23	9531.0	12.500	4130.0	40.500	102.00	.86702
6	25	9531.0	12.500	5770.0	44.800	125.00	.81542
6	26	9531.0	12.500	5110.0	44.300	123.00	.83588
6	27	9531.0	11.600	5710.0	43.200	125.00	.81985
6	30	9531.0	11.600	5030.0	44.300	87.200	.83915
6	31	9531.0	11.600	5199.0	40.500	65.000	.83601
6	32	9531.0	11.600	4180.0	36.700	171.00	.86814
7	19	9521.0	.0	5000.0	43.200	109.00	.84538
7	21	9521.0	.20000	4030.0	42.100	102.00	.84381
8	7	9472.0	6.2000	5020.0	40.000	94.500	.85762
8	8	9472.0	6.1000	5000.0	40.500	79.100	.85857
8	9	9472.0	5.5000	5160.0	40.500	88.600	.85527
9	13	9455.0	12.800	5070.0	38.900	82.900	.83626
9	17	9455.0	13.100	5030.0	38.900	84.900	.83663
9	20	9455.0	14.300	5090.0	39.500	94.300	.83127
9	21	9455.0	14.100	5060.0	39.500	96.000	.83278
10	7	9484.0	12.400	4930.0	43.200	102.00	.84183
10	9	9484.0	12.000	4930.0	43.200	68.400	.84301
11	11	9476.0	4.1000	4540.0	39.500	61.200	.87647
11	22	9476.0	4.1000	4420.0	39.500	54.300	.87060
11	23	9476.0	5.0000	4860.0	39.500	72.700	.86649
11	11	9484.0	14.000	5240.0	34.600	81.900	.82912
10	12	9484.0	16.000	4980.0	37.300	106.00	.82979
10	13	9484.0	16.000	4910.0	37.800	98.500	.83508
11	14	9484.0	15.000	4890.0	42.100	124.00	.83548
10	15	9484.0	15.000	4110.0	41.100	123.00	.86014
10	16	9484.0	15.000	4880.0	26.100	61.100	.83579
10	17	9484.0	15.000	4820.0	26.700	58.900	.86302
11	7	9476.0	7.9000	3910.0	39.500	160.00	.89175
11	14	9476.0	9.3000	3770.0	35.600	97.800	.91872
11	15	9476.0	6.8000	5100.0	33.400	83.000	.85936
11	17	9476.0	6.8000	5090.0	32.300	84.100	.85969
11	18	9476.0	6.2000	4750.0	31.800	84.400	.86632
11	19	9476.0	7.8000	3850.0	31.800	79.000	.89041
22	5	9513.0	8.2000	5530.0	42.100	108.00	.83539
22	6	9513.0	5.9000	5630.0	42.700	113.00	.83912
22	7	9513.0	5.9000	4910.0	38.900	-.10000E+15	.86208
22	8	9513.0	5.9000	3170.0	35.600	-.10000E+15	.91965
22	9	9513.0	5.3000	4330.0	38.400	110.00	.85325
22	10	9513.0	5.0000	4880.0	38.900	110.00	.85356
22	12	9513.0	5.0000	5050.0	39.900	109.00	.84815
22	13	9513.0	5.0000	5180.0	39.500	110.00	.84403

Flight	Oscillograph Counter	Variable Number					
		19	20	21	22	23	24
22	14	9513.0	9.0000	5220.0	34.500	110.00	.84277
22	15	9513.0	9.0000	5220.0	30.600	-.10000E+15	.84277
112	496	7530.0	17.200	3530.0	29.000	96.400	.87316
112	497	7531.0	17.200	3340.0	44.600	154.00	.87835
112	498	7530.0	17.200	3340.0	43.400	128.50	.86223
112	520	7750.0	14.400	3580.0	35.300	106.20	.87906
112	521	7750.0	14.400	3550.0	38.500	103.00	.88003
112	522	7750.0	14.400	3700.0	38.500	100.30	.87516
112	523	7750.0	15.000	3470.0	38.900	91.000	.88081
112	524	7750.0	15.000	3210.0	48.200	123.00	.88932
112	525	7750.0	15.000	3480.0	50.700	125.00	.88048
114	635	7594.0	8.9000	3530.0	80.900	95.000	.89786
114	636	7594.0	8.3000	3540.0	76.400	101.00	.89611
114	637	7594.0	7.8000	3640.0	81.000	95.000	.89771
114	638	7594.0	8.9000	3350.0	81.400	101.00	.90386
116	723	7599.0	17.800	4090.0	69.800	155.00	.85249
116	724	7599.0	21.100	3550.0	50.700	147.00	.86000
116	725	7599.0	21.100	3600.0	70.300	143.00	.85841
116	726	7599.0	21.100	3670.0	70.700	148.00	.85614
116	727	7599.0	21.100	3770.0	78.200	147.00	.85301
118	814	9479.0	13.900	3730.0	75.900	83.000	.87571
118	815	9479.0	13.900	3900.0	77.100	87.000	.87020
118	816	9479.0	13.900	4020.0	76.600	83.000	.86633
118	817	9479.0	13.900	3520.0	82.200	86.000	.88255
118	818	9479.0	13.900	3550.0	86.900	90.000	.88157
118	819	9479.0	13.900	3430.0	74.100	112.00	.88549
118	825	9479.0	15.000	2350.0	53.100	170.00	.91795
117	772	7599.0	13.900	3950.0	65.800	74.300	.86858
117	773	7599.0	13.900	3950.0	74.300	79.000	.86858
117	774	7599.0	13.900	3950.0	75.000	89.000	.86858
117	775	7599.0	13.900	4000.0	80.000	74.000	.86697
117	785	7599.0	11.100	3300.0	69.400	94.000	.89853
117	786	7599.0	11.700	3950.0	61.500	110.00	.87529
117	787	7599.0	11.700	4190.0	61.700	104.50	.86752
117	789	7599.0	11.700	3680.0	71.000	103.00	.88411
117	790	7599.0	11.700	3880.0	62.800	44.000	.87751
119	838	9479.0	1.7000	3810.0	58.200	81.000	.91220
119	839	9479.0	1.7000	3900.0	24.300	86.500	.90882
119	840	9479.0	2.8000	3900.0	60.200	112.50	.90520
120	879	7599.0	13.300	3300.0	56.600	35.000	.89163
120	881	7599.0	13.300	3700.0	70.100	31.000	.87852
120	882	7599.0	13.300	3350.0	81.900	26.000	.88998
120	883	7599.0	13.300	3650.0	44.700	33.000	.88015
120	884	7599.0	12.200	2950.0	79.200	33.000	.90671
120	885	7599.0	13.300	3850.0	77.800	30.500	.87364
111	336	7805.0	17.800	2000.0	49.100	92.000	.92086
111	337	7805.0	16.100	2000.0	51.800	85.000	.92627
113	596	7694.0	9.4000	3000.0	31.700	85.300	.91400
113	597	7694.0	9.4000	2600.0	28.900	94.200	.92758
113	598	7694.0	9.4000	2480.0	33.900	102.50	.93168
113	599	7694.0	10.000	2630.0	35.300	107.50	.92459
113	600	7694.0	10.000	3750.0	47.700	139.00	.88711
113	601	7694.0	11.100	2430.0	47.500	139.00	.92781
113	602	7694.0	11.100	2330.0	45.600	143.00	.93123
113	603	7694.0	12.700	1780.0	38.100	147.00	.94487
116	737	7599.0	18.300	3630.0	76.000	125.00	.86569
116	738	7599.0	18.900	3370.0	70.300	115.00	.87227
116	739	7599.0	18.300	3690.0	69.400	116.00	.86377
118	820	9479.0	13.900	3500.0	76.600	100.00	.88320
118	821	9479.0	13.900	3200.0	53.800	100.00	.89306
118	822	9479.0	13.900	3160.0	79.700	108.00	.89438
118	823	9479.0	17.200	3040.0	72.100	108.00	.88814
118	824	9479.0	15.000	3120.0	74.400	105.00	.89228
116	740	7599.0	18.900	3130.0	49.100	147.00	.88004
116	741	7599.0	19.400	3100.0	46.700	139.00	.87951
119	841	9479.0	3.9000	2600.0	51.100	130.00	.94599

Flight	Oscillograph Counter	Variable Number 25	26	27	28	29	30
5	11	5.4300	5.8900	.65100	.65100	-8.3600	-8.6000
5	13	7.7300	7.9600	1.8100	1.8100	-9.3100	-9.5500
5	14	9.0000	9.2300	2.3900	3.5400	-9.7900	-10.300
5	15	9.9200	10.000	.65100	1.8100	-10.000	-10.300
5	16	12.900	12.900	1.8100	1.8100	-11.000	-11.000
5	21	6.8100	6.9300	2.9600	2.9600	-2.6400	-3.0000
5	23	4.9700	5.2000	1.8100	2.3900	-6.6900	-6.9300
5	25	7.9600	8.3100	1.2300	1.2300	-7.7600	-7.8800
5	28	4.5100	4.5100	.72600E-01	.72600E-01	18.900	18.900
5	29	4.4000	5.3200	1.2300	1.2300	-5.6200	-6.1000
5	36	4.6300	4.7400	-.50600	-.50600	4.7500	4.9800
5	37	6.8100	7.2700	.65100	.65100	6.6500	6.6500
5	38	6.8100	7.6200	.72600E-01	.72600E-01	8.0800	8.5600
6	5	12.000	12.100	6.7200	6.7200	-8.1200	-8.1200
6	6	16.500	16.500	6.1500	7.3000	-9.4300	-9.9100
6	9	16.600	17.900	10.500	10.500	-10.400	-11.000
6	9	10.400	10.400	4.1200	5.2800	-2.2800	-2.6400
6	10	11.000	11.000	5.2800	6.4300	-6.2200	-6.6900
6	11	13.500	13.500	8.7500	8.7500	-7.8800	-7.8800
6	17	10.700	10.700	4.7000	6.4300	-3.8300	-5.2600
6	18	9.4600	9.4600	-52.000	-52.000	-5.0200	-5.2600
6	19	11.400	11.900	7.0100	7.0100	-5.9800	-5.9800
6	21	11.600	11.600	5.8600	5.8600	-5.9800	-5.9800
6	22	13.900	13.900	7.5900	7.5900	-5.9800	-6.9300
6	23	13.500	13.900	4.1200	4.1200	-6.9300	-7.6400
6	25	7.8500	7.8500	5.5700	5.5700	-4.1900	-4.1900
6	26	10.600	10.700	5.8600	5.8600	-5.0200	-5.0200
6	27	10.800	10.800	.74100	.74100	-4.7900	-5.7400
6	30	14.500	15.600	7.0100	7.0100	-12.200	-12.600
6	31	13.400	13.400	5.5700	6.1500	-10.400	-13.700
6	32	4.7400	5.6600	5.2800	5.8600	-3.2400	-3.2400
7	19	11.400	11.500	.72600E-01	2.3900	-7.4100	-7.6400
7	21	12.600	14.400	2.3900	3.5400	-5.9800	-7.1700
8	7	14.300	14.400	.65100	1.8100	-8.1200	-8.8400
9	9	14.200	15.800	2.3900	2.3900	-11.500	-11.700
9	9	15.100	15.100	-1.0800	-1.0800	-9.7900	-10.000
9	10	9.3400	9.8000	-1.9500	-3.1100	-7.8800	-8.0000
9	13	7.7300	8.6500	.72600E-01	.94000	-8.1200	-8.6000
9	20	13.500	15.000	-.50600	-.50600	-8.6000	-9.0700
9	21	12.300	13.900	.65100	4.7000	-7.6400	-8.8400
10	7	9.6900	9.6900	3.4300	4.1200	5.8200	5.8200
10	9	12.800	13.500	7.5900	11.900	7.1300	7.7300
11	21	21.300	21.400	8.7500	20.900	8.9000	10.500
11	22	19.500	19.500	2.3900	4.7000	11.500	12.400
11	24	14.200	15.000	-57.500	-57.800	9.7900	10.300
10	11	9.3700	9.0300	.65100	.65100	8.0300	8.0800
10	12	9.1100	9.8000	.65100	.94000	6.1800	6.6500
10	13	6.7300	6.7000	-1.6600	-1.6600	5.7000	5.9400
10	14	4.0500	4.1700	-.79500	-.79500	4.6300	4.5100
10	15	6.8100	7.5000	-1.0900	-2.2400	5.8200	5.9400
10	16	11.600	11.600	-.21700	-1.3700	9.3700	10.500
10	17	12.000	12.600	-1.9500	-2.2400	10.600	12.100
11	7	7.5000	9.6500	.65100	.65100	5.4600	5.4600
11	14	10.500	10.800	-.50600	-1.0800	8.3200	8.8000
11	16	10.000	11.000	-1.6600	-1.6600	8.5600	8.8000
11	17	9.3400	9.3400	.72600E-01	1.8100	8.0800	8.0800
11	18	11.600	11.900	-1.0800	-1.6600	6.4100	6.4100
11	19	12.100	12.100	-2.2400	-2.9200	9.7500	9.7500
22	5	7.8500	12.300	.65100	3.5300	-.49600	-.49600
22	6	11.900	16.000	2.9600	6.4400	7.8400	8.3200
22	7	4.0500	6.5800	.72600E-01	1.2300	-.49600	-.49600
22	8	9.5400	9.0000	.72600E-01	4.1200	1.6500	1.6500
22	9	10.800	10.800	-.50600	-.50600	-.73400	-.73400
22	10	-.10000E+10	-.10000E+10	2.3900	4.1200	-.25800	-.73400
22	12	4.1900	14.200	4.1200	7.5900	-1.0900	-1.0900
22	13	11.400	19.700	4.7000	7.0100	-.49600	-.49600

Flight	Oscillation Counter	Variable Number					
		25	26	27	28	29	30
22	14	9.3400	19.500	2.3930	6.4400	-.25600	-.49800
22	15	2.4400	3.4800	.72600E-01	.65100	.21900	.45700
112	520	15.900	18.600	.23400	.46900	-2.3900	-4.5800
112	521	4.9300	17.100	.31300	.54700	-.69700	-1.2900
112	522	5.2100	13.800	.78200E-01	.46900	-.31800	-1.6900
112	523	4.6900	4.6900	.23400	.39100	-.19900	-.39800
112	521	5.6500	6.5100	.31300	.54700	-1.1900	-1.1900
112	525	5.6100	11.300	.39100	.62500	-.29900	-1.1900
112	526	7.6500	15.700	.31300	.46900	-.19900	-1.6900
112	527	7.6400	11.300	.31300	.54700	-.99600E-01	2.0900
112	528	13.400	15.100	.23400	.46900	.69700	1.5900
114	635	13.800	14.800	2.0600	5.6100	1.2200	2.6400
114	636	15.300	15.900	.79000	8.0600	.71000	3.3500
114	637	13.100	14.700	-2.6900	-3.8700	-1.9300	-2.3300
114	638	7.6000	18.400	-.15800	-6.0600	-.40600	-.91400
115	723	8.4700	12.300	-4.1400	-6.4000	1.5900	3.5800
115	724	11.200	15.400	.39000	10.700	1.6900	2.9800
115	725	9.5600	16.400	1.5600	6.6300	.99500	2.6900
115	726	11.900	16.700	.78300	4.0600	.69600	1.7900
116	727	10.900	14.800	-.85800	-6.2400	1.6900	2.7900
116	814	9.3800	14.500	-1.8200	-1.8200	1.0000	3.9200
116	815	4.9600	12.900	.98900	8.1400	.80400	2.0100
116	816	10.800	13.500	-.39500	-2.7700	.20100	1.4100
119	817	13.600	18.700	-1.0300	-1.1100	-.90500	.0
119	818	13.000	17.700	-2.0500	-2.0500	.50200	5.0200
118	819	9.6000	11.300	.94800	4.5000	.0	2.2100
114	825	1.3600	3.1000	.31600	2.4500	-.10100	-.30700
117	772	3.4100	9.0900	-.15900	-3.3900	-1.1000	-7.0300
117	773	2.2500	9.0000	.78800E-01	2.6800	-2.0100	-10.000
11	774	4.2700	8.6100	-4.6500	-4.6500	-4.1200	-12.100
117	775	-.31300	-1.3200	3.8600	4.9700	-1.0000	-9.6400
117	785	.85400	11.400	-4.7300	-4.7300	-5.3200	-7.3300
117	786	6.9100	11.300	-3.7800	-7.0200	-1.5100	-2.2100
117	787	1.7800	9.3900	.86700	5.6800	-1.3100	-5.8300
117	789	4.4200	12.300	-.55200	-5.2000	-.90400	-6.2300
117	790	-1.3200	-1.4200	2.0500	7.3300	.50200	.60300
119	838	-.23300	-1.0900	-.23200	-1.7800	-2.5900	-4.8900
119	839	4.8900	5.9000	-1.1600	-1.1600	1.1000	1.1900
119	840	2.5600	10.000	-2.9400	-2.9400	-.59700	-1.2900
120	879	-3.1600	-3.1600	3.0200	3.0200	.59700	1.2900
120	881	-1.5400	-1.9300	2.2500	2.2500	.19900	1.7900
120	882	-1.4200	-2.3100	-1.0900	-4.1100	.29800	.29800
120	883	-2.2300	-2.2300	3.2600	3.2600	.79600	1.3900
120	884	-1.6200	-1.6200	3.4100	3.4100	-.59700	-1.6900
120	885	-2.5400	-2.5400	2.1900	6.5900	-.99500E-01	-2.2900
111	836	21.300	21.800	-2.6300	-21.100	-14.300	-14.600
111	837	17.300	18.900	3.9900	17.200	8.7600	11.200
113	596	5.6800	7.7400	-25.600	-39.700	2.2900	7.4700
113	597	5.4500	7.5000	-28.900	-46.600	3.8800	6.7700
113	598	1.8900	5.1300	12.300	66.800	4.9800	5.5700
113	599	-.15800	-.71100	-8.7500	-49.400	-9.3600	-9.3600
113	600	1.8200	3.7900	13.300	47.600	2.4900	2.6900
113	601	1.5800	4.1800	1.1500	4.2200	-5.7700	-6.2700
113	602	5.6100	5.6100	-28.300	-40.700	-4.5800	-4.7800
113	603	1.4200	6.0800	-11.600	-58.800	-5.7700	-8.1600
116	737	9.4900	13.800	-15.100	-23.200	-1.5900	-2.2900
116	738	8.1900	12.100	13.600	26.400	1.5900	3.9800
116	739	7.5000	12.800	10.400	20.200	1.2900	1.2900
118	820	4.5700	11.700	-10.300	-17.600	-2.9100	-2.9100
118	821	10.500	16.400	-16.900	-19.100	-3.5200	-5.7300
118	822	9.3800	14.200	-16.900	-20.800	-.60300	-1.4100
118	823	10.800	14.400	18.200	21.300	.90400	6.1300
118	824	8.2100	16.900	9.7200	24.600	2.3100	3.5200
116	740	14.000	19.500	6.2400	9.2000	-6.4700	-6.5700
116	741	12.500	13.500	1.0900	8.5000	-6.2700	-6.4700
119	841	10.300	11.700	2.9400	5.6500	-4.6800	-4.6800

Flight	Oscillograph Counter	Variable Number 31	32	33	34	35
5	11	1107.4	.61572E-02	.94591E-01	.14057	1.1900
5	13	1108.4	.69275E-02	.10641	.14769	1.2500
5	14	1109.4	.73406E-02	.11276	.14493	1.3300
5	15	1108.4	.75727E-02	.11632	.14357	1.3700
5	16	1107.4	.79100E-02	.12151	.15095	1.4400
5	21	1110.2	.62477E-02	.95971E-01	.19830	1.2100
5	23	1110.0	.70210E-02	.10785	.19220	1.2600
5	25	1110.6	.71489E-02	.10981	.19126	1.3800
5	28	1111.3	.67716E-02	.10402	.24175	1.2200
5	29	1109.8	.70764E-02	.10871	.24592	1.2700
5	36	1110.9	.69775E-02	.10718	.24663	1.2500
5	37	1109.8	.71006E-02	.10907	.20234	1.2800
5	38	1109.6	.65449E-02	.10053	.14274	1.2600
5	5	1112.3	.79739E-02	.12249	.16336	1.3900
6	6	1112.3	.81993E-02	.12595	.15543	1.4700
6	8	1112.3	.87343E-02	.13417	.15865	1.5800
6	9	1112.3	.74484E-02	.11441	.21022	1.3600
6	10	1112.3	.83387E-02	.12809	.21166	1.4400
6	11	1112.3	.93114E-02	.14303	.20071	1.6800
6	17	1112.3	.86716E-02	.13320	.26074	1.5200
6	18	1112.3	.86017E-02	.13213	.24648	1.5000
6	19	1112.3	.92594E-02	.14223	.24433	1.6700
6	21	1112.3	.88566E-02	.13605	.25765	1.5300
6	22	1112.3	.94374E-02	.14497	.25135	1.6800
6	23	1112.3	.90577E-02	.13913	.24772	1.6600
6	25	1112.3	.85285E-02	.13101	.31304	1.4700
6	26	1112.3	.92253E-02	.14171	.30423	1.6300
6	27	1110.6	.99827E-02	.15334	.31219	1.7300
6	30	1110.6	.89639E-02	.13769	.21526	1.5900
6	31	1110.6	.88277E-02	.13560	.16076	1.5600
6	32	1110.6	.72297E-02	.10708	.41503	1.2900
7	18	1107.7	.89443E-02	.13739	.26809	1.6000
7	21	1099.1	.94091E-02	.14453	.25110	1.6800
8	7	1100.0	.94293E-02	.14484	.23076	1.7200
8	8	1099.8	.91450E-02	.14048	.19305	1.6700
8	9	1098.6	.96750E-02	.14862	.21665	1.7600
9	16	1112.9	.81936E-02	.12584	.20500	1.4600
9	19	1113.5	.90777E-02	.13940	.20990	1.4400
9	20	1115.8	.98805E-02	.15177	.23389	1.7500
9	21	1115.4	.10031E-01	.15409	.23783	1.7800
10	7	1112.1	.77729E-02	.11940	.25140	1.3900
10	9	1111.3	.82048E-02	.12609	.16847	1.4700
11	21	1095.8	.97473E-02	.13437	.14783	1.6300
11	22	1095.8	.85902E-02	.13195	.13162	1.5900
11	23	1097.6	.85224E-02	.13091	.17662	1.5730
1	11	1113.3	.77217E-02	.11961	.20116	1.3600
10	12	1113.1	.83962E-02	.12897	.26315	1.4800
10	13	1119.1	.80048E-02	.12296	.24375	1.4200
10	14	1117.2	.78484E-02	.12117	.30678	1.4000
10	15	1117.2	.86473E-02	.13293	.29991	1.5800
10	16	1117.2	.74911E-02	.11507	.15114	1.3390
10	17	1117.2	.75420E-02	.11647	.14338	1.3900
11	7	1103.8	.73316E-02	.11262	.38316	1.3900
11	14	1103.1	.83962E-02	.12897	.23074	1.6400
11	15	1097.6	.74264E-02	.12023	.20247	1.4300
11	17	1097.2	.75504E-02	.11598	.20617	1.3900
11	12	1104.8	.79284E-02	.12176	.20506	1.4600
11	13	1104.1	.85575E-02	.13145	.18932	1.4200
22	5	1104.9	.87064E-02	.13371	.26721	1.5400
22	6	1099.4	.93412E-02	.14349	.27346	1.6600
22	7	1099.4	.76683E-02	.11779	-.24356E+12	1.4030
22	8	1099.4	.77215E-02	.11861	-.23881E+12	1.5000
22	9	1099.4	.86331E-02	.13261	.26980	1.5600
22	11	1100.0	.72469E-02	.11132	.24943	1.3100
2	12	1100.0	.89833E-02	.13763	.26765	1.6100
22	13	1100.0	.95665E-02	.14695	.27376	1.7100

Flight	Oscillograph Counter	Variable Number 31	32	33	34	35
22	14	1105.5	.94128E-02	.14459	.27097	1.6800
22	15	1105.5	.90206E-02	[illegible]	-.24633E+12	1.6100
112	496	1121.4	.84755E-02	.13019	.23329	1.9800
112	497	1121.4	.94042E-02	.14446	.37159	2.2100
112	498	1121.4	.96814E-02	.14872	.31295	2.1700
112	520	1116.0	.61703E-02	.94781E-01	.25615	1.4100
112	521	1116.0	.63383E-02	.97362E-01	.24829	1.4500
112	522	1116.0	.76044E-02	.11681	.24244	1.7300
112	523	1117.2	.85601E-02	.13149	.21927	1.9600
112	524	1117.2	.83051E-02	.12757	.29495	1.9200
112	525	1117.2	.92623E-02	.14228	.30125	2.1200
114	635	1105.3	.89421E-02	.13736	.22672	2.1300
114	636	1104.1	.91699E-02	.14086	.24128	2.1800
114	637	1103.1	.92796E-02	.14254	.22674	2.2100
114	638	1105.3	.92998E-02	.14285	.24024	2.2300
116	723	1122.6	.91145E-02	.14001	.37963	2.0600
116	724	1128.9	.10088E-01	.15496	.35846	2.3000
116	725	1128.9	.10062E-01	.15457	.34903	2.2900
116	726	1128.9	.10573E-01	.16241	.36171	2.4000
116	727	1128.9	.10214E-01	.15690	.35993	2.3100
118	814	1115.0	.96711E-02	.14856	.20057	1.8000
118	815	1115.0	.95161E-02	.14618	.21090	1.7600
118	816	1115.0	.96672E-02	.14850	.20166	1.7800
118	817	1115.0	.10023E-01	.15396	.20702	1.8800
118	818	1115.0	.10087E-01	.15495	.21677	1.8900
118	819	1115.0	.98830E-02	.15181	.26915	1.8600
119	825	1117.2	.79959E-02	.12283	.40125	1.5600
117	772	1115.0	.10596E-01	.16276	.18028	2.4400
117	773	1115.0	.10639E-01	.16343	.19169	2.4500
117	774	1115.0	.10552E-01	.16210	.21595	2.4300
117	775	1115.0	.11051E-01	.16975	.17972	2.5400
117	785	1109.6	.10285E-01	.15798	.22425	2.4500
117	786	1110.8	.10730E-01	.16482	.26588	2.4900
117	787	1110.8	.10174E-01	.15628	.25372	2.3400
117	789	1110.9	.10666E-01	.16384	.24772	2.5000
117	790	1110.8	.94988E-02	.14591	.10672	2.2100
119	838	1091.1	.10058E-01	.15450	.19179	1.9500
119	839	1091.1	.70408E-02	.10815	.20519	1.3600
119	840	1093.3	.10967E-01	.16847	.26740	2.1100
120	879	1113.9	.91798E-02	.14101	.83821E-01	2.1700
120	881	1113.9	.97032E-02	.14905	.74793E-01	2.2600
120	882	1113.9	.91968E-02	.14127	.62325E-01	2.1700
120	883	1113.9	.10885E-01	.16721	.79545E-01	2.5400
120	884	1111.7	.10858E-01	.16679	.78371E-01	2.6100
120	885	1113.9	.10405E-01	.15983	.73792E-01	2.4100
111	336	1122.6	.99866E-02	.15187	.21680	2.3500
111	337	1119.3	.93687E-02	.14391	.19972	2.2400
113	596	1106.3	.58915E-02	.90499E-01	.20177	1.4100
113	597	1106.3	.56406E-02	.86645E-01	.22118	1.3700
113	598	1106.3	.56157E-02	.86263E-01	.24014	1.3700
113	599	1107.4	.68153E-02	.10469	.25282	1.6500
113	600	1107.4	.57257E-02	.87952E-01	.33374	1.3300
113	601	1109.6	.74914E-02	.11508	.32633	1.8200
113	602	1109.6	.72999E-02	.11213	.33511	1.7800
113	603	1112.7	.71945E-02	.11051	.34199	1.7800
116	737	1123.5	.10152E-01	.15594	.30381	2.3300
116	738	1124.7	.92538E-02	.14215	.27845	2.1400
116	739	1123.5	.89955E-02	.13818	.28229	2.0600
118	820	1115.0	.95890E-02	.14730	.24063	1.8000
118	821	1115.0	.10221E-01	.15700	.23930	1.9400
118	822	1115.0	.10100E-01	.15515	.25825	1.9200
118	823	1121.4	.10013E-01	.15380	.25915	1.8900
118	824	1117.2	.11021E-01	.16929	.25137	2.0900
116	740	1124.7	.11058E-01	.16986	.35436	2.5800
116	741	1125.7	.10378E-01	.15942	.33517	2.4200
119	841	1095.4	.10395E-01	.15968	.30226	2.0900

LIST OF SYMBOLS

b	number of rotor blades
b_i	intercept of the regression line with the axis of the dependent variable
C_L	rotor average lift coefficient, $6C_T/\sigma$
c	blade chord, feet
c_ℓ	blade element lift coefficient
C_T/σ	ratio of thrust coefficient to solidity, $\frac{T}{\rho(\Omega R)^2 bcR}$
d_{ij}	deviation from the mean of the j^{th} variable for the i^{th} observation
H_p	pressure altitude, feet
I_x	rotor blade chordwise moment of inertia, in.-lb-sec^2
I_y	rotor blade beamwise moment of inertia, in.-lb-sec^2
K	Southwell coefficient
k	number of independent variables
M_j	number of observations of j^{th} variable
m_{ij}	slope of the regression line
N	number of observations reduced by the number of constraints
n	number of observations
OAT	outside air temperature, degrees Fahrenheit
p	probability in Student-t distribution

LIST OF SYMBOLS - Continued

q	number of independant variables introduced in the analysis
R	rotor radius, feet
R	determinant of correlation coefficient matrix
$\bar{R}$	matrix of correlation coefficients
R_{ij}	cofactors of the correlation coefficient matrix
$R_{i.jkl...}$	multiple correlation coefficient
r_{ij}	simple correlation coefficient
$r_{ij.kl...}$	partial correlation coefficient
s_j	standard deviation, for the sample, of the j^{th} variable
T	thrust, pounds
TAS	true airspeed, knots
t	time, seconds
t	variable in Student-t distribution
t_{comp}	computed value of t used in Student-t test
tz	height of trace zero above reference line, inches
X_j	standard normal variable corresponding to x_j
X_j'	approximation to X_j computed from linear regression equation
x_j	value of j^{th} variable
$\bar{x}_j$	mean value of j^{th} variable
x_{ij}	value of j^{th} variable for i^{th} observation

LIST OF SYMBOLS - Concluded

Z, z	normalized variable used in z test
z_{crit}	critical value of z
α	angle of attack, degrees
α_r	retreating blade tip angle of attack, degrees
$\Delta ( )$	indicates the difference between the value at the time of maximum mean normal load factor and the value at the beginning of the maneuver
ζ_H	hypothetical mean used in Z test
μ	advance ratio, 1.688 TAS/ΩR
ρ	rotor blade weight per inch, pounds/inch
σ	rotor solidity, $\frac{bc}{\pi R}$
σ_j	population standard deviation of the j^{th} variable
σ_z	standard deviation of transformed variable z
Ω	rotor rotational rate, radians/second

4333-75